La borsa di dottorato è stata cofinanziata con risorse del
Programma Operativo Nazionale Ricerca e Innovazione 2014-2020 (CCI 2014IT16M2OP005),
Fondo Sociale Europeo, Azione I.1 "Dottorati Innovativi con caratterizzazione Industriale"

UNIVERSITY OF SALERNO
Department of Civil Engineering
Ph.D. school:
Risk and Sustainability in Civil, Architecture and Environmental Engineering Systems
Cycle XXXII (2016-2019)
Director:
Prof. Fernando Fraternali

UNIVERSITY OF LYON
University Claude Bernard Lyon1
Ph.D. school:
MEGA ED 162
Mechanic, Energetic, Civil Engineering, Acoustic

Director:
Prof. Jocelyn Bonjour

Ph.D. thesis in: Civil Engineering
Subject: Structural Engineering
Defended the 06/04/2020

FLAX TRM COMPOSITE SYSTEMS FOR STRENGTHENING OF MASONRY: FROM THE MATERIAL IDENTIFICATION TO THE STRUCTURAL BEHAVIOUR

Giuseppe Ferrara

Italian Supervisor
Prof. Enzo Martinelli

French Supervisors
Prof. Aron Gabor
Prof. Carmelo Caggegi

UNIVERSITY OF SALERNO
Department of Civil Engineering
Ph.D. school:
Risk and Sustainability in Civil, Architecture and Environmental Engineering Systems
Cycle XXXII (2016-2019)
Director:
Prof. Fernando Fraternali

UNIVERSITY OF LYON
University Claude Bernard Lyon1
Ph.D. school:
MEGA ED 162
Mechanic, Energetic, Civil Engineering, Acoustic
Director:
Prof. Jocelyn Bonjour

Ph.D. thesis in: Civil Engineering
Subject: Structural Engineering
Defended the 06/04/2020

FLAX TRM COMPOSITE SYSTEMS FOR STRENGTHENING OF MASONRY: FROM THE MATERIAL IDENTIFICATION TO THE STRUCTURAL BEHAVIOUR

Giuseppe Ferrara

Ph.D. Committee:

de Felice Gianmarco, Professor, University Rome III	President
Oliveira V. Daniel, Associate Professor, University of Minho	Reviewer
Papanicolaou Catherine, Associate Professor University of Patras	Reviewer
Aiello Maria Antonietta, Professor, University of Salento	Examiner
Thouraya Baranger, Professor, University CB Lyon 1	Examiner
Ribera Federica, Associate Professor, University of Salerno	Examiner
Martinelli Enzo, Associate Professor, University of Salerno	Supervisor
Gabor Aron, Associate Professor, University CB Lyon 1	Supervisor
Caggegi Carmelo, Associate Professor, University CB Lyon1	Invited

Université Claude Bernard – LYON 1

Président de l'Université	M. Frédéric FLEURY
Président du Conseil Académique	M. Hamda BEN HADID
Vice-Président du Conseil d'Administration	M. Didier REVEL
Vice-Président du Conseil des Etudes et de la Vie Universitaire	M. Philippe CHEVALLIER
Vice-Président de la Commission de Recherche	M. Jean-François MORNEX
Directeur Général des Services	M. Damien VERHAEGHE

COMPOSANTES SANTE

Faculté de Médecine Lyon-Est – Claude Bernard	Doyen : M. Gilles RODE
Faculté de Médecine et Maïeutique Lyon Sud Charles. Mérieux	Doyenne : Mme Carole BURILLON
UFR d'Odontologie	Doyenne : Mme Dominique SEUX
Institut des Sciences Pharmaceutiques et Biologiques	Directrice : Mme Christine VINCIGUERRA
Institut des Sciences et Techniques de la Réadaptation	Directeur : M. Xavier PERROT
Département de Formation et Centre de Recherche en Biologie Humaine	Directrice : Mme Anne-Marie SCHOTT

COMPOSANTES & DEPARTEMENTS DE SCIENCES & TECHNOLOGIE

UFR Biosciences	Directrice : Mme Kathrin GIESELER
Département Génie Electrique et des Procédés (GEP)	Directrice : Mme Rosaria FERRIGNO
Département Informatique	Directeur : M. Behzad SHARIAT
Département Mécanique	Directeur M. Marc BUFFAT
UFR - Faculté des Sciences	Administrateur provisoire : M. Bruno ANDRIOLETTI
UFR (STAPS)	Directeur : M. Yannick VANPOULLE
Observatoire de Lyon	Directrice : Mme Isabelle DANIEL
Ecole Polytechnique Universitaire Lyon 1	Directeur : Emmanuel PERRIN
Ecole Supérieure de Chimie, Physique, Electronique (CPE Lyon)	Directeur : Gérard PIGNAULT
Institut Universitaire de Technologie de Lyon 1	Directeur : M. Christophe VITON
Institut de Science Financière et d'Assurances	Directeur : M. Nicolas LEBOISNE
ESPE	Administrateur Provisoire : M. Pierre CHAREYRON

Research funding

Several institutions financially contributed to the research study:

- *the Italian Ministry for Education, University and Research (MIUR), as part of the program "Dottorati Innovativi a caratterizzazione industrial" funded by the European Union (Structural Funding ERDF-ESF for "Research and Innovation" 2014-2020), awarded the Ph.D. scholarship;*

- *the French Government provided a scholarship to cover the mobility expenses concerning the stay at the laboratory LMC2 (UCBL1, France);*

- *the Ph.D. school MEGA (UCBL1, France) contributed to the mobility expenses for participation to international conferences;*

- *the laboratory LMC2 (UCBL1, France) contributed to the mobility expenses for participation to international conferences;*

- *the European Union's Horizon 2020 Research and Innovation Program under Grant Agreement N° 645704 (H2020-MSCA-RISE-2014), by means of the "SUPERCONCRETE Project" (www.superconcrete-h2020.unisa.it), covered the mobility expenses concerning the stay at the laboratory NUMATS (UFRJ, Brazil);*

- *the company INNOVATION s.r.l. provided the materials tested in the experimental research activity.*

The author gratefully acknowledges the mentioned institutions for their financial support, essential for the fulfilment of the Thesis.

Acknowledgments

I would like to express my deepest gratitude and appreciation to the people without which the completion of the Ph.D. thesis would not have been possible.

My sincere thanks to:

Prof. Enzo Martinelli, my first mentor and the person who introduced me to the academic research world, for guiding me during the research, for the wise advices, for the constant encouragement, and for always believing in me;

Profs. Aron Gabor and Carmelo Caggegi, my French supervisors, for their fundamental guide and support during my research activity at University C.B. Lyon1, and for making me comfortable within the institution from the very first moment;

Mr. Rossano Petruzziello, the head of the company Engineering s.r.l. (Avellino, Italy), for giving me the possibility to spend time in his company;

Prof. Emmanuel Ferrier, the director of the laboratory LMC2 (University C.B. Lyon1, France), for gently welcoming me to the laboratory and for giving me the great opportunity to join it;

Prof. Luciano di Maio and Dr. Bartolomeo Coppola, who work at the Department of Industrial Engineering of University od Salerno, for their precious collaboration in fulfilling part of the experimental activity;

Prof. Romildo Dias Toledo Filho, director of the laboratory NUMATS (Federal University of Rio de Janeiro, Brazil), for kindly welcoming me to the laboratory, and giving me the great chance to cooperate with it;

Dr. Marco Pepe, researcher at University of Salerno, for the valuable support, and for the collaboration in part of the research.

I would also extend my sincere thanks to Dr. Carmine Lima and Dr. Roberto Falcone, who welcomed me in the research group from the very first moment with warmth and friendliness.

I am also grateful to the entire staffs of Ph.D. students, technicians, secretaries, researchers and professors of both the laboratories LMC2 and NUMATS, for their hospitality and for treating me like a family. Many thanks to Norbert Cottin and Emmanuel Janin for their essential help in the accomplishment of the experimental activity.

I need to express dutiful and sincere thanks to all the people I shared with my "Ph.D. adventure", who day by day cheered me up and supported me through tough times. Many thanks to Maria Rosaria Scoppettuolo, for her helpfulness and kindness, to Maria Grazia Stoppiello, for her wise advices, and all the "GNAMMMM" people, always ready to share with me funny moments and difficult times. Merci beaucoup to the Ph.D. students of the LMC2, in particular to Antoine Chalot, "mon père adoptif français", et Mohamed Saidi, for the good times we shared in our multicultural office, always with joy, consideration and respect.

Last, but certainly not least, I would express my extreme gratitude to my parents and family, for conveying to me the sense of duty and the responsibility without which I would never have accomplished such an important achievement.

English abstract

Thesis Title

FLAX TRM COMPOSITE SYSTEMS FOR STRENGTHENING OF MASONRY: FROM THE MATERIAL IDENTIFICATION TO THE STRUCTURAL BEHAVIOUR

Author

Giuseppe Ferrara

Textile Reinforced Mortar (TRM) composites represents nowadays an innovative and efficient technique for strengthening of masonry structural elements. In recent years, the use of plant fibres within the composite, instead of high strength synthetic fibres, emerged as a smart solution to increase the sustainability of such reinforcement system. However, several issues are still open concerning the use of such fibres in inorganic matrices, and the studies in the literature addressing this aspect, although showing a great potential of these systems, are not enough to widely promote such innovative and sustainable technique of reinforcement.

With the aim of raising the awareness in the use of plant fibres based TRMs, this study proposes a comprehensive mechanical characterisation of a Flax TRM system conceived as reinforcement of masonry elements. Prior to address the issue of the composite characterisation, its components, i.e. textile and mortar, were physically and mechanically characterised. Then, tensile tests on the composite and shear bond tests on Flax-TRM-to-masonry substrate elements were carried out to qualify the composite material and its adherence behaviour with a brick-masonry element. Consequently, on a structural scale, the contribution of the reinforcement system on the shear capacity of masonry elements was analysed by means of diagonal compression tests. Finally, innovative solutions to improve the mechanical performance of the studied reinforcement system were proposed and their efficiency was discussed.

The study confirms the potential in the use of plant fibre textiles as reinforcement in TRM systems, outlines the aspects on which it is necessary to act to increase their efficiency, and shows some technical solutions to improve it.

Italian abstract

Titolo della Tesi

SISTEMI COMPOSITI TRM A BASE DI LINO PER IL RINFORZO DI MURATURE: DALLA CARATTERIZZAZIONE DEI MATERIALI AL COMPORTAMENTO STRUTTURALE

Autore

Giuseppe Ferrara

L'impiego di sistemi compositi a matrice cementizia TRM (Textile Reinforced Mortar) rappresenta, oggigiorno, una soluzione innovativa per il rinforzo di elementi strutturali in muratura, che si contraddistingue per la sua efficienza. Negli ultimi anni, per far fronte alla sempre più crescente esigenza di soluzioni sostenibili anche nel campo dell'edilizia, si è valutato l'impiego di fibre vegetali come elemento di rinforzo del composito, al posto delle più comuni fibre sintetiche ad alta resistenza. Sebbene promettenti, i risultati scientifici mettono in evidenza anche degli aspetti di debolezza di tale sistema di rinforzo, che ne frenano la diffusione nei campi applicativi. Al fine di incoraggiare l'impiego di sistemi compositi TRM a base di tessuti vegetali, il presente studio si propone di fornire una ampia ed esaustiva caratterizzazione meccanica di un sistema TRM a base di fibra di lino per il rinforzo strutturale di elementi in muratura. L'analisi parte dall'individuazione dei principali aspetti fisici e meccanici dei materiali che costituiscono il composito, ovvero il tessuto e la malta. In secondo luogo, si analizza il comportamento meccanico alla scala di investigazione del composito stesso, attraverso lo studio della resistenza a trazione dell'elemento TRM e della sua aderenza con un supporto in muratura. Successivamente, viene analizzata l'efficienza del sistema di rinforzo nell'incrementare la capacità tagliante di pannelli murari, attraverso prove sperimentali condotte alla scala strutturale. In ultimo, considerando le potenzialità del sistema, e in luce dei limiti evidenziati, vengono proposte ed applicate delle soluzioni tecniche volte a migliorarne la risposta meccanica, dimostrando che c'è ancora un ampio margine di miglioramento della performance meccanica, e delineando la linea da perseguire per ottimizzare quest'ultima.

Lo studio conferma il grande potenziale nell'uso di fibre vegetali all'interno di sistemi compositi TRM, mette in luce gli aspetti sui quali è necessario lavorare affinché se ne aumenti l'efficienza, e propone delle soluzioni tecniche innovative volte al miglioramento della risposta meccanica.

French abstract

Titre de la Thèse

RENFORCEMENT DES MAÇONNERIES PAR TRM A BASE DE FIBRES DE LIN : DE LA CARACTERISATION AU COMPORTEMENT STRUCTUREL

Auteur

Giuseppe Ferrara

L'utilisation de matériaux composites TRM (Textile Reinforced Mortar) représente aujourd'hui une technique innovante et efficace pour le renforcement des structures en maçonnerie. Au cours des dernières années, l'utilisation de fibres végétales dans le composite, en remplacement des fibres synthétiques à haute résistance, est apparu comme une solution efficace pour réduire l'impact environnemental du système de renforcement. Toutefois, il subsiste des doutes quant à l'utilisation de cette technique. Les études de la littérature scientifique mettent en évidence le grand potentiel de ce système, mais elles ne sont pas suffisamment exhaustives pour permettre une diffusion massive des systèmes TRM à base de fibres végétales.

Dans le but d'encourager l'utilisation de systèmes composites TRM à base de fibres naturelles, la présente recherche propose une étude de la caractérisation mécanique d'un système TRM à base de fibre lin pour le renforcement des éléments de maçonnerie. En premier lieux, les caractéristiques physiques et mécaniques des éléments constitutifs du composite, c'est-à-dire le tissu et la matrice, ont été déterminées. Dans un second temps, le comportement en traction du système TRM et l'étude de l'adhérence avec le support de maçonnerie ont été étudiés. La troisième étape vise à caractériser, à travers des essais à l'échelle structurelle, la contribution du système de renforcement à la résistance au cisaillement de murs en maçonnerie. Finalement, des solutions innovantes visant à améliorer les performances du système de renforcement à l'étude ont été proposées.

L'étude confirme le grand potentiel de l'utilisation des fibres végétales comme renforcement dans les systèmes composites TRM. Elle souligne les aspects sur lesquels il est nécessaire de se concentrer pour améliorer leur comportement mécanique et présente des solutions innovantes pour améliorer leur performance.

Contents

About the Author

Giuseppe Ferrara was born in Italy, in 1991. He received his B.Sc. and M.Sc. degrees, with 110/110 cum laude, in Civil Engineering from the University of Salerno, Italy, in 2013 and 2016, respectively. In the period June-August 2016 he was trainee at the Federal Institute for Materials Research and Testing (BAM) in Berlin, Germany, dealing with the study of Ultra-High performance fibre-reinforced concrete. In November 2016 he started a bi-nationally supervised Ph.D. course between the University of Salerno (Italy), at the Department of Civil Engineering – doctoral school in Risk and Sustainability in Civil, Architectural and Environmental Engineering (Cycle XXXII) – and the University Claude Bernard Lyon 1 (France), at the Laboratory of Composite Materials for Constructions (LMC^2) – doctoral school in Mechanic, Energetic, Civil Engineering and Acoustic (ED 162, MEGA). His research deals with composites materials for strengthening of masonry structures. He published some of the achieved results on International Journals and presented his work in several International Conferences.

1. Introduction

1.1 Motivation

The Mediterranean basin is characterised by a significant seismic hazard, due to geographic and morphological aspects. The many earthquakes events happened over centuries, have affected human activities with consequences in terms of safety, economy and sociology. Nowadays, although a deep and established knowledge of the problem, and available technologies to conceive civil structures able to cope successfully with earthquake actions, seismic events still represent an actual threat for human safety. This concern is mainly due to the presence on the territory of several structures the construction of which often dates way back before the establishment of designing principles and methods specifically conceived to address such seismic issues [1].

The majority of the historical city centres are characterised by old masonry buildings, conceived to face gravitational loads, but very often lacking in capacity to resist to the horizontal forces caused by seismic events. The seismic hazard, combined with a massive presence of vulnerable structures, confers to the area a high seismic risk, against which it is necessary to provide urgent solutions to guarantee at least the preservation of human life [2-3].

The increased awareness toward the preservation of our environment, represents nowadays an aspect of fundamental importance that affects more and more our society at every level. Ecological solutions are strongly recommended, and in some cases imposed, by ruling governments, in every production process of our community, with the aim to achieve, in a more or less far future, a circular economy system based on the use of renewable sources, recycling processes, and the reduction, as much as possible, and at any level, of the environmental impact.

In this framework, the field of the building materials is fully involved in such epoch-making phase of transition. Manufacturing companies, practitioners and scientific research groups are constantly looking for innovative solutions that may meet both mechanical and ecological requirements, giving rise to a new class of systems referred to as green building materials.

Inorganic matrix composites, consisting in high strength fibres embedded in cementitious or lime mortars (referred to as Textile Reinforced Mortar, TRM),

represents an innovative and efficient strengthening technique to enhance the capacity of structural elements, very suitable in the case of masonry buildings. With the aim of combining the aspects aforementioned, the research focuses on the study of a more sustainable TRM composite, and on the investigation of its efficiency as reinforcement of masonry structural elements.

The sustainability of the system lies in the use of plant fibres, instead of high strength synthetic ones. In fact, several plant fibres, such as hemp, flax, sisal, jute, coconut, curaua, etc…, already gained attention as reinforcement in composites in several fields (aeronautic, naval, automotive, etc…) thanks to several good properties, such as: availability, satisfactory mechanical characteristics, affordability, high resistance over density ratio, sustainability. In recent years few studies addressed the problem of the use of plant-based composites also in the building material field. The use of plant fibre-based textiles in TRM composites showed up as a very promising reinforcement system with a great potential, but still characterised by several issues that prevent their diffusion on the market in the same manner of most traditional synthetic-based composites. As a consequence, it is necessary to intensify the research in the field in order to deeply define the mechanical behaviour of such innovative composite systems, and to improve their efficiency according to the performance required in structural applications.

In order to comply with this need, the present study strives to provide a comprehensive investigation of an innovative sustainable plant based TRM system, i.e. Flax TRM, aiming at defining its mechanical behaviour, and at identifying its efficiency and limitations in strengthening of masonry structural elements.

In order to have the elements to deeply understand the behaviour of the system, the analysis starts from the investigation on a small scale of the composite constituent materials, to move until an experimental study on the structural element scale of investigation.

In addition, the issue of the durability of the composite was addressed as well, being the latter one of the main aspects that feed scepticism about the use of plant fibre-based composites.

Finally, the study aims at showing that there is still room for improvement with respect to the mechanical behaviour of plant based-TRMs, by proposing the application of some improving techniques conceived on the basis of the outcomes deriving from the reach multi-scale analysis proposed.

1.2 Contents and structure of the thesis

The thesis consists of the analysis of results deriving from experimental investigations carried out at different scales of study. From a small scale of investigation aimed at analysing the microstructure of flax fibres, passing through the assessment of the mechanical response of TRM composites, up to the study of masonry structural elements externally strengthened by Flax TRMs, the thesis provides a comprehensive identification of the behaviour of plant based composites.

Each chapter deals with a different scale of investigation. A critical analysis comparing the results at different scales of investigation is proposed as well. Finally, some modifications of the TRM components, aimed at improving the performance of the reinforcement, are experienced as conclusion of the work.

The structure of the thesis, with the main contents and outcomes of each section, are reported as follow:

- Chapter 1 presents the context of the research. It comprises the main contents and the aim of the thesis;
- Chapter 2 presents a review of the literature state of the art, concerning the topic of interest, is presented. Specifically, the main research outcomes available in the literature, are presented with respect to the of TRM composites as reinforcement systems in civil engineering, and with respect to the use of plant fibres in TRMs. The aims of the thesis are reported as well;
- Chapter 3 reports the outcomes of the investigation of the flax textile adopted in the research. It aims, by providing the main physical and mechanical properties of the textile, and its durability performance, at defining whether or not the fabric is suitable as reinforcement in mortar-based composites;
- Chapter 4 proposes the characterisation of the system on the composite scale of analysis. According to standardised procedures, and with respect to different reinforcement configurations proposed within the research, the composite mechanical behaviour was assessed by means of Flax TRM tensile tests, and by means of Flax TRM-to-masonry substrate systems shear bond tests. In addition, the issue of the durability of TRM elements was addressed as well;
- Chapter 5 deals with the assessment of the efficiency of Flax TRMs as external strengthening system of masonry structural elements to enhance their in-plane shear capacity. The results of the experimental study were discussed and compared with similar studies available in the literature, and with the model proposed by standard regulations;

- Chapter 6 proposes some observations concerning the displacement field of the TRM strengthened masonry walls subjected to diagonal compression tests, by compering such response with that exhibited by Flax TRM tested in tension;
- Chapter 7 comprises the application of innovative techniques aimed at improving the mechanical performance of Flax TRMs. The aim is to show that there is still room for improvement in the performance of plant based TRMs employed as reinforcement of structural elements, and that such enhancement of performance is easily achievable by means of available technical solutions;
- Chapter 8 shows the main outcomes and the perspectives of the research study.

1.3 Context of the research

The study is the result of a Ph.D. scholarship awarded by the Italian Ministry for Education, University and Research (MIUR) as part of the programme "Dottorati Innovativi a caratterizzazione industriale" financed by the European Union (Structural Funding ERDF-ESF for "Research and Innovation" 2014-2020).

The Ph.D. project, carried out at the Doctoral school "Risk and Sustainability in Civil, Architecture and Environmental Engineering Systems" (Department of Civil Engineering of University of Salerno), included a collaboration with the company Engineering s.r.l. (Avellino, Italy), and with the Laboratory of Composite Materials for Construction, LMC2 (University Claude Bernard Lyon 1, France).

The collaboration with the French institution was strengthened by means of bi-nationally supervised Ph.D. thesis collaboration agreement between University of Salerno and University Claude Bernard Lyon 1, that entailed the enrolment of the Ph.D. student also to the Doctoral school "Mechanic, Energetic, Civil Engineering, Acoustic" (ED 162, MEGA) of University Claude Bernard Lyon 1 (France). Therefore, the Ph.D. research was developed at both the institution partners in the collaboration agreement.

The large experimental plan pursued in the research study, includes several investigations at different scale of analysis, and with respect to several aspects, such as mechanical, physical and chemical. It required, therefore, many instrumentations and appropriate expertise to be properly executed. In addition to the Ph.D. candidate institutions, a collaboration with external institutions was established as well. The main contribution of each institution is reported below.

Ph.D. candidate institutions:

- the Structural Engineering Testing Hall, Str.Eng.T.H. laboratory (Department of Civil Engineering of University of Salerno, Italy): a laboratory with expertise in the characterisation of the mechanical behaviour of civil engineering structures. Within the laboratory, to which the Ph.D. candidate is affiliated, the mechanical characterisation of the Flax TRM composite was carried out;
- the Laboratory of Composite Materials for Construction, LMC2 (University Claude Bernard Lyon 1, France): a laboratory with expertise in the field of composite systems for application in civil engineering structures. Within the laboratory, to which the Ph.D. candidate is affiliated, the analysis concerning the interaction between the composite and the masonry, and the structural investigation of masonry externally strengthened by Flax TRMs, were carried out;

External institutions:

- the Industrial Engineering Department of University of Salerno, Italy: a structure with expertise in the physical, mechanical and chemical characterisation of materials. The collaboration concerned the physical and mechanical characterisation of the flax textile adopted within the study. Moreover, the institution provided the chemical equipment and expertise necessary to carry out the durability tests;
- the Centre of Sustainable Materials and Technologies, NUMATS (COPPE-Federal University of Rio de Janeiro, Brazil): a laboratory with expertise in the study of sustainable materials and solution in the construction field. At the laboratory, within a three months research stay, the application of technologies to improve the mechanical performance of Flax TRMs, was carried out;
- the company Engineering s.r.l. (Avellino, Italy): within the company, which operates in the field of structural diagnostic of existing constructions, a six months internship provided an overview of the fields of application in which it is possible to concretely apply the results of the research.

2. State of the art review and aims of the thesis

Through the ages, the Mediterranean basin was interested by earthquakes events considered among the most destructive natural hazards, if not to the human life itself, then more likely to the works of man. The region, densely populated since ancient times, is characterised by historical buildings created using traditional construction techniques, hence not specifically designed to bear earthquake actions [1]. Most of these constructions, especially in the centres of old towns, consists of masonry structures, typically characterised by significant capacity towards gravity loads, but not always capable to resist horizontal loads applied both in-plane or out-of-plane. Typical collapse mechanisms observed as a result of catastrophic seismic events were out-of-plane failures due to poorly connected crossing walls or lack of connection of non-structural hollow clay tile walls, and in-plane failure mainly due to a lack in shear capacity, especially in presence of window or door openings [2, 3]. It is therefore essential to implement efficient strategies aimed at reducing the vulnerability of existing buildings in order to lower the seismic risk. Several retrofitting techniques were developed over the years aimed at conferring to the entire building a global response in accordance with the safety performances proposed by the standards.

The concept of seismic retrofitting is based on two main approaches: the first one aims at reducing the earthquake "demand" on the structure, the other one aims at increasing the "capacity" of the building [4]. Different retrofitting solutions may be chosen by adopting one of the two approaches, or by combining them, generally depending on the construction typology, structural scheme and the specific use of the building. With respect to the first approach, the reduction of the seismic demand of the building can be achieved by implementing measures specifically designed to optimise its structural dynamic behaviour. Building base isolation, installation of dumper devices and remodulation of the mass distribution are possible retrofitting techniques falling within this category. With respect to the second approach several solutions are nowadays available to upgrade the individual element strength: confinement/jacketing techniques; addition of thin surface treatments (shotcrete, coatings, grouted steel bars); repointing; internal reinforcement (typically by means of steel bars inserted within masonry); tying; grout injections, filling in door or window openings. The use of these techniques, also defined as traditional retrofitting

interventions, is well-established and is largely adopted for retrofitting of masonry elements. In the last decades innovative techniques were developed to enhance the strength of structural elements by using composite materials. The so called Fibre Reinforced Polymer (FRP) composite systems, thanks to the employment of high performance fibres, are considered a viable solution to solve, or lessen, the effects of overloading. FRP systems in the form of laminates or rods consist of long fibres embedded in polymeric matrices. High strength fibres, such as carbon, glass, aramid, PBO or basalt, are typically adopted. The success in the use of such innovative retrofitting systems mainly lies in their tailorable performance characteristics, ease of application and low life cycle costs together with high strength-to-weight and stiffness-to-weight ratios [5]. Although resulting particularly suitable in concrete structural applications, FRP systems showed some drawbacks when applied to masonry elements. The non-permeable nature of the polymeric resins, and a strength much higher than that one of the substrates on which FRP are applied, may create a problem of compatibility between the composite and the masonry. Moreover, they are characterised by lack of ductility, susceptibility to fire, and installation problems related to the process of thermosetting adhesive being moisture and temperature dependent, and to the toxicity of the resin that requiring specialised workers [6]. To overcome such issues during the last years inorganic-matrix composite systems were developed by embedding high strength fibres in cement or lime-based mortars rather than within polymeric resins. Such innovative materials, herein defined as Textile Reinforced Mortar (TRM) composite systems, result particularly suitable as reinforcement of masonry elements, and besides, they do not present some drawbacks typical of FRPs such as low fire resistance and toxicity nature of the resins [7].

2.1 Textile Reinforced Mortar Composite Systems

Textile Reinforced Mortar composite systems, hereinafter referred to as TRMs, consist of high strength long fibres embedded in inorganic matrices, cement- or lime-based mortars, as creating laminates capable to significantly improve the strength of the structural elements on which they are applied. Several acronyms were adopted in literature to define the same kind of inorganic-matrix composite system, such as Fabric Reinforced Cementitious Matrix, FRCM; Textile Reinforced Concrete, TRC; Cementitious Matrix Grid, CMG; Inorganic Matrix Grid, IMG; Composite Reinforced Mortar, CRM [8].

TRMs represent an innovative reinforcement technique particularly suitable for applications to masonry elements, in respect of which they are preferred to the

FRPs. The latter, due to a high specific strength, are often implemented in the form of strip laminates that once applied on masonry surfaces create significant concentration of stress on the substrate typically characterised by a low adhesion capacity. The use of mortar, characterised by fine aggregates, entails the necessity to use fabrics arranged with less dense meshes. As a consequence, TRMs are typically applied all over the masonry elements, allowing a more uniform distribution of the stress on the substrate. Moreover, the affinity between the material employed and the masonry, and their permeability, make TRMs more compatible to masonry substrate with respect to FRPs [9].

TRMs are characterised by good mechanical performance, reversibility and versatility of the intervention, and they offer the possibility to perform several different solutions by choosing between several types of fabric and mortar available on the market. In the light of these considerations, they are considered an effective, practical and cost-efficient solution for the seismic retrofitting and repair of structures. The use of TRMs significantly increased in recent years with numerous applications in civil engineering field as strengthening of existing masonry element.

In the last decade TRM systems were more and more proposed and developed as externally bonded reinforcements with several applications to cultural heritage after significant earthquake events such as “L’Aquila 2009” and “Emilia 2012” [10]. Masonry vaults were strengthened by applying TRMs in order to provide a structural stability of the element also when subjected to significant horizontal actions. The composite can be applied, below and over the vaults, in the form of strips to improve the strength of more stressed specific sections, or all over the vault surface when bidirectional oriented fabrics are adopted (Figure 2.1).

a)  b) 

Figure 2.1: Extrados retrofitting of masonry vaults by applying: a) TRM strips; b)TRM all over the surface [10].

Masonry walls were reinforced by applying all over the surface TRMs in order to improve both the in-plane and the out-of-plane capacity of the element (Figure 2.2a). In some applications the upgrading intervention by means of TRM was integrated by steel plates to guarantee a correct anchorage and post-tensioning of the composite strip (Figure 2.2b).

a)  b) 

Figure 2.2: a) Reinforcement of a masonry wall by means of TRMs; b) TRM-steel mixed intervention to upgrade a masonry element capacity [10].

Since their emergence in the market, TRMs suddenly became a very popular solution, even though there were still a lack of knowledge with respect to mechanical performance and durability of such composite systems. In order to cover this gap, and to encourage an aware use of composites in the rehabilitation of cultural heritage, several researches focused their attention on the investigation of the mechanical behaviour of TRM systems. Scientific committees were created with the aim of providing guidelines on qualification, installation, design and control, which represent crucial aspects for the effectiveness of the strengthening work.

2.1.1 TRM characterisation tests

Several kinds of fibres can be adopted to create TRMs by embedding them in cement, lime or geopolymer mortar matrices, possibly enriched with short fibres and/or polymeric additives. Carbon, glass, basalt and PBO fibres are commonly adopted because of their mechanical features such as high rupture stress, high stiffness, very low weight and linear elastic behaviour up to failure. The combination of these materials and the possibility to choose the best suited geometry, make it possible to produce a large variety of TRMs depending on the need of the specific case of application. This wide choice necessarily entails a significant variability of the mechanical properties that this reinforcement technique can offer. It is necessary, therefore, to standardize the qualification procedures and to define the best

characterisation methods in order to provide a valuable support for both producers and practitioners in the material selection and/or design. The scientific community focused great attention on the understanding, hence the improvement, of TRMs mechanical behaviour with the aim of providing the necessary tools for the correct designing of technical interventions by using such composite systems.

2.1.1.1 Tensile Test

Although the elements reinforced by TRMs are generally subjected to several load conditions (such as compression, bending moments, shear, etc…), the composite itself is meant to exhibit its strength in tension. Therefore, the qualification procedure includes direct tensile tests to derive the basic material mechanical properties [11]. TRM coupons rectangular in shape, are tested in tension monotonically, in displacement control, up to the failure of the composite. The mechanical response, strongly depends on the specimens' geometry, the test set-up and the monitoring technique employed to derive the mechanical parameters. A scientific technical committee, RILEM TC 232-TDT, was specifically organised with the aim of providing recommendations concerning the test method to determine the load bearing behaviour of tensile specimens made of textile reinforced concrete [12]. The document represented a valid reference both for researchers and practitioners to reproduce a standardised qualification procedure in order to obtain reliable results, comparable with similar experimental activities.

The specimens to test in tension are usually sandwich-type, performed by applying several layers of mortars, 3÷5 mm thick, alternate with textile plies. The thickness of the specimens varies between 6 and 20 mm, the width between 40 and 80 mm and the length between 400 and 600 mm. Specimens are cured in ambient conditions for a period generally considered of 28 days, due to the use of cementitious- or lime-based mortars whose characteristic mechanical properties are computed at that time [13, 14].

The specimens include two gripping areas at the edges, through which the load is applied to the specimen, followed by a transition zone in proximity to the clamping system and a measurement range in the middle (Figure 2.3). Strains are registered by means of strain gauges and/or are derived by LVDT measurements. Due to developments of cracks along the free length of the specimens, displacement and strain transducers should be accurately placed along such distance, close enough to each other so that a large number of them is within the base length. The use of Digital Image Correlation (DIC) analysis, integrated with traditional devices, may provide useful information concerning the strain and displacement field of the specimen

external surface, hence an accurate analysis of the crack pattern within the matrix [15].

The typical tensile stress-strain behaviour of TRM systems is characterised by a response in which three stages can be identified (Figure 2.4). In the Stage I the mortar is uncracked, and the response is linear elastic up to the achievement of the tensile strength of the matrix in correspondence of which a first crack appears in the matrix. In this phase the tensile modulus of elasticity, E_I, can be estimated referring to a homogeneous cross section with the assumption of a perfect matrix-to-textile bond. The transition point between the first and the second Stages is identified by the couple of values σ_I and ε_I. The higher are the strength of the mortar and the bond capacity at the matrix-to-textile interface, the higher is the stress σ_I.

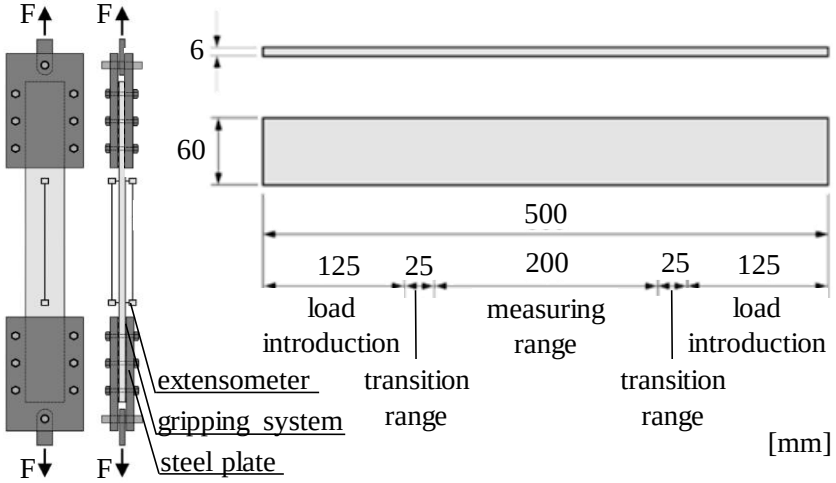

Figure 2.3: Specimen typical geometry and test set-up [12].

Multiple cracking of the mortar is assuming to occur during the Stage II. Generally, the development of a cracks within the matrix leads to a load drop whose significance mainly depends on the ratio between the mortar and the dry textile tensile stiffness and on the bond behaviour at the matrix-to-textile interface. The response curve in this stage may often result uneven due to the crack pattern occurred, therefore the stiffness E_{II} can be derived by a linear interpolation in a suitable range of data. It is important, to this purpose, that the strain and/or displacement recorded during the tests are referred to a measuring range long enough to include a sufficient number of cracks being representative of the mechanical behaviour of the system. Several aspects influence the form and the number of the cracks, such as the grid spacing of the textile, the interlocking behaviour between

textile and mortar, the boundary conditions reproduced during the test, the amount of textile reinforcement, the specimen length.

Once the crack pattern has completely developed, transition point II, a nearly linear and stiffer response is observed. This phase, named as Stage III, is characterised by a widening of the existing cracks with no developments of further other ones. In the Stage III the stiffness of the composite relies on those of the dry textile and so assumes values similar to the one of the fabric alone tested in tension. In the case of a failure mode characterised by the tensile failure of the textile yarns, the bearing capacity of the composite in terms of stress assumes values close to the tensile strength of the dry textile [16].

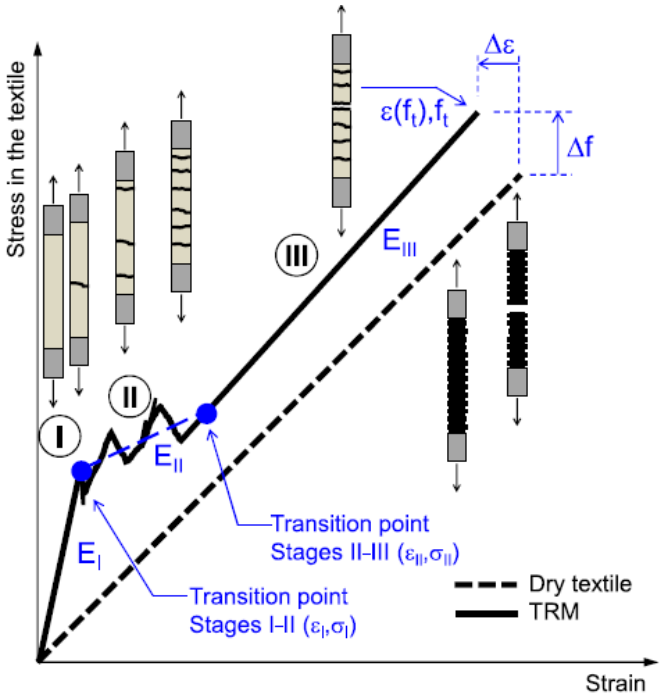

Figure 2.4: TRM typical tensile response [16].

The three stages in the TRM tensile response may be more or less identifiable according to the volume fraction and the stiffness of the textile adopted. TRM designed with relatively low reinforcement volume ratio may end up in a mechanical response characterised by Stage III showing zero strain-hardening behaviour. Conversely, Stage III mainly governs the response of TRMs characterised by relatively high-volume fraction of a stiff textile. In the case of significantly dense fabrics combined to weak and deformable matrices, the first two stages even become hardly identifiable [17]. Considering the poor tensile strength of cementitious

matrices, and the environmental conditions to which TRM systems are exposed during their service life, is it reasonable to think the composite system to work in a cracked configuration. It is, therefore, fundamental to choose a proper amount of textile reinforcement when designing a TRM system.

The failure mode concerning TRM coupons in direct tensile tests may occur due to rupture of the textile in proximity of the gripping area, due to rupture of the textile in a section included within the measurement range or due to slippage of the textile within the mortar (Figure 2.5). The type of failure mode is strictly related to the boundary conditions reproduced during the test, hence the gripping system adopted. If a lateral pressure is applied on the gripping area (clamping method) the compressive stress transferred to the coupon hinder the textile to slip within the matrix in the gripping area during the test. This method induces a failure mode characterised by the rupture of the textile. If the lateral pressure is insufficient, or absent by choice (clevis method), the tensile stresses are transferred from the machine to the specimen only by means of resins glued between the steel tabs and the TRM element, and, depending on the length of the gripping area, the textile tensile strength, and the bond at the textile-to-matrix interface, the failure may occur with a slippage of the textile within the gripping area. In the case of the clamping method, in order to avoid premature failure within the transition range due to crushing of the mortar due to the lateral compression, the TRM element may be stiffened by applying FRP strips within the gripping area [18, 19].

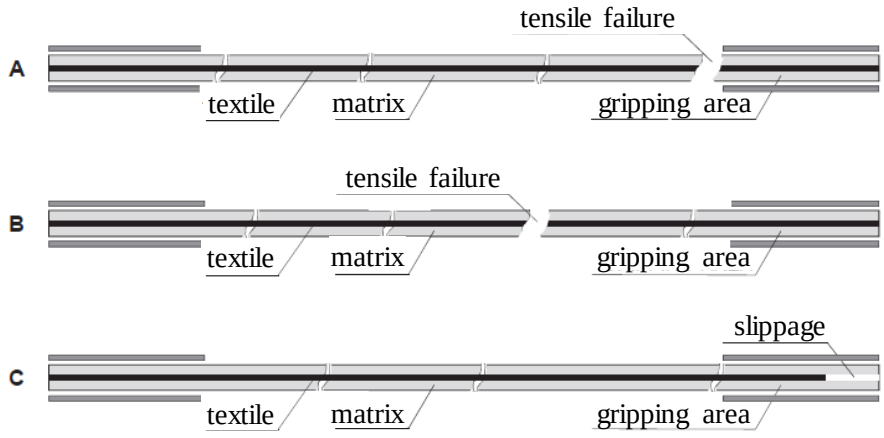

Figure 2.5: Classification of TRM failure modes in direct tensile test [16].

With the aim of providing a solid database concerning the mechanical response of different TRMs subjected to direct tensile test, several research groups carried out round robin tests comparing the results deriving from different

laboratories. The most common and efficient high-strength fibre textiles available in the market were considered during such tests, i.e. carbon [20], steel [21], glass [22], basalt [23] and PBO [24] fibres. The tests showed in almost all the cases the typical trilinear behaviour. When glass fibres were adopted the TRM specimens exhibited a response without a clear Stage II, showing in some cases the development of a single crack. The clamping method test set up resulted the most suitable, able to guarantee almost in all the studies an entire exploitation of the fibres' strength with a failure mode characterised by textile rupture. As PBO fabrics were adopted the most common failure mode occurred consisted in a slippage of the textile within the mortar. Such behaviour highlighted a poor bond capacity with inorganic matrices of such material, with respect to its tensile strength. The increase of fibre amount obtained by overlapping more textile plies leads to higher tensile loads, however, in terms of stress a loss of efficiency may occur with a reduction of the textile exploitation due to a reduction of the bond between textile and matrix [25, 26]. The use of fabrics treated by means of coating specifically designed to improve the bond with matrix (based on the use of epoxy resins and quartz sands) may lead to higher ultimate tensile strength of the TRM and to a stiffer behaviour in the cracked stage [26].

Significant designing parameters may be derived from the direct tensile test: with respect to the Service Limit State, the crack spacing and the stress of the first crack (σ_I) may be assumed as important designing parameters; with respect to the Ultimate Limit State the Stage III stiffness, and ultimate stress and strain are fundamental parameters in such applications in which the tensile capacity of the TRM may be fully exploited [16].

2.1.1.2 Shear Bond Test

TRMs are conceived as an external reinforcement of structural elements (herein masonry), hence it is necessary to consider the nature of the substrate on which they are applied to get a proper identification of the system efficiency. When the substrate gets deformed it transfers the stresses to the TRM matrix. The composite, subjected to tension, develops cracks, and in proximity of the cracks the load can be assumed to be completely borne by the textile. In such configuration, restrained by the masonry substrate, and by the stretched textile, the TRM-to-masonry system is submitted to shear loads. The shear bond test, performed on specimens characterised by a TRM strip applied on a masonry substrate, reproduces such loading conditions, and it represents, therefore, a necessary test in order to obtain an exhaustive qualification of the TRM-to-substrate system.

The assessment of the shear bond behaviour is a fundamental aspect to define, as it is the weakest mechanical phenomena, conditioning the type of failure mode, among a debonding at the TRM-to-substrate or textile-to-mortar interface bond loss and a tensile failure of the textile. It is worth emphasising that any premature bond failure, not involving the rupture of the textile, may be a solution poorly optimised since the fibres often represent the most expensive component of the reinforcing system [13].

Several test set-up configurations were devised in order to reproduce the actual shear bond conditions existing in real applications: single-lap or double-lap configuration, respectively for the TRM strip applied on one or both the sides of the masonry block; with one prism or two symmetric prisms, respectively if the reinforcement is applied on one block or on two blocks symmetrically pulled [26-28]. Generally, the substrate is characterised by masonry prisms, but in some cases individual masonry blocks are adopted [29-30]. Comparison between the double-lap/double-prisms test configurations and the single-lap one showed that the different test set-up led to the same mechanical response up to the peak load, but double-lap configurations failed to retain symmetric debonding on both the sides. Due to the randomness of this last aspect, and to the easier reproducibility of the test, single-shear lap test is preferred to study the bond behaviour of TRM-to-masonry systems [31].

The RILEM Technical Committee 250-CSM was created with the aim of providing recommendations to standardise the test method for the TRM-to-substrate bond characterisation [32]. The geometry of the specimen and the test set-up are shown in Figure 2.6. The textile is partially left unbonded, clamped by using steel plates and pulled by means of the testing machine. The specimen has to be correctly arranged so that the masonry block remain locked during the test. The textile should be be perfectly in line with the TRM axis to ensure that a pure shear stress is applied to the TRM-to-substrate system. Any possible eccentricity may lead to a mixed failure mode in which both normal and shear stress develop. The test is carried out in displacement control and the relative displacement between the reinforcement and the substrate in correspondence to the loaded end is recorded by means of LVDTs and by a steel element connected to the textile [16]. This solution proves efficiency in recording the slipping of the textile within the matrix. However, in the post peak phase, and in case of a failure mode including fibres rupture, the displacement data recorded may be inaccurate.

Several shear bond failure mode may be identified: loss of cohesion due to either shear failure within the substrate (mode A) or at the TRM-to-substrate interface (mode B); detachment of the textile with the outer layer of mortar (mode

C); sliding of the textile within the matrix (mode D) and textile rupture either out (mode E1) or within the mortar (mode E2) (Figure 2.7).

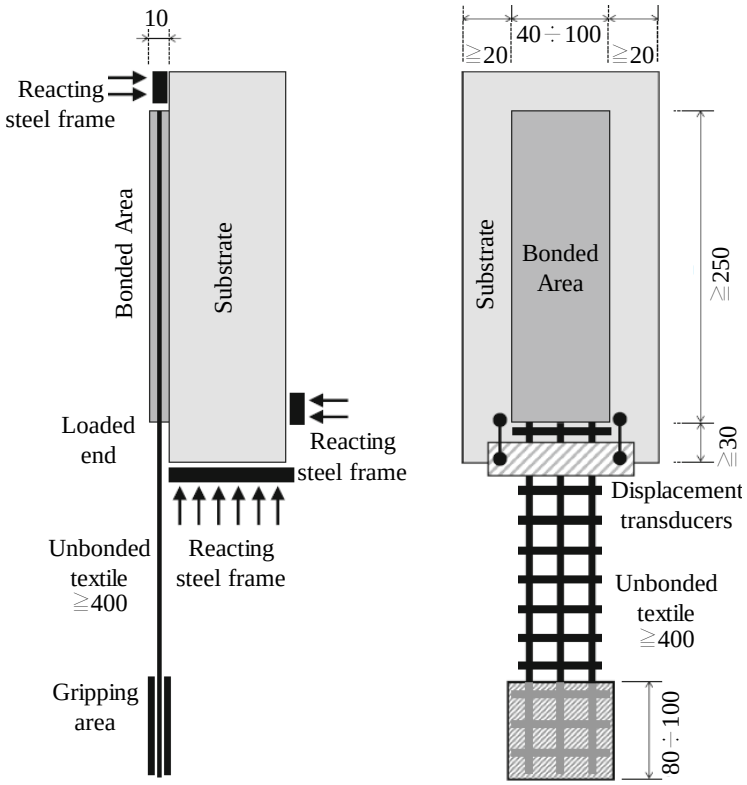

Figure 2.6:Single-Lap Shear bond test set-up [32].

The cohesive failure at the TRM to substrate interface depends on the shear properties of the substrate and the adherence between mortar and masonry. The abrupt detachment of the outer layer of mortar at the textile-to-mortar interface generally occurs when dense fabrics are employed inhibiting a proper protrusion of matrix through the voids. Failure modes A, B and C are characterised by a shear-slip curve with a brittle load drop, generally with short displacement values in the modes B and C (Figure 2.8a).

Failure mode D occurs when the composite is characterised by weak textile-to-matrix bond. This aspect depends on the mechanical properties of both the mortar and the fibres, the arrangement of the fabric and the geometry of the single threads. In this case the stress-slip response is characterised by a post-peak load decrease due to the progressive loss of adherence of the textile within the mortar due to the advancement of the slippage (Figure 2.8 b). When such behaviour occurs, it is

possible to improve the shear bond performance by means of fibres treatment (coating) specifically designed to improve the textile-to-mortar adherence [33].

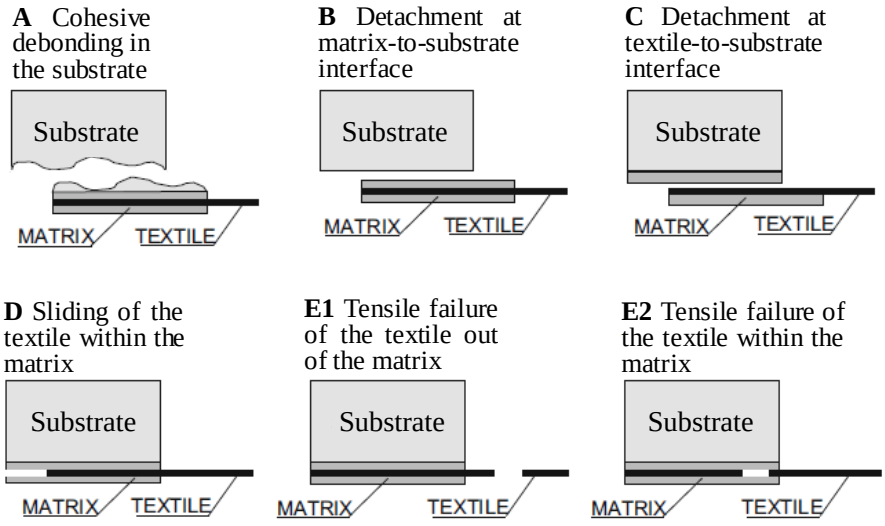

Figure 2.7: Classification of TRM failure modes in Single-Lap Shear test [32].

Failure mode E may occur in case of TRM systems characterised by textiles with poor tensile strength with respect to the textile-to-mortar bond. The consequent stress-slip response is characterised by instantaneous drops of the load corresponding to the rupture of the textile bundles (Figure 2.8 c). A non-uniform distribution of the stress over the different textile threads, due - for example - to fabrics characterised by relatively sparse meshes, may contribute to the occurring of this mechanical behaviour.

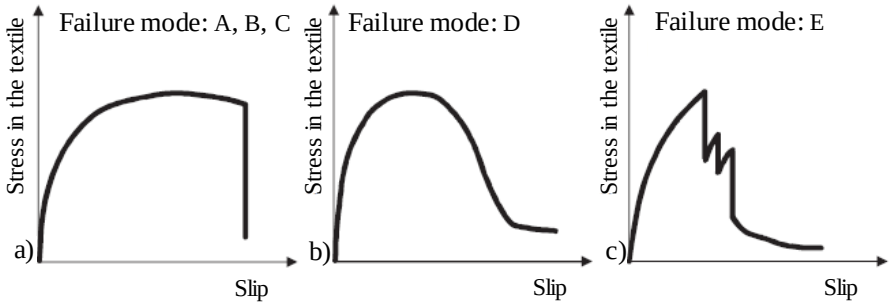

Figure 2.8: Typical textile stress-slip curves observed in Single-Lap Shear bond tests on externally bonded TRMs related to failure modes: a) A, B, C; b) D; c) E [11].

Whether the failure is due to loss of textile-to-matrix bond or to the textile rupture, the TRM system should be properly designed taking into account the type of failure mode in order to avoid unexpected premature collapse in the applications.

Round robin tests were carried out to compare the shear bond response of TRM-to-masonry systems performed in different laboratories by using the most common high strength fibres, such as carbon, steel, glass [22], basalt and PBO fibres. Several failure modes were observed. In the case of steel fibres an exploitation ratio up to 94% led to cohesive failure modes in the substrate [20]. The failure mode characterised by slipping of the fibres within the mortar was observed in several cases where the smooth surface of the threads is combined with low strength mortars [21-23]. The use of PBO textiles often led to the rupture of the fibres along the free length of the specimens, and damage within either the matrix or the substrate was observed [24]. It was in general observed that the matrix-textile bond capacity plays a key role in the mechanical response of the system. Specifically, it is affected by the textile geometry, treatment of yarn (coating or impregnation), mesh size and the capability of the matrix to penetrate in the core filaments of the yarns. Specimens constructed by using fibres of the same nature, but differing in these parameters, may end up in failure mode and exploitation ratio significantly different.

It is necessary, in order to get an exhaustive characterisation of the TRM system, to carry out both tensile and shear bond tests: the first one provides the maximum strength that the composite can exhibit in tension, the second one takes into account any possible debonding phenomena that prevent such maximum capacity to be achieved. It is possible, therefore, to combine the results of both the tests to get designing parameters: the maximum stress and strain can be derived from the tensile response by superiorly limiting the stress at the maximum value achieved in the shear bond test (Figure 2.9) [13].

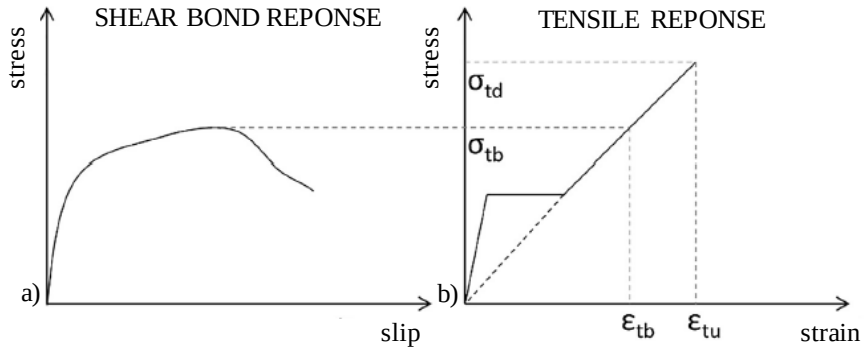

Figure 2.9:Definition of the maximum bond stress (a) and strain (b) of TRM systems [13].

This qualification method is suitable in case the maximum stress of the shear bond curve corresponds to a point included in the stage III of the tensile test response. Besides, it is worth emphasising that when TRM-to-masonry specimens fail in shear bond test due to a rupture of the textile along the free length, the maximum shear stress generally coincides with the maximum one observed in tensile test.

2.1.2 Diagonal compression test

Tensile and shear bond represent easy reproducible tests to characterise, on a local scale, the mechanical behaviour of the composite itself and of the TRM-to-masonry system. However, it is necessary to carry out mechanical tests on larger scales of analysis in order to investigate the efficiency of the external reinforcement by TRMs on actual masonry structural elements, and to verify that qualification tests on smaller scales are enough to predict such behaviour. Depending on the load conditions to reproduce, several tests may be carried out on unreinforced and reinforced masonry elements to assess the contribution of TRMs. Masonry column were tested in compression to study the efficiency of TRM confinement [34]. In-plane capacity of masonry elements externally strengthened by TRM can be assessed by shear or bending tests [35]. Out-of-plane bending test can be carried out to reproduce the collapse that may develop as overturning, vertical flexural failure or horizontal flexural failure [36, 37].

One of the aspects of crucial importance, especially for strengthening of masonry elements toward seismic actions, is the in-plane shear capacity. Shear strength can be assessed by means of cyclic or static direct shear tests or by means of diagonal compression tests. The latter, due to the loading configuration, induces a failure mode of diagonal cracking in a stepwise form along bed and head joints or crossing masonry units. Due to the reproducibility and the reliability of the results, diagonal compression tests were often adopted to mechanically characterise the efficiency of the masonry strengthening by means of TRM systems in various types of specimens, such as two and single leaf walls, with bricks of tuff volcanic elements and by using various TRM systems differing in the geometry, nature of mortar and textile [8].

Diagonal compression (or tension/or shear) tests are typically carried out on 1.2 m x 1.2 m masonry assemblages loaded in compression along one diagonal, thus causing a diagonal tension failure with specimen splitting apart perpendicular to the direction of the load (Figure 2.10). The test set up and procedure is described in the standard ASTM E519-2 [38]. The shortening of the loaded (typically vertical) diagonal and the lengthening of the other diagonal (typical horizontal) are recorded during the test by means of specific instrumentation. On the basis of such

displacements, combined with the applied load values, the maximum shear strength, strain and stiffness in the middle of the panel can be computed.

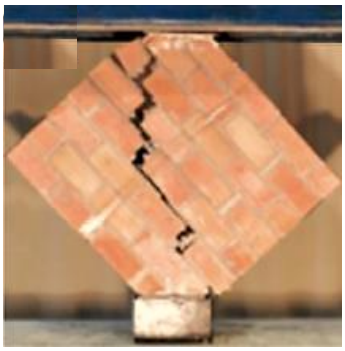

Figure 2.10: Clay brick wall subjected to diagonal compression test [8].

A large number of parameters strongly affect the effectiveness of TRM systems in enhancing the in-plane shear capacity masonry panels, such as geometric and mechanical properties of the matrix and mesh reinforcement, the presence of mechanical anchors, the properties of the masonry substrate. It was observed that the mechanical properties of the TRM matrix strongly affect the peak capacity of the panels. Moreover, the axial stiffness of the mesh reinforcement affects the peak capacity: when TRMs characterised by low axial stiffness textiles were adopted a smaller capacity increase was achieved with respect to those with higher axial stiffness [8]. In all cases, the reinforcing textile seemed to play a significant role in the inelastic post-peak behaviour, and even where the reinforcement was not sufficient to provide any increase of strength capacity, it seemed to enhance efficiently the displacement capacity [13].

2.1.3 Durability

Significant efforts were carried out by the scientific community to provide information about the mechanical behaviour of TRM systems and of their applications on structural elements. However, most of the study available in literature concerning such strengthening technique are pertinent with its short-term performance. Although being important to find increasingly better performing solutions, it is equally fundamental to verify that the reinforcing intervention preserve its effectiveness in time and under in-service conditions. Thus, it appears necessary to experimentally assess the long-term structural efficiency of TRM-strengthened masonry elements under various environmental exposure conditions.

Different approaches may be adopted to investigate the TRM durability performance. In some studies, the issue was addressed by ageing the reinforcing

textile, exposing it to specific conditions, taking care of reproducing the environment created by the mortar [39, 40]. Micelli and Aiello showed that glass and basalt fibres are highly sensitive to alkaline environments, while steel and carbon textiles are less susceptible to that environment (Figure 2.11). Moreover, it was highlighted that the alkalinity of the environment cannot be related to the pH value of the solution in which the fibres are immersed alone, but it should be ensured that the solution contains chemical components able to reflect the real service conditions created by mortars, i.e. lime- or cement-based. The temperature represents an important parameter to reproduce accelerated ageing processes, however, further investigations are needed to accurately correlate the accelerated protocols with the actual mortar environmental conditions [41].

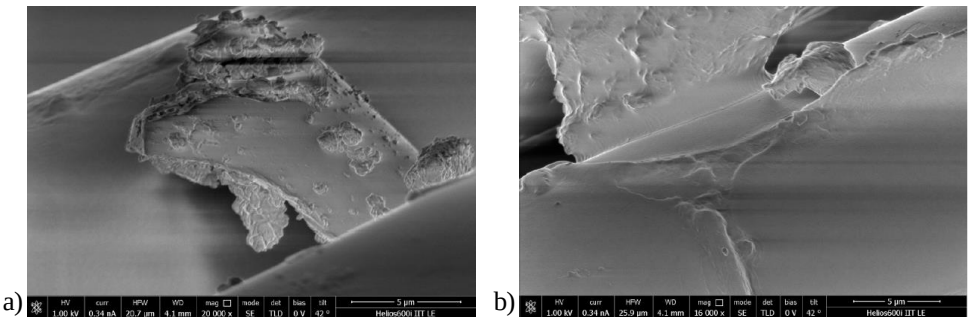

Figure 2.11: Glass fibre deterioration through a) the surface and b) the thickness due to exposure to alkaline environment [41].

Another approach consists in assessing the decay of properties in the time directly on TRM coupons aged in specific environmental conditions and then subjected to direct tensile tests [42, 43]. In order to get an exhaustive evaluation of the durability performance of TRM composites, the specimens may be immersed, for a time of 1000 h, in alkaline (sodium bicarbonate solution with a pH level of 10), saline (3.5% sodium chloride solution) and water solutions at a temperature of 23 °C [44]. Moreover, in order to reflect the temperature changes to which TRMs are subjected in service conditions, freeze-thaw cycles were reproduced by alternating periods of 12 hours at constant temperature of 37.7 °C to period of 4 hours at -18 °C. Durability protocols represent an efficient solution to analyse the TRM ageing processes, and so to propose and verify solutions to improve the long-term efficiency of the reinforcing system. However, aggressive environments may significantly reduce the design limits and so they should be carefully considered [45]. On the other hand, ageing protocols at environmental temperature do not allow to assess the long-term durability of the composite. More elaborated protocols, perhaps by adopting

higher temperatures to reproduce accelerated ageing conditions, would be needed to define the decay of the mechanical performance of TRMs in the time.

Some studies focused their attention on the efficiency of TRMs when submitted to high temperatures [46-51]. It was observed that textile coating treatments can improve the high-temperature performance of the system delaying the deterioration of the fibres [52]. However, such types of treatment should be specifically designed to this purpose: inappropriate coating treatments may lead to even worse performances with respect to untreated fibre based TRMs by causing a loss of adherence at the textile-to-mortar interface [53].

As well as for the short-term mechanical response, also in the case of the durability assessment it is important to analyse the entire TRM-to-masonry system to take into account any ageing phenomena involving the substrate. To this purpose masonry block specimens reinforced by TRM strips were subjected to shear bond test after being exposed to ageing protocols: such as immersion in water and salt solutions, and/or subject to wet-dry cycles. Franzoni et al. proposed an ageing protocol that produced a realistic salt accumulation in the specimens. By analysing a steel-TRM-to-masonry system, it was showed a limited effect of sulfate exposure on the stress-transfer mechanism between the composite and masonry highlighting the good efficiency of the reinforcement under the analysed exposure environment [54]. Glass-TRM-to-masonry elements showed a significant change in the mechanical response after different environmental exposures: the short term response was characterised by a failure mode with a slipping of the textile within the mortar; specimens immersed in salt solution experienced a rupture of the fibres in the free length; specimens subjected to wet-dry cycling were characterised by a debonding crisis at the TRM-to-masonry interface [55].

Although pioneering studies showed various solutions to study the durability of TRM systems, further efforts are required to better define the efficiency of the proposed ageing protocols, and to deeply understand the long-term mechanical response of the composite. To this purpose the technical committee RILEM TC IMC was recently created with the aim of clarifying scientific aspects concerning the strengthening of existing masonry structures with TRM materials, particularly focusing on those aspects related to durability and structural reliability in the long-term [56].

2.1.4 Codes and guidelines

Ever since they appeared on the market, TRM composites immediately gained great interest from practitioners finding increased application in interventions of reinforcement of masonry structures. Therefore, it became necessary to implementat

guidelines and acceptance criteria as support of the materials' qualification and of the strengthening interventions design. The aim of this paragraph is to provide an overview of the main specifications required by standards and recommendations available today concerning the use of TRMs.

The AC434, acceptance criteria for masonry and concrete strengthening using Fabric-Reinforced cementitious Matrix composites (FRCM, herein referred to as TRM), were developed in the US with aim of providing guidelines for the evaluation of such innovative strengthening method where the codes did not provide yet requirements for testing and determination of structural capacity, reliability and serviceability of these products [57]. Within the document a FRCM is defined as "a composite material consisting of a sequence of one or more layers of cement-based matrix reinforced with fibres in the form of open grid (mesh). When adhered to concrete or masonry structural members, they form an FRCM system". The document provides an overview of the mechanical tests needed to characterise TRM systems. Characterisation tests are needed on the components of the composite system, such as mortar and textile mesh. Moreover, it is suggested to carry out tensile tests to be conducted on coupons cut from TRM panels laid up using a procedure similar to that in the actual in-service applications. In addition, in order to define the bond strength, it is mentioned to carry out tensile bond tests on TRM systems applied onto substrates in accordance with the applicant's instructions. An overview of the test methods to investigate the structural performance of TRM reinforced elements is provided as well, such as wall flexural tests, wall shear tests, columns axial and flexural tests. With respect to the characterisation of the mechanical performance of TRM systems, the document provides a general comprehensive approach rather than detailed specifications. Conversely, as regard the durability aspects, ageing protocols and conditions of acceptance are described in detail. According to the document specimens should be conditioned for one week in humidity chamber, then subjected to twenty freeze-thaw cycles, each one consisting in a minimum of four hours at -18°C, followed by 12 hours at 37.7 °C. The specimens shall retain at least the 85 % of the tensile and shear properties of control specimens in order to be in line with the conditions of acceptance. Environmental durability tests consist in the immersion of TRM coupons in three different solution: deionised water, salt-water, alkaline solution (with pH equal to 9.5 or higher). The three treatments should last for 1000 h and 3000 h and should lead to a retainment respectively of the 85 % and 80 % in order to respect the conditions of acceptance [57].

The American Concrete Institute developed the ACI 549.4R-13, guide to design and construction of externally bonded FRCM systems for repair and strengthening concrete and masonry structures [58]. Within the guidelines background information and field applications concerning TRM systems are widely

discussed. The main properties of TRM systems and TRM-strengthened structures are reported, and the structural design procedures are described. No novelties with respect to the TRM qualification procedures and durability requirements are introduced in this document with respect to the AC434. The guidelines provide the main tools in view of designing of interventions for the maintenance and repairing of existing structures. Specifically, formulations are proposed to evaluate the capacity to resist out-of-plane and in-plane loads of masonry elements externally strengthened by TRM systems. The section analysis is based on the following assumptions: strain compatibility between masonry and TRM composite, plane sections remain plane, the TRM is characterised by a bilinear behaviour to failure and its contribution prior to cracking is neglected. The mechanical strength parameters considered are the maximum tensile strength and strain of the TRM, and the stiffness concerning the response of the composite in tension in the cracked configuration. The approach proposed by the guidelines for the assessment of both out-of-plane flexural strength and in-plane shear strength of TRM strengthened masonry elements consists in adding up the two contributions of strength of the unreinforced masonry member and if the TRM system. The latter is calculated on the bases of the TRM strength parameters, by superiorly limiting the maximum strain to the values of 0.012 and 0.004 respectively for the case of out-of-plane and in-plane load configuration. With the aim of making easier the use of the guidelines, the ACI 549.4R-13 also provide with designing examples of TRM external reinforcement of several structural elements subjected to different load conditions [58].

With the aim of standardising the qualification test procedures of TRM and TRM-to-masonry systems scientific technical committees were created ad hoc. Recommendation of RILEM TC 232-TDT illustrates the test method to determine the load bearing behaviour of TRM tensile specimens [12]. Recommendation of RILEM TC 250-CSM defines the test method for TRM to substrate bond characterisation [32]. Both documents describe in detail the geometry of the specimens, the test condition and equipment, the test procedure and the evaluation of test results.

With respect to the Italian legislative context, the technical code for constructions [59] requires that all materials and products adopted in constructions, when used with a structural function, should be identified, qualified and controlled. To this purpose, guidelines for the identification, qualification and acceptance criteria of TRM to be used for retrofitting of existing structures, were recently developed [60]. An interesting aspect present in the latter concerns the application of the reinforcement system. As known, the mechanical efficiency of TRMs is strictly related to a proper implementation in situ. Therefore, it is necessary that the

manufacturer provides technical handbook explaining the installation procedure, specifying the range in which the thickness of the composite may vary and possible needed preparatory treatments of the substrate. Such instructions, to be respected during the reinforcement application, also represent the reference for control inspections. Also in Italy instructions for the design, execution and control of reinforcement interventions by means of TRMs were developed, provided by the Italian National Research Institute (CNR) [61]. Similar to what is proposed by the American guidelines, the document includes an overview of the possible applications of the retrofitting system, the basic principles for conception of retrofitting interventions and designing formulas. The qualification procedure provides for tensile test of the textile, tensile test of TRM coupons and shear bond test of TRM-to-substrate systems. The mechanical parameters deriving from the characterisation tests, and to consider in designing formulas, are defined as follow:

- σ_{uf}, ε_{uf} and E_f, respectively representing the maximum tensile stress and strain and the tensile stiffness of the dry textile;
- $f_{c,mat}$, representing the compression strength of the matrix;
- σ_u, ε_u, respectively representing the maximum tensile stress and strain of the TRM deriving from direct tensile test (clamped configuration);
- E_1, representing the stiffness in tension of the TRM with respect to the Stage I (linear elastic phase in the uncracked configuration);
- $\sigma_{lim,conv}$, $\varepsilon_{lim,conv}$, defined as conventional limit stress and strain.

The normal stresses are conventionally referred to the cross section of the dry textile in the direction of loading. The conventional limit stress, $\sigma_{lim,conv}$, represents the maximum strength of a TRM-to-substrate system derived from the shear bond test. The conventional limit strain, $\varepsilon_{lim,conv}$, represents the deformation corresponding to the conventional limit stress in the tensile stress-strain response of the dry textile (Figure 2.12).

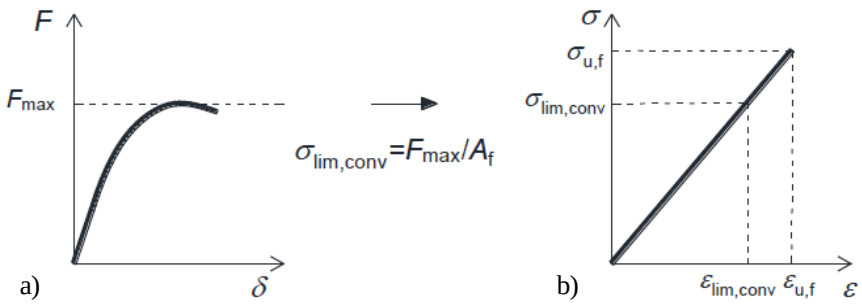

Figure 2.12: Conventional limit stress and strain assessment by means of: a) TRM-to-substrate shear bond test; and b) dry textile tensile test responses [61].

2.2 Use of plant fibres in TRM composites

During the last decades, the sensitivity of the public opinion toward environmental issues has significantly increased. The first definition of "sustainable development" was given by the Brundtland Report "Our Common Future" in 1987, in which it is highlighted that "*Humanity has the ability to make development sustainable to ensure that it meets the needs of the present without compromising the ability of future generations to meet their own needs*" [62]. Such concept implies the improvement of technology and social organization to make way for a new era of economic growth in line with the current elaborated model of circular economy, defined as "*a regenerative system in which resource input and waste, emission, and energy leakage are minimised by slowing, closing, and narrowing material and energy loops*" [63]. Moreover, the need of more sustainable solutions is recognised as one of the main "societal challenges" of our days also by the EU Research and Innovation program "Horizon 2020". Therefore, limiting the environmental "impact" of human activities is nowadays considered as a priority in all industrial fields. Among others, the construction sector needs to get "greener" by reducing both the demand of energy and raw materials, and the emission of green-house gases [64]. Moving in this direction new sustainable building materials are conceived by promoting the reuse of waste-materials and the use of the so-called eco-friendly raw material sources characterised by a low environmental impact [65].

Composite materials lend themselves well to the implementation of several solutions aimed at obtaining more sustainable systems. For instance, the adoption of natural fibres (also called bio-fibres or cellulosic fibres and hereinafter referred to as plant fibres), in lieu of industrial ones, as reinforcement of both organic and inorganic matrices, is one of the possible features of a new class of materials generally referred to as biocomposites. In recent years, such use experienced a considerable increase in engineering applications. In 2003, the use of plant fibres in composites in EU, was estimated to be around 43000 tonnes [66]. In 2010, the amount increased to around 315000 tonnes, representing about the 13% of the all types of reinforcing fibres available (carbon, glass, etc…) and estimated to be around 28% by 2020 [67]. The US Departments of Agriculture and Energy set goal of having at least 50% of all basic chemical construction blocks created from renewable and/or plant-based sources by 2050 [68]. It is reasonable to consider bio-composite as the next generation of structural materials. For this reason, several efforts are made by the scientific community to investigate the mechanical behaviour of plant-fibres-based composites, and to improve it according to the performance levels required by structural applications.

2.2.1 Plant fibres

Based on their origin, natural fibres can be classified as plant, animal or mineral [69]. Plant fibres, in turn, are subdivided into wood fibres and non-wood fibres. The latter include different kinds of fibres depending on the part of the plant they are taken out: leaf (sisal, pineapple, àbaca), bast (hemp, flax, jute, kenaf, ramie), seed (cotton), fruit (coir, kapok), straw (rice, corn), grass (bamboo). The great availability in many countries, their cost-effectiveness and low density, are some of the advantages that led to a great interest in the use of such fibres (Table 2.1). Due to their nature, they result to be biodegradable, renewable, non-hazardous and non-abrasive. Moreover, they proved to have good mechanical properties, sometime comparable to those of synthetic fibres. However, a successful commercialization of such fibres is prevented by some issues still unsolved. The lack of data related to the durability creates a widespread scepticism that prevents the implementation of these materials in engineering areas. In addition, significant fibre contents are needed in order to have adequate reinforcement effects, with possible difficulties in mortar mixing due to reduction in workability. Another drawback is related to the reliability of the mechanical properties of plant fibres, frequently characterised by a significant scattering due to their dependence on random variables such as chemical composition, filaments geometry (diameter and length) and surface roughness [69].

Table 2.1: Estimation of the plant fibres global production [70].

Fibre type	Production per year (Million tonnes)	Main producer countries
Abaca	0.10	Philippines, Equator
Cotton	25	China, USA, India, Pakistan
Coir	0.45	India, Sri Lanka
Flax[a]	0.50-1.5	China, France, Belgium, Ukraine
Hemp[b]	0.10	China
Henequen	0.03	Mexico
Jute	2.5	India, Bangladesh
Kenaf	0.45	China, India, Thailand
Ramie	0.15	China
Silk	0.10	China, India
Sisal	0.30	Brazil, China, Tanzania, Kenya

[a] The real production of flax was underestimated because the production of Canada is not considered.

[b] China has announced plan to substantially increase the hemp production for textiles in the coming years to 1.5 million tonnes of fibres per year.

Plant fibres (also named as cellulose/lignocellulose fibres) may themselves be considered as a composite whose basic chemical components are cellulose, hemicellulose and lignin. The cellulose represents the stiffest and strongest

component and its amount affects the fibre strength, stiffness and stability. Plant fibres can be classified with respect to the chemical composition, and so the proportion among the different components: i.e. cotton, hemp, flax, sisal, ramie, with an amount of about 70% of cellulose of the entire chemical composition, are considered as fibres reach in cellulose. Several other aspects may also affect the chemical composition, such as geographical and climatic conditions, the variety of the plant, soil quality, level of plant maturity and the fibre manufactory process. The combination of these features determines the mechanical properties of the fibres [71].

Depending on their nature, plant fibres may present different structures. In general, they are arranged as bundles of elementary fibres, each one characterised by a multilayer cylindrical structure. In Figure 2.13 the typical structure of a flax fibre is represented from the stem (macroscopic scale) to the elementary fibre components (nanoscopic scale).

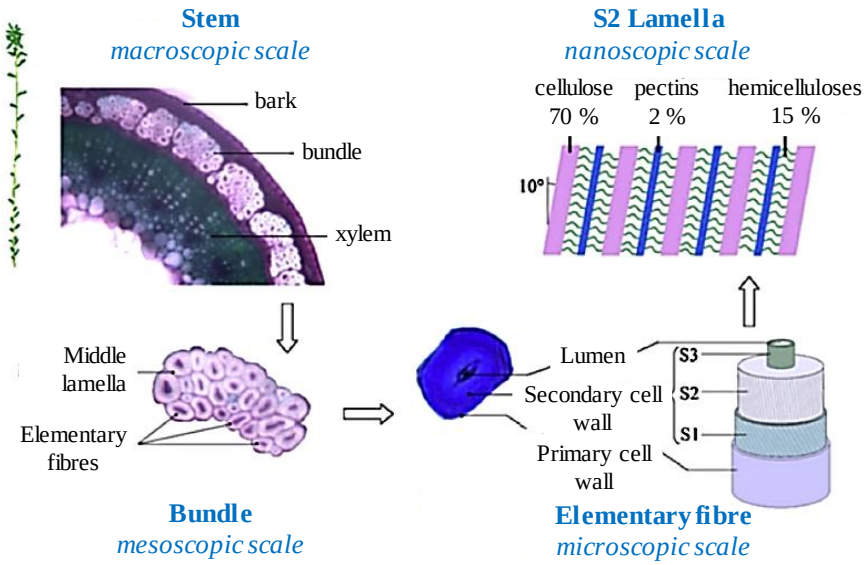

Figure 2.13: Schematic multi-scale flax fibre structure [69].

The stem is characterised by several layers. Bundles of fibres are placed right under the bark. The cross section of a bundle contains between 10 and 40 elementary fibres. At the microscopic scale the elementary fibre is characterised by concentric cell walls, differing each other in terms of thickness and chemical components. The centre part, with a small open channel in the middle, is called lumen, and it is the part responsible of water uptake. On the outer side, the primary cell wall is located

around the secondary wall. The latter, with a high content of cellulose, is responsible for the strength of the fibre [70].

Physical properties also play an important role in the mechanical performance of plant fibres. Generally, the tensile strength decreases when the fibre length increases in line with the principle according to which the longer the fibre, the higher the probability of presenting imperfections leading to premature failures compared to shorter fibres [69]. The main mechanical properties of cellulosic fibres, compared with those of synthetic fibres such as carbon, aramid and glass, are shown in Table 2.2.

Table 2.2: Mechanical properties of main plant and synthetic fibres [69].

Fibre type	Relative density (g/cm^3)	Tensile strength (MPa)	Elastic modulus (GPa)	Specific modulus ($GPaxcm^3/g$)	Elongation at failure (%)
Abaca	1.5	400-980	62-20	9	1.0-10
Alfa	0.89	35	22	25	5.8
Bagasse	1.25	222-290	14-27.1	18	1.1
Bamboo	0.6-1.1	140-800	11-32	25	2.5-3.7
Banana	1.35	500	12	9	1.5-9
Coir	1.15-1.46	95-230	2.8-6	4	15-51.4
Cotton	1.5-1.6	287-800	5.5-12.6	6	3-10
Curaua	1.4	87-1150	11.8-96	39	1.3-4.9
Flax	1.4-1.5	343-2000	27.6-103	45	1.2-3.3
Hemp	1.4-1.5	270-900	23.5-90	40	1-3.5
Henequen	1.2	430-570	10.1-16.3	11	3.7-5.9
Isora	1.2-1.3	500-600	-	-	5-6
Jute	1.3-1.49	320-800	30	30	1-1.8
Kenaf	1.4	223-930	14.5-53	24	1.5-2.7
Piassava	1.4	134-143	1.07-4.59	2	7.8-21.9
Palf	0.8-1.6	180-1627	1.44-82.5	35	1.6-14.5
Ramie	1.0-1.55	400-1000	24.5-128	60	1.2-4.0
Sisal	1.33-1.5	363-700	9.0-38	17	2.0-7.0
Aramid	1.4	3000-3150	63-67	46.4	3.3-3.7
Carbon	1.4	4000	200-240	157	1.4-1.8
E-glass	2.5	1000-3500	70-76	29	0.5
S-glass	2.5	4570	86	34.4	2.8

Flax, ramie and hemp represent the most performant fibres, whose strength and stiffness ranges of values are relatively close to those of synthetic fibres, such as glass. Nevertheless, the same cannot be said with respect to the strain at failure. Such discrepancy is due to the mechanical response in tension of plant fibres, that, unlike

synthetic fibres, shows a first less stiff branch prior to achieve a linear behaviour. Such behaviour, typical of plant fibres, consists of an elasto-visco-plastic deformation due to the re-arrangement of the amorphous parts of the thickest cell wall, the cellulosic microfibrils, aligning with the tensile axis [72]. The Ashby plot in Figure 2.14 shows the density of several types of fibres and fibre-based composites in function of the tensile strength on logarithmic scale. This graph, although confirming that plant fibres strength is comparable to those of glass ones, also highlights a wide gap of performance with respect to carbon and polymeric based composites with high strength fibres.

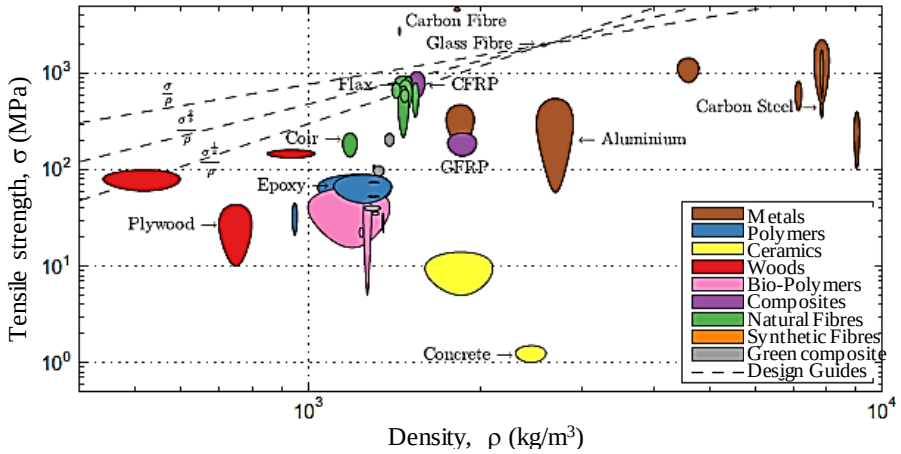

Figure 2.14: Density – tensile strength relationship of different types of fibres and fibre-based composites [73].

As known, in addition to mechanical aspects, several other features affect the interest in the use of a construction materials. Among them surely economic criteria play a fundamental role. With this respect it was observed that the cost per weight of most plant fibres results to be relatively lower than those of synthetic fibres, such as glass ones (Figure 2.15a). The economic criteria can also be assessed by considering a more significant parameter defined as the cost per length for an amount of fibres capable of resisting a tensile load of 100 kN (Figure 2.15b). According to the latter such cost discrepancy between plant and glass fibres clearly decreases, even though such fibres, i.e. flax, still exhibit a good potential combination of low cost, light weight, high strength and stiffness. The same conclusions can be drawn by considering a greater population of materials of comparison (Figure 2.16). It is necessary to point out that specific treatments to adjust the mechanical behaviour of plant fibre-based composites to the required performances may lead to additional costs related to their use. In addition, being plant fibres materials a relatively young

market concerning their supply and use, great uncertainty exists concerning the future price of these materials. For these reasons, further investigations are needed in order to accurately define such economic aspects.

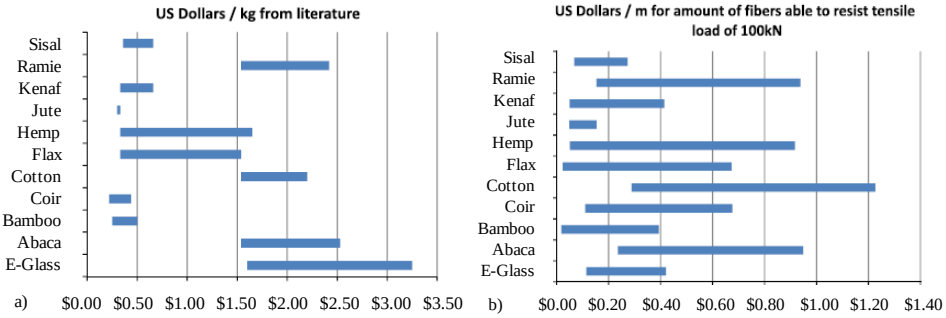

Figure 2.15: Comparison between E-glass and plant fibres: a) cost per weight; b) cost per unit length capable of resisting 100 kN load [74].

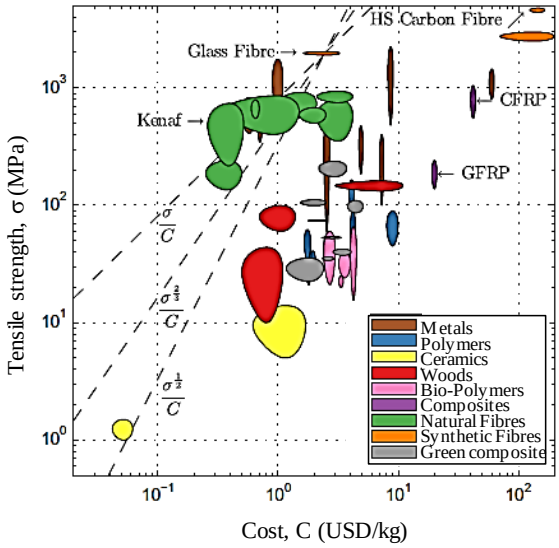

Figure 2.16: Cost – tensile strength relationship of different types of fibres and fibre-based composites [73].

A more comprehensive analysis aimed at investigating the potential use of plant fibres in construction materials, cannot neglect the aspect of the environmental impact, an issue of primary importance nowadays. Plant fibres are known to be characterised by relatively low embodied energy, representing, the latter, the energy consumed by all processes associated with the production of a construction material (or of a building) from the mining and processing of natural resources, to

manufacturing and transport. By putting in relationship such a parameter with the tensile strength, over a wide population of different types of fibres and fibre-based composites, an exhaustive comparison can be provided (Figure 2.17). In absolute terms, the embodied production energy concerning synthetic fibres is approximately 10 times larger than that of plant fibres, and it is highlighted that synthetic fibre-based composites require around five times more energy of production than green composites [73].

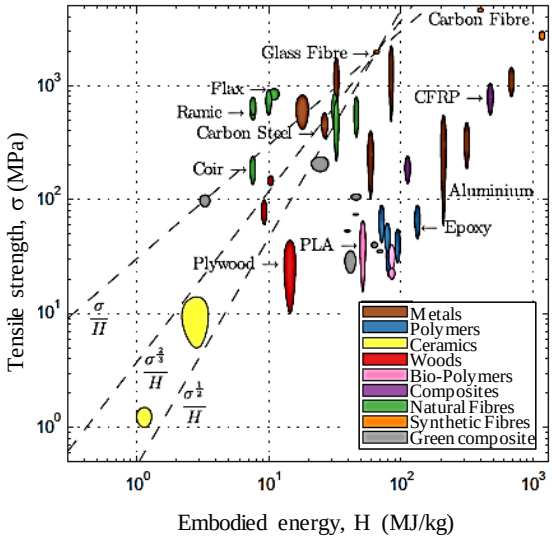

Figure 2.17: Embodied energy – tensile strength relationship of different types of fibres and fibre-based composites [73].

By taking into account the several aspects discussed above, such as physical, mechanical, economic and ecologic ones, among the various plant fibres, flax, hemp, cotton, sisal and jute concretely represent potential candidates as reinforcement of innovative composites in civil engineering applications [69].

2.2.2 Plant fibres as reinforcement in TRMs

The use of plant fibres as reinforcement in inorganic matrices represents a smart solution to employ the potential of the fibres in TRMs, and to improve the sustainability of such an innovative retrofitting technique. Several research studies, carried out to investigate the efficiency of plant-based TRMs, showed it as a valuable and promising solution [75]. Due to their nature, physical structure and mechanical properties, plant fibres are characterised by a mechanical performance different from that exhibited by synthetic fibres. Therefore, the scientific outcomes deriving from

the several studies carried out in the last decade on the use of TRMs, mainly conducted by using high strength fibres, cannot be directly extended to plant fibre based TRMs. For this reason, many researchers focused their attention on the mechanical behaviour of lime/cement-based matrices reinforced by plant fibre textiles, often referred to as Natural TRMs, with the aim of assessing their efficiency. Several aspects were investigated on different scales of analysis from the fibre-to-matrix bond, to the application of Natural TRMs as reinforcement of masonry elements.

The bond behaviour at the fibre-to-matrix interface represents a fundamental aspect that affects the mechanical behaviour of the entire TRM composite and its performance as reinforcement of structural elements. Pull-out test, consisting in pulling a textile yarn embedded in a mortar cylinder (Figure 2.18), provides shear stress vs slip (also named bond-slip) curves representative of the bond capacity between the two elements.

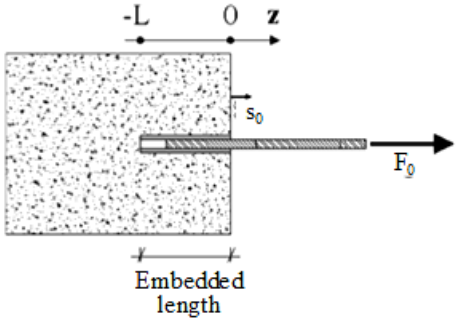

Figure 2.18:Single fibre pull-out test scheme [76].

The bond-slip law is typically characterised by a first linear branch followed by a frictional bond phase. The maximum shear bond stress, and the magnitude of the residual force depend on the materials' properties and on the embedded length. The shear-bond response of jute fibres in a cementitious matrix was studied by Ferreira et al. [76], in which a debonding failure showed that the critical transfer length is larger than 10 mm. The study also proposed an analytical model providing a bilinear bond-slip law representative of the experimental evidences. The bond between plant fibres and matrix can be improved by means of treatments applied on the fibres before embedding them within the mortar [77].

Different treatments may be applied to the fibres to improve their strength: hornification, consisting in wet-drying cycles in hot water; alkaline treatment, consisting in immersion of fibres in low alkaline concentration solutions for 50 minutes and in drying for 24 h; polymer impregnation; hybrid treatments, combining fibres hornification and polymer impregnation. By adopting the aforementioned

treatments to sisal fibres immersed in a cement-based matrix, an increase of both fibres' tensile strength and fibre-to-matrix bond was observed in all the cases [78]. The alkali treatment modifies the fibre composition by removing the amorphous constituents of the fibre and by increasing its crystallinity. The polymer coating increases the interfacial bond creating a layer acting as a bridge between matrix and fibre.

Several researchers devoted their attention to the mechanical characterisation of the tensile behaviour of TRM coupons made with plant fibre textiles. Ghiassi et al. [79] produced TRMs with lime mortar and flax fabric and induced tensile stresses by applying the load trough clamping of the textile on the two sides of the specimen. By comparing the results with the tensile response of the dry textile, although a decrease of stiffness was observed, a significant increase of the tensile strength was evidenced, due to the increased integrity of the system provided by the mortar presence. Codispoti et al. [80] carried out tensile test on TRMs performed by using several types of textile, such as jute, sisal, coir, flax, hemp (Figure 2.19). The different types of Natural TRM exhibited a promising mechanical response with a good exploitation rate of the entire dry textile strength. However, it was emphasised that it is fundamental to adopt appropriate thickness of the mortar, and hence appropriate volume fraction of fibre, in order to produce a mechanically efficient system.

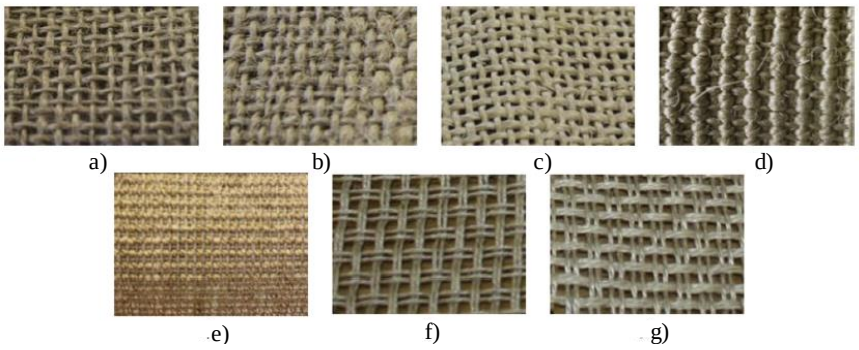

Figure 2.19: Different types of plant fibre fabrics: jute (a, b and c); sisal (d and e); hemp (f); flax (g) [80].

The tensile response of Natural TRMs is characterised by the typical three phases generally exhibited by the conventional synthetic fibre-based system [81]. Unlike the latter, Natural TRMs are characterised by a second stage in which, in correspondence to the occurrence of a crack, a significant drop of the load is observed due to a discrepancy in the axial stiffness of the textile (A_f x E_f) and the axial stiffness of the mortar (Figure 2.20).

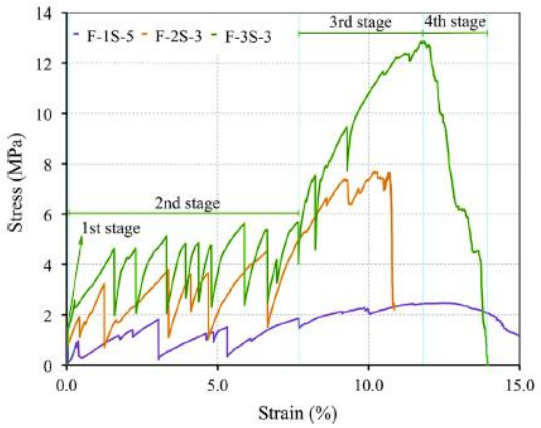

Figure 2.20: Stress-strain response of composite specimens reinforced with one, two and three layers of flax fabrics [82].

The fibre volume fraction plays a key role in the mechanical response of Natural TRMs. Figure 2.21 shows the tensile strength of plant fibre composites (assessed referring to the entire cross-section area of the coupons), performed by using flax and sisal, as a function of the fibre volume fraction. It can be noted that starting from a volumetric ratio of about the 3%, a significant enhancement of the mechanical performance was experienced [82].

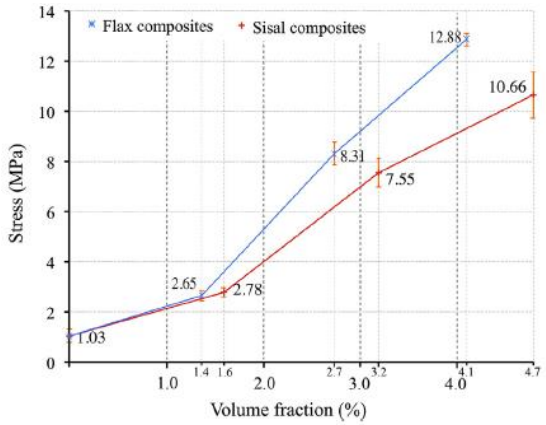

Figure 2.21: Effect of the fibre volume fraction on tensile strength of Natural TRMs [82].

Natural TRM tested in tension typically exhibited a failure characterised by the rupture of the fibres. However, depending on the test set up, a slippage of the fibres within the clamped zone may occur [83].

The influence of fibre treatments, i.e. coating, on the mechanical response of several types of Natural TRMs, performed by using flax, hemp, sisal and cotton

fabrics, was investigated as well. Mercedes et al. employed two different treatments by coating the fabrics either with epoxy resin or with polyester. In both cases, an increase of the tensile response of the textile was observed. In regards to the tensile strength of Natural TRMs, when epoxy-coated meshes were adopted, a larger exploitation rate of the textile was observed with respect to polyester-coated mesh based TRMs, that presented debonding phenomena at the fibre-to-matrix interface [84]. Few studies focused their attention on the experimental investigation on bond adhesion between Natural TRMs and masonry support. Olivito et al. carried out double-lap shear bond tests on masonry clay bricks externally strengthened by a Flax TRM composite and compared the mechanical behaviour with a similar system characterised by conventional high strength fibres (PBO) [85]. Two configurations were taken into account, respectively characterised by a bonded length of 50 mm and 100 mm. The experimental results highlighted clear differences between the two reinforcing systems adopted: the flax-based system exhibited a failure mode characterised by the rupture of the textile yarns in the unbonded length, whereas PBO-based systems experienced a brittle cohesive failure mode. Flax fibres exploited their potential strength to a high degree during the test achieving almost 60% of the dry fibre tensile strength, unlike PBO textiles that used only between the 20% and the 30% of their strength (Figure 2.22). Such experimental evidences point out the good collaboration between flax fibres and inorganic matrix, in some cases showing even more compatibility than synthetic fibres. It is important to notice that in case of TRM strengthened masonry elements under cyclic/dynamic loading, a controlled debonding of the textile within the matrix would be more desirable in terms of energy dissipation. Still it is important emphasising the possibility to increase the capacity of the system by increasing the textile amount, due to the good bond behaviour between plant fibres and mortar.

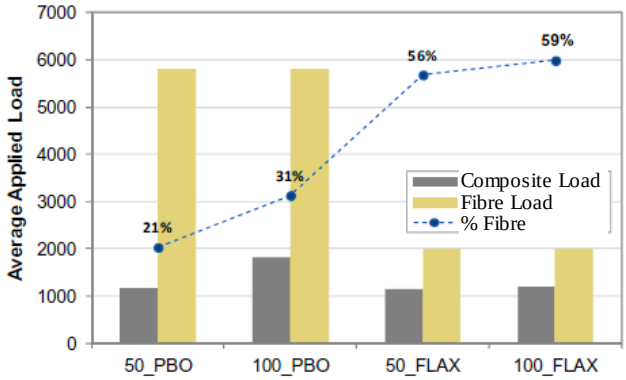

Figure 2.22: Fibres exploitation ratio in PBO-TRMs and Flax-TRMs [85].

Carvalho Bello et al. [83] carried out single lap shear tests on Sisal TRM-to-masonry systems according to RILEM recommendations [32]. Sisal fibres were impregnated by an adhesive promoter prior to the inclusion in the inorganic matrix. The failure mode observed was characterised by the tensile failure of the yarns along the free (unbonded) length, and no slip was observed at masonry-to-mortar interface. Due to an uneven distribution of the stresses among the sisal yarns, the maximum tensile strength attained was about 30% lower than the potential strength of the dry textile. Some applications of Natural TRMs as external reinforcement of masonry elements are present in literature. Cevallos et al. assessed the efficiency of a Flax-TRM system for strengthening of masonry structural elements subjected to eccentric loads (Figure 2.23). The mechanical response of different sized specimens was compared to those of elements externally strengthened by PBO-TRM composites. The reinforcement conferred to the masonry elements a substantial gain in strength and deformability. By comparing the plant fibre-based system with the synthetic based one, it was highlighted that the higher ductility of flax fibres allowed for a higher strain in the TRM forming cracks in the mortar. Such behaviour resulted in a more ductile behaviour, unlike the case of PBO TRM-strengthened elements, in which the lower strain capacity of the fibres led to debonding of the strengthening system with a consequent brittle collapse of the element [86].

Figure 2.23: Application of the Flax-TRM system on masonry structural elements: a)application of the first layer of mortar; b) embedment of the fabric into the matrix; c) smoothing of the outer layer of mortar [86].

With the aim of assessing the contribution of Natural TRMs to the in-plane shear capacity of masonry elements diagonal compression tests were carried out. Menna et al. investigated the in-plane response of either clay bricks or tuff masonry elements externally strengthened, uniformly all over the surface, by a TRM system

comprising a hemp textile, properly impregnated in a flexible epoxy resin, and either a pozzolanic or a lime-based mortar [87]. The experimental outcomes showed enhanced mechanical properties in all tested panels, with a maximum shear strength increased by a factor of about 2-5. The failure occurred with a mostly uniform crack pattern that developed until the entire exploitation of the textile that achieved its tensile strength in the most stressed points (Figure 2.24).

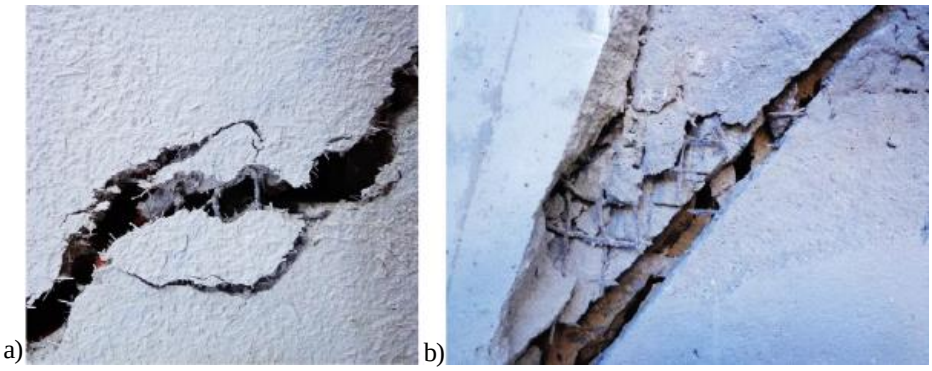

Figure 2.24: Tensile failure of textile in proximity of cracks in Hemp-TRM externally strengthened clay brick (a) and tuff (b) masonry elements [87].

Different configurations of reinforcement, with either Flax-TRM and Hemp-TRM unidirectional strips applied on the surfaces of clay brick walls, were also investigated (Figure 2.25). An increase of the strength was observed in the range of the 20% and 40% with respect to unreinforced masonry walls tested in diagonal compression [88].

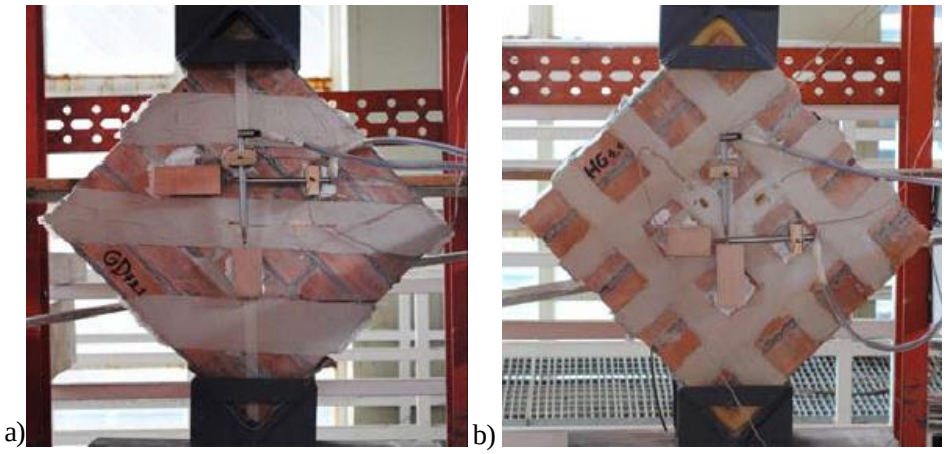

Figure 2.25: Clay brick walls eternally strengthened by Natural TRMs arranged in strips oriented in the tensile direction (a); and applied in the form of bidirectional grids (b) [88].

In order to define the effectiveness of plant fibre-based cementitious composites, it is necessary, in addition to mechanical investigations, to focus the attention on durability aspects with the aim of assessing the ability of the system to resist both external (weather conditions) and internal damage (compatibility between matrix and fibres). Plant fibres embedded in Portland cement undergo a degradation process due to the high alkaline environment [89]. Such degradation is due to the alkaline pore water that dissolves the lignin and hemicellulose in the middle lamellae of the fibres, weakening the link between the individual fibre structure elements. An additional phenomenon consists in the alkaline hydrolysis of cellulose, that causes degradation of the molecular chains with a consequent decrease of polymerisation of the fibre structure. Toledo Filho et al. investigated the degradation of sisal and coconut fibres by immersing them in alkaline solutions [90]. It was observed that in sodium hydroxide (NaOH) solutions between the 30% and 40% of the strength was lost after 420 days of exposure. Even a more aggressive exposure was that of a calcium hydroxide ($Ca(OH)_2$) solution in which a complete loss of strength was evidenced after 300 days of immersion. The heavier attack of the calcium hydroxide may be attributed to the crystallization of lime in the fibre's pores [91].

Another aspect that contributes to the degradation of plant fibres in inorganic matrix composites is related to the capacity of such fibres to absorb water [92]. The latter may lead to volume changes that can induce cracks within the matrix, as in the case of hygral fatigue (Figure 2.26).

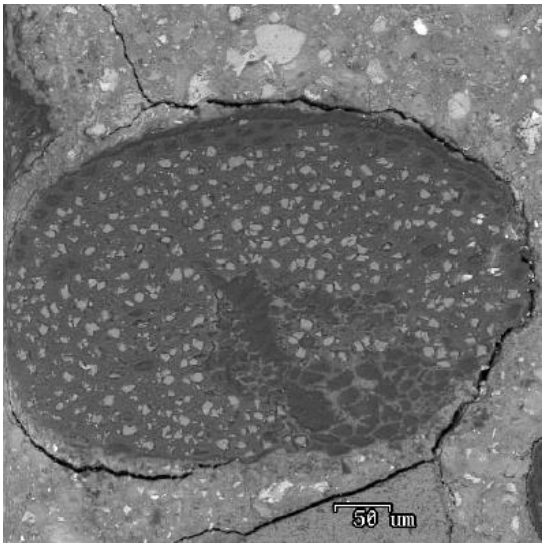

Figure 2.26: Coconut fibre-cementitious matrix interface after 25 cycles of wetting and drying [90].

In order to improve the durability of plant fibres in inorganic matrices two approaches can be adopted: matrix modification and fibre modification [93]. With respect to the first strategy using low alkaline matrices can reduce their aggressivity, for instance by adding pozzolanic products, rice husk or fly ashes [94]. D'Almeida et al. showed that by replacing part of the Portland cement by metakaolin it is possible to obtain a matrix totally free of calcium hydroxide, hence avoiding a damage of the fibre lumen, middle lamella and cell walls [95]. As regards fibre treatments to improve the durability performance, the coating procedure may result in being useful with respect to both water absorption and alkaline aggression. Toledo et al. recommended the immersion of plant fibres in a silica fume slurry to improve such behaviour, before adding them into the mix [96]. The choice of coating treatment has to be accurately defined by taking into account not only durability aspects, but also the mechanical behaviour of the fibres themselves and with respect to the fibre-to-matrix bond. Fibre hornification treatments may also improve their durability by reducing the water absorption capacity [97].

The available literature data concerning the use of plant fibres in inorganic matrices shows a significant potential of such a reinforcement technique with respect to mechanical aspects. The experimental results, in some cases deriving by pioneering studies in the field, encourage to invest further efforts to improve the performance and to shed light on several aspects still unclear. Moreover, with respect to durability issues, it is important to spend more energy in improving the available treatments already existent, and eventually develop new ones. Finally, it is necessary to enrich the knowledge with respect to the efficiency of the application of Natural-TRMs as reinforcement of masonry, at scales of analysis being representative of the structural elements [93].

2.3 Aims of the Thesis

The state of the art review emphasizes the importance in the development and improvement of innovative construction techniques, such as those characterised by the use of plant fibres-based materials, to provide sustainable solutions becoming more and more indispensable.

In the light of what it was presented in the previous sections, several outstanding issues still remain unsolved concerning the use of plant fibres as reinforcement in inorganic matrix composites. It is necessary, on the basis of the potential exhibited by such systems, and on the basis of their limitations with respect to conventional reinforcement systems, to intensify experimental analysis in order to have a more robust scientific background. However, such investigations have to be

carefully conceived in a targeted manner with respect to the crucial aspects affecting either the strong points and the weaknesses of the reinforcing system.

In this context, the present thesis aims at providing a comprehensive investigation of a plant fibre-based TRM system. Specifically, due to its satisfying mechanical and physical properties, a flax textile was adopted as reinforcement of a hydraulic lime-based mortar. The overall interest of the work is to provide, by means of experimental investigations, a detailed analysis concerning the contribution of such composite systems on the mechanical behaviour of structural masonry elements.

However, too many aspects may play a more or less significant role in the global response of the system, and the existing studies in literature, although providing valuable information, are not enough to get a standardisation of the material. Therefore, in order to get a deep understanding of the overall mechanical behaviour, the investigation cannot be limited to the analysis of the response of masonry structural elements externally strengthened by Flax TRMs, but must start from more detailed scales of analysis.

The comprehensive characterisation carried out in the study moves from the physical investigation of the microstructure of the employed plant fibres, to the analysis of the global response of externally strengthened structural elements. For each scale of analysis, the main objectives pursued are defined in detail.

- At the smallest scale of analysis, a physical and morphological characterisation of the adopted plant fibres is presented aiming at providing the necessary information to evaluate the mechanical behaviour on greater scales of analysis, and to compare the adopted fibres with others of the same, or different, nature.
- A mechanical characterisation of the employed flax textile is proposed with the aim of defining to what extent it can be both mechanically and chemically suitable as reinforcement in inorganic matrices. Both mechanical and durability tests provide more information on such aspect and represent the basis from which possible necessary improvement solutions may be properly conceived.
- Mechanical and durability tests on the composite scale of analysis were planned with the aim of qualifying the material according to standardised procedures, and of comparing its performance with similar systems. At this scale of investigation too, the analysis of results provides both potential aspects and limitations of the system.
- The global mechanical response of masonry assemblage aims at quantifying the contribution of the Flax TRM external strengthening system on the in-plane capacity of the panel. Such scale of analysis

provides more realistic strength values with respect to smaller scales of investigation.

A further objective of the present study consists of taking advantage of the adopted multi-scale approach of the analysis to define the connection between the mechanical performance assessed on the material scale of investigation and the global response of the structural elements. This aspect is of fundamental importance since, according to standard codes concerning structural interventions by means of TRM systems, the main mechanical designing parameters are assessed on the composite scale of analysis. In addition, since only few studies in the literature have been carried out with a similar multi-level analysis approach, it represents a valuable contribution.

Therefore, in a global perspective, the comprehensive characterisation herein proposed has the aim of investigating the efficiency of a Flax TRM composite as external strengthening of masonry elements, by highlighting both the potentials and the limitations, with respect to a mechanical point of view.

Moreover, to move a step further than a mechanical characterisation for its own sake, the study aims to preliminary investigate technical solutions, i.e. fibre treatment and mortar mix design modification, to prove that the composite system, already characterised by a promising potential, still presents room for improvement.

3. Mechanical behaviour and durability of Flax textiles to be used as reinforcement in TRMs

Prior to addressing the investigation of Natural TRMs, and to studying its influence on structural elements, it is necessary to characterise the reinforcing fabric. Such step, conducted at the constituent *"materials"* scale of analysis, is of fundamental importance for the interpretation of the mechanical behaviour at greater scales of analysis. Due to the randomness of plant fibre properties, it is not enough to limit such investigation to the assessment of mechanical properties, such as tensile strength and stiffness. It is, however, essential to accurately define the geometry and the morphology of the fibres, and to face the issue of the compatibility of the textile with the mortar. The aim of this chapter is to provide such information by reporting the results of an experimental research intended at determining the fundamental properties of Flax fibres, yarns and fabrics, and assess their behaviour when subjected to various environmental exposures and ageing protocols.

The experimental work moves from determining the relevant geometric properties, such as length, cross-section and relevant sizes, and physical parameters, such as water absorption capacity. Then, tensile tests on differently sized flax samples lead to determining the tensile strength and its natural variability. Lastly, regarding durability, different ageing protocols are considered with the aim of reproducing specific environmental conditions, i.e. the exposure to water, salt-water, and alkali solutions or to lime- and cement-based mortars.

The experimental activity performed to physically and mechanically characterise the flax textile, and to investigate its durability were almost entirely carried out at the Department of Industrial Engineering (DIIN) of University of Salerno. Few experimental investigations were performed at the laboratory NUMATS-COPPE of the Federal University of Rio de Janeiro in order to deeply analyse such aspects.

3.1 Physical characterisation

The flax fabrics under consideration in the study was provided by the company Innovation s.r.l. with the name of *FIDFLAX Grid 300 HS20*® [98]. The textile consists of a bi-directional woven flax fabric with plain weave. Warp and weft yarns are arranged so that they form a simple cross pattern. Yarns are laid in twos along

the same row in both the directions. Each one is a combination of two smaller yarns, assembled to create a double twisted thread. The yarns are in their turn characterised by a bundle of filaments that represent the smaller components of the fabric structure. The double twisted thread is considered in the present study as the reference sample and hereinafter it is referred to simply as thread. Figure 3.1 shows the fabric structure at different scale levels.

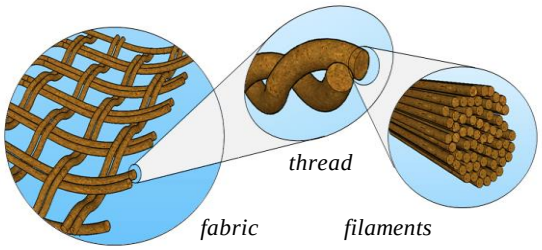

Figure 3.1: Flax fabric structure.

The textile grid, with 4.3 threads per centimetre in both directions, and a clear opening size of about 3 mm, is accurately sized to be used as a reinforcement within inorganic matrices, allowing the transit of fine aggregates. The identification of physical and geometric properties starts from analysing the single filaments constituting the fabric yarns, up to the assessment of the thread's density and cross section. One of the main aspects in the identification of plant fibres is the size of the filaments. A Scanning Electron Microscope (SEM) analysis was adopted to assess the mean diameter of the flax filaments (Figure 3.2). Specifically, 4 SEM images with a magnification of 1000X, and representing 4 different samples, were analysed providing a value of the filament diameter by means of 28 measurements.

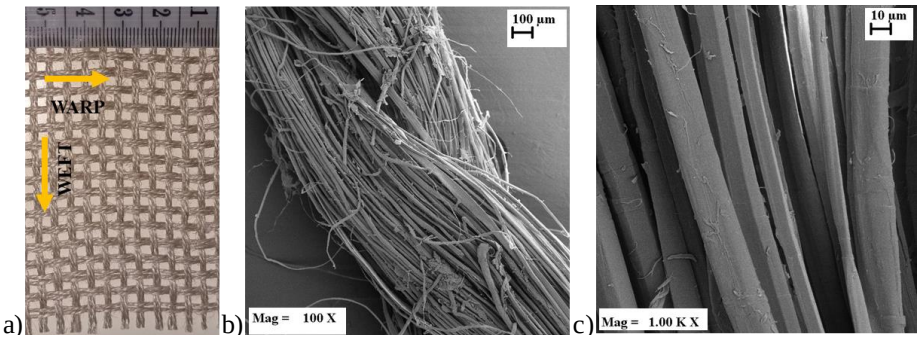

Figure 3.2: a) Flax fabric; b) thread (magnification 100X); c) filaments (magnification 1000X).

The cross-section area was indirectly determined from the density of the textile. Particularly, the specific gravity of 5 saturated thread samples with a length

of 15 cm was assessed by means of hydrostatic balance. The indirect estimate of the thread cross-section was obtained by dividing the weight of the samples for their density and length.

The flax fibres water absorption was defined as well (Figure 3.3). Five thread samples 15 cm long, were immersed in deionised water and weighted with regular intervals of 24 h up to the achievement of a negligible weight gain. The value of the water absorption ratio is equal to 222% with a coefficient of variation of 19 % and it is in line with the evidences of similar studies available in literature [99].

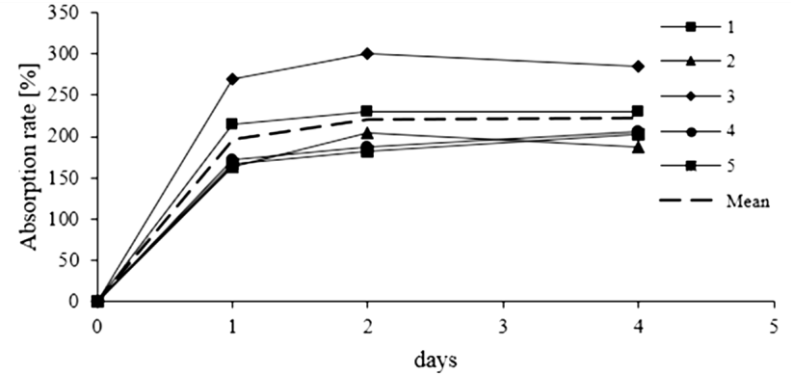

Figure 3.3: Flax thread water absorption rate.

The mean values of the physical properties, together with the respective coefficients of variation are listed in Table 3.1.

Table 3.1: Flax fabric physical properties.

	Mean	Co.V. (%)
filament diameter (μm)	16.78	29.64
density (g/cm^3)	1.19	3.29
linear density (Tex)	302	15.27
n° threads/cm	4.3	-
Thread's cross-section area (mm^2)	0.25	16.62

A more detailed investigation of the morphology of the flax threads was carried out at the laboratory NUMATS-COPPE of the Federal University of Rio de Janeiro. SEM images were taken to analyse the transversal shape of the fibres with a magnification of 60X. A total of 30 images were analysed. The presence of the voids within the yarns, due to the chaotic arrangement of the filaments, makes it difficult to get an accurate estimation of the threads cross section area. Consequently, an image manipulation software was used to analyse the SEM images. The contrast

of each picture was modified so that a black-and-white image was obtained, in which the white part represented the filaments section. An estimation of the yarn cross section area was obtained by converting in square millimetres the number of white pixels contained in the modified picture. Moreover, by tracking the border of the white region, an estimation of the actual perimeter of each thread was obtained as well (Figure 3.4).

The mean value of the thread cross section and of the perimeter are respectively equal to 0.28 mm^2 (Co.V. 18%) and 4.89 mm (Co.V. 21%). Considering the variability of the results and the accuracy of the adopted techniques it can be observed that the cross section mean value estimated by means of analysis on SEM images is in line with the indirect estimation obtained from the density of the fibres.

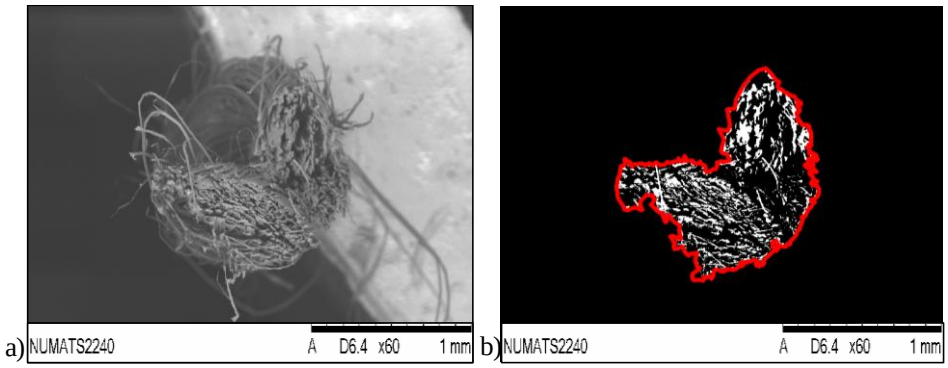

Figure 3.4: Thread's morphology identification: a) thread SEM image; b) thread manipulated image.

3.2 Mechanical characterisation

3.2.1 Methods

The mechanical characterisation of flax textile mainly consists in the assessment of its response in tension. Plant fibres are typically characterised by a variability of the mechanical properties that also depends on the arrangement of the textile. That's the reason why the characteristic properties of the specific fibres utilised are generally assessed on the single element constituting the thread. With the aim to compare the performance of the adopted flax fibres with those of other types of plant fibres from literature, tensile tests were preliminary carried out on the single filaments, representing the smallest component of the flax textile. Moreover, the single flax threads were tested in tension so as to get mechanical properties more representative of the scale of analysis of the composite itself. Being the textile a combination of smaller thread, the size of the sample to be subjected to tension may affect itself the

estimation. Therefore, four kinds of specimens, differing in the number of flax yarns, were tested in tension to assess the tensile strength and to analyse the variability of the response with the size. The different series considered are defined hereafter:

- *filament*: which consists of the smaller component of the textile. The samples, having a length of 30 mm, were randomly extracted from the fabric (Figure 3.5);
- *Flax-Y*: which consists of one of the two yarns constituting the main thread. Each sample, having a length of 15 cm, was extracted from threads in the weft direction (Figure 3.6a);
- *Flax-T (warp and weft)*: which consists of the thread representing the main element of the textile. The samples, having a length of 15 cm, were extracted in both weft and warp directions of the fabric (Figure 3.6b);
- *Flax fabric-2cm:* which consists of a flax fabric strip 2 cm large, characterised by 8 threads. The samples, having a length of 15 cm, were extracted from the fabric in weft direction (Figure 3.6c). This configuration was chosen on the basis of having a specimen comprising at least 3 yarns in the strip;
- *Flax fabric-6cm (warp and weft):* which consists of a flax fabric strip 6 cm large, characterised by 24 threads. The samples, having a length of 30 cm, were extracted from the fabric in weft and warp direction (Figure 3.6d).

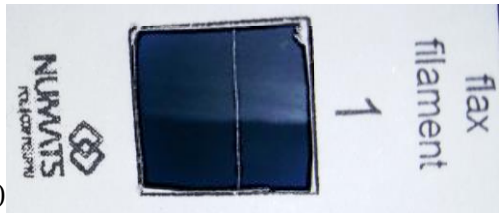

Figure 3.5: Flax filament tested in tension.

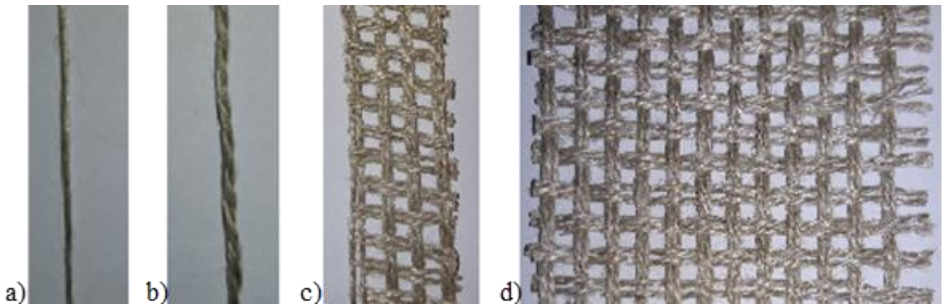

Figure 3.6: Flax samples: a) Flax-Y; b) Flax-T; c) Flax fabric-2 cm; d) Flax fabric-6 cm.

The filament series consisted of 10 samples with a gauge length of 10 mm that were clamped at each edge for a length of 10 mm. The tests were carried out at the laboratory NUMATS-COPPE of the Federal University of Rio de Janeiro by a microforce testing machine (Tytron 250, MTS System Corporation, Eden Prairie, MN, USA), with 50 N load cell in displacement control by using a rate of 0.5 mm/min. Tensile strength of the samples Flax-T and Flax fabric-6 cm was assessed in both the directions of the fabric in order to check if there was any direction-related difference. The samples of the series Flax-Y, Flax-T and Flax fabric-2 cm were characterised by a gauge length of 100 mm and were clamped in along each edge for a length of 25 mm. The gripping was guarantee by the rough clamping elements of the testing machine. Tensile tests were carried out at the Department of Industrial Engineering of the University of Salerno by means of a CMT4000 SANS Series dynamometer machine (by MTS, China), in displacement control with a rate of 4 mm/min by using a cell load of 1 kN (Figure 3.7a).

The samples of the series Flax fabric-6 cm were characterised by a gauge length of 200 mm and were clamped along both the edges for a length of 50 mm. The gripping was guaranteed by gluing the textile between two steel plates 5 mm thick, by means of an epoxy resin, and by putting the plates within the machine clamps (Figure 3.7b). Tensile tests were performed at the STRENGTH laboratory of the University of Salerno, by means of a Zwick Roell Schenck Hydropuls S56, with a maximum capacity of 630 kN and according to the ISO 13934-1 [100]. The tests were conducted in displacement control with a rate of 4 mm/min.

a) 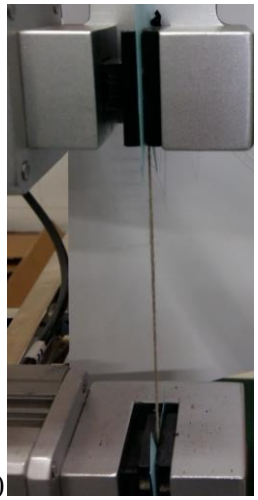 b) 

Figure 3.7: Tensile test set-up of series: a) Flax-T and b) Flax fabric-6 cm.

The mean values of the axial strains were assessed by dividing the displacement between the clamping edges for the free length of the specimens.

3.2.2 Results and discussion

Axial displacement and applied force were recorded in each tensile test. They were easily converted to stress and strains and the corresponding results are reported in this section. Specifically, the tensile strength, ft, the Young's modulus, E, and the strain at the peak, ε_u, were defined as parameters characterising the tensile behaviour of the fibres. Due to morphologic (microstructure of the fibres) and geometric (fabric arrangement) reasons, the tensile behaviour is always characterised by a lower initial stiffness that increases up to a constant value before failure. For this reason, the Young's modulus is calculated in the linear branch within the stress range from 20 % to 50 % of the maximum strength.

Figure 3.8 shows the tensile response of the filaments in terms of stress-strain. The cross-section area considered to get the stress values of filaments was obtained by assuming a circular section and by considering the diameter value reported in Table 3.1.

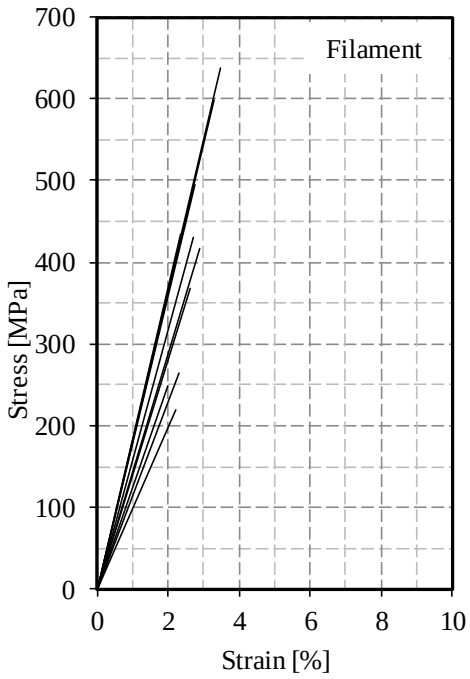

Figure 3.8: Tensile stress-strain diagram of the flax filament series.

The stress-strain response of the other series of specimens is shown in Figure 3.9. The cross-section area considered to get the stress values for all the types of samples was obtained from the value estimated from the threads of the Flax-T series, knowing that a thread consists in two twisted yarns, and the 2 cm and 6 cm flax strips were respectively characterised by 8 and 24 threads. The main values of the mechanical properties obtained from the tensile tests, with their respective coefficient of variation, are listed in Table 3.2.

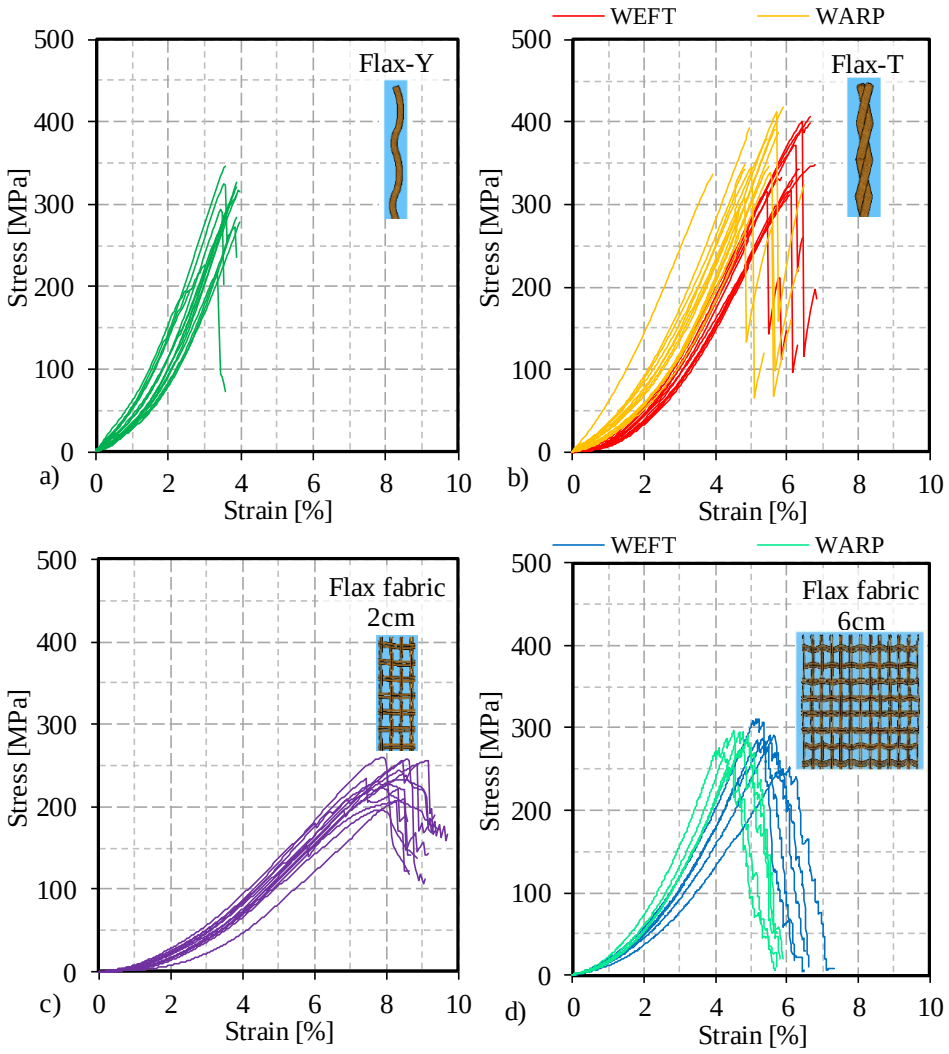

Figure 3.9: Tensile stress-strain response of the different flax specimens: a) Flax-Y; b) Flax-T; c) Flax fabric 2 cm; 4) Flax fabric 6 cm.

The mechanical parameters that arose from the experimental tests on the filaments assume values partially out of the range of values found in literature for flax, and more generally, plant fibres [69]. Specifically, the Young's modulus presents lower values. This might be due to the manufacturing process of the filament roving from which the samples were extracted, that may have made the fibres to be subjected to distortion.

Table 3.2: Mechanical properties of flax samples tested in tension.

	Direction	Numb. of spec.	P_u		f_t		E		ε_u	
			Mean (N)	Co.V. (%)	Mean (MPa)	Co.V. (%)	Mean (GPa)	Co.V. (%)	Mean (%)	Co.V. (%)
filament	-	10	0.29	35	411	35	15.1	21	2.66	18
Flax-Y	Weft	15	37	16	293	16	11.61	10	3.58	12
Flax-T	Weft	12	88	13	345	13	8.53	6	6.14	9
Flax-T	Warp	14	92	10	361	10	10.07	7	5.20	11
Fabric-2cm	Weft	14	476	9	233	9	4.39	8	8.27	6
Fabric-6cm	Weft	5	1759	7	288	7	8.25	10	5.56	6
Fabric-6cm	Warp	5	1744	4	285	4	9.81	3	4.63	5

The tensile tests carried out on different kinds of threads and fabrics confirm that flax fibres, as all other types of plant fibres [75], present variability of the mechanical properties both among samples of the same size and in terms of main values among the different series of specimens. Tensile strength assumes values varying in the range of 290 ÷ 360 MPa concerning the threads and 230 ÷ 290 MPa concerning the fabric strips. The Young's modulus assumes values between the range of 8.3 ÷ 11.6 GPa in both the threads and fabric specimens except from the series Flax-fabric-2cm in which significantly lower values of stiffness were observed. Such inconsistency may be attributed to an inefficient clamping system adopted during the test. For this reason, further analysis would be needed to get more certain values of stiffness and strain parameters concerning the Flax-fabric-2cm series. Both strength and stiffness resulted to be lower with respect to the values deriving from the tests on the flax filaments. Such trend is in line with research carried out by using flax textile in which a loss of stiffness is recorded as well by increasing the size of the samples [82]. Also the strain at failure, varying in the range 3.6 ÷ 6.1 %, is in line with similar studies in which the analysis was conducted at the level of thread rather than of the single filaments.

In Figure 3.10 the mean values of the strength of different series are compared. The filaments get the highest strength value, equal to 411 MPa, while the threads of the series Flax-T, assume a mean value of strength equal to 354 MPa. The latter,

being assessed on threads meant to reinforce matrices, can be considered as the nominal strength of the textile adopted as reinforcement in inorganic matrix composites. The lower strength observed in the flax strips may be attributed to a non-uniform stress distribution in the different threads, yarn and filaments constituting the fabric. However, this aspect, seems to provide greater uniformity in the mechanical response of the material as confirmed by the coefficient of variation associated to the tensile strength that significantly decreases by increasing the size of the specimen (Table 3.2). The mechanical behaviour of the series Flax fabric-6cm is the most representative of the textile adopted in TRM applications (and for instance in Flax TRM tensile tests). The tensile response of the strip is characterised by an initial lower stiffness up to a quasi-linear branch in which the stress-strain curve slope is constant (Figure 3.9d). The less stiff initial branch is due, as discussed in the literature review section, to the microstructure of the filaments, and to the arrangement of the filaments within the yarns. However, a third contribution is due to the structure of the fabric itself, characterised by yarns differently loaded due to the non-uniform distribution of the stresses. The mean axial strain corresponding to the failure is equal to 5%. It is important to underline that this value take into account also of the initial less stiff behaviour of the textile. In the applications, such behaviour can be modified in order to have a linear elastic response of the textile.

The experimental analysis showed above provides the main mechanical parameters concerning the flax textile. Such values are of fundamental importance in designing process of composite materials reinforced with flax fabric.

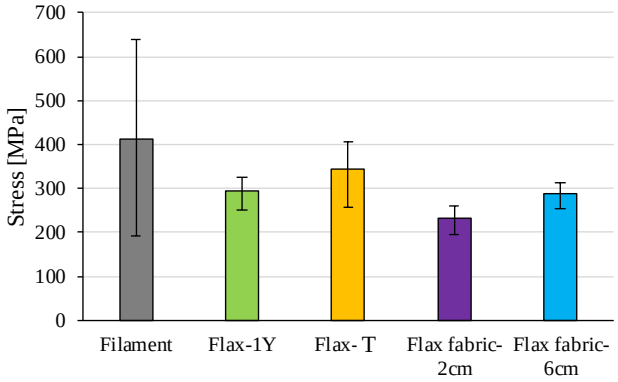

Figure 3.10: Tensile strength of different sized falx samples.

3.3 Durability of flax fibres

The flax textile under consideration is meant to be used as reinforcement in composite systems with different kinds of binders (mainly lime and cement) as

matrix, depending on the field of application of the composite. In case the system is used as reinforcement of existing masonry buildings, it is required the use of materials to be as consistent as possible with the ones the masonry structure is made of. In such cases, the use of hydraulic lime-based mortars is recommended. In many other cases the use of cement-based matrices may be more appropriate.

The use of plant fibres in cement-based materials gives rise to several problems in terms of durability. The two main ageing effects that arise in such alkaline environments are the alkaline hydrolysis and the mineralisation process of fibres constituents [101]. As known, plant fibres are characterised by three main components:

- cellulose, the main structural component;
- hemicellulose, generally present along with cellulose in almost all plant fibres;
- lignin, a binding phase for cellulose.

The high alkaline water content of the pores leads to the dissolution of hemicellulose and lignin and causes the alkaline hydrolysis of cellulose cells reducing the degree of polymerisation and the strength of the fibres. The mineralisation process, instead, is the result of the migration of hydration products, mainly $Ca(OH)_2$, into the voids and lumen walls of the fibre structure [102].

3.3.1 Methods

With the aim of studying the durability performance of flax fibres considering their application in inorganic matrices, in this section three ageing protocols are presented. They consist in putting flax threads in specific environments and in testing them after a period of exposure. After the removal from the exposure environment the samples were dried in environment conditions for 24 hours before being tested. The samples were flax threads, defined before as Flax-T, 15 cm long, and they were tested in tension by means of a SANS Universal Testing Machine having a capacity of 10 kN, in displacement control mode with a rate of 4 mm/min by using a load cell of 1 kN. The gauge length during the test was 100 mm. Each series of specimens was characterised by a number of samples between 12 and 15. The tensile strength obtained by testing the specimens of series Flax-T was considered as a reference value.SEM analysis was carried out on representative specimens to deeply investigate the state of the fibres after the exposure periods. The implementation of ageing protocols, the tests and the SEM analysis were executed at the Department of Industrial Engineering of University of Salerno.

3.3.1.1 Ageing protocol 1

According to acceptance criteria reported in the literature [57], fabric reinforced cementitious matrix composite systems are required to comply with various limitations related to the durability of the material. Specifically, three different ageing environments have to be considered for the samples to be exposed; exposure time and target limits in terms of strength decay are also defined.

The different environments consist of water, saltwater (to reproduce the marine environment), and alkali water. As a preliminary step of a more detailed study to be carried out on the entire composite, fibres were exposed to these environments to check their sensitivity on that. A period of exposure of 1000 h was chosen. The ageing conditions are listed in detail as follow:

- *Flax-T Water 1000*: the threads were immersed in 500 ml of deionised water for a period of 1000 h (~42 days);
- *Flax-T Salt 1000*: the threads were immersed in 500 ml of saline solution of deionised water with a concentration of 3.5 % in weight of NaCl for a period of 1000 h (~42 days);
- *Flax-T Alk 1000*: the threads were immersed in 500 ml of alkaline solution with a pH of 9.5 obtained by adding to deionised water NaOH with concentration of 0.32% in weight, for a period of 1000h (~42 days).

All the above-mentioned ageing conditions were performed at laboratory temperature and relative humidity (20 °C and 50 %, respectively).

3.3.1.2 Ageing protocol 2

The ageing protocol 2 represents a preliminary study aiming at assessing the decay of mechanical properties of flax threads once embedded in mortars. On the basis of similar studies in the literature [81], flax fibres were embedded in fresh mortar, then removed after a given period of embedment, and then tested in tension to check any loss of strength. Two types of mortars were chosen:

- a hydraulic lime-based mortar: a structural grout of natural hydraulic lime for the impregnation of fabrics for structural reinforcement provided by the company Innovation s.r.l. with the name of *FIDCALX NHL5®*;
- a cement-based mortar: a mortar based on hydraulic cement binders for bonding and embedment of fabrics provided by the company Innovation s.r.l. with the name of *Kimisteel LM Sta-0217*.

Both mortars are suitable to be used as matrices in fibre reinforced composite systems. For each type of mortar three series of flax threads were considered respectively having a time of exposure of 7, 28 and 56 days. This method allows monitoring the loss of strength with the time of exposure. According to the technical

data sheets provided by manufacturers the compressive strength of the mortars employed was, respectively, 15 MPa for the hydraulic lime-based and 45 MPa for the cement-based. The ageing conditions adopted are listed in detail as follow:

- *Flax-T H-lime (7-28-56 days)*: the threads were embedded in hydraulic lime mortar for a period of 7, 28 and 56 days;
- *Flax-T Cement (7-28-56 days)*: the threads were embedded in cement mortar for a period of 7, 28 and 56 days.

Both ageing conditions were performed at laboratory temperature and relative humidity (20 °C and 50 %, respectively).

3.3.1.3 Ageing protocol 3

The ageing protocol 3 considered a specific water solution, appropriately designed to reproduce hydraulic lime- or cement-based mortar conditions [41]. Two solutions were considered differing in the type of chemical components. Controlled temperature conditions were chosen to reproduce an accelerated ageing process. The ageing conditions are listed in detail as follow:

- *Flax-T Environment A (7-28-56 days)*: the threads were immersed for a period of 7, 28 and 56 days in solution thought to reproduce hydraulic lime conditions (16 wt% of $Ca(OH)_2$ in distilled water, pH=12.37). A closed container with fibres immersed in the solution was kept at 55 °C;
- *Flax-T Environment B (7-28-56 days)*: the threads were immersed for a period of 7, 28 and 56 days in a solution thought to reproduce cement conditions (16 wt% of $Ca(OH)_2$, 1 % of Na(OH) and 1.4 % of K(OH) in distilled water, pH=13.1). A closed container with fibres immersed in the solution was kept at 55 °C.

This ageing protocol was conceived to reproduce the real decay of mechanical properties of the fibres in the long term once embedded in inorganic matrices.

3.3.2 Results and discussion

Figure 3.11 shows the stress-strain response of the series of specimens subjected to the ageing protocol 1. Specifically, the three graphs concern the threads immersed for 1000 h respectively in water, saltwater and alkaline solution. The threads were extracted from the fabric in the warp direction, therefore, the series Flax-T-warp was considered as a control series representing the response before the ageing process. The main values of the mechanical properties, with the respective coefficient of variation, are listed in Table 3.3. According to the ageing protocol 2 samples embedded either in a cement- or in a hydraulic lime-based mortar were tested after a conditioning period of 7, 28, and 56 days. The tensile response, in terms of stress-

strain, for each conditioning environment and for each conditioning period, is shown in Figure 3.12 and Figure 3.13. The main values of the mechanical properties, with the respective coefficient of variation, are listed in Table 3.4.

The results of stress strain curves concerning the specimens subjected to the ageing protocol 3 are shown in Figure 3.14 and Figure 3.15. Tensile tests were respectively performed after 7, 28 and 56 days. Due to the high degradation of the specimens subjected to the Environment A for a conditioning period of 56 days, no tensile response was recorded concerning this series. The main values of the mechanical properties, with the respective coefficient of variation, concerning the samples aged in Environment A and B are listed in Table 3.5.

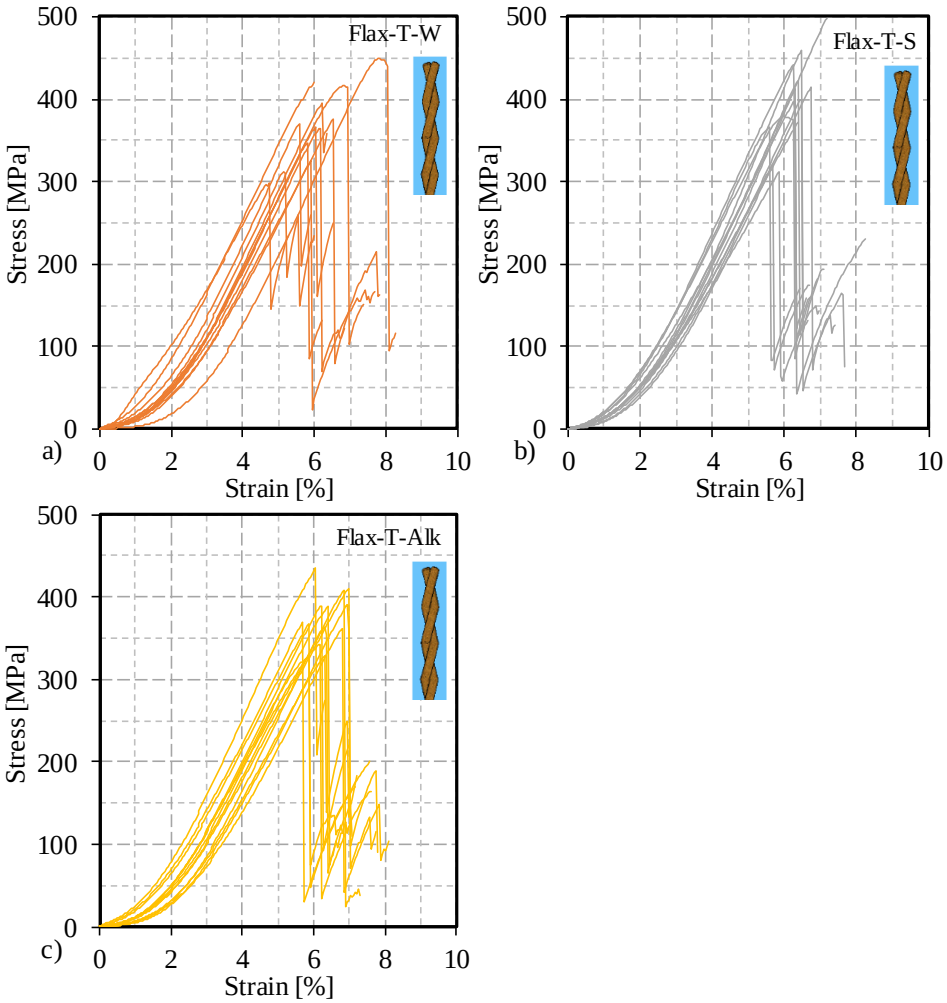

Figure 3.11: Tensile stress-strain diagrams of flax threads subjected to ageing protocol 1.

Table 3.3: Mechanical properties of flax samples subjected to ageing protocol 1.

	Ageing environment	Curing period	Numb. of spec.	P_u		f_t		ε_u	
				Mean (N)	Co.V. (%)	Mean (MPa)	Co.V. (%)	Mean (%)	Co.V. (%)
Flax-T	Control	-	12	92	10	361	10	5.20	11
Flax-T	Water	1000h	12	96	11	377	11	6.08	13
Flax-T	Saltwater	1000h	13	102	13	401	13	6.29	7
Flax-T	Alkaline water	1000h	13	96	9	376	9	6.34	7

Some of the series are characterised by less than 15 samples. Few specimens were discarded due to a not correct execution of the test. Tensile strength, f_t, was calculated based on the nominal cross-section of Flax-T specimens in the unexposed configuration. The ageing protocol 1 represents a preliminary analysis of the durability of the fibres in view of its application in textile reinforced composites according to what is suggested by acceptance criteria [57]. As shown in Figure 3.17, no significant reduction in terms of strength was observed for each conditioning environment considered, with respect to the reference series of unexposed specimens. A similar behaviour was observed in another study available in the literature [44], in which the small strength variations recorded after the conditioning period were attributed to causes of statistic nature. An appreciable increase of deformability was indeed observed with larger main values of the ultimate strain, ε_u. This experimental evidence may be attributed to some material degradation (weight loss) leading to the loosening of the twisted yarn, and, hence, to larger strain values.

Table 3.4: Mechanical properties of flax samples subjected to ageing protocol 2.

	Ageing environment	Curing period	Numb. of spec.	P_u		f_t		ε_u	
				Mean (N)	Co.V. (%)	Mean (MPa)	Co.V. (%)	Mean (%)	Co.V. (%)
Flax-T	Control	-	12	92	10	361	10	5.20	11
Flax-T	Hydraulic lime mortar	7 days	15	78	10	306	10	3.45	7
Flax-T		28 days	12	75	8	295	8	3.68	9
Flax-T		56 days	15	75	6	293	10	3.44	9
Flax-T	Cementitious mortar	7 days	15	72	10	284	10	3.34	9
Flax-T		28 days	14	71	10	280	10	3.45	12
Flax-T		56 days	15	67	13	262	13	3.04	11

Although representing a preliminary study that precedes an investigation at the level of the composite material, this analysis highlights the low aggressive nature of the conditioning protocol that does not trigger any ageing phenomena. A longer immersion period and/or higher temperature conditions may enhance the efficiency

of the ageing protocol applied on the flax threads and possibly also on the composite system itself.

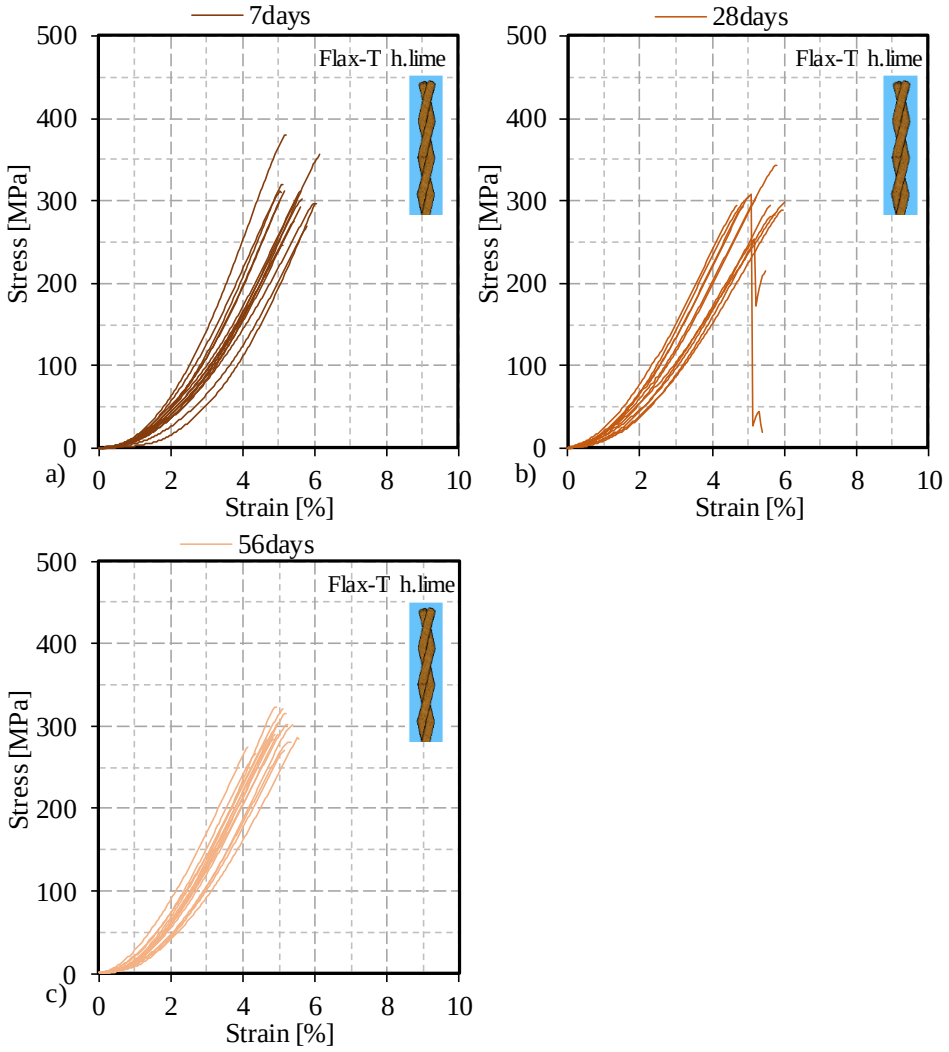

Figure 3.12: Stress-strain curves of threads in hydraulic lime mortar (ageing protocol 2).

The mean values of the tensile strength of the specimens subjected to the ageing protocol 2 are shown in Figure 3.18. A moderate loss of strength was observed in hydraulic lime and cement matrices conditioning environments. Concerning the decreasing deterioration over time in both cases the damage seemed to mainly occur during the first days of the mortar hydration process and to stop then up to 56 days. The reduction of tensile strength consisted of about the 16 % in case of hydraulic lime-based matrix environment, and of about the 22 % in case of

cement-based matrix. Besides the short exposure time, the results seem to confirm that the cement mortar environment is more aggressive than the hydraulic lime one [102].

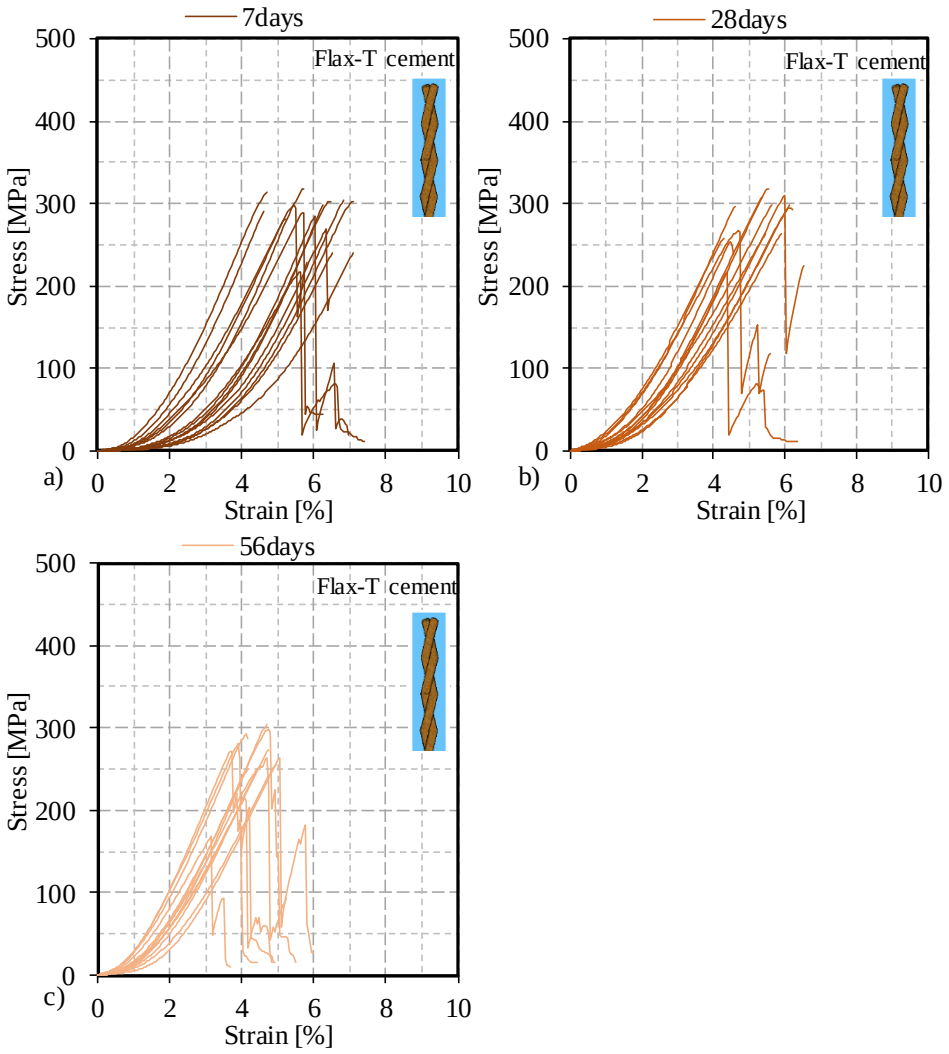

Figure 3.13: Stress-strain curves of threads in cementitious mortar (ageing protocol 2).

It is worth to highlight that such slight decay of strength may also be partially attributed to a superficial damage of the bundle as a consequence of an abrasive effect when fibres were extracted from the hardened mortar prior the testing. Further investigation, complying with long term exposures conditions, are needed to deeply define the ageing of flax fibres due to the aggressiveness of the mortar hydration products. Aiming at investigating in depth the degradation phenomena a Scanning

Electron Microscope analysis was performed. Figure 3.20 and Figure 3.21 depict filaments comprising flax threads, after 28 days of immersion in hydraulic lime and cement mortars, respectively. For comparison, an unexposed reference sample is shown in Figure 3.22.

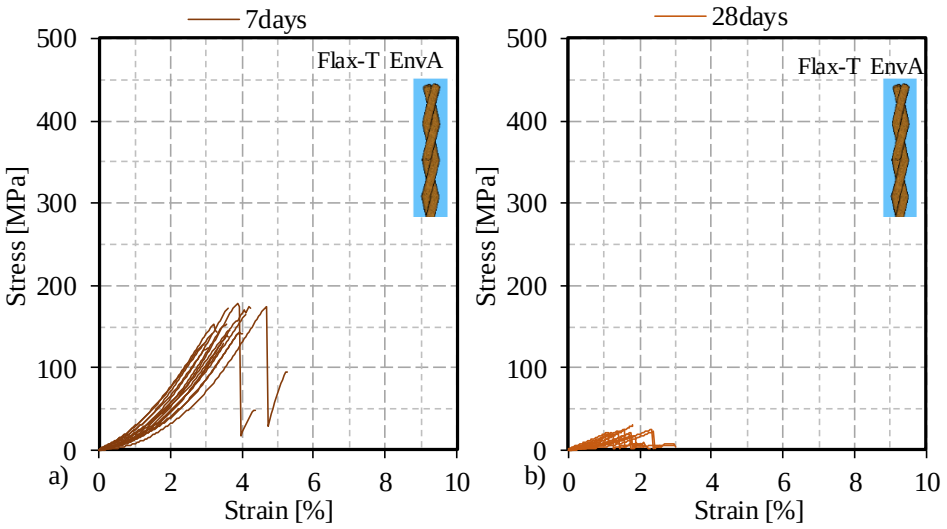

Figure 3.14: Stress-strain diagram of flax threads in Environment A (ageing protocol 3).

The pictures show the widespread presence of hydration products on the flax filaments' surface attesting a good interaction, in terms of adhesion, between fibres and matrix. Due to the alkaline hydrolysis process, the external wall of the filaments is clearly damaged with respect to the non-aged filaments, causing on a global scale a reduction in terms of tensile strength.

Table 3.5: Mechanical properties of flax samples subjected to ageing protocol 3.

	Ageing environment	Curing period	Numb. of spec.	P_u		f_t		ε_u	
				Mean (N)	Co.V. (%)	Mean (MPa)	Co.V. (%)	Mean (%)	Co.V. (%)
Flax-T	Control	-	12	92	10	361	10	5.20	11
Flax-T	Environment A	7 days	15	39	12	151	12	2.48	8
Flax-T		28 days	12	5	10	21	10	1.18	9
Flax-T		56 days	-	-	-	-	-	-	-
Flax-T	Environment B	7 days	15	36	11	141	11	2.69	11
Flax-T		28 days	14	18	12	70	12	1.89	8
Flax-T		56 days	15	19	12	76	10	1.66	9

However, fibre/matrix adhesion is very important in fibre reinforced composites for stress transfer at the interface both for synthetic and plant fibres [103, 104].

Thus, even if fibres' mechanical properties slightly decrease, an increase of surface roughness may improve fibre/matrix adhesion and, consequently, fibre reinforced composite mechanical properties.

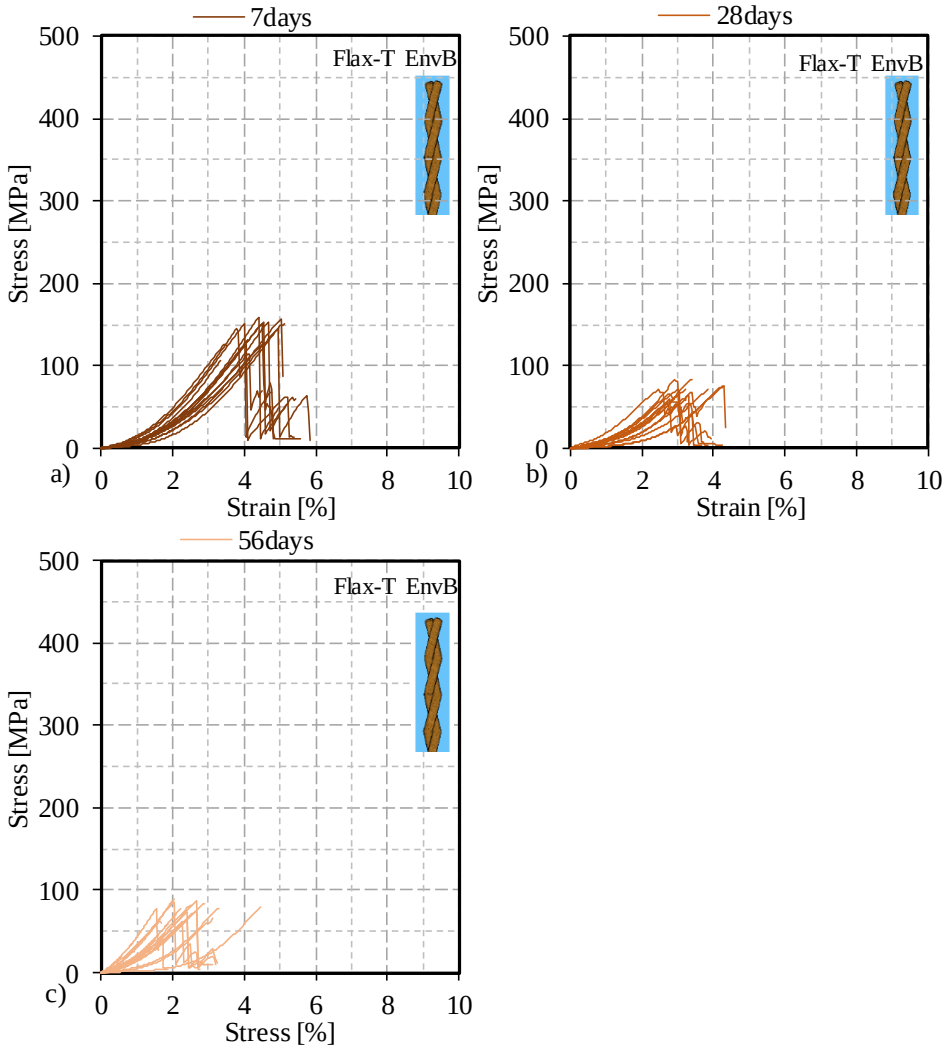

Figure 3.15: Stress-strain diagram of flax threads in Environment B (ageing protocol 3).

The ageing protocol 3 consists in two specific water solutions designed to accelerate the effects of the hydraulic lime and cement mortars on the mechanical behaviours of the reinforcement. Although the use of high temperatures helps to

accelerate the degradation phenomena providing information on a long-term, it also creates difficulties in quantifying the corresponding time in natural temperature conditions.

According to [41], 7, 28, and 56 days of accelerated exposure at a temperature of 55 °C should respectively correspond to about 3, 11, and 20 years in natural conditions. The mean values of the tensile strength concerning the series of specimens subjected to the ageing protocol 3 are shown in Figure 3.19.

Both series exposed to Environments A and B showed a loss of tensile strength of about 60 % after 7 days of conditioning. Flax threads exposed to Environment A for a period longer than 7 days were characterised by a strength loss equal to 95 % after 28 days and completely disintegrated after 56 days (Figure 3.16).

Flax threads exposed to Environment B showed a decrease of the mechanical properties of about 80 % after 28 days staying mainly constant up to 56 days. The degradation of the fibres may be attributed to the alkaline hydrolysis of lignin and non-cellulosic constituents of flax, accelerated by the exposure to 55 °C.

Figure 3.16: Degraded Flax-T Env A threads after 56 days of exposure.

Figure 3.23 and Figure 3.24 show SEM images of samples exposed for 28 days to Environment A and B, respectively; while a reference sample is shown in Figure 3.25. By comparing the pictures it can be seen that Environment A resulted to be more aggressive than Environment B, in terms of impurities, waxes and non-cellulosic compounds removal, confirmed by the higher amount of degradation products mixed to solution residues (Figure 3.23) compared to Flax-T Env-B 28 days sample (Figure 3.24).

Moreover, as reported in the literature [105], increasing the alkalinity of the solution an increase of the crystallinity index is obtained, probably due to a better packing of cellulose chains thanks to the removal of non-cellulosic materials. Thus, the higher mechanical properties of Flax-T Env-B samples can be explained considering an increase of cellulose crystallinity.

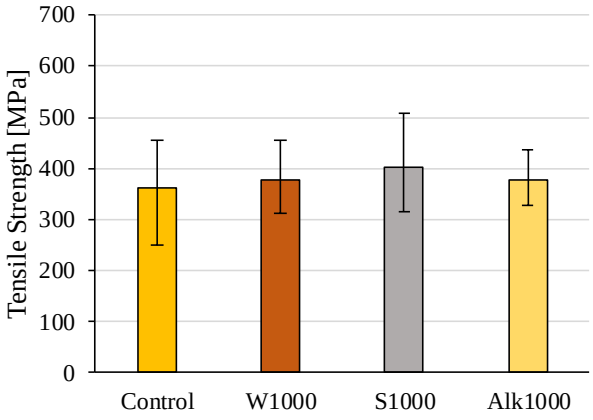

Figure 3.17: Tensile strength of series belonging to the ageing protocol 1.

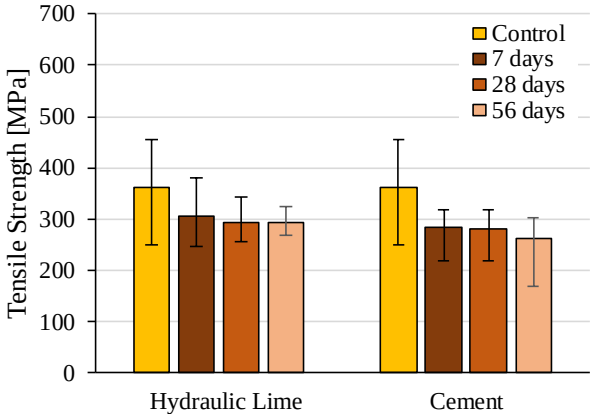

Figure 3.18: Tensile strength of series belonging to the ageing protocol 2.

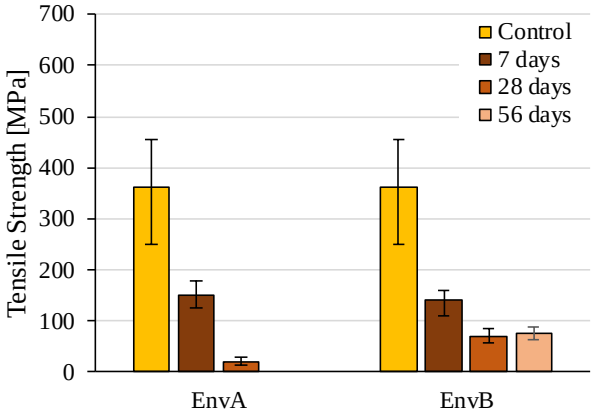

Figure 3.19: Tensile strength of series belonging to the ageing protocol 3.

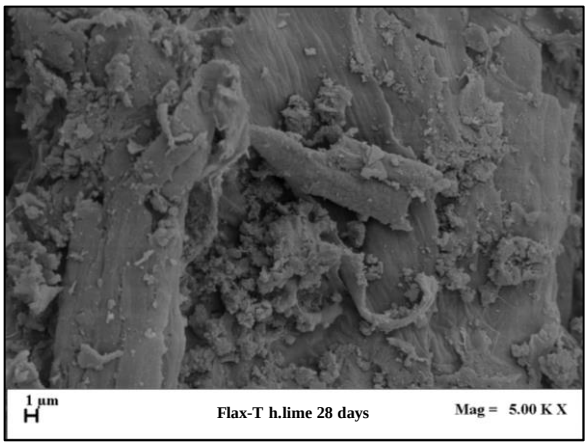

Figure 3.20: SEM image of Flax-T h.lime 28 days sample (5000X).

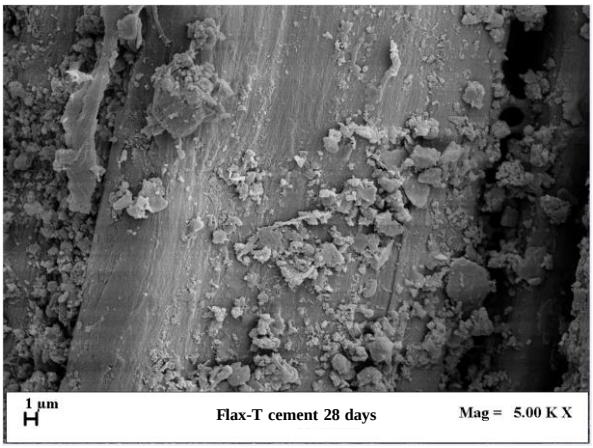

Figure 3.21: SEM image of Flax-T cement 28 days sample (5000X).

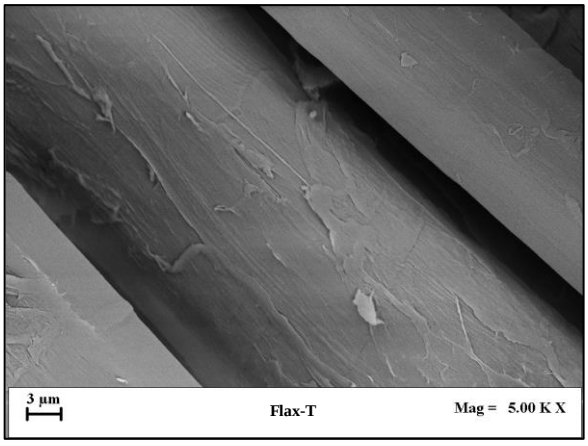

Figure 3.22: SEM image of a reference Flax-T sample (5000X).

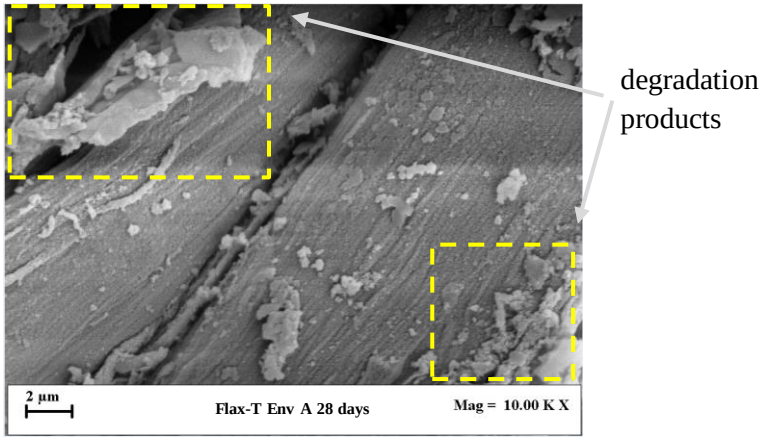

Figure 3.23: SEM image of Flax-T Env-A 28 days sample (10000X).

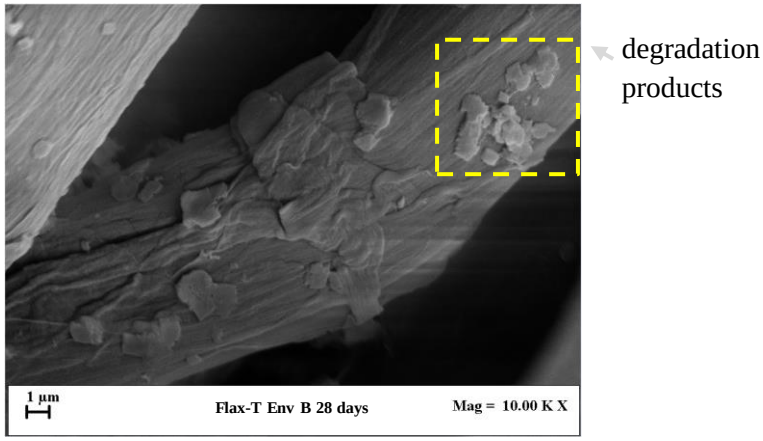

Figure 3.24: SEM image of Flax-T Env-B 28 days sample (10000X).

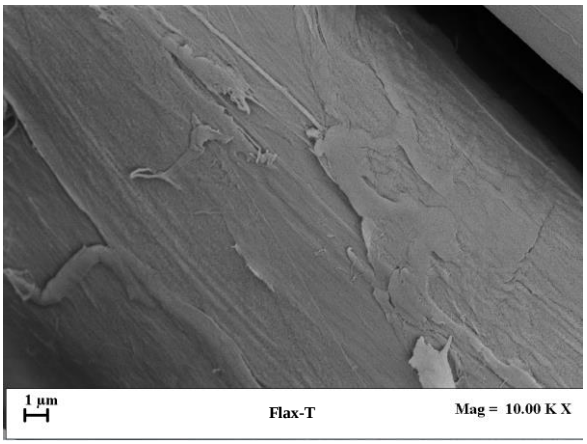

Figure 3.25: SEM image of a reference Flax-T sample (10000X).

3.4 Conclusions

The present chapter proposes a comprehensive characterisation of flax textile to be used as reinforcement in Textile Reinforced Mortar (TRM) composite systems. The main findings of the experimental analysis are summarised as follows:

- the flax main thread exhibits a tensile strength of 354 MPa, a Young's modulus of 9.3 GPa and a strain at failure of 5.6 %, which is consistent with other results recently reported in the literature on similar fibres [106];
- on the contrary, the degradation of mechanical properties induced by the three ageing protocols considered was significantly lower than expected;
- specifically, ageing protocol 1 (immersion in water, saltwater and alkali water solutions for 1000 h) did not lead to any significant decay in the tensile strength of flax threads;
- similarly, flax threads after 7 days of immersion in either hydraulic-lime or cement mortar (ageing protocol 2) suffered a reduction in strength of about 16 % and 22 %, respectively; however, no further reduction was observed in either cases for longer immersion durations until 56 days;
- conversely, in ageing protocol 3, a more significant decay in mechanical properties was observed with a complete loss of strength in specimens immersed for 56 days at a temperature of 55 °C: this was due to the prolonged exposure at harsh ageing conditions, in terms of pH and temperature, that promoted flax fibre degradation;
- finally, SEM investigations proved the good adhesion between fibres and the investigated matrices (i.e. cement and hydraulic lime) thanks to the interlocking positions created onto fibres surface as result of alkaline hydrolysis.

These results demonstrate that the flax fibres and fabrics under investigation, with promising mechanical properties can be utilised as internal reinforcement for TRM systems that appear to be particularly appropriate in strengthening masonry structures. In terms of durability the fibres showed a good performance in the short term, and significant decreases of strength in accelerated ageing exposures. This behaviour can be extended to that of the fabric adopted as reinforcement in TRMs.

Further investigations are needed, perhaps by focusing on fabric treatments and/or coating, with the aim of improving both the mechanical behaviour and the long-terms performance. Moreover, the mechanical and durability investigation needs to be extended to the Flax TRM systems as whole to confirm the potential of this kind of sustainable composite system.

4. Mechanical behaviour and durability of Flax TRMs: tensile and shear bond tests

Once defined the properties of the TRM constituent materials, i.e. mortar and textile, to get an exhaustive analysis it is necessary to move from a *"material"* scale of analysis to the investigation of the composite itself. As widely discussed in *Chapter 2*, in order to qualify and characterise a TRM composite, it is necessary to identify its mechanical behaviour in tension and its interaction with a masonry substrate. With the aim of providing the mechanical response of the studied Flax TRM system, an experimental study is proposed at the *"composite"* scale of analysis. Specifically, the results of tensile, carried out on Flax TRM coupons, and of shear bond tests on Flax TRM-to-masonry substrate elements, are presented in this section. In addition, in view of a more comprehensive characterisation, and in line with what is proposed by standards and guidelines, the results of an experimental campaign aimed at investigating the mechanical performance of Flax TRMs exposed to several ageing environments, is presented as well.

4.1 Tensile test on Flax TRM systems

4.1.1 Materials

A hydraulic lime-based matrix was employed for the production of the Flax TRM system, as, in recent years, several studies demonstrated the efficiency of using these kinds of binders for producing composite systems to be implemented as reinforcement in historical masonry structures [13]. Specifically, the pre-mixed mortar used in the research, labelled FIDCALX NHL5® [107], is commercialised by the Italian company "Innovation s.r.l." [108]. It consisted of a premixed mortar with pure natural hydraulic lime binder and selected inert materials with a maximum granulometry of 2.5 mm. Figure 4.1 shows its grain size distribution curve, obtained by means of a vibrating test sieve machine for the grains greater than 0.074 mm [109], and by means of a laser diffraction particle sizing machine for the finest particles. As known, in TRM implementation, the mortar penetrability within the textile is hindered if the maximum aggregate diameter is about 2÷2.5 times larger than the fabric clear opening. Being the 99% of the aggregates smaller than 1.19 mm

and being the flax textile clear opening of about 3 mm, it can be considered a compatibility between the two composite components.

The mortar was produced by mixing an amount of water equal to 19 % (in weight) of the pre-mixed formula of binder and aggregates, as recommended by the manufacturer. The water-to-binder ratio of the mixture was equal to 0.60. It was characterised by a consistency at the fresh state of 230 mm, according to the EN 1015-3 [110]. The mechanical performance of hardened mortar was evaluated, at every TRM reinforcement casting, for each mortar batch, at 28 days, in accordance to the EN 191-1 [111] on prismatic samples in order to get the flexural and compressive strength. The mean values of the flexural and compressive strength were respectively equal to 3.58 MPa and 8.02 MPa.

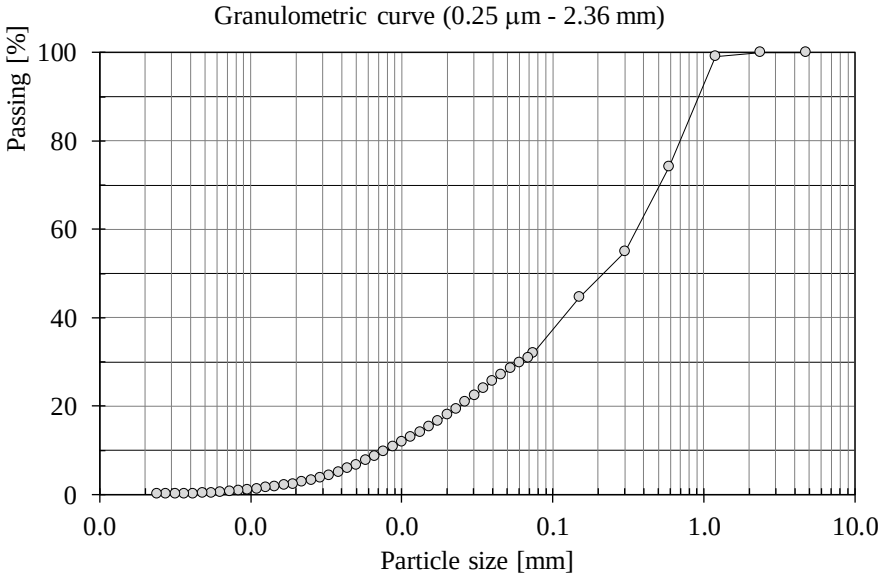

Figure 4.1: Grain size distribution curve for lime-based premixed matrix powder.

The textile adopted consists in the flax fabric described in *Chapter 3*, whose physical properties are listed in Table 3.1 and whose mean mechanical properties, assessed on a single thread, are a tensile strength of 354 MPa, a Young's modulus of 9.3 GPa and a strain at failure of 5.6 %.

4.1.2 Methods

Flax TRM coupons were performed, by means of a wet lay up method, according to the guidelines reported in the ACI 549 [58]. The specimens were cast by alternating mortar layers and flax textile plies. The first layer of mortar, of about 2.5 mm, was applied on the base of the mould, then the flax strip was placed on it by ensuring it

to be clamped along two edges of the specimens, so that it was kept as stretched as possible (Figure 4.2a). The textile was pressed by means of a roller to guarantee full impregnation of the fabric within the mortar (Figure 4.2c). The next layer of mortar, having the same thickness of the first one, was placed on it. The procedure was iterated for multi-plies' configurations in which more than one textile layer were placed within the system, always making sure a layer of mortar to be placed between two fibre strips to completely fill the grid voids. The application of the outer layer of mortar was performed by thoroughly smoothing it (Figure 4.2b).

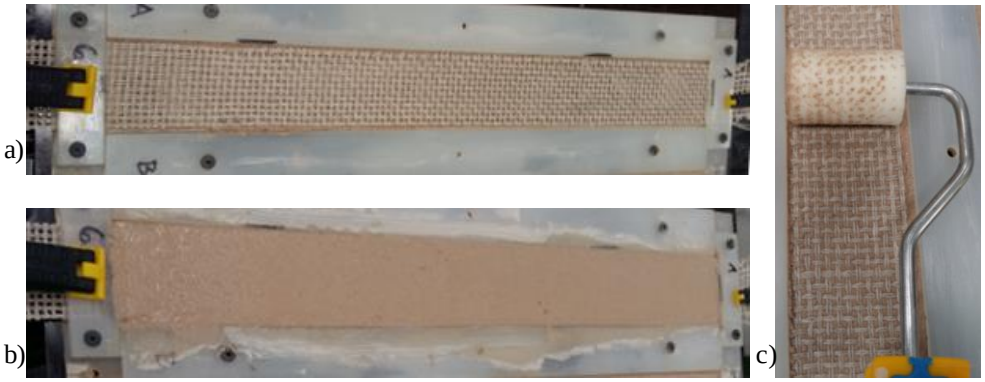

Figure 4.2: Flax TRM specimen implementation: a) application of the textile; b) application of the outer layer of mortar; c) pressure application on the textile.

Two reinforcement configurations were taken into account in the present study: the first one, labelled as Flax-TRM-1L, consisted of a TRM characterised by a thickness of 5 mm and by one layer of reinforcing flax textile, with a fibre volumetric ratio equal to 2.04 %; the second one, labelled as Flax-TRM-2L, was characterised by a thickness of 8 mm and by two plies of flax fabric overlapping each other by means of a thin layer of mortar, with a resulting fibre volumetric ratio equal to 2.55 %.

Two series of specimens, performed by means of the two above mentioned reinforcement configurations, were considered:

- Flax-TRM-1L-T: specimens characterised by the reinforcement configuration Flax-TRM-1L, and tested in tension (Figure 4.3 a);
- Flax-TRM-2L-T: specimens characterised by the reinforcement configuration Flax-TRM-2L, and tested in tension (Figure 4.3 b).

The specimens were characterised by a length of 500 mm, of which 300 mm in the middle represented the free length between the steel tabs glued to the specimen edges to transfer the load from the testing machine to the TRM. Further details concerning the two series of specimens are shown in Table 4.1, in which $f_{textile}$

represents the main tensile strength exhibited by flax strips 60 mm large (series labelled as Flax fabric-6 cm in *Chapter 3*), and *vf* the fibre volumetric reinforcement ratio. The coupons, characterised by a width of 60 mm (Figure 4.4a), contained, with respect respectively to the Flax-TRM-1L-T and Flax-TRM-2L-T series, 24 and 48 flax threads (the thread to which reference is made is the one defined as Flax-T in *Chapter 3*). For each series of specimens three mortar prisms were cast to mechanically characterise the matrix (Figure 4.4b).

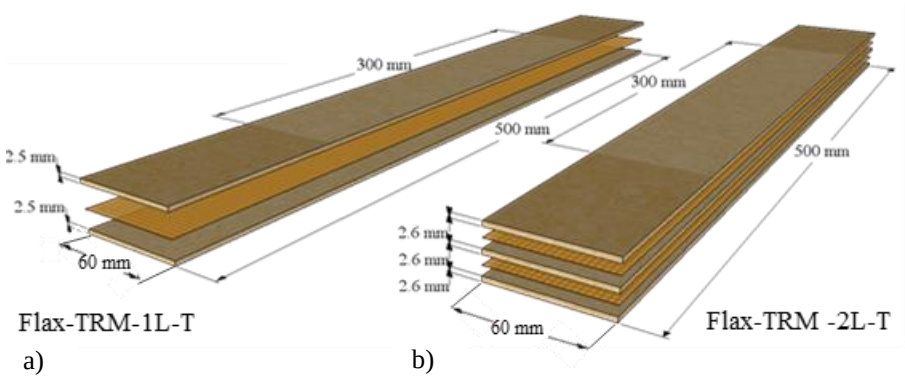

a) b)

Figure 4.3: Flax-TRM coupons tested in tension: Flax-TRM-1L-T, characterised by one layer of flax textile; Flax-TRM-2L-T, characterised by two flax textile plies.

Table 4.1: Main properties of the tensile test series of specimens.

Series	Number of specimens	Section (mm x mm)	A_{mortar} (mm^2)	$A_{textile}$ (mm^2)	*vf*	$f_{textile}$ (MPa)
Flax TRM-1L-T	4	5 x 60	300	6.1	2.04%	286
Flax TRM-2L-T	5	8 x 60	480	12.2	2.55%	

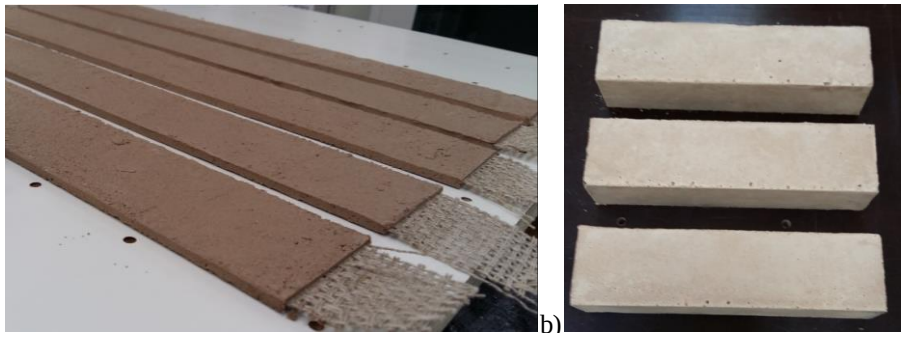

a) b)

Figure 4.4: a) Flax-TRM-1L-T specimens; b) mortar prisms.

Tensile tests were carried out at the laboratory STRENGTH of University of Salerno by means of a Zwick Roell Schenck Hydropuls S56, with a maximum

capacity of 630 kN (Figure 4.5b). The tests were executed under displacement control and the load and the displacement between the clamping wedges of the test machine were recorded. The displacement was increased monotonically with a constant rate of 0.25 mm/min.

A gripping system specifically studied for TRM tensile tests was adopted to clamp the coupons at the two charged edges for a length of 100 mm. (Figure 4.5a). Two stiff steel plates were glued at the edges of the specimens by means of an epoxy resin, with a bond length of 100 mm, so that the tensile load is transferred by shear stresses (clevis system). On the edges of the plates four bolts were placed in order to eventually apply a compression stress, when needed (clamping system). A further bolt was placed in the middle with the aim of realising a rotational release in the specimen plane. The latter was connected to a metallic system that constituted a hinge allowing the rotations out of plane. The hinge system was specifically studied to prevent bending and twisting moments to be transferred to the specimens in tension. If needed, the two hinges bolts may be tightened to create a perfectly clamped configuration. In the present study both rotations were permitted, and no compression was applied at the edges of the specimens.

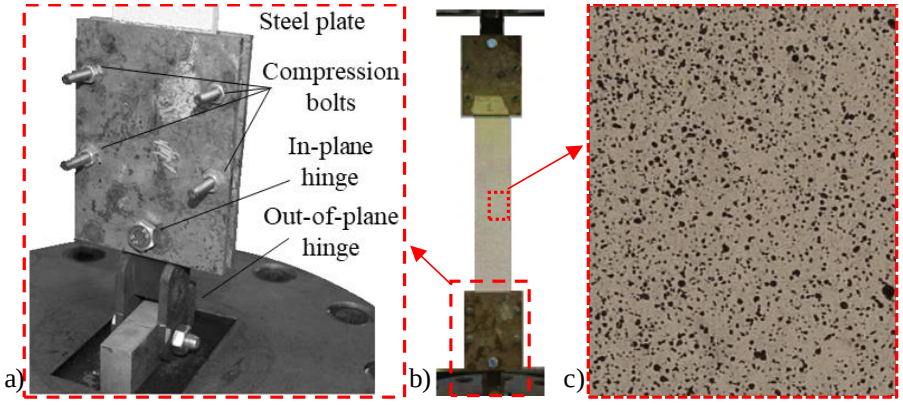

Figure 4.5: a) TRM tensile test clamping system; b) TRM tensile test set-up; c) surface treatment for Digital Image Correlation photos.

The external surface of the specimens, along the gauge length, was treated in order to get, during the test, images to be used for a Digital Image Correlation (DIC) analysis. The treatment consisted in creating a white background on which black dots were stochastically sprinkled by means of a spray can (Figure 4.5c). DIC analysis showed to be an efficient method to study the displacement field of TRMs under tensile tests [15]. During the test the camera for the acquisition of the photos was placed at a focal distance of 50 cm. The acquisition rate was of 3 ph/min and the resolution of the photo was of 3454 x 5184 pixels (0.06 mm/pix).

4.1.3 Results and discussion

The tensile response of Flax TRMs in terms of load-displacement is shown in Figure 4.6 and Figure 4.7.

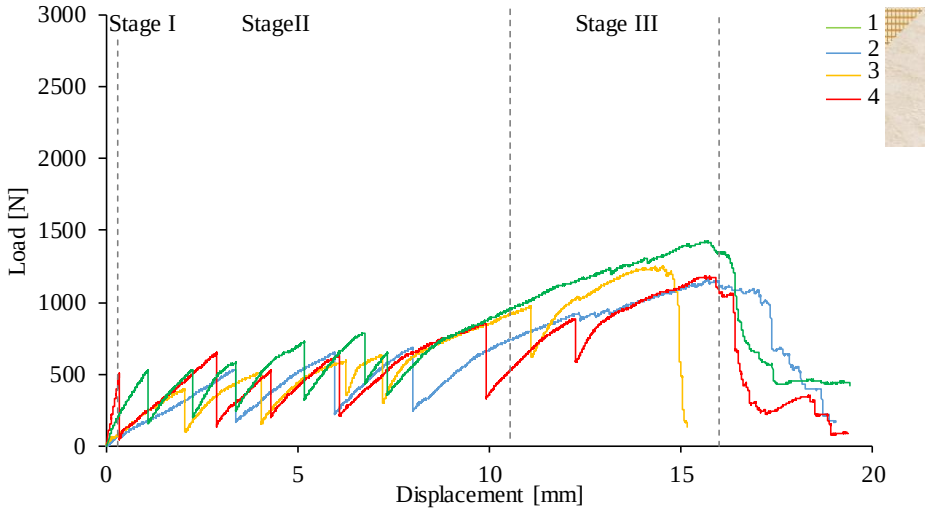

Figure 4.6: Load-displacement curves concerning Flax TRM-1L-T specimens.

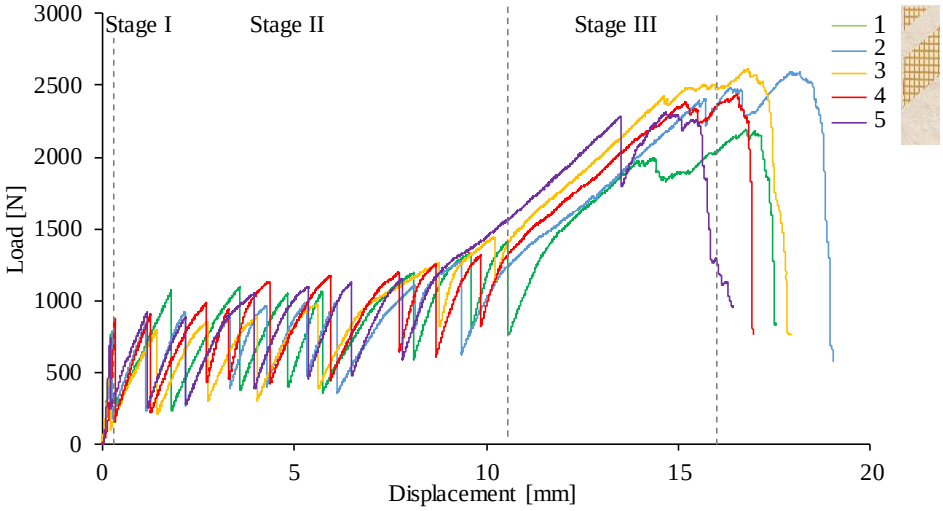

Figure 4.7: Load-displacement curves concerning Flax TRM-2L-T specimens.

The tensile response in terms of stress-strain is shown in Figure 4.8 and Figure 4.9. When the specimen is uncracked, it can be assumed that the entire cross-section is characterised by a constant normal stress, while in the cracked configuration, in proximity of the cracks, it can be assumed that the dry textile is charged of the entire

applied load. Therefore, the normal stress was assessed with respect to both the mortar cross section and the dry textile cross section. The strain was approximately evaluated as the ratio between the global displacement and the gauge length.

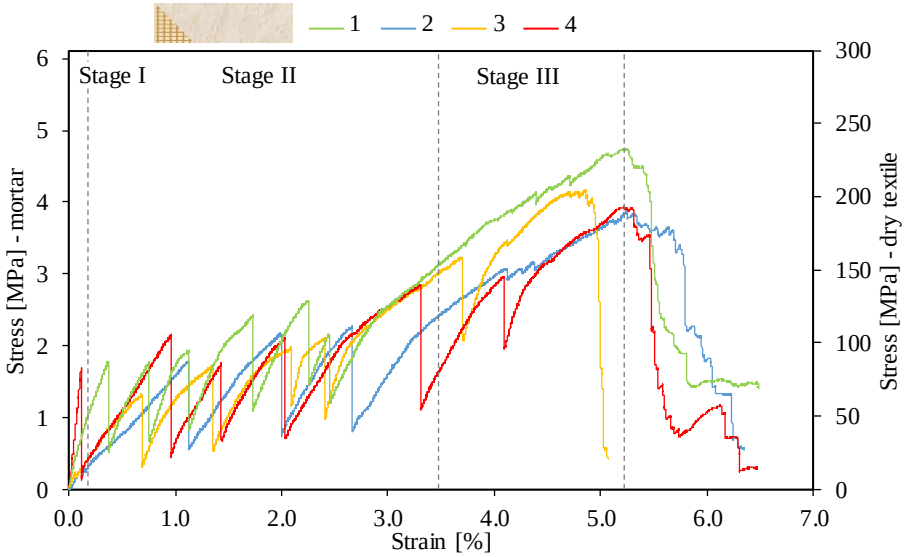

Figure 4.8: Stress-strain curves concerning Flax TRM-1L-T specimens.

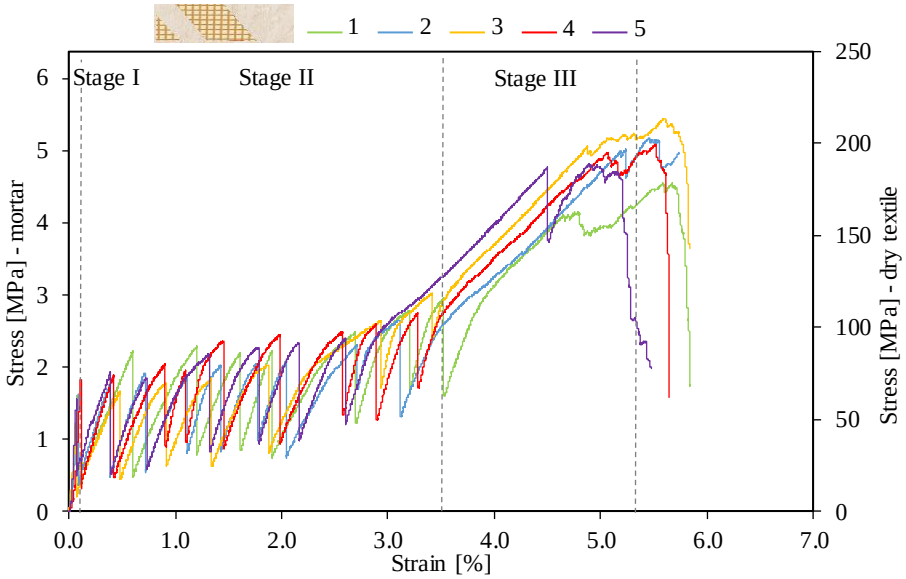

Figure 4.9: Stress-strain curves concerning Flax TRM-2L-T specimens.

As expected, the mechanical response was characterised by three stages:

- the first stage represented the elastic response up to the occurrence of the first crack;
- the second one represented a transition behaviour characterised by the development of several cracks;
- the third was mainly governed by the textile mechanical behaviour.

The transition point between the second and the third stage (σ_2, ε_2) corresponds to the point, after the last crack, in which the slope of the stress-strain curve changes (Figure 4.10). In same cases, where the last crack occurred in proximity of the failure mode, this transition point is considered in correspondence of the penultimate crack.

In the elastic response stage, the coupon remained uncracked and the entire composite bore the applied load. Being the specimen characterised by a constant section along the length, the first crack randomly occurred at any point, depending on geometric imperfections, or concentrations of stress in proximity of the loaded edges. Except for the specimen Flax TRM-1L-T-4, the other specimens belonging to the series Flax TRM-1L-T did not present an elastic phase because, due to their thinness, they were cracked before being tested.

The transition phase was characterised by large displacements and by a sequence of significant drops in the applied load corresponding to the occurrence of cracks. Such mechanical response, in line with similar research studies in which plant fibres were employed [81, 82], resulted not consistent with the typical behaviour exhibited by TRM composite with high strength synthetic textiles. Moreover, such behaviour may be also due to a not adequate degree of mechanical interlock between matrix and reinforcement. This issue may be solved by correctly defining the matrix mix design (aggregates granulometry and consistency).

Such behaviour may be attributed to two aspects. On one hand, the (out of plane) deformability of the textile, due to the absence of any impregnation treatment, unavoidably resulted in the textile not to be uniformly stretched during the specimens' implementation, even though great attention was devoted to this aspect during the manufacturing process. The latter is a common aspect also in the conventional TRM coupons when dry textile is adopted. On the other hand, as widely discussed in *Chapter 3*, the mechanical response of plant fibre textile loaded in tension is typically characterised by a lower stiff initial response, due to specific macro- and micro-structure of the threads. As a result, in the elastic behaviour, at low strain levels, the textile was only partially activated, while the load is almost entirely borne by the mortar. Indeed, in terms of stress, the σ_1 is approximately equal to 50% of the mortar flexural strength (being the latter un overestimation of the

uniaxial direct tensile strength of the mortar). Consequently, at the occurrence of the first crack, leading to partial loss of the contribution of the matrix, the lower contribution of the textile caused significant drops of the load. To qualitatively deeper understand such behaviour, in Figure 4.10, the stress-strain response of a representative specimen (Flax TRM-2L-T4) was compared with the response of a representative flax strip tested in tension (series labelled Flax fabric-6cm in *Chapter 3*). Such comparison, although being approximated due to the different test conditions of the two specimens compared (the flax strips were characterised by a free length of 15 cm and were clamped; the textile within the TRM, in proximity of a crack, was under a significant concentration of stress over a short length), emphasises the discrepancy in terms of stiffness between the TRM and the dry textile at a low strain level. The comparison also highlights a similarity between the TRM stiffness in the third stage, and the dry textile stiffness in the final linear branch, confirming that, once crack saturation has been achieved, the response is mainly governed by the dry textile.

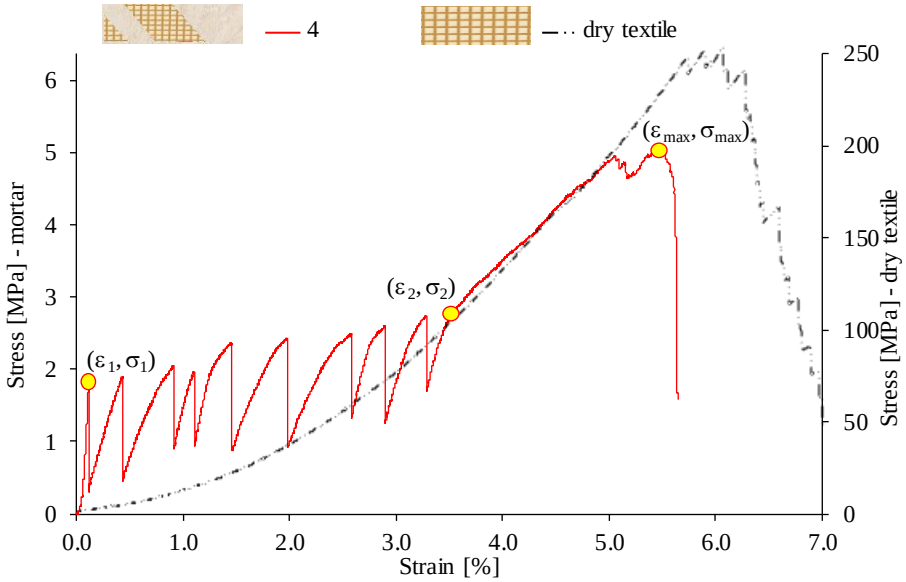

Figure 4.10: Comparison between stress-strain response in tension of a representative TRM specimen (series Flax TRM-2L-T), and a representative dry textile (series Flax fabric-6cm).

The main mechanical parameters deriving from tensile tests on the two series of specimens, together with the mean value and the coefficient of variation for each series, are listed in Table 4.2. Specifically, P_{max} represents the maximum load, $disp_{max}$ represents the displacement corresponding to the maximum load, σ_{max} represents the

maximum tensile stress assessed with respect to the entire TRM cross section, ε_{max} represents the axial strain corresponding to the maximum stress, $\sigma_{textile}$ represents the maximum tensile stress assessed with respect to the flax textile cross section, $\sigma_{max}/f_{textile}$ represents the exploitation ratio evaluated as the ratio between the maximum textile stress achieved during the test and the textile strength. The failure mode is reported as well and named as A, when the fibres failed in a section in proximity to the end-fixtures, with B in the case of a random section through the length. As expected, the results from the two series show that by doubling the amount of textile, the maximum capacity in terms of load nearly doubled. Such experimental evidence emphasises two aspects: it confirms the maximum load to be strongly affected by the amount of textile; it points out that by increasing the fibre volumetric reinforcement ratio interlaminar shear phenomena were not recorded, hence any decrease in textile-to-mortar bond properties related to higher concentration of stress within the cross section occurred. In terms of maximum displacement, and strain, the two series of specimens exhibited a quite similar trend.

Table 4.2: Mechanical parameters of Flax TRMs tested in tension.

Specimen	P_{max} (N)	$disp_{max}$ (mm)	σ_{max} (MPa)	ε_{max} (%)	$\sigma_{textile}$ (MPa)	$\sigma_{max}/f_{textile}$ (%)	Failure mode
Flax TRM-1L-T-1	1426	15.7	4.75	5.2	233	81	A
Flax TRM-1L-T-2	1161	16.3	3.87	5.4	190	66	B
Flax TRM-1L-T-3	1249	14.5	4.16	4.8	204	71	B
Flax TRM-1L-T-4	1181	15.7	3.94	5.2	193	67	B
Mean	1255	15.6	4.18	5.2	205	72	-
Co.V. (%)	10	5	10	5	10	10	-
Flax TRM-2L-T-1	2189	16.8	4.56	5.6	179	62	A
Flax TRM-2L-T-2	2591	17.9	5.40	6.0	212	74	A
Flax TRM-2L-T-3	2615	16.8	5.45	5.6	214	75	B
Flax TRM-2L-T-4	2443	16.5	5.09	5.5	200	70	B
Flax TRM-2L-T-5	2312	14.7	4.82	4.9	189	66	A
Mean	2430	16.5	5.06	5.5	199	69	-
Co.V. (%)	7	7	7	7	7	7	-

The values of stress and strain in correspondence to the two transition points between the various stages were evaluated as well and are reported in Table 4.3.

The mean value of the stress corresponding to the occurrence of the first crack resulted lower to the flexural strength of the mortar (3.58 MPa). Such aspect is attributed to the different loading conditions between the TRM tensile test and the mortar characterisation flexural test, and to possible geometric or test set-up imperfection that may anticipate the development of the mortar cracking. With

respect to the transition point between stages II and III, it was observed a similar value with respect to the two series in terms of strain, while a slightly higher value was observed in terms of stress in the Flax TRM-2L-T series with respect to the other one. Such result is distorted by the cross section adopted, i.e. the entire TRM area. By referring to the dry textile cross section the trend would invert, with slightly lower values recoded in the Flax TRM-2L-T series.

Table 4.3: Stress and strain corresponding to the different stage transition points.

Specimen	σ_1 (MPa)	ε_1 (%)	σ_2 (MPa)	ε_2 (%)	$\sigma_{1,textile}$ (MPa)	$\sigma_{2,textile}$ (MPa)
Flax TRM-1L-T-1	-	-	2.47	2.9	-	121
Flax TRM-1L-T-2	-	-	2.22	3.3	-	109
Flax TRM-1L-T-3	-	-	2.13	2.7	-	104
Flax TRM-1L-T-4	1.65	0.11	2.92	4.3	81	143
Mean	1.65	0.11	2.43	3.3	81	119
Co.V. (%)	-	-	15	22	-	15
Flax TRM-2L-T-1	1.56	0.08	3.00	3.9	61	118
Flax TRM-2L-T-2	1.62	0.09	2.66	3.6	64	104
Flax TRM-2L-T-3	1.37	0.08	2.99	3.6	54	117
Flax TRM-2L-T-4	1.76	0.11	2.90	3.6	69	114
Flax TRM-2L-T-5	1.50	0.07	2.50	2.9	59	98
Mean	1.56	0.08	2.81	3.5	61	110
Co.V. (%)	9	19	8	10	9	8

The maximum stress achieved in the textile, in both series of specimens, was about 70 % of the maximum tensile strength of the flax textile. No differences, between the two series, in the exploitation ratio value, confirmed that the mechanical properties remained unchanged by increasing the amount of textile. Although the tensile strength of the textile was not attained, the failure mode was characterised by a sequence of sudden drops of the load, attributed to the rupture of threads (Figure 4.11c) (mode B). Such a discrepancy may be attributed to the different loading conditions of the textile when tested alone with respect to the case in which it is restrained by the TRM mortar. Moreover, during the test the slippage between mortar and textile may damage the latter. Lastly, as shown in *Chapter 3*, the inclusion of flax within the lime-based mortar causes a slight reduction of its tensile strength.

4.1.4 Analysis of the crack pattern

During the elastic stage, specimens are characterised by a roughly uniform state of stress along their length until the cracking process starts at the weakest section, whose position is uncertain. The subsequent cracks will occur in locations depending

on this initial random event. In correspondence to a crack, the entire load is borne by the textile. Such load is transferred from the textile to the mortar by means of shear stress at the fibre-to-matrix interface. According to this behaviour, the stress within the mortar increases with the distance from a cracked section, up to a value next to the mortar tensile strength, so as, to cause to cracking of the mortar section. This process of transfer of normal stress from the textile to the matrix, mainly depends on the fibre-to-matrix bond properties, and on the quantity of interfacial surface available (i.e. the volumetric fibre reinforcement ratio). In fact, by looking at Figure 4.11a and b it is clear that the presence of a larger number of cracks in the specimen characterised by a higher amount of textile.

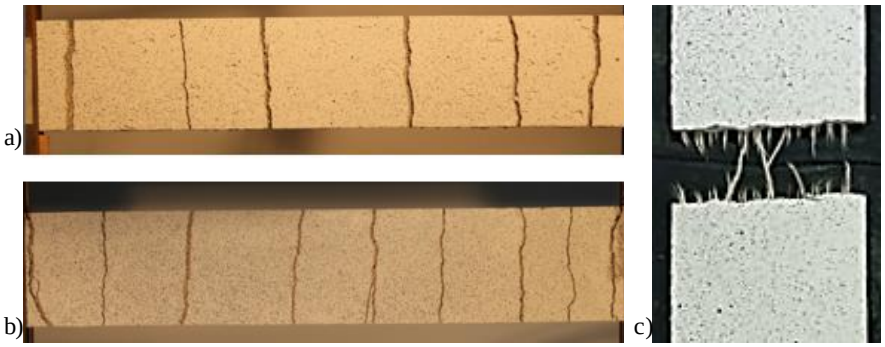

Figure 4.11: a) failure mode of specimens Flax TRM-1L-T-4 and b) Flax TRM-2L-T-4, c) close-up of fabric threads rupture.

Therefore, the analysis of the crack pattern, and of the distance between cracks and their opening, may represent an important tool to better understand the mechanical behaviour of the TRM and to get information about the interaction between the composite components. Such investigation was carried out by means of the Digital Image Correlation (DIC) analysis. By means of an image processing software [112], the displacement field along a longitudinal section in the middle of the external surface of the composite was obtained for each specimen, and with an interval of 20 s during the entire test. Such analysis was carried out on a portion of the specimen, 200 mm long, placed in the middle of the free length. By selecting significant images, corresponding to the transition between two different stages, or to the occurrence of cracks, it is possible to get curves describing the evolution of the displacements along the specimen and during the test. In Figure 4.12 and Figure 4.13 such curves are shown with respect of two representative specimens of the series Flax TRM-1L-T and Flax TRM-2L-T (curves from all the specimens are shown in Appendix A). The different colours represent the displacement field in the surface of the specimens. Each curve represents the image that corresponds to the strain reported on the right side. It can be observed that when the crack occurs, a relative displacement between

the two sides of the interested section is recorded. As a result, each step of the curve corresponds to the occurrence of a crack. In the final configuration, the represented by the upper curve in the graph, the distance between the cracks can be easily evaluated being the distance between two consecutives steps. Each step represents the width of a crack. By getting such curve at different values of the strain, it is possible to get the order in which the cracks developed, and the evolution of each crack opening at different strain levels. The evolution of the cracks opening during the test is plotted in Figure 4.14 and Figure 4.15 with respect of two representative specimens of the series Flax TRM-1L-T and Flax TRM-2L-T. The curves derive from the displacement field along a gauge length of 200 mm in the middle of the sample. During the tests some cracks occurred out of this length. Normally the strain interval between the development of two consecutive cracks is quite constant for all of them. However, by looking at Figure 4.14 and Figure 4.15 such a thing is not verified for all the cracks. This aspect is due to the development of cracks out of the gauge length. The analysis of crack pattern, hence the mean crack spacing between the cracks, is not affected by the neglecting of the cracks developed out of the gauge length. By analysing the graphs, for each specimen the mean value of the distance between two consecutives cracks, the mean crack spacing $\delta_{0,mean}$, and the maximum value of the crack opening, w_{max}, were extracted and reported in Table 4.4.

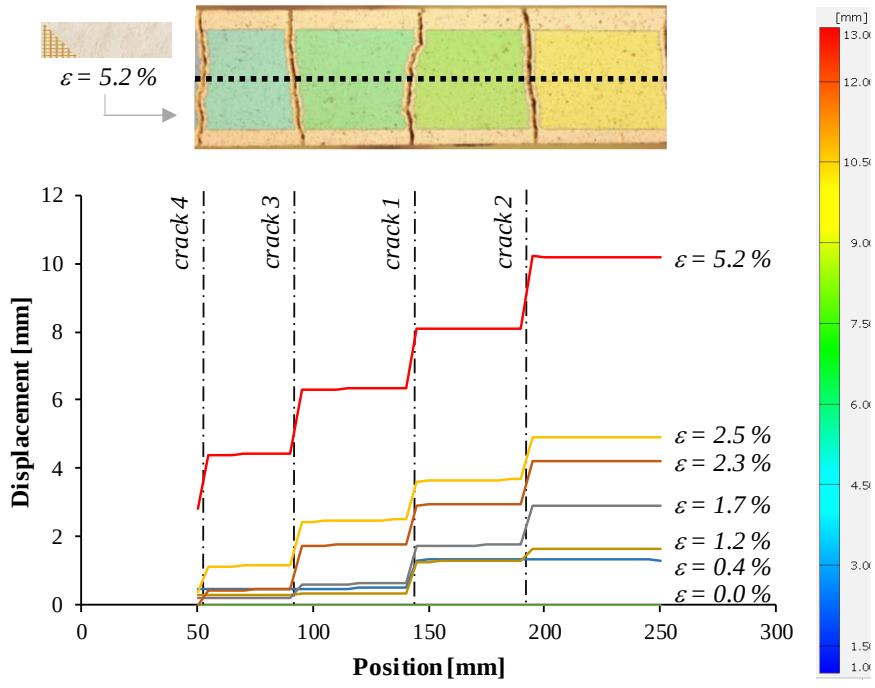

Figure 4.12: Displacement field of the mean longitudinal section (spec. Flax TRM-1L-T-1).

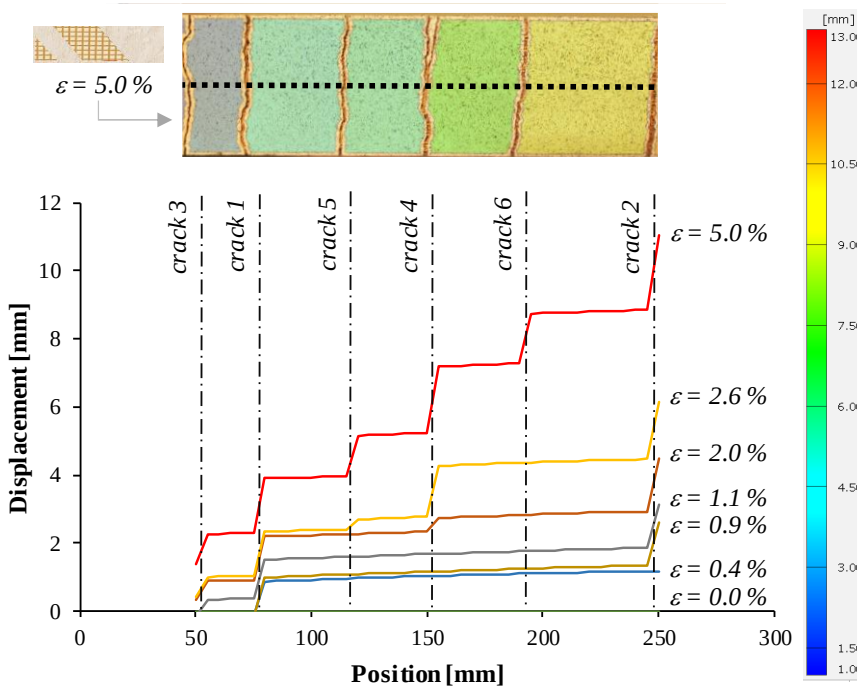

Figure 4.13: Displacement field of the mean longitudinal section (spec. Flax TRM-2L-T-4).

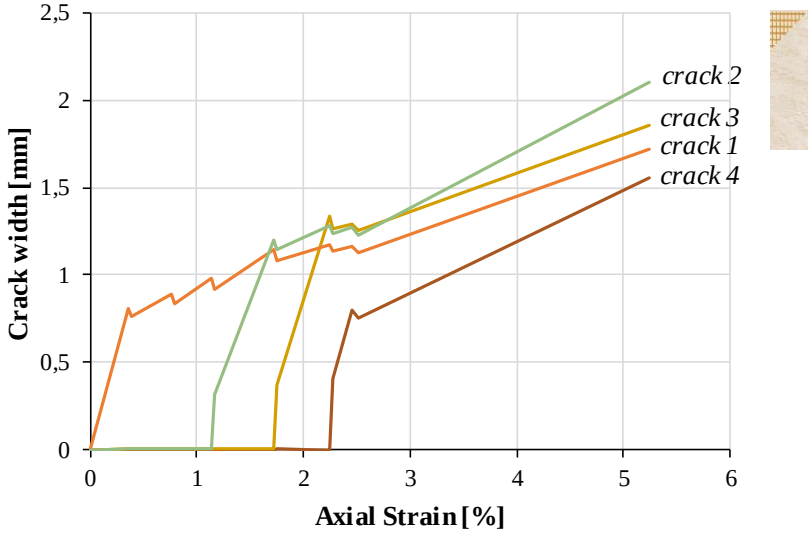

Figure 4.14: Cracks development of mean longitudinal section (spec. Flax TRM-1L-T-1).

By looking at the mean values of the maximum crack width it is highlighted that both reinforcement configurations adopted, by respectively using one and two plies of flax textiles, led to a similar maximum crack opening in correspondence to

the specimen failure. Such evidence was expected being the stress within the textile not significantly different between the two series of specimens.

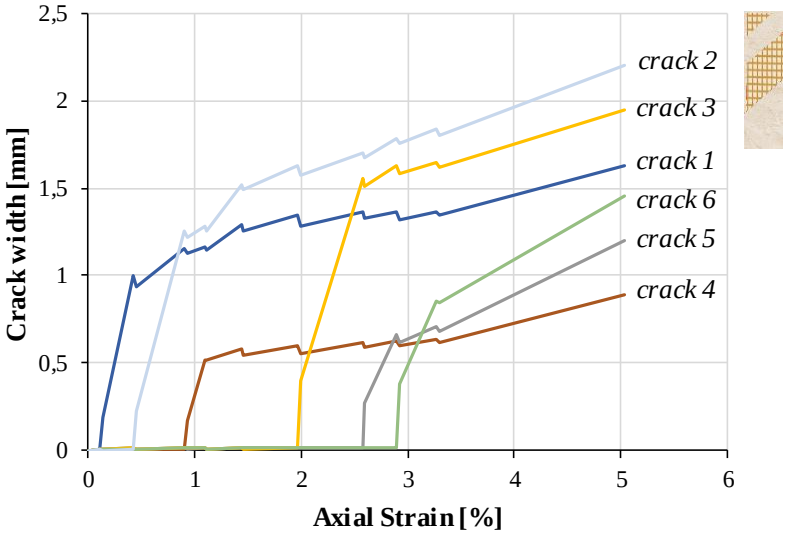

Figure 4.15: Cracks development of mean longitudinal section (spec. Flax TRM-2L-T-4).

With respect to the mean value of the distance between two cracks, δ_{0mean}, it was observed that the mean value concerning the Flax TRM-1L-T series was linearly proportional to the analogous distance observed in the Flax TRM-2L-T series, with a proportionality coefficient factor equal to the ratio between the two volumetric reinforcement ratios, vf_2/vf_1 (being vf_1 and vf_2 respectively equal to 2.04 % and 2.55 %). Such dependence of the distance between cracks from the fibre volumetric reinforcement ratio, emphasises that the two series of specimens were characterised by the same fibre-to-matrix bond behaviour.

A method to analyse the development of the cracks of TRM in tensile tests, consists in tracing the evolution of the mean distance between the cracks during the test [113]. Figure 4.16 shows such curve with respect to a representative specimen of the series Flax TRM-2L-T, evaluated as a logarithmic interpolation of descreet data. The graph shows that with the occurrence of cracks during the test, the mean distance between them decreases, until the end of the test at which the value corresponds to the mean distance δ_{0mean}. In Figure 4.17 the development of the mean crack spacing is plotted for each specimen for both series. As expected, the comparison shows that the specimens of the series Flax TRM-2L-T, in the final part, resulted to be below the curves concerning the other series. Such trend pointed out that, taken a generic value of the strain, the specimens reinforced by a higher amount of textile exhibited a higher number of cracks. This aspect is of fundamental

importance in the assessment of the efficiency of the composite: the higher is the number of cracks developed, the more the system responds as a composite material in which stress and strain are distributed along the entire coupon, and the drops of strength observed in the second stage reduce their size.

Table 4.4: Analysis of cracks main parameters.

Specimen	$\delta_{0,mean}$ (mm)	w_{max} (mm)	τ (MPa)
Flax TRM-1L-T-1	47	2.03	0.23
Flax TRM-1L-T-2	55	2.33	0.18
Flax TRM-1L-T-3	44	2.26	0.26
Flax TRM-1L-T-4	57	2.70	0.26
Mean	51	2.33	0.23
Co.V. (%)	12	12	16
Flax TRM-2L-T-1	40	2.22	0.21
Flax TRM-2L-T-2	31	2.48	0.29
Flax TRM-2L-T-3	40	2.80	0.21
Flax TRM-2L-T-4	39	2.19	0.29
Flax TRM-2L-T-5	45	2.07	0.21
Mean	39	2.35	0.24
Co.V. (%)	13	12	19

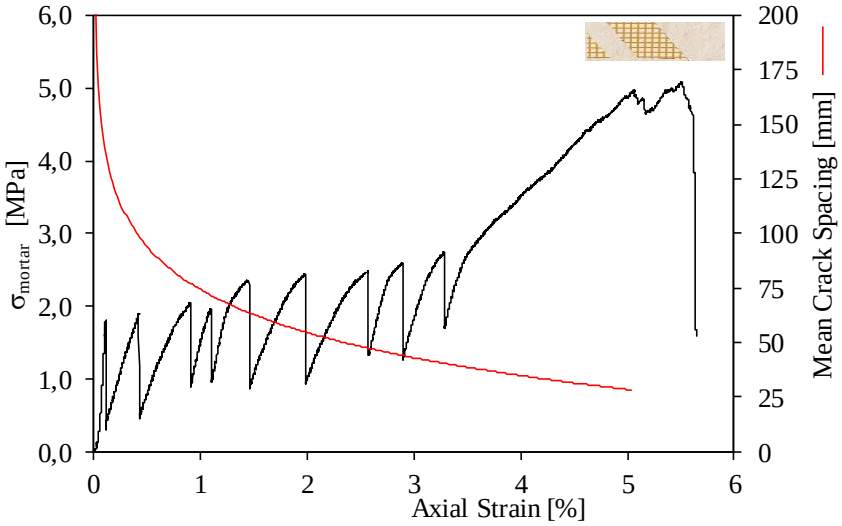

Figure 4.16: Mean crack spacing as a function of the strain (spec. Flax TRM-2L-T-4).

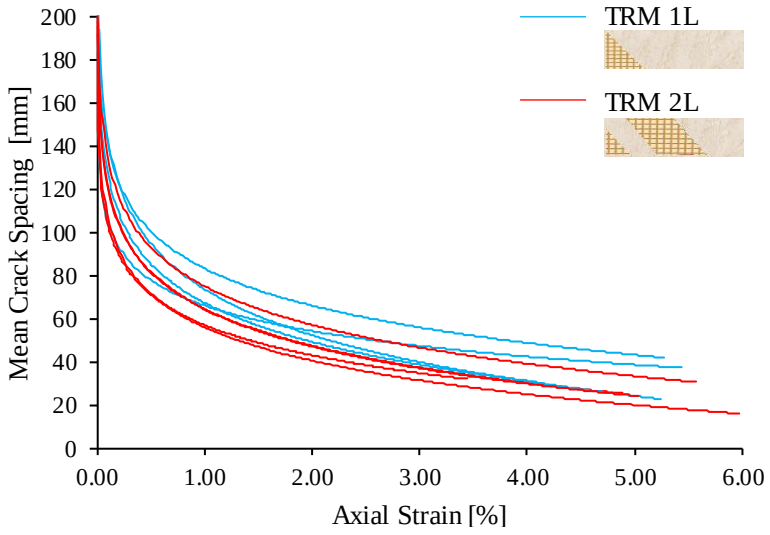

Figure 4.17: Mean crack spacing as function of strain (series Flax TRM-1L-T and 2L-T).

By analysing the crack pattern at the end of the test for each specimen, it is possible to get information about the shear stress at the fibre-to-matrix interface. An approximated estimation model is proposed as follows.

In the elastic phase it can be assumed that at any time the applied force, F, is in part borne by the matrix and in part by the textile (Equation 4.1):

$$F = \sigma_m(z)A_m + \sigma_t(z)A_t \qquad \text{Equation 4.1}$$

where σ_m and σ_t represent the normal stress in the matrix and the textile, A_m and A_t are the cross-section area of the matrix and the textile. By assuming null the σ_m in correspondence to the crack, and by assuming the shear stress transferred from the textile to the mortar to be constant along the z, the stress distribution in the damaged area in proximity to the crack takes the approximated form showed in Figure 4.18.

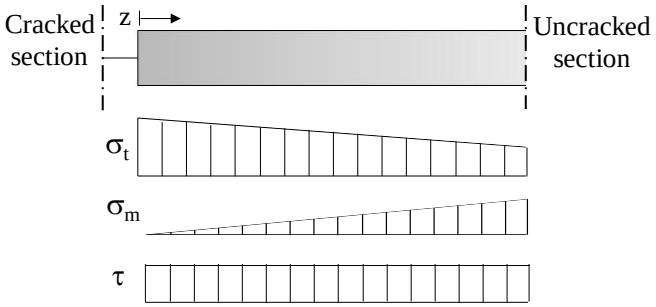

Figure 4.18: Normal and shear stress approximated distributions in the proximity of a cracked section.

Moving along the z, it can be assumed that the amount of force transferred from the textile to the matrix is equal to the integral of the shear stress τ along the z (Equation 4.2):

$$\sigma_t(z)A_t = F - \tau \cdot p \cdot z \quad \text{Equation 4.2}$$

Where p represents the lateral surface per unit length of the fibres (assessed in *Chapter 3*). δ_0 can be defined as the distance z so that the maximum tensile strength is achieved within the mortar ($\sigma_m=f_{t,m}$, being $f_{t,m}$ the uniaxial tensile strength of the mortar). By substituting Equation 4.1 in Equation 4.2 the following relationship between the stress τ and the distance δ_0 is obtained (Equation 4.3):

$$\tau = f_{t,m} \cdot A_m/(p \cdot \delta_0) \quad \text{Equation 4.3}$$

By assuming δ_0 as the smaller distance between two consecutive cracks (assessed by means of DIC analysis), by adopting Equation 4.3 an estimation of the shear stress at the fibre to matrix interface, τ, can be calculated. The values of such estimation are shown in Table 4.4. According to the results obtained, the shear stress assumed almost the same value for the two series of specimens.

It is worth pointing out that the shear values assessed represent an approximated estimation, due the hypothesis considered with respect to the interfacial stress distributions. In fact, in the in the Stages II and III there is a strain incompatibility between matrix and fibres, due to the relative displacements and damaging of the interface surface. Moreover, in this configuration the shear stress distribution is far to be constant over the z direction. However, the same order of magnitude of the shear stress with respect to the two series of specimen confirms that no significant changes in terms of bond properties occurred in the TRM system when the amount of textile was increased.

4.2 Shear bond test on Flax TRM-to-masonry systems

4.2.1 Materials and Methods

Shear bond (SB) tests were carried out by adopting the single-lap shear test configuration aiming to reproduce an intermediate crack-induced failure mode, characterised only by shear stresses distributed on the interfacial surfaces of the system components. In order to be consistent with studies present in the literature, the recommendations of the Committee TC 250 CSM RILEM [32] were respected in the definition of the experimental setup and the mechanical parameters of the study.

The specimens consisted of prismatic masonry substrates comprising five clay bricks and four 10 mm-thick mortar joints, externally strengthened by Flax TRM strips. In line with the tensile characterisation, two series of specimens were considered (Table 4.5):

- Flax TRM-1L-SB: specimens characterised by five bricks masonry element externally strengthened by the composite in the reinforcement configuration Flax TRM-1L, subjected to shear bond test (Figure 4.19);
- Flax TRM-2L-SB: specimens characterised by five bricks masonry element externally strengthened by the composite in the reinforcement configuration Flax TRM-2L, subjected to shear bond test (Figure 4.19).

Two of the specimens of the series Flax TRM-1L-SB were discarded because of an incorrect recording of the displacements during the test. That is why there is an inconsistency in the number of specimens of each series.

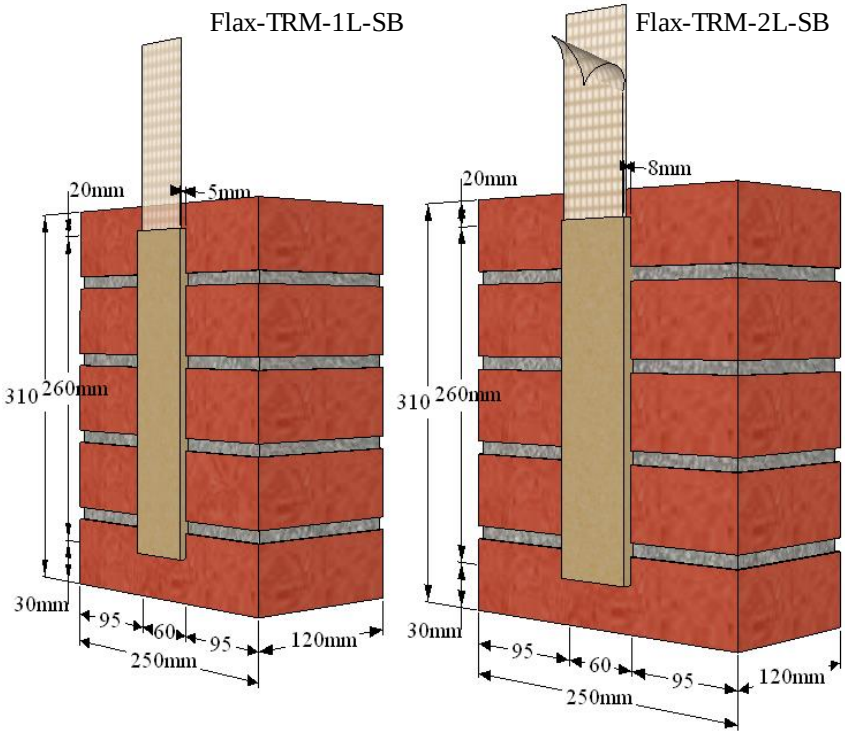

Figure 4.19: Flax TRM-to-masonry specimens subjected to shear bond test: Flax-TRM-1L-SB, characterised by one layer of flax textile; Flax TRM-2L-SB, with two layers.

The Flax TRM strips, with a bond length of 260 mm, were placed centrally along the vertical axis of the prism and at a distance of 20 mm from the upper side of the support. The textile free length at the loaded edge of the specimen was of 300

mm. The reinforcement was applied on the masonry elements by adopting the same manufacturing process utilised for tensile test specimens.

The clay bricks, belonging to the commercial line "Rosso Vivo A6R55 W" produced by San Marco-Terreal, Valenza AL, Italy [114], were 250 mm long, 120 mm wide, and 55 mm thick, with a compression strength (perpendicular to the larger face) of 18 MPa (manufacturer technical specifications).

The bed joints of the masonry consisted of a low strength hydraulic lime-based mortar, specifically designed to be representative of mortar that can be typically found in existing masonry buildings. It was characterised by the volumetric composition suggested by the Italian Guidelines [59], in order to reproduce a low strength hydraulic lime mortar, consisting of 2 parts of binder, 4 parts of sand, and 1.3 parts of water.

The main mechanical properties, assessed according to standard specifications [111], consisted in a compression and flexural strength respectively equal to 2.45 MPa (Co.V. 14 %) and 0.50 MPa (Co.V. 37 %).

Table 4.5: Main properties of the shear bond test series of specimens.

Series	Number of specimens	TRM section (mm x mm)	A_{mortar} (mm^2)	$A_{textile}$ (mm^2)	vf	$f_{textile}$ (MPa)
Flax TRM-1L-SB	3	5 x 60	300	6.1	2.04%	286
Flax TRM-2L-SB	5	8 x 60	480	12.2	2.55%	

The flax textile mechanical properties were shown in *Chapter 3*. The hydraulic lime-based mortar adopted to perform the Flax TRM systems was characterised by a compression and a flexural strength respectively equal to 10.55 MPa (Co.V. 8 %) and 3.56 MPa (Co.V. 5 %), assessed after 28 days of curing from the casting.

The experimental investigation was performed at the Laboratory of Composite Materials for Constructions (LMC2) of the University Claude Bernard Lyon 1. Single-lap shear tests were carried out by using a Zwick/Roell 1475 electro-mechanical testing machine, with a 50 kN capacity in tension and compression, in displacement control using a cross-head rate of 0.3 mm/min. A steel system, consisting of two metallic plates connected by four threaded rods, locked the masonry prisms so that no rotation of the reinforced substrate could occur (Figure 4.20). Steel plates bonded to the end of the flax textile were placed by a clamping steel device. In order to avoid load eccentricity and, consequently, out-of-plane tensile stresses (peeling) at the interface between the masonry substrate and the reinforcing system, each specimen was duly placed to ensure that the textile was aligned with the direction of the load, with no intentional eccentricity. Moreover, a

hinge was placed between the clamping steel device and the head of the universal machine so that no bending moments could be transmitted to the Flax TRM system.

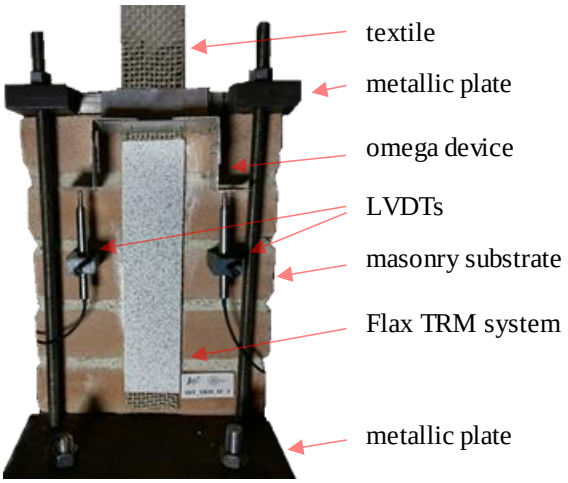

Figure 4.20: Shear bond test set-up.

In order to record possible slipping of the textile within the mortar matrix, an aluminium device, named "Ω" for its shape, was bonded to the flax textile at a distance of 5 mm from the TRM edge. Two displacement transducers (Linear Variable Differential Transformer, LVDTs) bonded to the masonry substrate, were used to monitor any motion of the "Ω" plate during the test.

4.2.2 Results and Discussion

The shear bond test response is expressed in terms of stress-slip curves (Figure 4.21 and Figure 4.22).

The normal stress, σ, was obtained by dividing the applied load for the cross-section of textile; the slipping, s, of the textile within the mortar matrix was computed as the average value among the two displacements recorded by the transducers, LVDTs, monitoring the "Ω" device.

The main parameters obtained from the tests are shown in Table 4.6. P_{max} represents the maximum load, s_{max} represents the corresponding main displacement of the "Ω" device, σ_{max} is the corresponding normal main stress within the textile. In order to quantify the fibres exploitation, the ratio between the maximum stress, σ_{max}, and the tensile strength of the textile, $f_{textile}$, is reported as well for each specimen.

The stress-displacement curves show that both the series of specimens exhibit the same trend characterised by a linear elastic branch up to the achievement of the maximum capacity. Such response may be interpreted as a combination of the linear

elastic deformation of the textile portion placed between the "Ω" device and the TRM system, and possible relative displacements between mortar and fibres within the composite. The post peak phase is mainly characterised by a sequence of drops of the load due to the rupture of the single flax threads until the failure of the specimen.

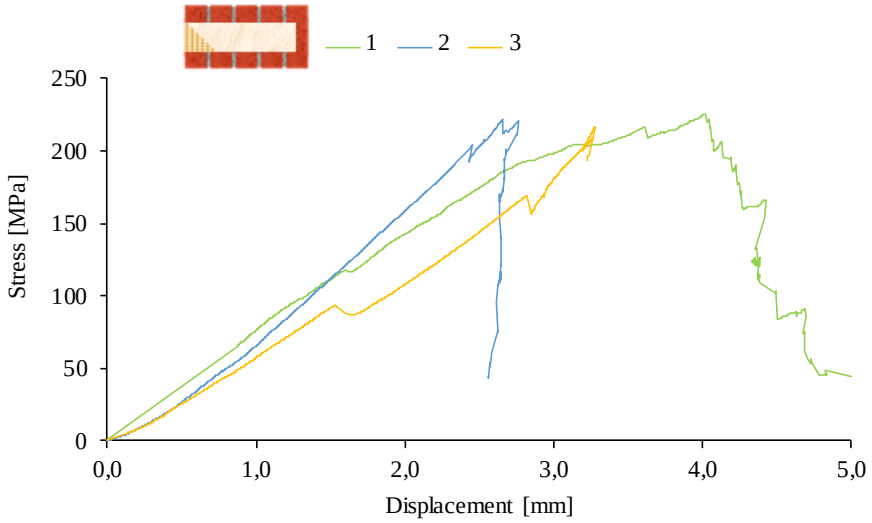

Figure 4.21: Stress-slip curves of shear bond tests concerning the Flax TRM-1L-SB series.

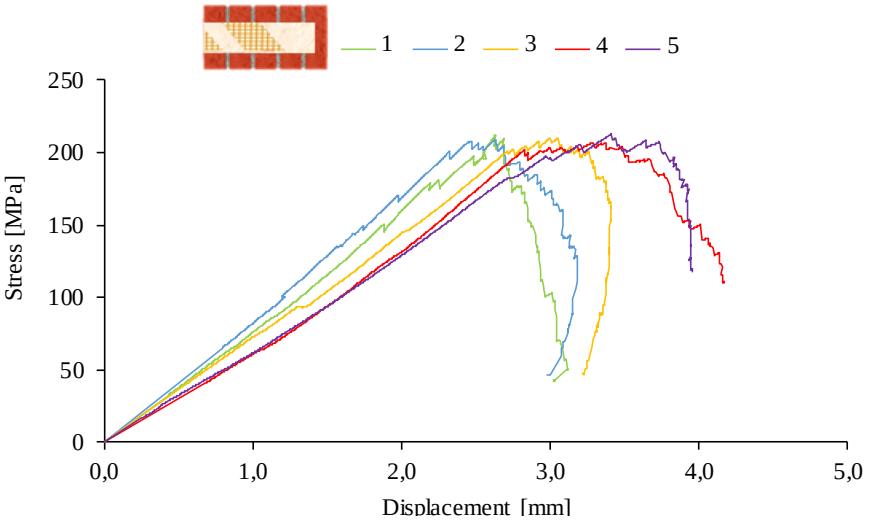

Figure 4.22: Stress-slip curves of shear bond tests concerning the Flax TRM-2L-SB series.

For all specimens the failure mode consisted in the rupture of the flax threads in the free length of the textile (mode E) (Figure 4.23a). Such rupture did not involve

a specific cross section: it was rather due to a process of redistribution of the stress within the textile after each thread rupture; at each step, the most charged thread randomly failed at the weakest point of its length. Figure 4.23b shows a close-up in which few threads already failed while the others were stretched due to a concentration of stress.

Table 4.6: Mechanical parameters of Flax TRM-to-masonry systems tested in shear.

Specimen	P_{max} (N)	s_{max} (mm)	σ_{max} (MPa)	$\sigma_{max}/f_{textile}$ (%)	Failure mode
Flax TRM-1L-SB-1	1379	4.0	226	79	E
Flax TRM-1L-SB-2	1355	2.7	222	77	E
Flax TRM-1L-SB-3	1325	3.3	217	76	E
Mean	1353	3.3	221	77	-
Co.V. (%)	2	21	2	2	-
Flax TRM-2L-SB-1	2598	2.6	212	74	E
Flax TRM-2L-SB-2	2551	2.6	209	73	E
Flax TRM-2L-SB-3	2572	3.1	210	73	E
Flax TRM-2L-SB-4	2530	3.4	207	72	E
Flax TRM-2L-SB-5	2604	3.4	213	74	E
Mean	2571	3.0	210	73	-
Co.V. (%)	1	13	1	1	-

Both series of specimens achieved an exploitation of the fibres of about 75 %. Although the fibres achieved tensile failure, the mean maximum stress never reached the value recorded during the dry textile tensile tests. Such behaviour, already showed also in the case of tensile tests, may be attributed to two aspects: on one side the free length is of 300 mm, while the dry textile was tested with a gauge length of 150 mm, as also shown in Chapter 2 the higher is the size of the specimen, the higher is the probability of having geometric and mechanic imperfection, the lower is the tensile capacity; on the other side, while in dry textile tensile tests the fabric is perfectly clamped at both the edges, in the case of shear bond test one of the sides is embedded in the mortar, allowing for deformation of the textile also within the TRM system, hence causing a lower strength.

It is worth to notice that the average tensile capacity observed in shear bond tests is slightly higher of that exhibited by composite specimens tested in tension, even if the same geometry of the Flax TRM system was adopted. Such experimental evidence may be explained by the fact that in tensile tests the distribution of the stress within the composite during the test create a damage at the matrix to fibre interface with a deterioration of the threads that result in a lower global capacity of the system.

a) 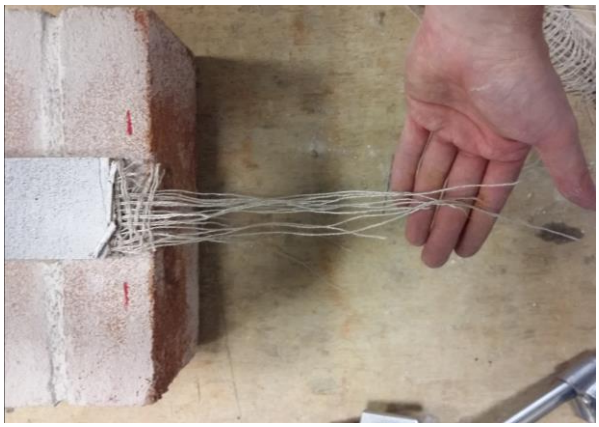 b) 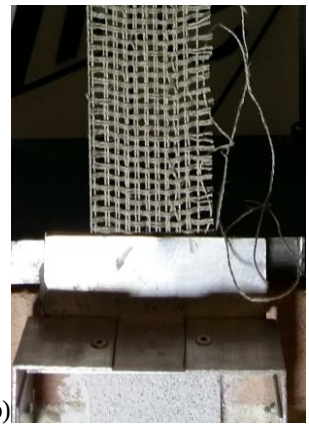

Figure 4.23: a) failure mode of a representative specimen (Flax TRM-2L-SB-5); b) close-up of the flax threads' failure in the free length.

The shear bond test showed that, among the different capacities associated to the possible failure mechanisms, i.e. loss of bond strength at the TRM-to-substrate interface, loss of bond at the textile to mortar interface, loss of strength of the textile in tension, the one associated to the latter is the lower. On one hand, this aspect emphasises that such failure mode is the most brittle, hence it has to be properly considered on the analysis of the global behaviour of structural elements, that are often required to exhibit a ductile behaviour. On the other hand, such a failure mode allows to increase the load capacity of the system by increasing the textile amount since the good adhesion at the fibre-to-matrix interface does not lead to a premature failure of the system due to the slippage of the textile within the mortar. The latter, in fact, results as one of the main limitations showed by most of high strength synthetic fibres (such as carbon and basalt), and in such cases, the improvement of the textile-to-mortar bond, by means of fibre treatments or matrix modifications, results to be a challenging task.

4.2.3 Determination of the Flax TRM designing conventional strength

As also discussed in paragraph 2.1.4, according to Italian guidelines for designing of rehabilitation interventions by means of TRMs [61], a conventional strength, to be used for designing and verification problems, can be derived by the mechanical characterisation strength. Specifically, such strength consists of a value of the normal stress, $\sigma_{lim,conv}$, corresponding to the maximum strength deriving from shear bond tests, and in a value of the axial strain, $\varepsilon_{lim,conv}$, corresponding to the value of the strain corresponding to the stress $\sigma_{lim,conv}$ in the stress-strain tensile response of the dry textile. By considering both series of specimens the conventional maximum

stress, $\sigma_{lim,conv}$, results equal to 215 MPa. The conventional strain is assessed as the average among the values corresponding to all the stress-strain curves of the series Flax-strip-6cm analysed in *Chapter 3* (Figure 4.24).

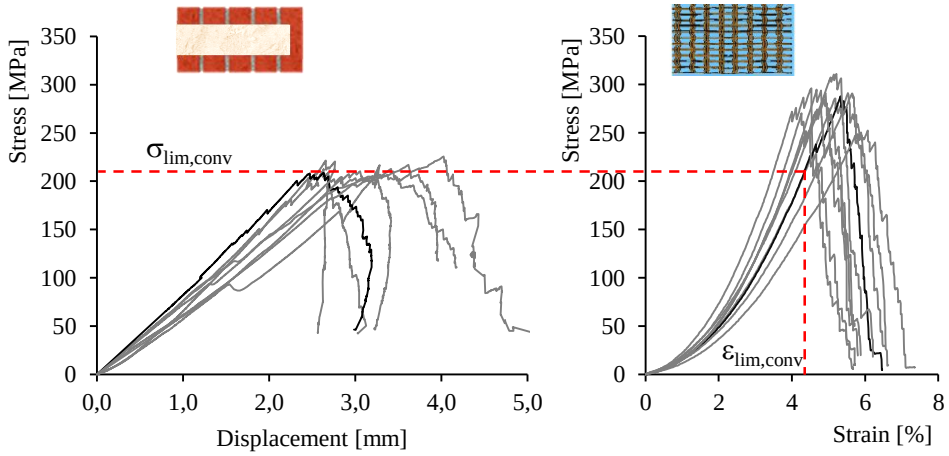

Figure 4.24: Determination of Flax TRM conventional strength according to [61].

The conventional strain, $\varepsilon_{lim,conv}$, assumes the mean value of 4.58 %. However, within the instructions it is assumed that the tensile textile response is linear. In the case of plant fibres, a less stiff branch is typically exhibited at low strain levels, due to the morphology of the fibres at a microscale, and of the textile on a macroscale.

Being this stiffness, E_f, determined in the linear branch, it is necessary to define a modified value of the limit strain, ε^*, as the difference between strain values ε_1 and ε_2 (Figure 4.25), so that the product between the conventional limit strain and the mean stiffness results to be equal to the conventional limit stress, $\sigma_{conv,lim}$.

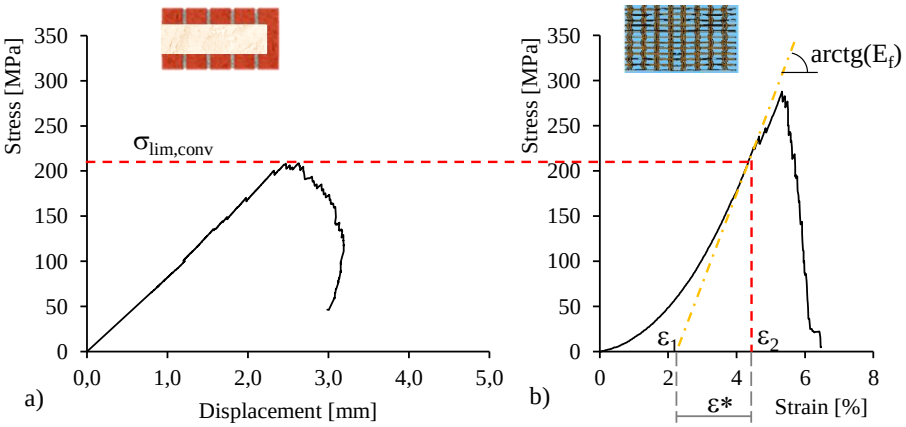

Figure 4.25: Modified value of the conventional limit strain assessed by comparing shear bond test and flax tensile test representative responses.

The graphical assessment of the conventional strain is shown in Figure 4.25 where, to make the image clearer, two representative specimens are plotted: a shear bond test response characterised by a maximum stress of about the $\sigma_{lim,conv}$, and a flax textile tensile response characterised by a linear stiffness of about E_f.

The outcoming mean values are: conventional limit stress, $\sigma_{lim,conv}$, of 215 MPa; a mean dry stiffness of the textile, E_f, of 9.03 GPa (*Chapter 3*); and a modified conventional limit strain, ε^*, equal to 2.4 %.

4.3 Durability

The durability of plant fibre-based TRMs represents one of the main concerns that feeds scepticism in the use of the composite system. Such distrust seems to be due to a lack of knowledge rather than to exhaustive scientific outcomes. This is the reason why, with the aim of providing a comprehensive analysis of the effectiveness of Flax TRMs, such aspect was addressed within the study. However, being mechanical aspects the core of the discussion, durability issues were boarded with a secondary attention, with the aim of at least proving Flax TRMs to comply with the existing standards and guidelines. As a consequence of the ageing investigation conducted on flax threads, and discussed in *Chapter 3*, in this paragraph the attention is focused directly on Flax TRM coupons.

4.3.1 Materials and Methods

The qualification procedure adopted consisted in the exposure of Flax TRM specimens in specific ageing conditions chosen according to the acceptance criteria AC434 [57]. The durability performance was computed by comparing the tensile behaviour of the specimens tested after the period of exposure, with the response of reference specimens stored in ambient conditions.

The composite material components (namely, the mortar matrix and the flax threads) were subjected to the same treatments to quantify their influence in the global response. The following ageing protocols were adopted:

- Ambient: the specimens were stored in ambient conditions for 3000 h (125 days) and were used as reference;
- Water: the specimens were immersed in deionised water for a period of 3000 h (125 days);
- Salt-water: the specimens were immersed for a period of 3000 h (125 days) in a saline environment consisting in 3.5 % in weight of sodium chloride (NaCl) aqueous solution, that was meant to reproduce the world's ocean seawater average salinity;

- Alkaline solution: the specimens were immersed for a period of 3000 h (125 days) in an alkaline environment with 9.5 PH level, reproduced by adding sodium hydroxide (NaOH) to the deionised water.

For each conditioning environment, in line with procedures of the literature [44], the following specimens were considered:

- Flax-T: consisting in flax threads tested in tension with a gauge length of 100 mm (the same type of specimen adopted in *Chapter 2*) (Figure 4.26a);
- H-Lime-Matrix: consisting in mortar prisms (40x40x160 mm^3) to be tested in bending and compression in accordance to the EN 196-1 [111] (Figure 4.26b);
- Flax TRM-1L-T: consisting of TRM coupons reinforced by the configuration Flax TRM-1L, characterised by 5 mm of thickness, 60 mm of width and 500 mm of length (of which 300 mm of gauge length), and tested in tension (Figure 4.26c).

The main characteristics of all series of specimens, curing conditions and the respective type of test are listed in Table 4.7. Tensile tests on fibres and bending tests on mortar, were performed by means of a Universal Testing Machine by using respectively a 1 kN load cell, with a displacement rate of 4 mm/min (Figure 4.27a), and a 5 kN load cell, with a displacement rate of 0.2 mm/min (Figure 4.27b).

Figure 4.26: Specimens tested for durability analysis: a) Flax-T; b) H-Lime-Matrix; c) Flax TRM-1L-T.

The immersion of the Flax TRM specimens in the different solutions was performed by taking care of avoiding the direct absorption of water through flax textile. To this purpose, the two edges of the specimens were sealed by means of silicon before the immersion in the water solutions (Figure 4.28). Tests were carried out at the Department of Industrial Engineering of University of Salerno.

Mortar compression tests (Figure 4.27c) and TRM tensile tests (Figure 4.27d) were carried out by means of a Zwick Roell Schenck Hydropolus S56, with

maximum capacity of 630 kN, respectively with a displacement rate of 0.3 mm/min and 0.25 mm/min, at the Strength Laboratory of University of Salerno.

Table 4.7: Series of specimen considered in the experimental durability analysis.

Series	Conditioning environment	Conditioning period	n° of spec.	Geometry	type of test	textile section
Flax T-Amb	Ambient	3000 h	14	150 mm	Tensile test	0.25 mm^2
Flax T-W	Water	3000 h	14			
Flax T-S	Salt	3000 h	14			
Flax T-Alk	Alkaline	3000 h	14			
H-Lime-Matrix-Amb	Ambient	-	3 / 6	40x40x160 mm^3 / ~40x40x40 mm^3	Three-point bending test / Compression test	---
H-Lime-Matrix-W	Water	3000 h	3 / 6			
H-Lime-Matrix-S	Salt	3000 h	3 / 6			
H-Lime-Matrix-Alk	Alkaline	3000 h	3 / 6			
Flax TRM-1L-T-Amb	Ambient	-	5	5x60x500 mm^3	Tensile test	6.12 mm^2
Flax TRM-1L-T-W	Water	3000 h	5			
Flax TRM-1L-T-S	Salt	3000 h	5			
Flax TRM-1L-T-Alk	Alkaline	3000 h	5			

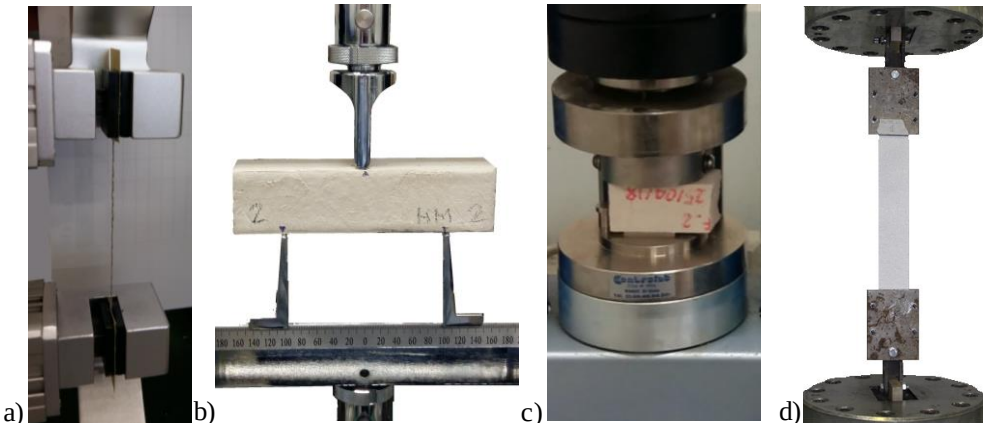

Figure 4.27: Test set-up of series: a) Flax T; b) H-Lime-Mortar (bending); c) H-Lime-mortar (compression); d) Flax TRM-1L-T

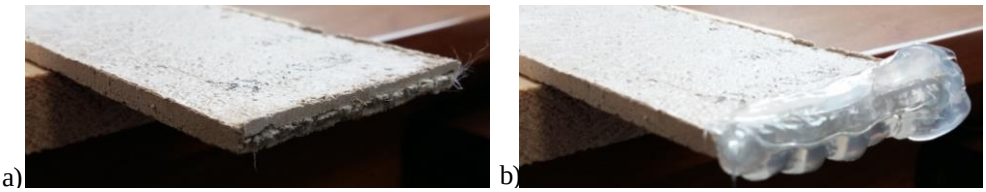

Figure 4.28: a) Flax TRM-1L-T edge before sealing; b) sealing of the edge.

4.3.2 Results and Discussion

The effect of application of the ageing protocols on the flax threads is analysed in terms of tensile strength, $\sigma_{t,max}$, of the corresponding strain, ε_{max}, and of stiffness, E (Table 4.8) (Coefficient of variation in round brackets). In terms of strength a slight increase of the mean maximum stress was observed in the series Flax-T-W. The series Flax-t-S and Flax-T-Alk exhibited a slightly less stiff response.

The effect of different environmental exposures on the mortar is analysed in terms of compression, $\sigma_{c,max}$, and flexural strength, $\sigma_{f,max,}$ of the mortar prisms (Table 4.9). The specimens aged in water and in alkaline solution exhibited a compression strength slightly higher of that shown by the reference series.

For both TRM components it can be affirmed that no significant changes were brought by the application of the durability protocols, and few variations of the mechanical properties may be attributed to the statistical variability of the results.

Table 4.8: Parameters concerning the Flax-T specimens.

Series	$\sigma_{t,max}$ (MPa)	ε_{max} (%)	E (GPa)
Flax T-Amb	283.67 (15)	3.3 (12)	9.07 (12)
Flax T-W	309.38 (12)	3.5 (13)	9.13 (7)
Flax T-S	294.02 (12)	3.6 (7)	7.98 (9)
Flax T-Alk	267.74 (9)	3.7 (8)	7.09 (11)

Table 4.9: Parameters concerning the H-Lime-Mortar specimens.

Series	$\sigma_{f,max}$ (MPa)	$\sigma_{c,max}$ (MPa)
H-Lime-Mortar-Amb	4.81 (3)	11.79 (4)
H-Lime-Mortar-W	4.05 (5)	13.73 (5)
H-Lime-Mortar-S	4.54 (7)	12.21 (7)
H-Lime-Mortar-Alk	4.39 (16)	14.10 (7)

The TRMs response is shown in terms of stress-strain curves for each series of specimens: the reference specimens in ambient conditions (Figure 4.29), the specimens aged in water (Figure 4.30), the specimens immersed in saltwater (Figure 4.31), and the specimens exposed to alkaline environment (Figure 4.32).

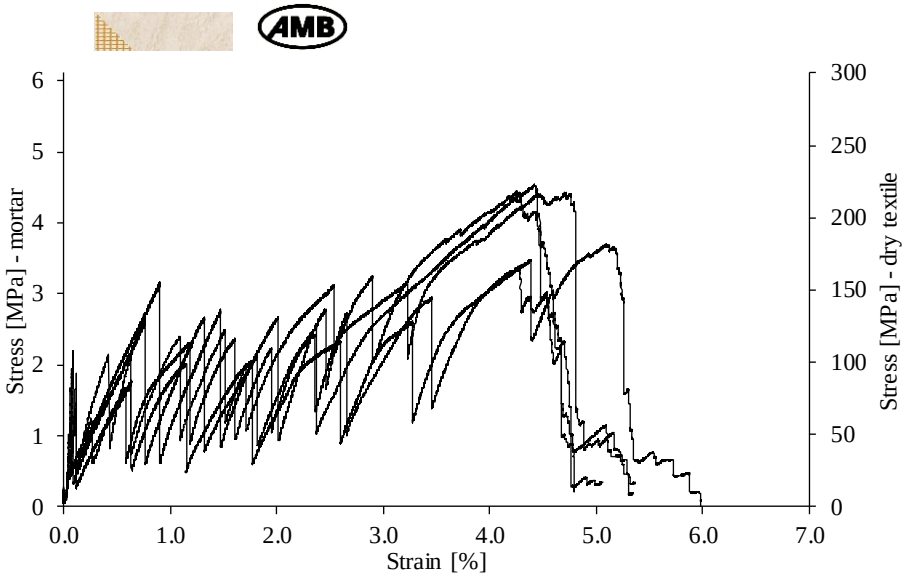

Figure 4.29: Stress-strain curves of the series Flax TRM-1L-T-Amb.

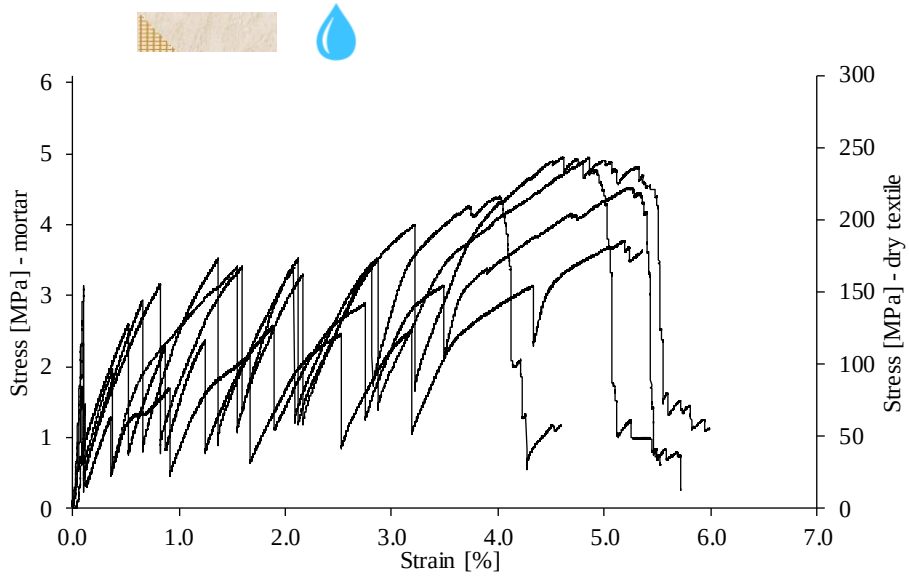

Figure 4.30: Stress-strain curves of the series Flax TRM-1L-T-W.

As expected, the response was characterised by the tri-phase behaviour widely discussed in paragraph 4.1.3. The main mechanical parameters concerning Flax TRM tensile tests for the different ageing environments, are shown in (Table 4.10 and Table 4.11).

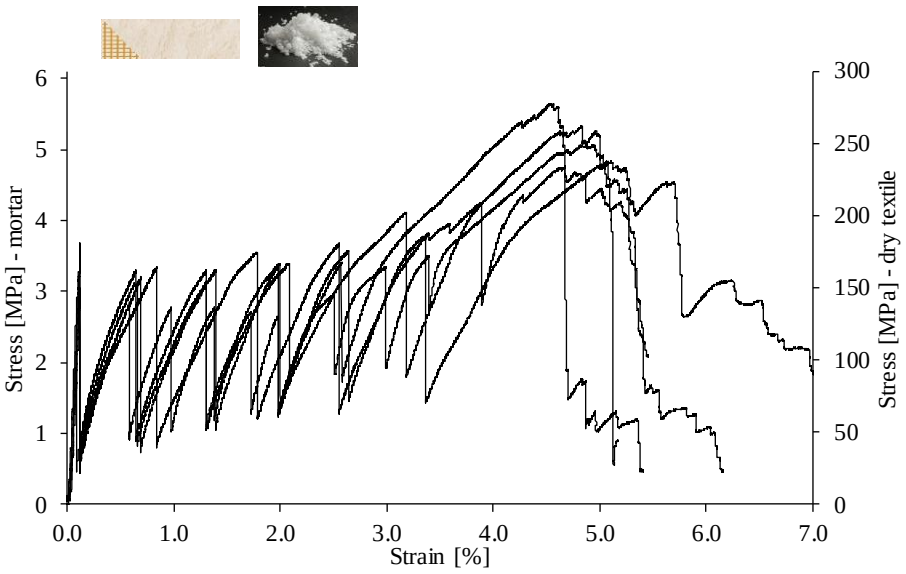

Figure 4.31: Stress-strain curves of the series Flax TRM-1L-T-S.

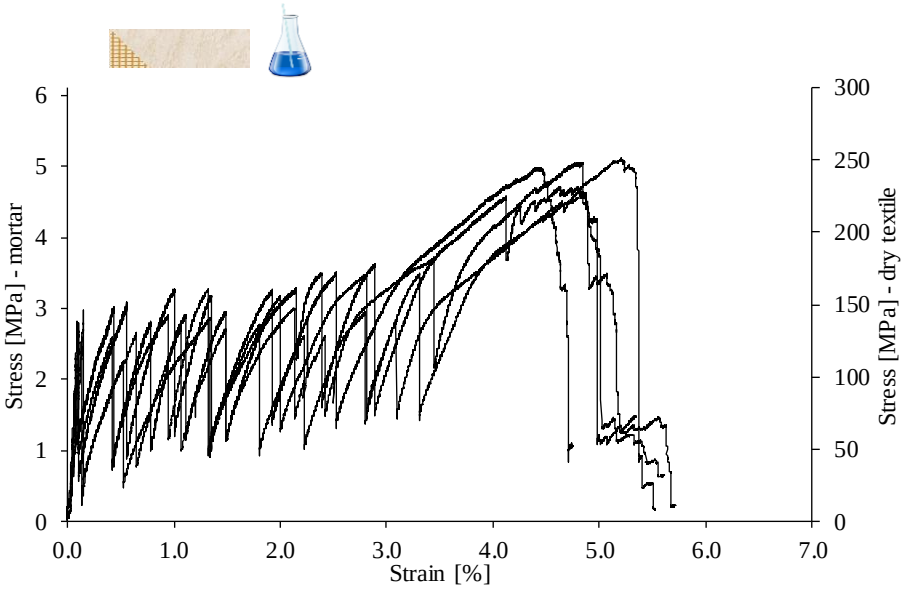

Figure 4.32: Stress-strain curves of the series Flax TRM-1L-T-Alk.

In line with the mechanical response exhibited by the TRM components, no significant changes were observed also in the behaviour of the whole composite tested in tension. More in details, the three environmental exposures conferred to the composite a slight increase of maximum strength. In fact, the textile exploitation ratio (assessed with respect to the non-aged textile), of about 70 % in the reference series, gets values included in the range between the 80 % and 85 % in the aged series. It is worth highlighting that the exploitation ratio of the series Flax TRM-1L-T-Amb, tested after 124 days, was the same of the one observed in the series Flax TRM-1L-T (paragraph 4.1), tested after 28 days. Such aspect confirms that no significant degradation of the textile in contact with the hydraulic lime mortar occur in the period between 28 and 124 days.

The low increase in the mortar strength led to transition points between the stage I and II, and between the stages II and III, characterised by higher stress, σ_1 and σ_2. Such experimental evidence may be attributed to the fact that the conditioning in water facilitates the hydration processes of the mortar.

Table 4.10: Parameters concerning the Flax TRM-1L-T specimens.

Series	P_{max} (N)	$disp_{max}$ (mm)	σ_{max} (MPa)	ε_{max} (%)	$\sigma_{textile}$ (MPa)	$\sigma_{max}/f_{textile}$ (%)
Flax TRM-1L-T-Amb	1224 (13)	13.6 (8)	4.08 (13)	4.5 (8)	200 (13)	70 (13)
Flax TRM-1L-T-W	1380 (7)	15.0 (16)	4.60 (7)	5.0 (16)	226 (7)	79 (7)
Flax TRM-1L-T-S	1540 (7)	14.4 (4)	5.13 (7)	4.8 (4)	252 (7)	88 (7)
Flax TRM-1L-T-Alk	1468 (5)	14.4 (6)	4.89 (5)	4.8 (6)	240 (5)	84 (5)

Table 4.11: Stress and strain corresponding to the different stage transition points.

Series	σ_1 (MPa)	ε_1 (%)	σ_2 (MPa)	ε_2 (%)	τ (MPa)
Flax TRM-1L-T-Amb	1.85 (15)	0.1 (23)	2.87 (12)	3.4 (11)	0.24 (18)
Flax TRM-1L-T-W	2.13 (34)	0.1 (11)	3.29 (16)	3.6 (6)	0.17 (18)
Flax TRM-1L-T-S	3.12 (11)	0.1 (12)	3.73 (8)	3.6 (13)	0.21 (32)
Flax TRM-1L-T-Alk	2.58 (16)	0.1 (29)	3.51 (9)	3.6 (9)	0.23 (18)

The typical failure mode of the specimens was characterised by a sequence of sudden drops of the load, corresponding to the mortar cracks, up to the rupture of the textile in one of the cracked sections (Figure 4.33) (modes A and B). It can be observed that in all specimens the distance between two consecutive cracks is roughly the same. Consequently, being the amount of textile, and the specimen size, the same for all samples, it can be affirmed that also the interface behaviour at the fibres-to-matrix interface did not significantly change after the application of the ageing protocol. In Table 4.11 the mean fibre-to-matrix interfacial shear stress, τ, assessed with the simplified model proposed in paragraph 4.1.4, is reported for each series of specimens. It can be seen that no significant differences were observed.

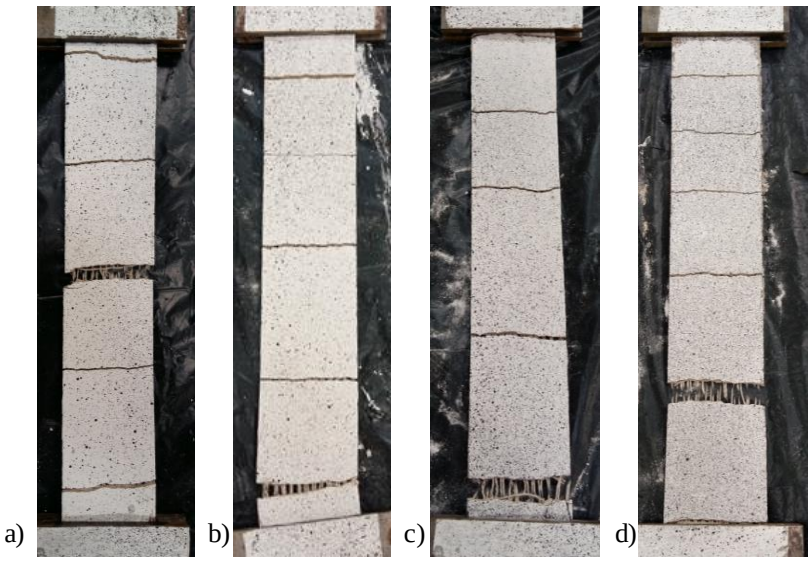

Figure 4.33: Failure mode of representative specimens of the series: a) Flax TRM-1L-T-Amb; b) Flax TRM-1L-T-W; c) Flax TRM-1L-T-S; d) Flax TRM-1L-T-Alk.

As a matter of fact, not having experienced any decrease of strength, it can be affirmed that the investigated Flax TRM system, exposed to conventional protocols provided by AC434 [57], complies with the acceptance criteria generally considered for qualifying composite materials.

4.4 Conclusions

The present chapter aims at providing an exhaustive mechanical characterisation of the Flax TRM system under investigation, at the scale of analysis of the composite. Both tensile behaviour and the shear bond performance with a masonry substrate were considered. Moreover, the characterisation was enriched with a preliminary

experimental analysis of the durability of Flax TRM composites. The main findings of the experimental analysis are summarised as follows:

- Tensile tests carried out on Flax TRM coupons showed that the response in tension is characterised by the typical three stages. However, unlike what is observed in high strength fibre based TRMs, the stress-strain response of Flax TRMs exhibited significant drops of the stress in correspondence to crack occurrence, due to the low initial stiffness of plant fibre textiles, to bond properties at the fibre-to-matrix interface and to the utilised mortar mix design;
- All specimens tested in tension exhibited a failure mode characterised by rupture of the fibres, with an exploitation ratio of about 70 %, due to the different load conditions of the textile when tested alone with respect to the case in which it is restrained by the mortar:
- By varying the fibre volume fraction no reduction in strength was observed, showing that the textile grid was well designed allowing the mortar to correctly penetrate through the voids. Such statement was confirmed by analysing the fibre-to-matrix shear stress assessed by means of a simplified model;
- Digital Image Correlation analysis was confirmed to be a suitable and powerful technique to deeply investigate the failure mechanisms of TRMs in tension;
- With respect to the Flax TRM-to-masonry substrate shear bond behaviour, the experimental evidences showed an elastic response of the textile in the free length of the loaded edge ending up in a rupture of the textile in such area. This behaviour, occurred in both reinforcement configurations, emphasising that the system is characterised by a good adhesion at the fibre-to-mortar interface with respect to the tensile strength of the flax textile itself, and that a bond length equal to 260 mm is adequate for preventing TRM-to-masonry debonding;
- The experimental investigation carried out to analyse the durability of Flax TRM composites showed that the system, exposed to a conventional ageing protocol, complies with the acceptance criteria proposed by standards in the field.

The promising outcomes of the comprehensive investigation carried out at the composite scale of analysis, encourage the employment of Flax TRM systems as reinforcement of structural masonry elements. Experimental studies with the application of such composite system on structural elements, are needed in order to confirm the potential of the strengthening technique, and perhaps to highlight the limitations of the system. The latter is a fundamental aspect:

the experimental study, together with the encouraging results, pointed out that there is still room for improvements of the mechanical performance of plant based TRMs. The definition of the crucial aspects on which it is necessary to focus the attention plays a key role in the process of improvement and refinement of the reinforcing technique.

5. Mechanical behaviour of masonry walls externally strengthened by Flax TRM composites

As shown in the previous chapters, the use of plant fibres as reinforcement in mortar-based composites represents a promising solution to improve the sustainability of the material. However, due to the specific mechanical properties of plant textiles, inferior in regard to "conventional" ones, (i.e. lower strength and stiffness) some differences in the mechanical behaviour emerged with respect to TRM composite performed by conventional textiles. Therefore, further studies are needed to better understand the behaviour of these types of TRM as a possible technological solution for enhancing shear capacity of masonry walls.

To respond to this need, this chapter reports experimental observations obtained on clay-brick masonry walls externally strengthened by the Flax TRM systems under study. Specifically, the reinforced masonry structural elements are subjected to diagonal compression tests in order to assess the contribution of the intervention to the shear capacity of the system. After discussing the experimental evidence into detail, a comparison of results with similar studies present in the literature, and with models proposed by standards in this area, is shown as well.

5.1 Methods

Masonry assemblages externally strengthened by Flax-TRM systems were subjected to diagonal compression tests in order to assess the diagonal shear (or tensile) strength. The test consisted in loading the wall along one diagonal, thus causing a diagonal tension failure with the specimen splitting apart perpendicular to the direction of load. The tests were carried out at the Laboratory of Composite Materials for Construction (LMC2) of the University Claude Bernard Lyon 1.

Three different series of specimens were considered (Figure 5.1):

- the first one, labelled as USW, was characterised by unstrengthened walls and was conceived so as to obtain the reference mechanical behaviour;
- the second one, labelled as SW-1L, was characterised by walls externally strengthened by the system Flax TRM-1L;

- The third one, labelled as SW-2L, was characterised by walls externally strengthened by the system Flax TRM-2L.

The TRM reinforcement system and the masonry substrate were performed with the same characteristics of the specimens subjected to tensile and shear bond test, whose experimental outcomes are discussed in *Chapter 3*. The bricks were arranged in the running bond pattern, a monolayer configuration characterised by a single row of bricks in thickness of one head. The low strength hydraulic lime-based mortar adopted for wall bed and head joints was characterised by a flexural strength of 0.94 MPa (Co.V. 20 %) and by a compression strength of 4.11 MPa (Co.V. 21 %). The main mechanical properties of the hydraulic lime mortar utilised as matrix of the Flax TRM systems consisted in a flexural strength of 3.13 MPa (Co.V. 13 %) and a compression strength of 11.13 MPa (Co.V. 8 %).

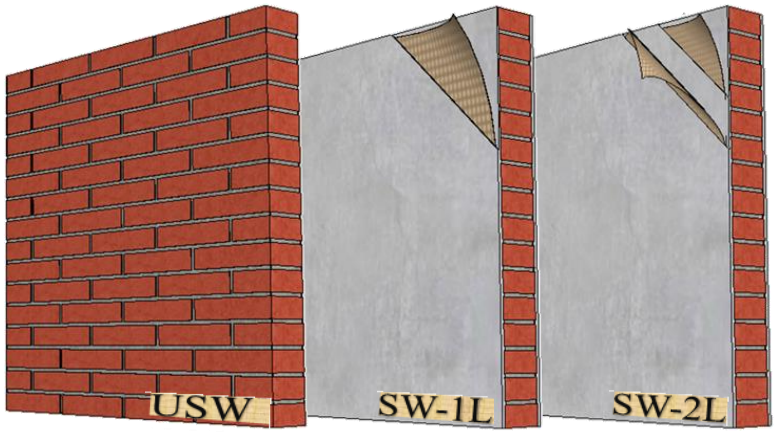

Figure 5.1: Specimens subjected to diagonal compression test: UnStrengthened (USW), Flax TRM-1L Strengthened (SW-1L) and Flax TRM-2L Strengthened (SW-2L) walls.

In both reinforcing configurations the strengthening system was applied uniformly to all the wall surface and symmetrically on both sides of the masonry elements. The installation of the Flax-TRM reinforcing system consisted in the application of the first layer of mortar on the masonry surface (Figure 5.2a), the application of the textile by ensuring it to be properly tight and embedded within the matrix (Figure 5.2b), the application of the next mortar layer and possible application of further flax textile layers, application and smoothing of the external layer of mortar (Figure 5.2c). Table 5.1 lists the main properties of the three series of specimens considered, including the reinforcement rate defined as the maximum capacity in tension of the textile included in a TRM strip one meter wide.

Figure 5.3 depicts the apparatus adopted to carry out the diagonal compression tests.

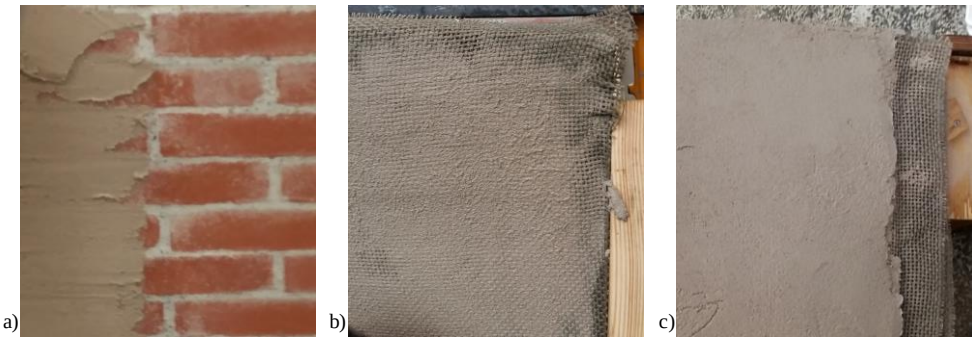

Figure 5.2: Application of the Flax TRM system: a) application of the first layer of mortar; b) application of the flax textile and impregnation in the matrix; c) application of the last layer of mortar and smoothing of the surface.

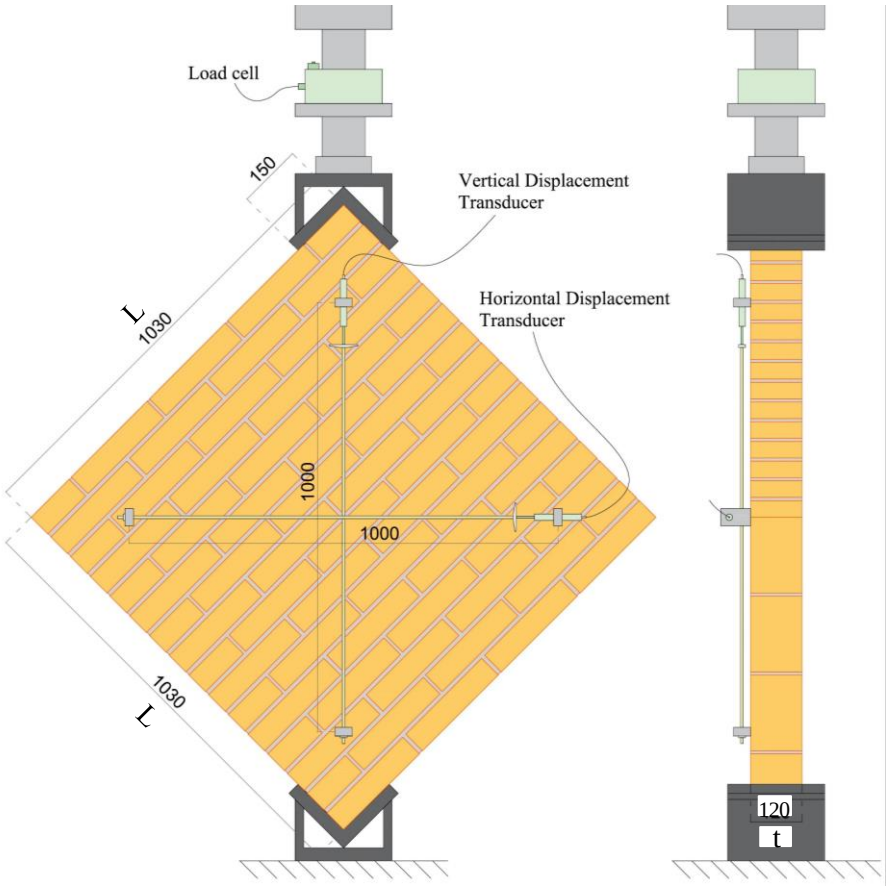

Figure 5.3: Test set-up of Diagonal Compression Tests.

The test machine, with maximum compressive lead capacity of 500 kN, was equipped by a load cell placed along the loading axis to record the load values during

the test. The test was carried out in displacement control with a rate of 1mm/min. The load was transmitted to the specimen by means of two loading shoes placed at the two edges of the vertical axis. The loading shoe consisted of a steel device characterised by a high stiffness (30 mm of thickness), and by a length of bearing of 150 mm specifically designed to avoid excessive local stress in the bearing zone and in correspondence to the mortar bed joints present in the loaded corners of the wall. The loading shoe was connected to the masonry assemblage by means of a high strength fast-setting cement-based mortar. The walls were instrumented by means of two linear displacement transducers, with a gauge length of 1000 mm, to measure the shortening of the vertical diagonal and the lengthening of the horizontal one under load.

Table 5.1: Properties of the three series of specimens tested in diagonal compression.

Series	n° spec.	Masonry type	Wall size t x w x h (mm^3)	Reinforc. type	Type of mortar	thick. (mm)	Reinf. rate (kN/m)
USW	3	clay brick	120x1030x1030	-	-	-	-
SW-1L	3	clay brick	120x1030x1030	Flax TRM-1L	hydraulic lime	5	31
SW-2L	3	clay brick	120x1030x1030	Flax TRM-2L	hydraulic lime	8	62

One of the two sides of the walls was treated in order to get, during the test, images to be used for a Digital Image Correlation (DIC) analysis. The treatment consisted in a white background on which black dots were stochastically sprinkled by means of a spray can. The camera was placed at a focal distance of 260 cm. The acquisition rate was of 2 ph/s and the resolution of the images was of 2560 x 2048 pixels (0.51 mm/pix). The analysed surface size was of 1 m x 1 m (Figure 5.4).

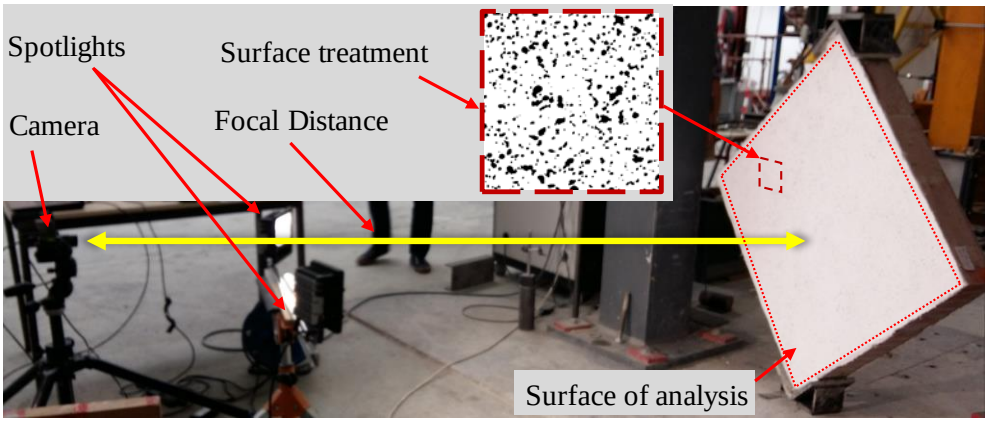

Figure 5.4: Digital Image Correlation equipment for walls tested in diagonal compression.

5.2 Results and discussion

5.2.1 Failure mode

As expected, the failure mode was characterised by the development of cracks along the loaded vertical diagonal, due to a stress concentration in correspondence to the tensile principal direction. The unreinforced walls were characterised by a brittle failure mode with the splitting of the two parts of the wall by means of a quasi-vertical cracks that mainly followed the mortar bed joints and in some parts broke the clay bricks (Figure 5.5a).

The same crack development trend was observed on the externally strengthened walls in which the cracks spread to the mortar matrix of the Flax-TRM system adopted (Figure 5.5b). During the post-peak phase, the rupture of the flax threads was observed in correspondence of such transversal cracked surfaces in both the reinforced series of specimens, SW-1L and SW-2L (Figure 5.6). This aspect is consistent with what was observed in the characterisation tests at local scale, tensile and shear bond tests, in which in both the cases, the ultimate failure was mainly governed by the tensile capacity of the flax textile (*Chapter 4*).

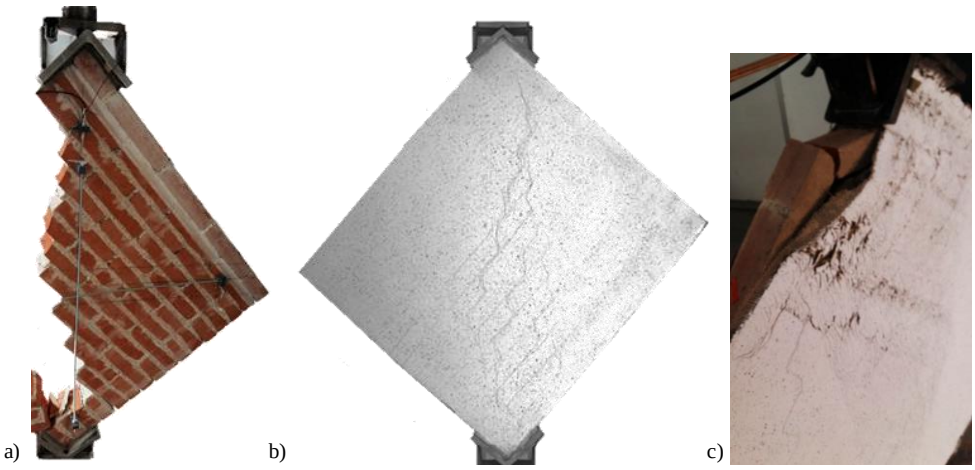

Figure 5.5: Failure modes: a) USW representative specimen; b) SW representative specimen; c) failure for local debonding (Specimen SW-1L-1).

This behaviour, although being due to the relatively low tensile capacity of flax fabric (for instance compared to the more common high strength fibre textiles), emphasised that the system was characterised by an effective bond between its components, i.e. good properties at both TRM-to-masonry and fibres-to-mortar interface surfaces. Also, this behaviour did not change by increasing the amount of textile, leaving room for the possibility of further investigations aimed at improving

the global shear capacity of the system, by increasing even more the amount of textile reinforcement. Only in one case, specimen SW-1L-1, local debonding phenomena were observed, with a detachment of the Flax-TRM system from the masonry substrate in one of the edges of the wall (Figure 5.5c). This behaviour, due to its isolated nature, may be attributed to possible inaccuracy during the installation of the TRM composite to on the wall that led to a local buckling of the reinforcing layer.

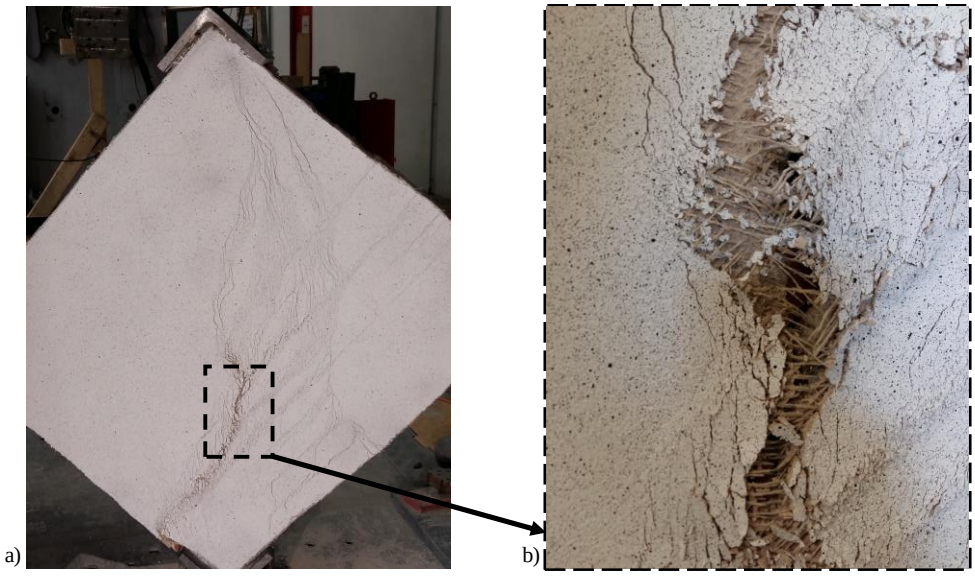

Figure 5.6: Failure mode: a) specimen SW-2L-3; b) close-up of the textile rupture.

5.2.2 Shear stress vs shear strain response

The results of diagonal compression tests carried out on the three series of specimens, USW, SW-1L, SW-2L, are shown in terms of applied load versus vertical and horizontal displacements (ΔV and ΔH), respectively. Specifically, the shortening of the vertical diagonal and the lengthening of the horizontal one are presented in Figure 5.7, Figure 5.8 and Figure 5.9. In accordance with standards ruling diagonal compression tests [38], on the basis of the recorded data, load and displacements, the values of the shear stress, τ_0, and the shear strain, γ, in the centre of the masonry assemblage were assessed, under the hypothesis of pure shear conditions in the middle of the panel, by means of Equation 5.1 and Equation 5.2:

$$\tau_{0,ASTM} = \frac{P}{\sqrt{2} \cdot A_n} \quad \text{Equation 5.1}$$

$$\gamma = \frac{\Delta V + \Delta H}{L_g} \quad \text{Equation 5.2}$$

were P is the applied load, A_n, the net transversal area of the specimen, ΔV, the vertical shortening, ΔH, the horizontal lengthening and L_g is the gauge length of 1m.

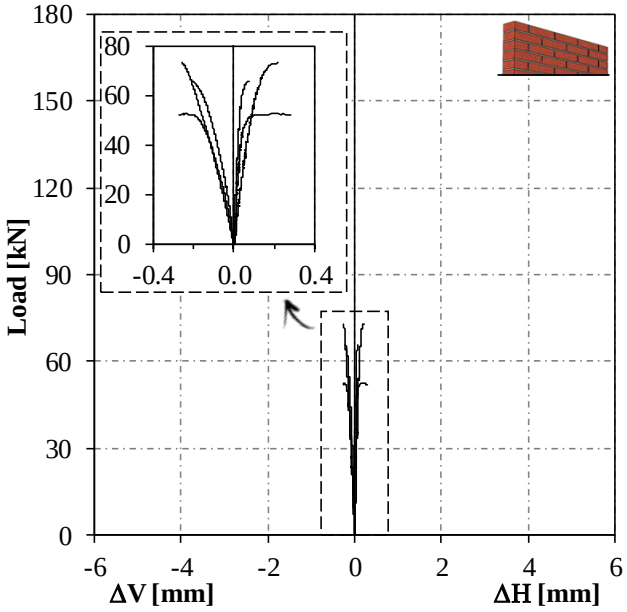

Figure 5.7: Load-Vertical/Horizontal displacements curves of diagonal compression tests of series USW.

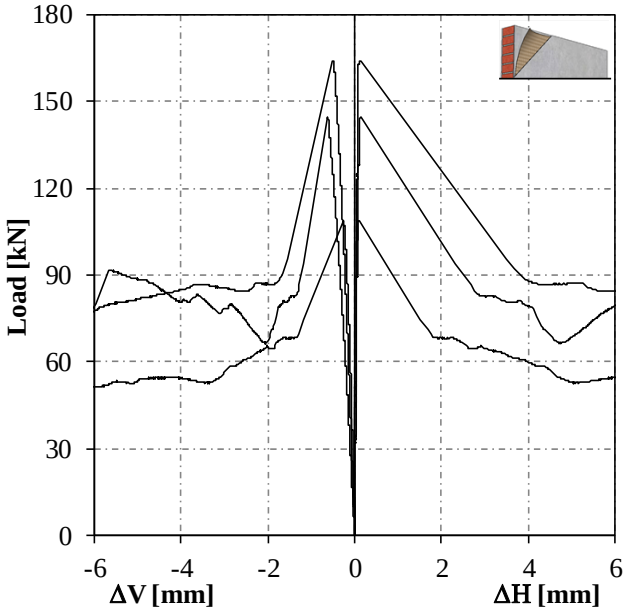

Figure 5.8: Load-Vertical/Horizontal displacements curves of diagonal compression tests of series SW-1L.

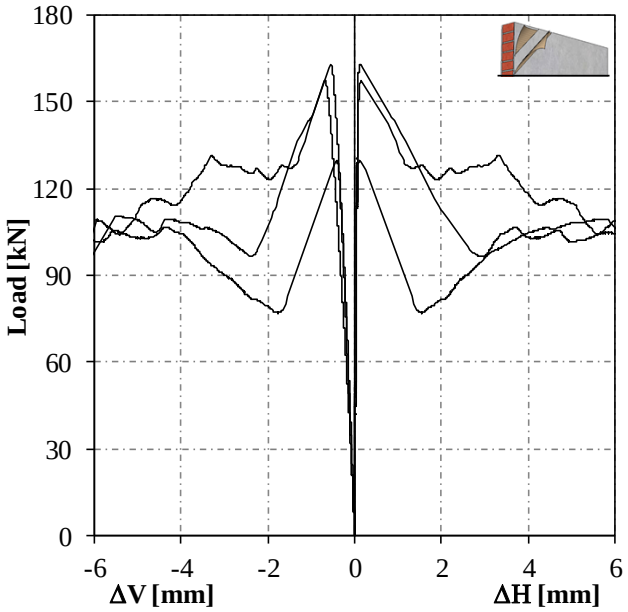

Figure 5.9: Load-Vertical/Horizontal displacements curves of diagonal compression tests of series SW-2L.

The curves in terms of shear stress, τ_0, and shear strain, γ, for all series of specimens are plotted in Figure 5.10, Figure 5.11 and Figure 5.12.

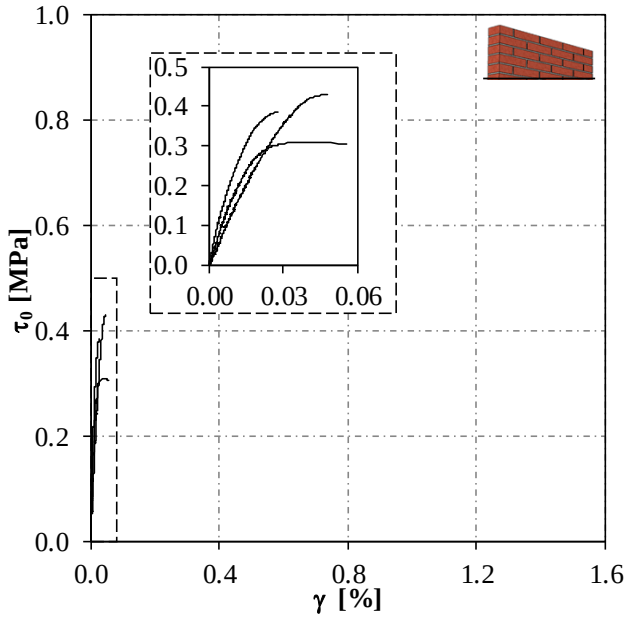

Figure 5.10: Shear stress – shear strain displacements curves of series USW.

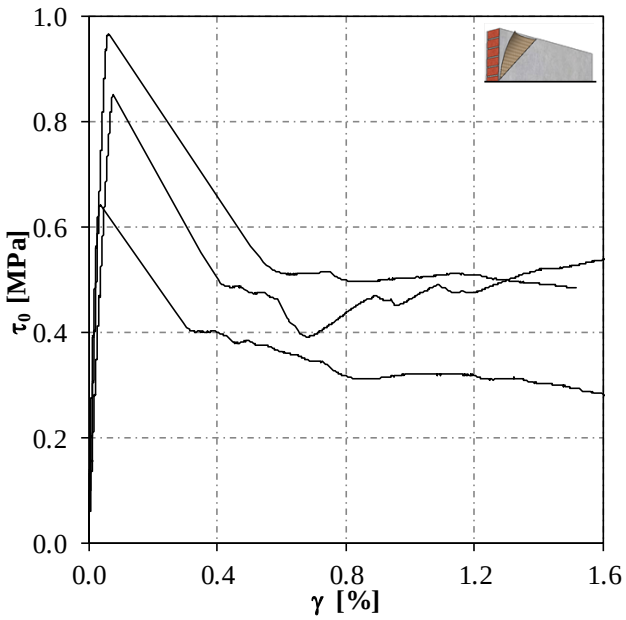

Figure 5.11: Shear stress – shear strain displacements curves of series SW-1L.

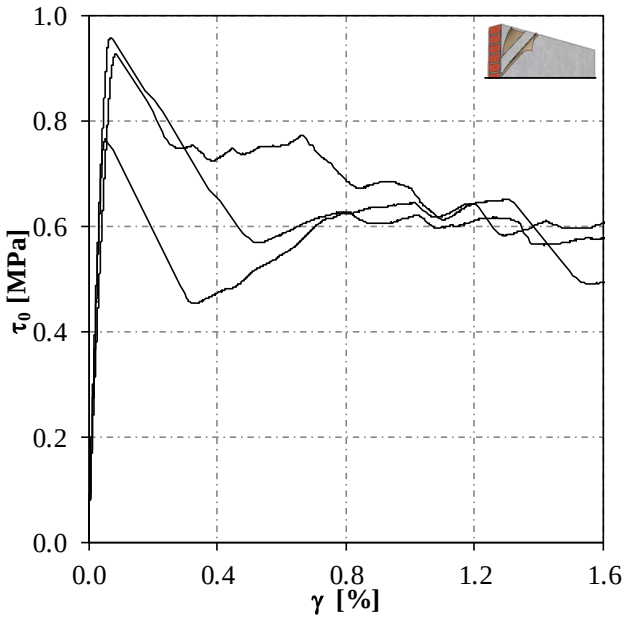

Figure 5.12: Shear stress – shear strain displacements curves of series SW-2L.

The behaviour of the unstrengthened specimens, USW, was characterised by an elastic branch followed by a short plastic branch and a brittle failure of the wall due to the opening of a crack along the vertical direction (Figure 5.10). The

externally strengthened walls, SW-1L and SW-2L, exhibited a pseudo-elasto-plastic behaviour as well, up to the achievement of the maximum capacity. Moreover, in these cases the end of the elastic phase is due to the development of cracks within the wall and the mortar of the Flax TRM system in correspondence the loaded diagonal. Unlike the USW specimens, the reinforced ones exhibited a post peak phase in which the textile was properly tight and conferred to the system the capacity of bearing significant loads at high values of displacements. As a matter of fact, although a considerable strength loss after the attainment of the maximum load occurred, the implementation of the Flax TRM systems over the masonry assemblages insures the post-failure integrity of wall, as shown by the residual load which is sustained for large values of shear deformation. This aspect, as known, represents a fundamental aspect, especially in view of solutions aimed at improving the structures performance toward horizontal actions.

The inelastic phase was characterised by a progressive decrease of the load corresponding to the gradual failure of the textile bundles in correspondence to the cracks developed along the loaded diagonal. The main parameters concerning the diagonal compression tests carried out on the three series of specimens, are listed in Table 5.2 with respect to the single walls and in terms of mean values for each series together with the corresponding coefficient of variation. In terms of maximum load, P_{max}, the externally strengthened walls, SW-1L and SW-2L, gained an average value more than two times higher than the one attained by the unstrengthened walls, USW. However, by comparing the two reinforced series no significant differences are observed, even though the amount of textile reinforcement was doubled in the SW-2L series with respect to the SW-1L one. As it might be expected, the textile did not significantly affect the elastic phase, mainly governed by the contribution of the matrix. As a matter of fact, in correspondence of the maximum load the masonry and the mortar matrix started to crack, while the textile basically remained unbroken, except for few well-anchored yarns. The textile contribution played an important role when higher values of strains were gained, hence in the post peak phase when the mortar matrix was already cracked.

Similar considerations can be done for the shear modulus G, determined as the slope of the shear stress-shear strain curve in the elastic phase, which did not show any significant change between the three series of specimens.

In all strengthened walls, a significant load loss was observed immediately after the achievement of the peak load. However, this load loss, that was of about the 30% of the maximum load in the case of SW-1L specimens, halved in the case of SW-2L (about 15% of the maximum load). This aspect emphasized that in the post peak phase, at higher values of the strain, the contribution of the fibres got significant

and a better performance was attained by increasing its amount within the reinforcement system.

In order to quantify the strain capacity of the system, the coefficient μ was considered, defined as the ratio between the shear strain value corresponding to a loss of bearing capacity equal to 20% of the peak load, in the post peak phase, and the value of the shear strain corresponding to the maximum load.

Table 5.2: Parameters concerning diagonal compression tests carried out on the three series of specimens: USW, SW-1L and SW-2L.

specimen	P_{peak} (kN)	$\tau_{o,peak}$ (MPa)	γ_{peak} (%)	G (MPa)	μ	Γ_1 (J)	Γ_2 (J)
USW-1	66	0.39	0.03	2987	-	9	-
USW-2	73	0.43	0.05	1473	-	11	-
USW-3	53	0.31	0.05	2104	-	11	-
mean	64	0.38	0.04	2188	-	10	-
Co.V.	16	16	27	35	-	11	-
SW-1L-1	164	0.97	0.03	2412	4.25	48	881
SW-1L-2	145	0.85	0.05	1460	3.01	51	1552
SW-1L-3	109	0.64	0.05	3560	4.88	19	1019
mean	139	0.82	0.04	2478	4.05	39	1151
Co.V.	20	20	27	42	23	45	31
SW-2L-1	163	0.96	0.07	2335	4.17	54	1730
SW-2L-2	130	0.77	0.05	1945	4.84	31	2964
SW-2L-3	158	0.93	0.08	2002	4.14	65	3222
mean	150	0.88	0.07	2094	4.38	50	2639
Co.V.	12	12	22	10	9	35	30

The strengthened series, SW-1L, exhibited a significant increase of the strain capacity with respect to the USW series, and a further increase of about the 10% was attained by doubling the amount of reinforcing textile, in the SW-2L series of specimens.

In order to analyse the ductile behaviour until the ultimate conditions of the specimen, the value of the energy dissipated was determined as the area under the load-vertical displacement curve. Specifically, Γ_1 is the energy dissipated to achieve the peak load, Γ_2 represented the energy dissipated during the post peak phase corresponding to the range between the peak load and a load equal to the 30% of it. It was observed that by doubling the amount of flax textile, the mean value of the dissipated energy more than doubled (Figure 5.13). The analysis of this parameter,

in line with the others, confirmed the significant contribution of the textile during the post peak phase.

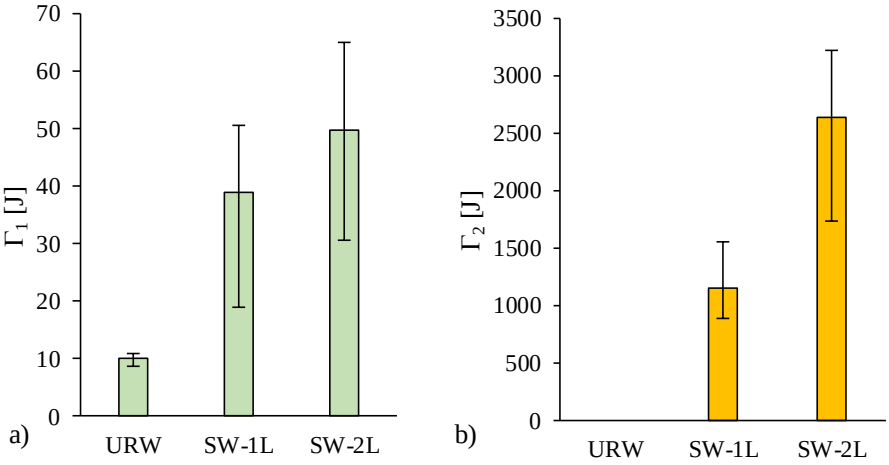

Figure 5.13: Mean values of the energy dissipated during diagonal compression tests for all the series of specimens: a) energy dissipated to achieve the peak load; b) energy dissipated during the post peak phase.

5.3 Comparison with standards

The aim of this section is to compare the experimental evidences with the strength value obtained theoretically by adopting the formulations proposed by standards concerning the assessment of the shear capacity of masonry elements and masonry elements externally strengthened by the application of TRM systems. First, the experimental strength of unstrengthened walls was compared with the strength assessed with respect to the Italian standard NTC 2018 [59], and specifically referring to chapter 8 of the explanatory circular concerning the assessment of the capacity of existing buildings. Secondly, the increase of shear capacity conferred by the TRM composite experimentally observed, was compared with the one evaluated according to the instructions provided by the CNR-DT 215/18 [61] proposed to design such retrofitting interventions.

The models adopted by the standards provide the shear strength of masonry elements in direct shear loading conditions while in the present experimental study the capacity of the wall was assessed by means of diagonal compression tests. For this reason, being not possible to directly compare the shear capacities, the comparison was carried out: in terms of shear stress attained in the centre of the masonry element, in the case of unstrengthened walls; in terms of increase of strength achieved by the reinforcement, in the case of strengthened walls.

5.3.1 Unstrengthened walls

The capacity of unstrengthened walls is expressed in terms of the parameter, labelled as τ_0, defined as the maximum shear stress attained in the centre of the panel in pure shear conditions, in absence of compression stress.

Considering diagonal compression test loading conditions several approaches are available to determine the shear stress, τ_0. According to the approach followed by the standard ASTM 519-2 [38] considering the element in the middle of the panel, with the axis oriented parallel to the two diagonals with the origin at their intersection, the two principal stress, oriented along these axis, attain the same value, and the shear stress in absence of normal stress, $\tau_{0,ASTM}$, can be defined according to Equation 5.3, where A_n represents the net area of the wall. According to the approach described by RILEM TC-76-LUM recommendations [115], the state of stress in the middle of the panel is the result of an elastic solution considering the wall a homogeneous and isotropic means. By that hypothesis the principal stress in compression and tension assume different values and the shear stress in absence of normal stress, $\tau_{0,RILEM}$, is determined in accordance to Equation 5.4.

$$\tau_{0,ASTM} = \frac{P_{peak}}{\sqrt{2} \cdot A_n} \quad \text{Equation 5.3}$$

$$\tau_{0,RILEM} = \frac{0.90 \cdot P_{peak}}{A_n} \quad \text{Equation 5.4}$$

We can assume that the experimental maximum value of the shear stress in the middle of the panel, with respect to the series of specimens URW, is included in range between $\tau_{0,ASTM}$ and $\tau_{0,RILEM}$. The theoretical estimation of the shear stress, τ_0, was assessed by taking into account the mean values proposed by the Italian standard code, according to which the strength of the masonry assemblages is assessed on the basis of the mechanical properties of the components of the wall. Specifically, with the mechanical strength of the bricks and the mortar of the bed joints being known, an estimation of the characteristic compression strength of the masonry was done by interpolating values proposed by the standard (Table 11.10.IV of the [59]). A mean compression strength of the masonry equal to 6.3 MPa was computed. In function of this strength, and considering a masonry typology of solid bricks with hydraulic lime-based mortar, a range of values $\tau_{0,1} \div \tau_{0,2}$, in which the shear stress is included, was assessed (Table C8.5.I and Table C8.5.II of the [59], chapter 8 of the explanatory circular). The values of the shear stress range, concerning both the experimental and theoretical estimations, are listed in Table 5.3. The value of shear stress τ_0 deriving from the tests were about 2.5 times the average value assessed by means of the formulation proposed by the standard code, highlighting that the strength values

conventionally used in the design phase, in absence of experimental data, guarantee a wide safety margin. This aspect also emphasises that the diagonal compression test does not perfectly guarantee pure shear conditions.

Table 5.3: Comparison of the shear strength between experimental and theoretical results of unstrengthened walls.

Experimental results		Standard model
$\tau_{0,ASTM}$	0.38 MPa	0.10 MPa $< \tau_0 <$ 0.25 MPa
$\tau_{0,RILEM}$	0.48 MPa	

The theoretical shear capacity of the unreinforced wall, in direct shear conditions, was assessed according to the modified formulation of Turnsek-Cacovic reported in the explanatory circular of the Italian standard NTC 2018, that in absence of normal stress takes the following form (Equation 5.5):

$$V_t = \frac{A_n \cdot 1.5 \cdot \tau_0}{b} \quad \text{Equation 5.5}$$

where A_n is the net area of the wall defined as the product of the length and the thickness, τ_0 is the shear stress in absence of normal stress defined as the mean value of the range $\tau_{0,1} \div \tau_{0,2}$ previously assessed, b is a corrective coefficient that takes into account the distribution of the shear stress over the section (assumed equal to 1). The theoretical value of the shear capacity of unreinforced wall in direct shear conditions, V_t, is equal to 31 kN.

5.3.2 TRM externally strengthened walls

The increase in strength experimentally observed by applying the TRM system on the masonry elements was compared with the increase of strength that can be theoretically assessed by means of models proposed by standards. According to the Italian instructions to design TRM interventions [60], the shear capacity of masonry elements loaded in their plane, $V_{t,R}$, externally strengthened by TRM systems symmetrically applied on both the wall sides, uniformly over the entire surface, and preferably with the fibres oriented in both vertical and horizontal directions, is calculated as the sum of the contribution of the unstrengthened wall, V_t, and the contribution brought by the application of the TRM composite system, $V_{t,f}$. The latter can be evaluated by means of the Equation 5.6:

$$V_{t,f} = 0.5 \cdot n_f \cdot t_{v,f} \cdot b_f \cdot \alpha_t \cdot \varepsilon_{f,d} \cdot E_f \quad \text{Equation 5.6}$$

where the product $n_f \cdot t_{v,f} \cdot b_f$ represents the area of the equivalent section of the actual shear reinforcement oriented parallel to the shear force; α_t is a coefficient that takes

into account the decrease of tensile test of the fibres when subjected to shear and it is equal to 0.8; ε_{fd} represents the maximum deformation of the textile superiorly limited by the maximum value attained during the shear bond test; E_f represents the dry textile stiffness. The strain was assumed to be equal to ε*, whose assessment procedure is shown in paragraph 4.2.3 (*Chapter 4*).

By applying Equation 5.6 to the case of the reinforcement Flax-TRM-1L and Flax-TRM-2L, considered uniformly applied to both the sides of the wall, it was obtained increases of strength, $V_{t,f}$, respectively equal to 19 kN and 38 kN. It is clear that the theoretical approach proposed by standards is conceived so that the TRM strength contribution linearly increases with the increasing of the reinforcing fibres amount. The values of the resulting global shear capacities of the TRM externally strengthened walls, $V_{t,R}$, obtained by summing the contribution of the unstrengthened wall strength, V_t, and the increase of strength provided by the TRM system, $V_{t,f}$, were respectively equal to 50 kN, for the SW-1L configuration, and 69 kN, for the SW-2L configuration. The ratio between the strength of the wall in the strengthened configuration and the strength of the unstrengthened wall are shown in Figure 5.14.

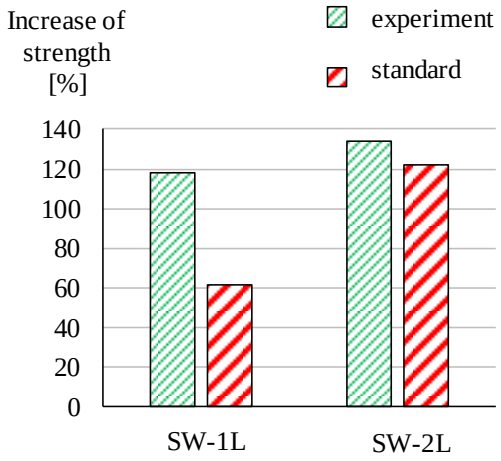

Figure 5.14: Comparison between the increases of strength deriving from the standard models and the experimental campaign, for series SW-1L and SW-2L.

It can be observed that in the case of the reinforcement Flax-TRM-1L the experimental increase of strength observed is much higher than what was observed by applying the theoretical model of the standard. In the case of SW-2L series, such difference between experimental and theoretical results decreases. In both cases the standard model was be conservative providing lower values of increase of strength. By looking at the increase of strength concerning the reinforcement system Flax-

TRM-2L, we can observe that, contrary to what is proposed by the standard, the experimental evidences showed that the increase of strength was not directly proportional to the increment in terms of fibre textile reinforcement. This discrepancy in the results emphasizes that the increase of the fibre mechanical ratio by overlapping different textile plies does not necessarily result in the same increase of strength obtainable with the use of a denser textile grid. Moreover, it seems that the textile arrangement plays a fundamental role in the global behaviour of the system, especially in the case of the use of plant fibres, already characterised by issues related to a uniform distribution of the stress between the several fibre bundles, due to the unavoidable imperfections of the natural fabric itself.

The approach of the standard seems to consider the maximum capacity of the system coinciding with the tensile failure of the reinforcing grid. However, in the specific case of study, although on one hand the ultimate state was actually characterised by the tensile rupture of the fibres, on the other hand the maximum capacity coincided with the end of the phase in which the masonry and the mortar matrix of the TRM system started to crack, and the textile still remained unbroken. This aspects, although prospecting a discrepancy between the experimental and theoretical results, also highlighted a limit in the standard model that did not take into account different failure modes, as the one occurred in the present study, and, for example, did not take into account the nature, and so the contribution, of the mortar employed in the TRM system. Probably, further analysis aimed at obtaining a more elaborated formulation, that would better consider the contribution of all the components of the TRM-to-masonry system, may provide a more efficient model capable to better predict the mechanical behaviour of the entire system.

5.4 Comparison with the literature

This section aims at providing a comparison of the results obtained in the present study with similar experimental outcomes from the literature concerning diagonal compression tests carried out on masonry elements externally strengthened by TRMs. The analysis was carried out on two levels: a general comparison of the main mechanical parameters performed with respect to a large heterogeneous database of walls, by also focusing the attention on the cases in which plants fibres were adopted as reinforcement; a comparison with similar studies in which reinforcement configurations obtained by overlapping several textile plies were considered.

In order to have a large database, unavoidably walls characterised by different building blocks, geometry and reinforcement system with respect to what presented in this study, were considered as comparison. Only studies concerning diagonal

compression tests carried out in laboratory were considered, excluding in-situ tests, in order have a uniformity in the test set-up. To take into account this heterogeneity, for each series of specimens considered, the main characteristics, such as wall size, masonry type, TRM adopted and reinforcement configuration, were listed in Table 5.4. As reported in Table 5.5, several parameters to describe the mechanical properties of the specimens were considered as well, such as the strength of both the mortar and the textile adopted in the TRM system and the reinforcement rate (defined as the maximum capacity in tension of the textile included in a TRM strip one meter wide, expressed in kN/m). As proposed in similar studies [8] the mortar mechanical ratio, ω_m and the grid mechanical ratio, ω_f, representing an index of the contribution in terms of strength, respectively of the TRM mortar and textile, were considered as well and computed according to Equation 5.7 and Equation 5.8:

$$\omega_m = \frac{f_t \cdot A_f}{\tau_0 \cdot A_{masonry}} \quad \text{Equation 5.7}$$

$$\omega_f = \frac{\sqrt{f_{cm}} \cdot A_{matrix}}{\tau_0 \cdot A_{masonry}} \quad \text{Equation 5.8}$$

where f_t is the ultimate tensile strength of the textile grid, τ_0 represents the capacity in terms of shear stress of the unstrengthened configuration, $A_{masonry}$ represents the wall section ($L \cdot t$, as defined in Figure 5.3), f_{cm} is the compression strength of the TRM mortar, and A_{matrix} represents the mortar matrix section ($L \cdot t_{matrix}$), A_f is the total area of the mesh reinforcement computed as defined in [8] (it is the product among: $n_{orientation}$, a coefficient related to the grid orientation equal to 1 for unidirectional fabric with angle 0°, equal to 2 for bidirectional grids with orientation angle 0°-90°; n_{side}, the number of strengthened sides of the wall; n_{layers}, the number of grid layers in each side; t_{eff}, the grid equivalent dry thickness; L, the wall edge lenght).

In order to compare the mechanical response under diagonal compression tests the following parameters were considered: the maximum capacity of the wall in terms of shear stress, τ_{max}, and the shear modulus, G, both defined according to the ASTM E519 [38], the ratio between their values in the strengthened configuration over the values concerning the unstrengthened reference one, τ_{max}/τ_{USW} and G/G_{USW}, the ductility, μ, computed as the ratio γ_u/γ_{el} between the shear strain at the elastic limit and at the ultimate configuration (γ_{el} corresponds to the furthermost point at which shear stress and strain are linearly correlated, depending on the shear stress-strain curve it corresponds either to the end of the elastic branch or to the point of the elastic phase corresponding to the 80% of the peak load, γ_u typically corresponds to a load equal to the 80% of the peak load in the post peak phase).

Table 5.4: Comparison of test results with data from the literature for TRM strengthened masonry panels in Diagonal Compression.

Paper	wall size mm^3	mas. type	TRM textile	TRM mortar	$f_{c,m}$ MPa	t_{TRM} mm	reinf. conf.	$f_{t,tex}$ MPa	ρ kN/m	τ_{max} MPa	$\frac{\tau_{max}}{\tau_{USW}}$	G MPa	$\frac{G}{G_{USW}}$	μ	Failure mode	ω_f	ω_m
SW-1L series	1000 x 1000 x 120	CB	Flax	HL	11.1	5	Unif.	354	31	0.82	2.2	2478	1.1	4.1	C-TRM, CS-Deb	2.7	0.7
SW-2L series	1000 x 1000 x 120	CB	Flax	HL	11.1	8	Unif. (2 pl.)	354	62	0.88	2.3	2095	1.0	4.4	C-TRM, CS-TRM	5.4	1.2
Menna et al. 2015 [87]	1200 x 1200 x 250	TB	Hemp	PM	16.1	15	Unif*	-	20	0.50	1.9	601	1.26	5.1	C-TRM, CS-TRM	1.2	1.8
	1180 x 1180 x 250	CB	Hemp	PM	16.1	15	Unif*	-	20	0.75	5.3	445	1.21	7.4	C-TRM	2.3	3.4
	1200 x 1200 x 250	TB	Hemp	HL	14.2	40	Unif*	-	20	0.75	2.8	1543	3.24	7.1	C-TRM	1.2	4.5
	1180 x 1180 x 250	CB	Hemp	HL	14.2	40	Unif*	-	20	0.76	5.4	2250	6.14	32.2	C-TRM	2.3	8.6
Olivito et al. 2012 [88]	510 x 510 x 120	CB	Hemp	-	-	-	Grid	240	27	1.34	1.2	3065	1.32	-	CS-TRM	0.8	-
	510 x 510 x 120	CB	Hemp	-	-	-	Grid	240	53	1.32	1.2	3096	1.33	-	CS-TRM	1.6	-
	510 x 510 x 120	CB	Flax	-	-	-	Grid	350	54	2.13	2.0	2870	1.23	-	CS-TRM	1.7	-
	510 x 510 x 120	CB	Flax	-	-	-	Diag	350	26	1.77	1.6	3043	1.31	-	C-TRM	0.8	-
	510 x 510 x 120	CB	Flax	-	-	-	Diag	350	13	1.56	1.5	3042	1.31	-	C-TRM	0.4	-
	510 x 510 x 120	CB	Glass	-	-	-	Grid	-	-	1.53	1.4	4128	1.77	-	CS-TRM	-	-
	510 x 510 x 120	CB	Glass	-	-	-	Diag	-	-	1.54	1.4	3772	1.62	-	C-TRM	-	-
Babaeidarabad et al. 2014 [116]	1200 x 1200 x 120	CB	Carbon	Cem	20.0	10	Unif	802	40	1.32	2.2	1520	1.8	18.2	C-TRM	2.2	1.2
	1200 x 1200 x 120	CB	Carbon	Cem	20.0	10	Unif (4 pl.)	802	160	2.86	4.7	2660	3.2	4.3	TC	8.8	1.2
Marcari et al. 2017 [117]	1000 x 1000 x 250	TB	Basalt	HL	15.0	6	Unif	3000	110	0.62	1.6	1017	1.4	6.7	C-TRM	4.6	0.5
Wang et al. 2018 [118]	910 x 910 x 110	CB	Carbon	Cem	32.0	15	Grid	3110	56	1.80	2.1	2806	1.6	4.3	C-TRM, TC	2.4	1.8
	910 x 910 x 110	CB	Steel	Cem	32.0	10	Grid	2800	72	1.50	1.8	2300	1.3	14.9	TC	3.1	1.2
	910 x 910 x 110	CB	Basalt	Cem	32.0	15	Unif (2 pl.)	1006	35	1.67	2.0	2529	1.5	1.0	C-TRM, CS-TRM	1.5	1.8

Continuation Table 5.4.

Paper	wall size mm^3	mas. type	TRM textile	TRM mortar	$f_{c,m}$ MPa	t_{TRM} mm	reinf. conf.	$f_{t,tex}$ MPa	ρ kN/m	τ_{max} MPa	$\frac{\tau_{max}}{\tau_{USW}}$	G MPa	$\frac{G}{G_{USW}}$	μ	Failure mode	ω_f	ω_m
	910 x 910 x 110	CB	Basalt	Cem	32.0	15	Unif (4 pl.)	1006	70	1.71	2.0	4538	2.6	13.4	TC	3.0	1.8
Almeida et al. 2015 [119]	990 x 990 x 140	HCB	Carbon	Cem	44.0	25	Unif	4300	185	2.09	4.2	4458	1.6	-	C-TRM, CS-Deb	11	4.8
Parisi et al.2013 [120]	1230 x 1230 x 310	TB	GFRP	HL	16.1	10	Unif	1270	51	0.65	3.0	570	1.4	5.4	C-TRM	3.1	1.2
Gattesco et al. 2015 [121]	1160 x 1160 x 250	CB	GFRP	HL-Cem	6.7	30	Unif	490	168	0.93	2.0	3481	1.64	16.8	C-TRM	5.8	1.3
	1160 x 1160 x 250	CB	GFRP	HL-Cem	6.7	30	Unif	490	84	0.97	2.1	3146	1.48	7.8	C-TRM	2.9	1.3
	1160 x 1160 x 250	CB	GFRP	HL-Cem	6.7	30	Unif	490	56	1.00	2.1	2953	1.40	4.7	C-TRM	1.9	1.3
	1160 x 1160 x 250	CB	GFRP	HL-Cem	6.7	30	Unif	490	168	1.02	1.6	5165	1.51	15.5	C-TRM	4.3	1.0
	1160 x 1160 x 250	CB	GFRP	HL-Cem	6.7	30	Unif	490	84	1.20	1.9	4783	1.40	5.3	C-TRM	2.1	1.0
	1160 x 1161 x 250	CB	GFRP	HL-Cem	6.7	30	Unif	490	56	1.23	2.0	4513	1.32	4.9	C-TRM	1.4	1.0
	1160 x 1161 x 380	CB	GFRP	HL-Cem	6.7	30	Unif	490	168	0.77	1.7	3843	1.48	15.7	C-TRM	3.9	0.9
	1160 x 1161 x 380	CB	GFRP	HL-Cem	6.7	30	Unif	490	84	0.77	1.7	3506	1.35	5.3	C-TRM	1.9	0.9
	1160 x 1161 x 380	CB	GFRP	HL-Cem	6.7	30	Unif	495	105	0.90	2.0	4258	1.64	11.0	C-TRM	2.4	0.9
	1160 x 1161 x 380	CB	GFRP	HL-Cem	6.7	30	Unif	495	70	0.70	1.5	3984	1.54	8.4	C-TRM	1.6	0.9
Ferretti et al. 2017 [122]	1200 x 1200 x 120	CB	Carbon	FR-PM	6.5	6	Unif*	2363	111	1.17	1.9	-	-	-	C-TRM	6.1	0.4
	1200 x 1200 x 120	CB	Glass	FR-PM	6.5	6	Unif*	991	63	1.24	2.1	-	-	-	C-TRM	3.5	0.4
Incerti et al. 2018 [123]	1100 x 1100 x 250	CB	Basalt	HL	12.6	6	Unif*	1016	33	0.85	1.5	2575	1.02	-	C-TRM	0.9	0.3
	1160 x 1160 x 250	CB	Basalt	HL	12.6	6	Unif*	1016	33	0.79	1.9	2537	1.71	-	C-TRM	1.3	0.4
Del Zoppo et al. 2019 [124]	1280 x 1280 x 140	CB	BFRP	FR-HL	14.5	15	Unif	1542	60	1.28	3.7	2350	1.38	5.0	C-TRM	4.9	2.3
	1280 x 1280 x 285	CB	BFRP	FR-HL	14.5	15	Unif	1542	60	0.90	1.6	2857	1.01	6.8	C-TRM	1.5	0.7

Continuation Table 5.4.

Paper	wall size mm^3	mas. type	TRM textile	TRM mortar	$f_{c,m}$ MPa	t_{TRM} mm	reinf. conf.	$f_{t,tex}$ MPa	ρ kN/m	τ_{max} MPa	$\frac{\tau_{max}}{\tau_{USW}}$	G MPa	$\frac{G}{G_{USW}}$	μ	Failure mode	ω_f	ω_m
De Lorenzis et al. 2004 [125]	461 x 461 x 100	CS	Carbon	PM	20.4	7	Unif	2800	132	1.75	1.2	-	-	-	C-TRM	3.7	0.4
Prota et al. 2006 [126]	1030 x 1030 x 250	TB	Glass	FR-Cem	24.1	10	Unif (2 pl.)	1276	87	0.59	2.5	731	1.43	3.3	C-TRM	5.8	1.6
	1030 x 1030 x 250	TB	Glass	FR-Cem	24.1	10	Unif	1276	44	0.50	2.1	492	1.00	3.5	CS-TRM	2.9	1.6
Faella et al. 2010 [127]	1160 x 1160 x 380	TB	Carbon	FR-Cem	38.0	10	Unif	4800	160	0.33	5.6	-	-	-	C-TRM, C-Deb	29	5.5
Balsamo et al. 2012 [128]	1000 x 1000 x 250	TB	GFRP	FR-PM	16.1	10	Unif	-	45	0.52	3.3	821	2.96	4.7	C-TRM	4.6	2.1
	1000 x 1000 x 250	TB	BFRP	FR-PM	16.1	10	Unif	-	60	0.39	2.5	369	1.33	2.4	C-TRM	6.2	2.1
	1000 x 1000 x 250	TB	GFRP	Cem	28.3	10	Unif	-	45	0.64	4.1	928	3.35	4.9	C-TRM	4.6	2.7
Del Zoppo et al. 2019 [129]	1200 x 1200 x 250	TB	Steel	Cem	18.8	40	Unif*	451	115	0.97	3.8	2338	3.93	1.1	C-TRM, C-Deb	7.2	5.4
	1200 x 1200 x 250	TB	Steel	FR-Cem	14.2	40	Unif*	451	115	0.93	3.6	2196	3.69	1.9	C-TRM, C-Deb	7.1	4.7
	1200 x 1200 x 250	TB	Steel	FR-HL	14.5	40	Unif*	451	115	0.76	2.9	1552	2.61	1.5	C-TRM, C-Deb	7.1	4.7
	1200 x 1200 x 250	TB	GFRP	FR-Cem	14.2	40	Unif*	1350	76	0.94	3.7	1857	3.12	2.7	C-TRM, C-Deb	4.7	4.7
	1200 x 1200 x 250	TB	GFRP	FR-HL	15	40	Unif*	1350	76	0.62	2.4	1646	2.77	2.2	C-TRM, C-Deb	4.7	4.8
	1200 x 1200 x 250	TB	GFRP	FR-Cem	14	40	Unif*	1480	53	1.02	4.0	2252	3.79	2.0	C-TRM, C-Deb	3.3	4.7
	1200 x 1200 x 250	TB	GFRP	FR-HL	15	40	Unif*	1480	53	0.78	3.0	1384	2.33	4.6	C-TRM, C-Deb	3.3	4.7
Babaeidarabad et al. 2014 [130]	1220 x 1220 x 92	ConB	Carbon	Cem	20.0	10	Unif	802	38	2.06	1.9	3747	1.22	3.2	TC	1.6	0.9
	1220 x 1220 x 92	ConB	Carbon	Cem	20.0	10	Unif (4 pl.)	802	154	2.49	2.4	4940	1.61	1.3	TC	6.3	0.9
Ismail et al. 2018 [131]	1050 x 1050 x 150	ConB	GFRP	FR-PM	40	10	Unif	-	105	1.23	2.5	18415	5.23	12.0	C-TRM	5.6	1.7
	1050 x 1050 x 150	ConB	Basalt	FR-PM	39	10	Unif	-	60	1.35	2.7	13190	3.74	13.2	C-TRM	3.2	1.7
	1050 x 1050 x 150	ConB	CFRP	FR-PM	51	10	Unif	-	240	1.10	2.2	15050	4.27	15.1	TC	13	1.9

Table 5.5: nomenclature adopted in Table 5.4.

Properties	
$f_{c,m}$	*compressive strength of TRM mortar*
t_{TRM}	*TRM thickness*
reinf. conf.	*TRM reinforcement scheme*
$f_{t,tex.}$	*tensile strength of TRM textile*
ρ	*tensile strength of the textile per unit wigth*
τ_{max}	*maximum shear stress in the centre of the panel evaluated according to ASTM E519*
τ_{max}/τ_{USW}	*ratio between the maximum shear stress in the reinforced configuration over the maximum shear stress of the reference*
G	*elastic shear modulus evaluated according to the ASTM E519*
G/G_{USW}	*ratio between the shear modulus in the reinforced configuration over the shear modulus of the reference unstrengthened wall*
μ	*ductility*
ω_f	*grid mechanical ratio*
ω_m	*matrix mechanical ratio*
Masonry types	
CB	*clay brick units*
TB	*tuff blocks*
HCB	*holed ceramic bricks*
CS	*calcareous stones*
ConB	*concrete blocks*
TRM mortar	
HL	*hydraulic lime mortar*
PM	*pozzolanic mortar*
Cem	*cement-based mortar*
FR	*short fiber reinfroced mortar*
Reinf. Conf.	
Unif	*TRM uniformly applied over all the surface*
(x pl.)	*number of overlapped textile plies in the TRM (in the absence of number, a single ply is implied)*
Grid	*reinforcement with TRM strips oriented parallel to the wall sides (45° with respect to the load direction)*
Diag	*reinforcement with TRM strips oriented along the two wall diagonals (0°-90° with respect to the load direction)*
*	*use of mechanical anchors*
Failure mode	
C	*loaded diagonal direction*
CS	*along the mortar joints*
TRM	*TRM failure, either for textile slippage or textile rupture*
Deb	*debonding at the masonry-TRM interface*
TC	*toe crushing at the loaded edges*

5.4.1 Description of the database

Several studies exist in literature concerning the mechanical characterisation of the shear capacity of masonry elements externally strengthened by TRM composite systems. Among them only those complying with some criteria imposed by the author were considered in order to be consistent with the experimental activity herein presented. Nevertheless, the database still resulted to be quite heterogeneous due to the intention of having a large amount of data.

All studies considered concerned externally strengthened walls subjected to diagonal compression test according to the ASTM E519 [38]. The walls taken into consideration included mostly clay brick masonry, both in single and double leaf configurations, and in some cases tuff blocks or other less common blocks masonry elements.

Concerning the TRM system the most common industrial fibres were considered, such as glass, carbon, basalt and steel; GFRP and CFRP reinforcement grids were considered too, as well as few cases in which plant fibres, such as hemp and flax, were employed.

The matrices adopted were mainly either cement-, hydraulic lime- or pozzolanic-based. In all cases, the TRM reinforcement was symmetrically applied on both sides of the wall, and almost in all cases the reinforcement was uniformly applied all over the surface. In few cases different TRM reinforcement configurations, performed by the use of TRM strips or by the use of mechanical anchors, were considered as well (in these studies plant fibres were adopted as reinforcement in TRMs).

Concerning the failure mode five different cases were considered: toe crushing at the loaded edges, cracking of masonry along the loaded diagonal, combined cracking of masonry and sliding along the mortar joints, TRM failure either due to textile slippage or rupture, debonding at the TRM to masonry interface. In some cases, the failure mode resulted a combination of the just mentioned modes.

5.4.2 Comparison with the entire database

The comparison was carried out by analysing the relationship between the mechanical parameters above mentioned with the grid and mortar mechanical ratios, ω_m and ω_f. Each one of the parameters τ_{max}/τ_{USW}, G/G_{USW} and μ was studied individually by distinguishing the case studied herein from the cases in which high strength fibre textile and plant fibre fabrics were adopted.

In Figure 5.15a and Figure 5.15b the relationship between τ_{max}/τ_{USW} and respectively, ω_m and ω_f is shown. As already observed in similar studies [8], the graphs confirmed the enhancement of strength capacity to be mainly depending on

the mortar contribution rather than on the fibres one. Moreover, the graphs showed that plant fibre TRM based systems were generally characterised by lower values of the grid mechanical ratio, ω_f. This aspect is mainly due to the lower strength of plant fibres with respect to the industrial ones. It is worth emphasising that the only value out of this range is the one concerning the author's case of study characterised by the double plies flax textile reinforcing configuration.

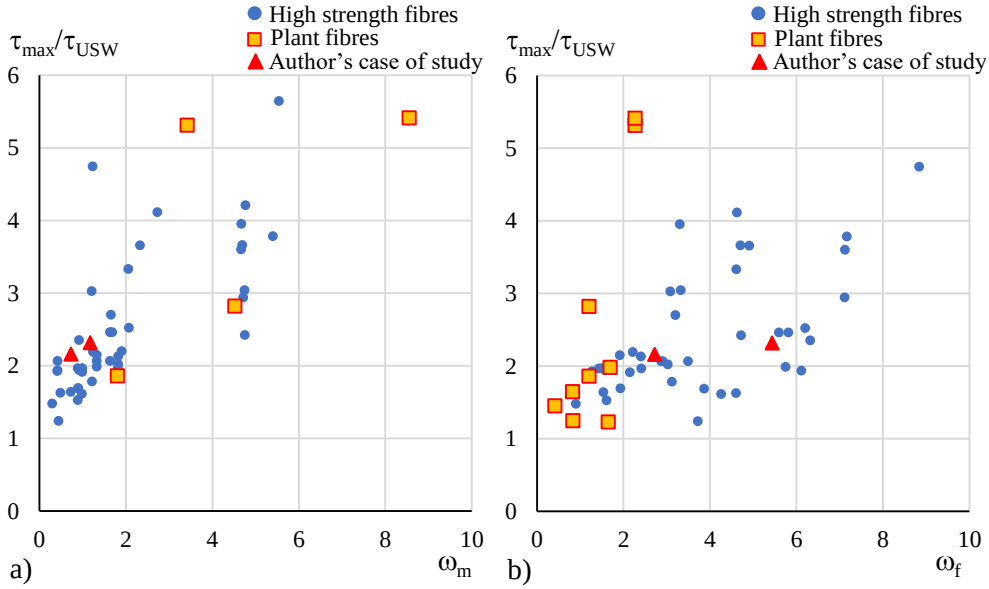

Figure 5.15: Effect of the mechanical ratios a) ω_m and b) ω_f, on the ratio τ_{max}/τ_{USW}.

The same comparison was proposed in terms of ductility, μ, in Figure 5.16a and Figure 5.16b. Although in both cases the data do not follow a clear trend, an increase of the ductility was observed in the range of greater values of the grid mechanical ratio, ω_f. Due to the low values of the grid mechanical ratio, ω_f, no significant information could be observed in terms relationship between ductility and amount of plant fibres. In the author's case of study, the grid mechanical ratio did not significantly affect the parameter of ductility, μ.

The comparison in terms of G/G_{USW} (Figure 5.17a and Figure 5.17b) showed that by increasing the mortar contribution, ω_m, a quasi linear increase of the shear modulus was observed. This trend was also confirmed in the plant fibre TRM based systems. Concerning the author's case of study, the mortar mechanical ratio, ω_m, appeared to be too low to register any significant shear stiffness enhancement. In all cases, no significant dependence seemed to exist between the fibre mechanical ratio, ω_f, and the shear modulus, G.

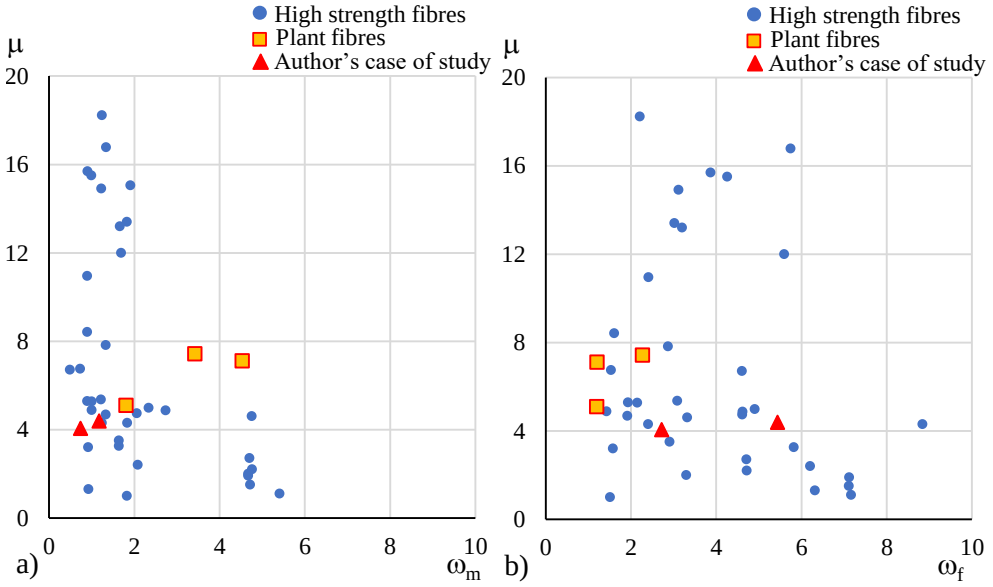

Figure 5.16: Effect of the mechanical ratios a) ω_m and b) ω_f, on the ductility μ.

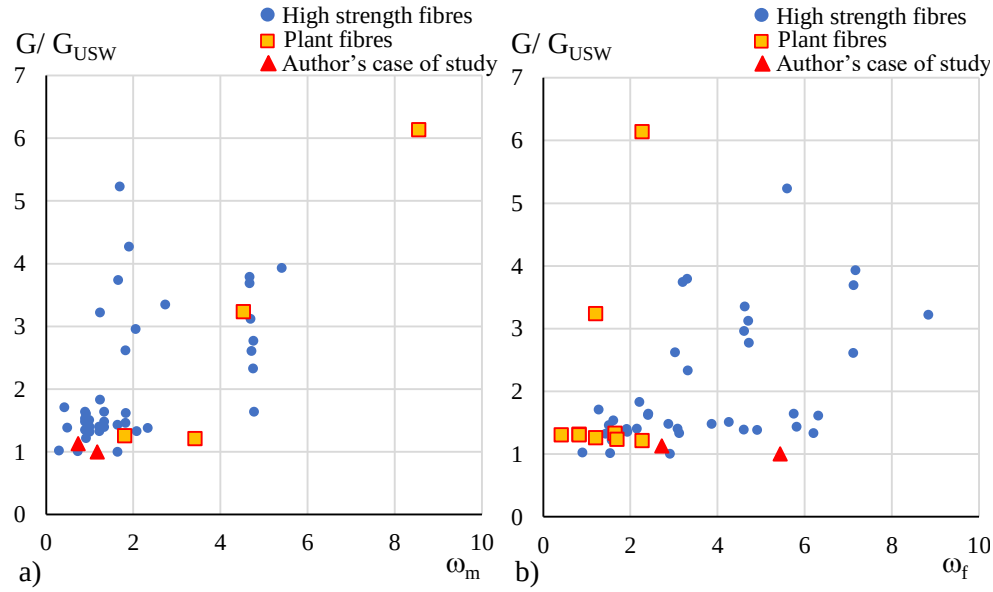

Figure 5.17: Effect of the mechanical ratios a) ω_m and b) ω_f, on the ratio G_{max}/G_{USW}.

This aspect, together with the outcomes deriving from the comparison in terms of shear stress, τ_{max}, highlighted that the elastic behaviour of masonry walls externally strengthened by TRM composite systems, is mainly governed by the strength contribution provided by the TRM mortar matrix, rather than by that one

deriving from the fibre reinforcing grid. Such evidence was expected, it is known that fibres are activated once the mortar (and the wall) is cracked.

5.4.3 Comparison between walls strengthened by multi-ply grids

Aiming at enhancing the shear capacity of TRM externally bonded systems by increasing the fibre mechanical ratio, ω_f, several studies, as well as the author's one, proposed a TRM composite system by applying overlapped textile plies (herein labelled as multi-ply grids technique), taking care that a thin layer of mortar is always introduced between the different textile grids. In order to assess the influence of the multi-ply grid technique on the mechanical behaviour of TRM externally strengthened walls subjected to diagonal compression test, the author's case of study was compared with other four cases of study in which the same reinforcement technique was adopted. Specifically, in two studies, similar to what is proposed in the thesis, the textile amount was doubled [118], [126], in other two studies it was quadrupled [116], [130]. The comparison was carried out in terms of maximum shear stress, τ_{max}, shear modulus, G and ductility, μ. The ratio between these parameters concerning the multi-ply configuration (mp) and the same parameters concerning the so-called standard-ply (sp) arrangement (τ_{mp}/τ_{sp}, G_{mp}/G_{sp}, μ_{mp}/μ_{sp}) are listed, for each case of study, in Table 5.6.

Table 5.6: Comparison between walls externally strengthened by TRMs performed with the multi-ply grid technique.

Case of study	*increase of plies*	τ_{mp}/τ_{sp}	G_{mp}/G_{sp}	μ_{mp}/μ_{sp}
Author's case of study	*x2*	1.07	0.85	1.1
Wang et al. 2018 [118]	*x2*	1.02	1.79	13.4
Prota et al. 2006 [126]	*x2*	1.19	1.49	0.9
Babaeidarabad et al. 2014 [116]	*x4*	2.17	1.75	0.2
Babaeidarabad et al. 2014 [130]	*x4*	1.21	1.32	0.4

In terms of maximum shear stress, τ_{max}, in the current study it was observed an increase of the 7% by doubling the amount of textile. This experimental evidence was in line with what observed in similar studies in which the 2-plies configuration was adopted. With respect to the case of the study [116] a significant enhancement of strength was observed by increasing the percentage of textile of the 300%. The same gain of strength was not attained in the study [130] in which the 4-plies configuration was adopted as wall. This discrepancy may be due to the fact that in the study [130] a stiffer masonry was adopted (see Table 5.4): the smaller is the strain

in the elastic phase, the smaller is the fibres contribution in this phase. In terms of elastic shear modulus, G, in all the cases of comparison an increase of stiffness was recorded, with increments in the range of the 30% to the 80%. On the contrary, in the author's case of study, the higher amount of textile lead to even lower values of the shear modulus. Regarding the ductility, μ, except for a value largely outside the mean trend [118], no important benefits were observed.

As a matter of fact, with the limitation of an analysis carried out on a small set of data, it could be affirmed that by overlapping several textile plies, no significant benefits were conferred to the system. This result may be due to the fact that the multi-ply reinforcing technique did not always guarantee the textile to be uniformly charged through the entire surface subjected to a stress concentration.

Moreover, it is worth underlining that the entire analysis was carried out without taking into account the reinforcing textile stiffness in tension. In the author's specific case of study, for example, the structure of the flax textile did not allow the grid to be tied, in a proper uniform way, during the implementation of the TRM composite system. This may be the reason why, during the elastic phase, the strain level resulted to be not enough to let the textile immediately contribute to the whole system strength. The poor capacity to uniformly distribute the stress through the entire textile is a typical aspect of non-made fibres, even more evident in the case of plant fibre textiles due to the morphology of the natural threads conferring to the fibres lower stiffness at low strain values.

With a view to future applications it may be interesting to investigate the increase of shear capacity of externally strengthened masonry panels by means of Flax-TRM composite systems, by varying the mortar mechanical ratio, ω_m, i.e. by adopting mortars with higher strength or by increasing the TRM thickness. It may be interesting also to investigate systems in which higher values of the fibre mechanical ratio, ω_f, are obtained by using specifically designed grids. This has to be done by increasing the specific surface of the textile in contact with the matrix, ensuring at the same time a good degree of mortar penetration trough the openings of the textile. Finally, impregnation treatments may make the textile tighter, facilitating its application within the fresh mortar, and so by adopting a better collaboration between textile and mortar also on smaller level of deformation.

5.5 Conclusions

This chapter aimed at investigating the efficiency of the studied Flax TRM systems as strengthening of structural masonry elements. The experimental evidences were discussed and compared with the values of strength deriving by the formulations

proposed by standards in the field, and with similar studies from the literature. The main findings are summarised as follow:

- the application of the Flax-TRM system significantly affects the mechanical response of clay-brick masonry walls tested in diagonal compression, by conferring them an increase of shear capacity equal to the 118% in the case of the system characterised by one ply of flax textile, SW-1L, 136% in the case of the system characterised by two overlapped flax textile plies, SW-2L;
- the failure mode of the walls is characterised by the development of cracks along the vertical loaded diagonal, followed by a gradual rupture of the fibres with the opening of the cracks. No significant debonding phenomena are observed at the interface surface between the TRM and the masonry substrate. Moreover, the externally strengthened walls exhibited a post-peak phase, completely absent in the brittle behaviour of the unreinforced walls, underlying the significance of the TRM reinforcement that confers a "pseudo-ductility" to the entire system consisting in a post-failure integrity of the wall;
- no significant differences are recorded in terms of maximum shear stress, $\tau_{o,max}$, between the two series of specimens SW-1L and SW-2L, however, the walls externally strengthened by the Flax-TRM-2L system exhibit in the post peak phase a value of the dissipated energy, E_2, more than two times higher than the one exhibited by the walls strengthened by the system Flax-TRM-1L;
- from the comparison of the experimental results with the models deriving from the formulations proposed by standards in the field, concerning the unstrengthened walls, the shear stress in absence of normal stress, τ_0, deriving from the experimental tests, was much higher than the one deriving by applying the formulation of the standards, confirming the latter is provided with a substantial safety margin;
- regarding the systems externally strengthened by TRMs it is observed that the increase of strength theoretically defined is conservative with respect to the values experimentally defined. Moreover, unlike the formulation proposed by the standard, in the experimental analysis the increase of strength is not directly proportional to the increase of the amount of reinforcing fibres;
- the comparison with the literature shows that the results are quite in line with similar studies, although showing a low value of the mortar mechanical ratio with respect to systems in which high strength fibres are

adopted. The experimental evidences confirm that the maximum shear stress, τ_{0max}, and the shear modulus, G, mainly depend on the mortar mechanical ratio, ω_m, rather than on the fibre mechanical ratio, ω_f; whereas regarding the ductility, μ, no specific trend is observed with either of the two mechanical parameters;

- the comparison with studies in which the multi-ply technique was adopted shows that, in line with the other results, no significant increase of both maximum shear stress, τ_{0max}, and ductility, μ, is observed by overlapping several textile plies. As regard the shear modulus, G, unlike the evidences from other studies, in the present study no increase of the stiffness is observed by doubling the amount of textile.

As a conclusion, the experimental investigation confirmed the potential in the use of plant fibres, i.e. flax textile, as reinforcement in TRMs to enhance the shear capacity of masonry assemblages. However, it also emphasized some limitations in the use of such technique, mainly related to the bond properties between fibres and mortar, the amount of either textile and/or mortar employed, the capacity of the textile to uniformly distribute the stress through all the stressed section. Therefore, there is still room for improvements, by studying possible solutions to solve the mentioned issues, perhaps by investigating fibre impregnation processes to let the grid respond in a more uniform way, or by conducting parametric studies by varying the textile amount to reach higher capacities in the post peak phase.

6. Observations on the displacement field of strengthened walls subjected to diagonal compression test

6.1 Introduction

As shown in the previous chapters, although plant-based TRM systems present a high potential, they are also characterised by several limitations that prevent their spread in the market. Most of the drawbacks are related to the variability of the properties of plant textiles, due to the nature of the fibres and to the fabric assembly techniques. A standardisation of textile production techniques, specifically conceived for applications in TRM composites, would help overcome some issues, such as the stiffening of the fibre bundles, or the thickening of the fabric. Many other aspects are still under investigation, such as coating and impregnation processes, fibres physical and chemical treatments, refinement of the geometry of the TRM.

These innovative techniques may lead to improvements in the mechanical performance of plant-based TRM composites. However, it is technically onerous to carry out experimental investigations on the structural scale of analysis, especially when several different solutions have to be compared. Therefore, the mechanical response is rather assessed on the composite scale of analysis, by means of textile and TRM tensile tests, pull-out tests to investigate the fibres-to-matrix bond, and shear bond tests to analyse the composite-to-substrate adherence.

Therefore, it is fundamental to define the parameters on which it is necessary to focus at the materials scale of analysis, to obtain an improvement of the response on the structural scale. It is necessary, to this purpose, to define a correspondence between the mechanical response of TRM systems tested at the composite scale, with the mechanical response of structural element externally strengthened by the TRM.

The aim of this chapter is to find a relationship between the strain field on the external surface of a Flax TRM externally strengthened wall tested in diagonal compression, and that of the external surface of Flax TRMs tested in tension. The objective is to define the crucial parameters on which it is necessary to focus during tensile test in order to have an improvement of the system when applied on structural elements,

6.2 Methods

The analysis was carried out by processing DIC images concerning the diagonal compression test of a representative specimen, i.e. the specimen SW-2L-1. A total of 26 images, representative of significant steps of the test, were processed. Six images represent the first phase of the response up to the peak load, the others are representative of the post peak phase. A picture, the number 26, was selected to represent the very ultimate state of the wall. Figure 6.1 shows the load-vertical displacement curve of the specimen SW-2L-1, on which the points corresponding to the selected photos are highlighted.

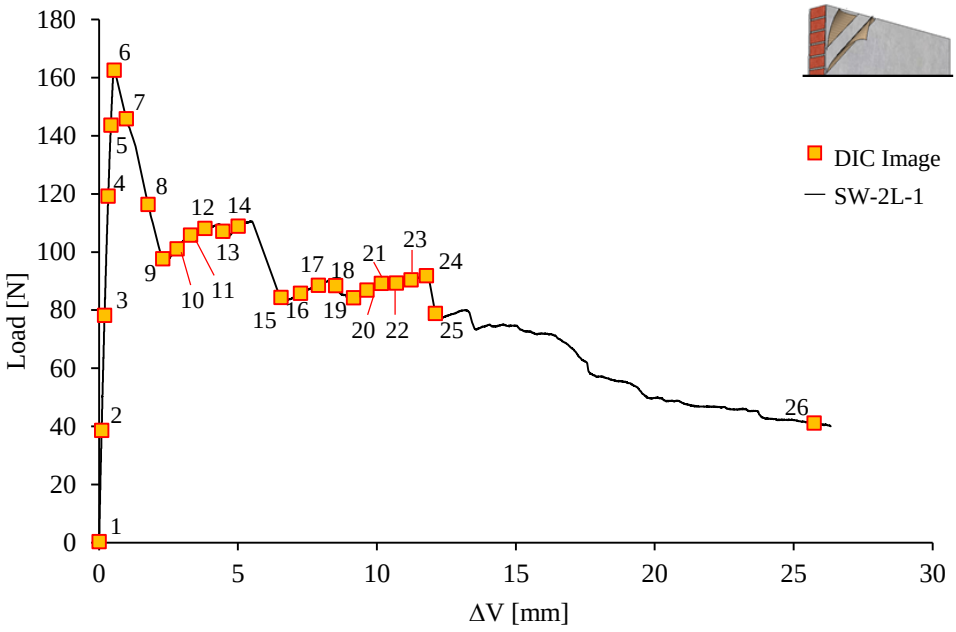

Figure 6.1: Load-vertical displacement curve of specimen SW-2L-1 with the selected photos highlighted by yellow squares.

The value of the load, the time of the photo captured, and the vertical displacement corresponding to each image, are reported in Table 6.1.

The analysis provides the displacement field on the entire surface of the specimen. However, with the aim of extrapolating parameters to compare to the tensile test response of TRMs, in this analysis the displacements along the horizontal diagonal were taken into consideration.

According to the hypothesis of pure shear conditions, such direction represents the principal stress direction in tension, therefore it is the direction that

comes closest to the pure tensile conditions reproduced in tensile tests. The scheme of the images processed is shown in Figure 6.2, where the zone and section of analysis, the reference system, the loaded corners and the two diagonals are highlighted.

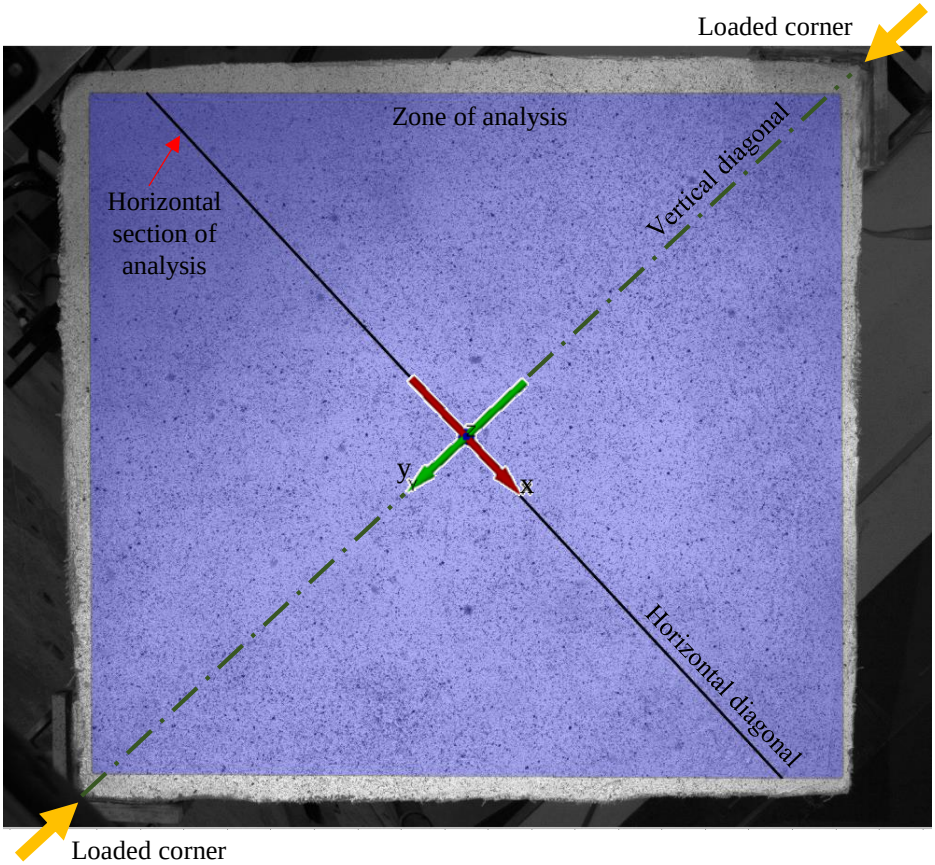

Figure 6.2: Scheme of the images processed by means of DIC analysis.

6.3 Analysis

From each image the value of the of the displacements along the x direction (herein after referred to as horizontal displacements) can be derived for all the points of the horizontal section of analysis (Figure 6.3). When a crack appears on the wall surface, the displacement curve corresponding to that instant is characterised by a discontinuity in correspondence to the abscissa at which the crack occurred.

By estimating the difference of displacement between points placed at different edges of the crack, the crack opening can be assessed, and by monitoring such value for the other photos, the evolution of the crack openings can be observed.

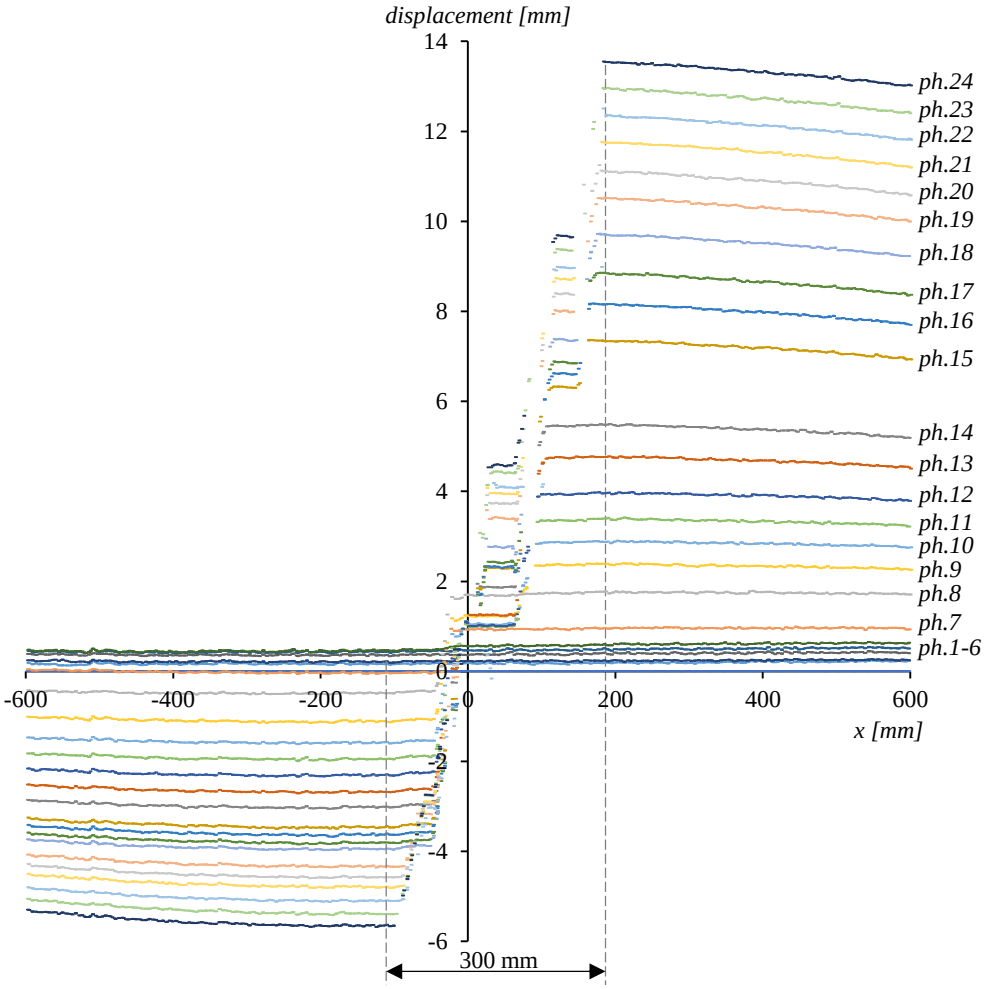

Figure 6.3: Displacement along the horizontal analysed section for all the selected pictures.

From image 1 to 6 no discontinuities are shown being the curves referring to the elastic phase of the response up to the achievement of the peak load. From picture 7 to 15 several discontinuities can be observed, representing the development of several cracks in the post peak phase. From picture 15 on an increase of the cracks opening is observed without the occurrence of new cracks.

A further aspect that can be observed is that the displacements are concentrated in a zone of about 300 mm in the middle of the length of the horizontal

section of analysis. Such area, referred to as the zone of deformation, corresponds to the centre of the panel, where the shear and normal stress attain their maximum values. The displacement curves of some marker images, corresponding to significant changing in the curve of displacement due to the occurrence of a crack, are shown more in detail with respect to the central zone of deformation analysed (Figure 6.4).

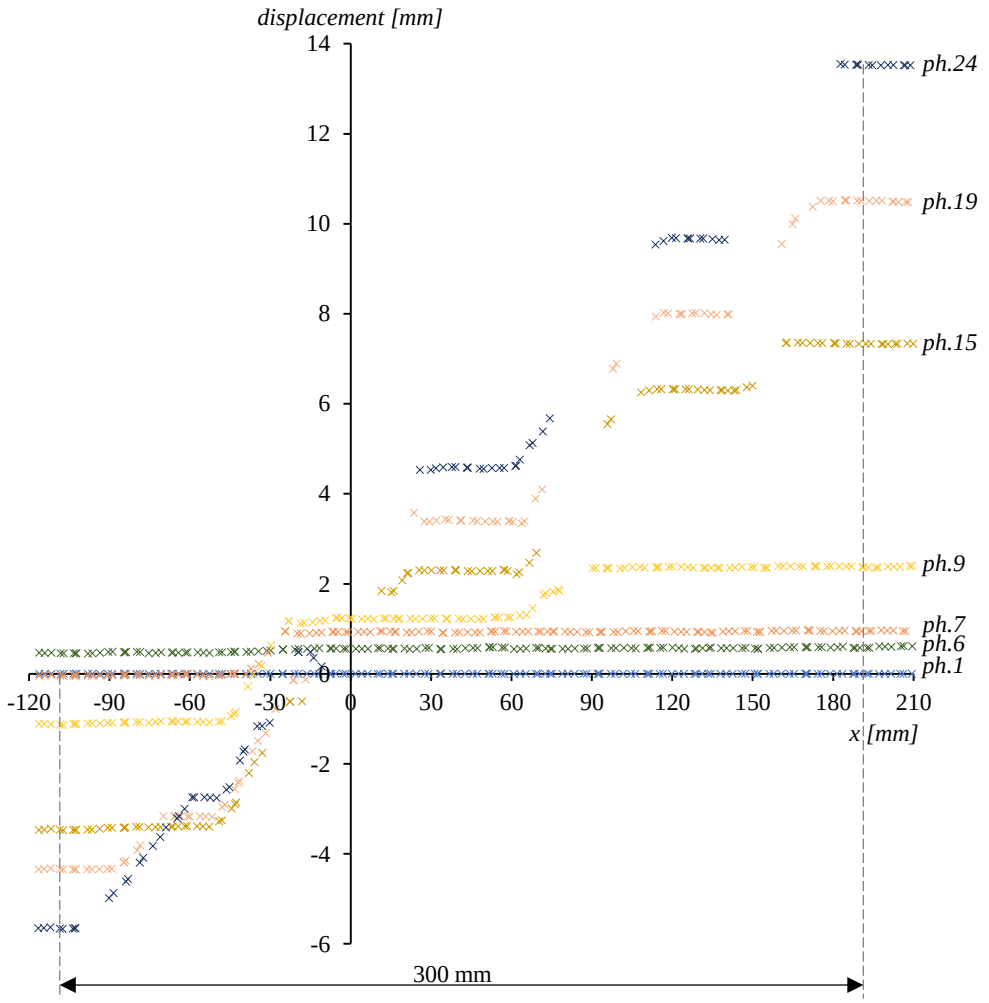

Figure 6.4:Displacement along the zone of deformation for significant images.

The horizontal displacement field of the entire surface for the significant pictures, deriving from the DIC analysis, is shown in Figure 6.5. Such representation emphasises the crack development and the concentration of the deformation in the central zone of the panel.

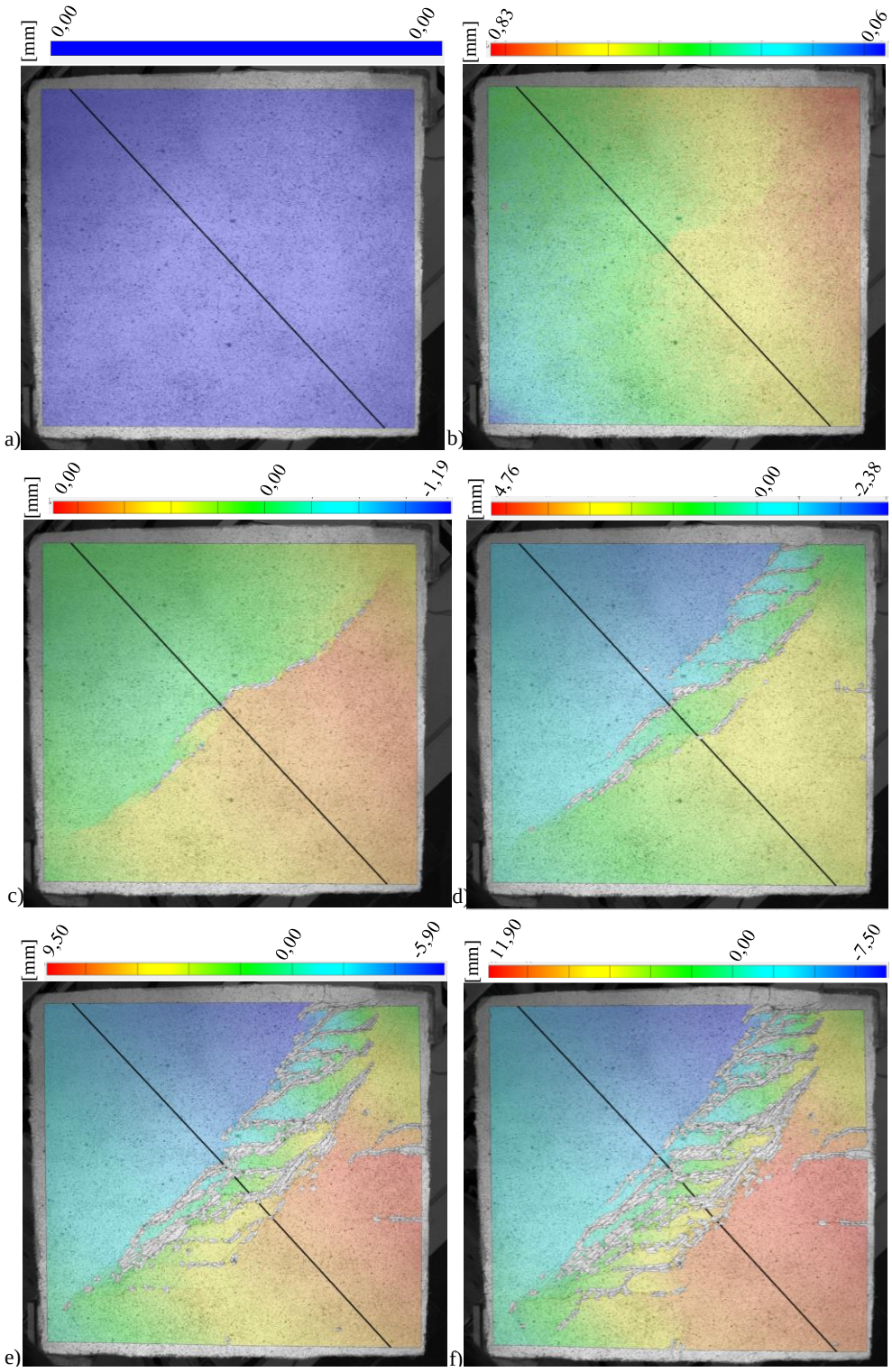
[mm]
0,00
0,00
a)
[mm]
0,83
0,06
b)
[mm]
0,00
0,00
-1,19
c)
[mm]
4,76
0,00
-2,38
d)
[mm]
9,50
0,00
-5,90
e)
[mm]
11,90
0,00
-7,50
f)

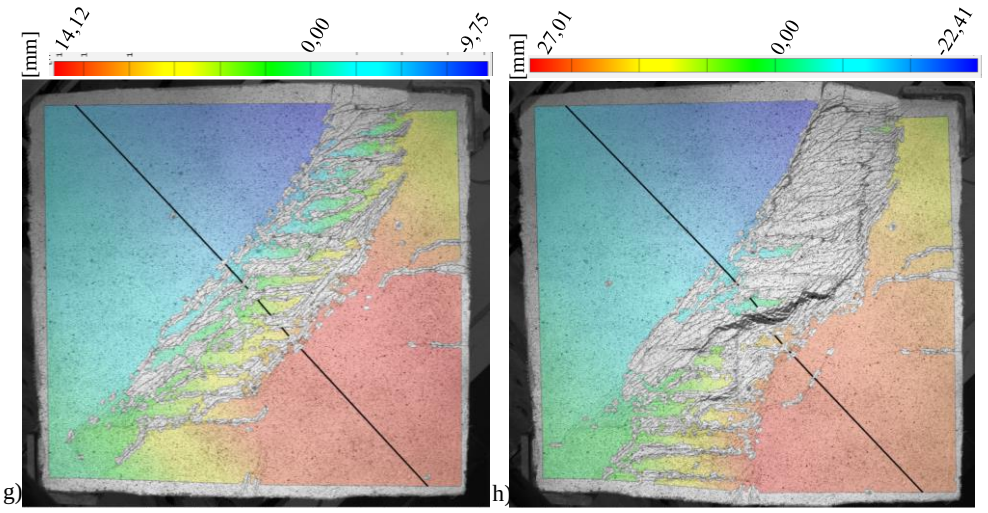

Figure 6.5: Horizontal displacement field of photos: a)1; b)6; c)7; d)9; e)15; f)19; g)24; h)26.

Image 26 (Figure 6.5h), not considered in the analysis, was shown so as to represent the ultimate state configuration of the specimen. By analysing the displacement in the central deformation zone, it is possible to assess, for each image, a mean value of the deformation, ε_{mean} (ratio between the difference of the displacements corresponding to the two edges of the zone of deformation and the length of this latter, 300 mm). It represents an approximated estimation of the strain of the most stressed point of the panel. The values of ε_{mean}, for each selected photo, are reported in Table 6.1. The values are also plotted in Figure 6.6 with respect to the vertical displacement attained during the test.

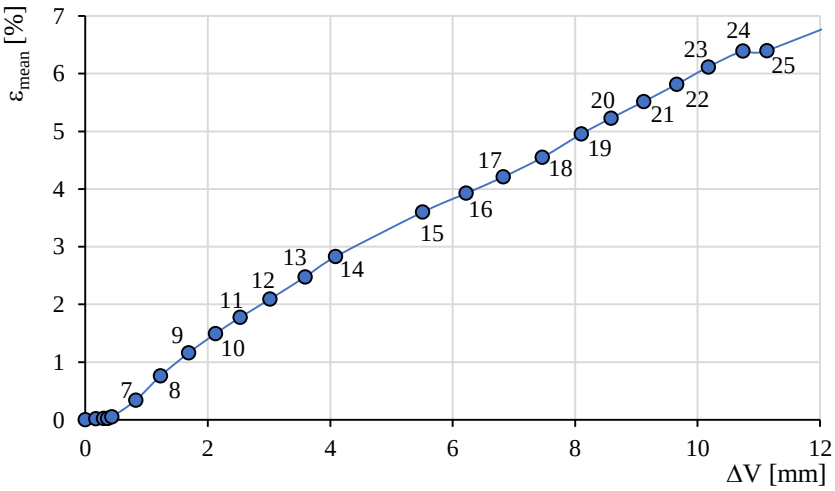

Figure 6.6: Mean strain in the zone of deformation versus vertical displacement.

Table 6.1: Main parameters concerning the selected photos for the DIC analysis.

Photo	time (s)	Load (kN)	ΔV (mm)	ε_{mean} (%)
1	0	0	0.00	0.00
2	88	39	0.09	0.01
3	172	78	0.20	0.02
4	249	119	0.33	0.02
5	295	144	0.42	0.02
6	333	163	0.54	0.05
7	335	146	0.98	0.34
8	339	116	1.77	0.76
9	344	98	2.29	1.16
10	379	101	2.81	1.49
11	414	106	3.29	1.77
12	449	108	3.82	2.09
13	484	107	4.45	2.48
14	519	109	5.01	2.83
15	554	84	6.55	3.60
16	589	86	7.25	3.92
17	624	89	7.89	4.21
18	659	88	8.51	4.55
19	694	84	9.16	4.95
20	729	87	9.64	5.23
21	764	89	10.16	5.51
22	799	89	10.70	5.81
23	834	90	11.23	6.11
24	870	92	11.78	6.39
25	875	79	12.11	6.40
26	1692	41	25.73	12.19

The mean value of the strain of the deformation zone can be compared with the axial strain deriving from TRM tensile tests. It is worth highlighting that the boundary conditions of the composite applied to the masonry are not the same of the conditions of pure tension to which the TRM is subjected in tensile tests. Moreover, along the horizontal direction of the walls the textile is differently oriented with respect to the axial direction of tensile coupons, rotated of an angle of 45°. Therefore, it cannot be assumed that a real correspondence between the two different behaviours exists. However, it may still be interesting to compare the strain field exhibited by

the composite in tensile tests, with the strain field of the portion of the wall solicited in tension.

To this purpose, the tensile response of the specimen of the series Flax TRM-2L-T are plotted in Figure 6.7. In the graph the mean values of the strain and stress corresponding to the transition between the different stages, are highlighted.

With respect to Table 6.1, it can be observed that in the range of photos 1-6, during the elastic phase of the diagonal compression response, the mean strain is included in the range of 0.00 % ÷ 0.05 %. Being such values less than the value ε_1 (the mean deformation of the transition point between Stages I and II in the tensile test response), it can be assumed that in correspondence of the elastic branch of diagonal compression response, the TRM works under elastic conditions. As a matter of fact, the TRM mechanically behaves as in the Stage I of the tensile response.

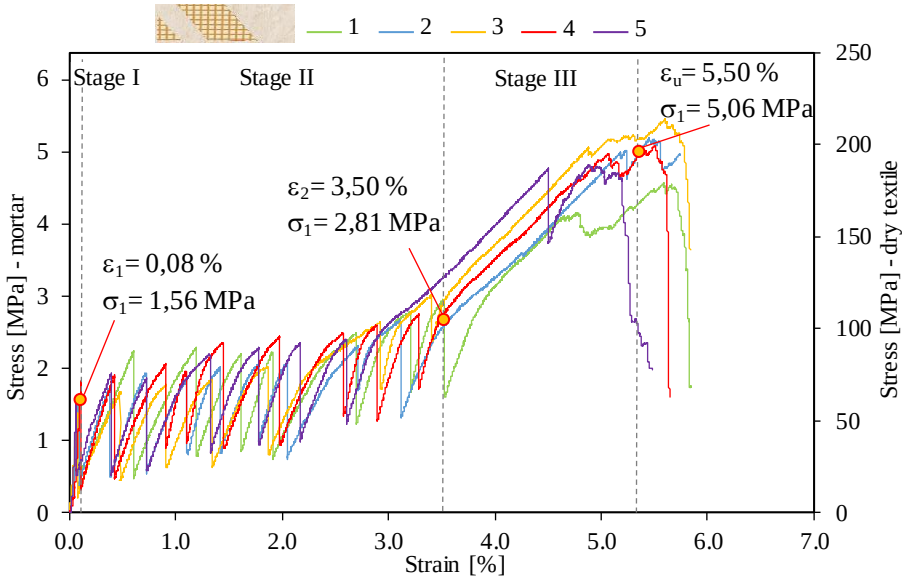

Figure 6.7: Stress-strain response of specimens of the series Flax TRM-2L-T.

It is difficult to find an accurate correlation with respect to the wall post-elastic behaviour, due to the gradual loss of the pure shear conditions in the plastic phase.

However, it can be observed that in correspondence to image 15 a value of mean strain, ε_{mean}, is attained equal to 3.60 %. Such is results very close to the mean value of the transition point between Stages II and III, ε_2. For the reasons explained above such similitude in the values does not represent an actual correspondence. However, it may be assumed that, in the post peak diagonal compression response, the TRM within the zone of deformation, exhibits a behaviour characterised by a range of strains similar to that exhibited during Stage II in tensile test conditions.

Therefore, may be reasonable to associate the post elastic behaviour in diagonal compression, characterised by several drops of loads corresponding to cracks in the wall, to the response of the TRM in tension during Stage II.

It is also interesting to remark that in the range of photos 15-25 no development of new cracks is observed, and the existing cracks increase their opening. Moreover, within this range, the response is characterised by a slightly hardening behaviour.

Starting from the image 25 a gradual decrease of strength is observed due to the progressive rupture of the textile along the vertical diagonal. Such behaviour can be associated to the ultimate configuration of tensile tests corresponding to the failure of the fibres.

6.4 Observations

With the aim of optimizing the global performance of the system, leaning towards a diagonal compression test response in which the post-elastic response comprises a hardening phase with an ultimate load higher than the elastic one, it is necessary to improve the tensile response of TRMs.
From the comparison between the tensile behaviour of Flax TRMs and their response once applied on the structural element, in terms of displacements, hence strains, it is possible to obtain interesting information.

On the basis of the considerations explained before, we can define the parameters on which the attention has to be focused on.

Having shown that the composite behaves in an elastic phase up to the achievement of the peak load, we can assume that a TRM system characterised by higher values of the normal stress σ_1 (transition point between Stages I and II) would lead to a higher value of the elastic load in diagonal compression.

The correlation between strains in the post peak phase, with the strain in Stage II, may lead to assume the post peak drop of load being associated to the significant drops of load observed during the tensile test. Therefore, a tensile response characterised by smaller values of the strain ε_2, hence by the developments of cracks closer to each other, and by higher values of the stress σ_2, may lead to elastic response in diagonal compression characterised by less significant losses of loads. Moreover, a higher stress level guaranteed by adequate textile amounts, proportionated with respect to the unreinforced wall strength, may even lead towards a hardening behaviour in the post elastic phase.

Several technical solutions are available to improve the response, such as stiffening of the textile, improving of the textile-to-mortar bond, matrix modifications, and optimisation of the reinforcement ratio.

Whatever the solution adopted is, the efficiency of a TRM system in view of applications as reinforcement of structural elements, has to be evaluated with respect to the considerations reported above.

It is worthy underlying that the analysis proposed in this chapter, rather than defining an accurate correspondence between the local and global behaviour, represents a starting point to further investigations, that with similar methods may find an exhaustive relationship, perhaps by taking into account also the shear-bond test behaviour, being the latter more representative to the actual behaviour of the composite once applied to structural elements, with respect to the tensile one.

A comprehensive model in these terms, would be fundamental in view of designing formulas aimed at assessing the strength of TRM externally strengthened masonry elements starting from the mechanical properties deriving from the local scale characterisation, i.e. tensile and shear-bond tests.

7. Influence of fibre treatment and matrix mix design modification on the behaviour of Flax TRMs

7.1 Aim and contents of the chapter

As shown in previous chapters, Flax TRMs are characterised by a promising mechanical behaviour. However, there is still room for improvements in order to design and manufacture a composite system being competitive, from a mechanical point of view, with respect to most common TRMs characterised by high strength industrial fibres. In *Chapter 2*, within the analysis of the state of the art, it was shown that to face such issues and to improve the composite system mechanical response it is possible to apply fibre treatments mainly consisting in hornification [78], alkali treatments [132], coating procedures [133], matrix modifications, optimization of the textile mesh and of the reinforcement ratio. These treatments, specifically designed, may improve either the strength and/or the durability performance. Moreover, in *Chapter 6* some considerations were reported in order to define the parameters to take into account to quantify the efficiency of an improvement technique, by means of TRMs tensile strength characterisation.

The present chapter aims at showing that by applying some of the improvement technique available in literature, it is possible to confer a better mechanical performance to the composite system. Specifically, a fibre impregnation treatment, and a modification of the mortar matrix, were considered.

The aim of the study is to show that by adopting simple technique measures it is possible to improve the mechanical response of Flax TRMs. It is important to highlight that the experimental evidences showed in this chapter represent a preliminary step toward the definition of satisfying improvement techniques, rather than the proposal of a specific treatment.

The fibre treatment proposed consisted in the application of a latex-based substance on the flax textile. Prior to applying such treated textile as reinforcement in TRMs, the problem of the influence of the treatment on the fibre morphology and strength, and on the fibre-to-mortar bond behaviour, was addressed. Subsequently, the tensile behaviour of Flax TRMs, performed by means of the treated textile, was investigated in order to analyse the efficiency of the treatment. Finally, the tensile behaviour of a Flax TRM, performed by means of the treated textile and by adding

within the matrix short curaua fibres, was assess as well with the aim of defining the contribution provided by improving the mortar matrix.

The experimental activity was carried out at the Laboratory NUMATS – COPPE of the Federal University of Rio de Janeiro (Brazil).

7.2 Influence of the fibre treatment on the morphology and mechanical behaviour of flax yarns embedded in hydraulic lime mortar

This section aims at investigating the effect of flax fibres treatment on their morphology, tensile strength and mortar-to-fibres adherence behaviour. To this purpose flax yarns, extracted from a textile and coated by means of a polymeric material, are subjected to tensile and pull-out tests and their response, compared with dry flax threads, is discussed taking into account the yarns geometry assessed by means of Scanning Electron Microscope (SEM) images analysis.

It represents a preliminary step to observe the influence of the treatment on the local behaviour at the fibre-to-matrix interface, before further analysis to be carried out at the composite scale by means of TRM tensile tests.

7.2.1 Materials and methods

The flax fibre and the hydraulic lime mortar employed are those whose physical and mechanical main parameters are shown in *Chapter 3* and *Chapter 4*.

A Carboxylated Styrene Butadiene Rubber (XSBR) latex was used to coat the flax yarns under investigation. Such material was chosen because it has been demonstrated that the copolymer, largely used in textile industry both with plant and synthetic fibres, can improve the bond between plant fibres and the surrounding matrices [76].

Although no specific investigations have been carried out in this regard, it is worth emphasising that further analyse are required to define the XSBR coating sustainability impact on the entire system. However, as a first step, it is fundamental to quantify the benefits of the impregnation in terms of mechanical properties. Further durability and life-cycle assessment analysis may clarify if the eventual gap in terms of environmental impact is offset by the mechanical benefits, and if more sustainable coating materials may be employed.

The flax yarns were cut from the fabric (Figure 7.1a) and fully immersed in the polymer in environmental temperature conditions (Figure 7.1b), then, the excess liquid was removed from the external surface (Figure 7.1c) and the threated fibres

were dried at a controlled temperature of 38 ± 2 °C for 24h. During the drying period the yarns were arranged in a frame specifically conceived to give them an elongated and regular shape (Figure 7.1d).

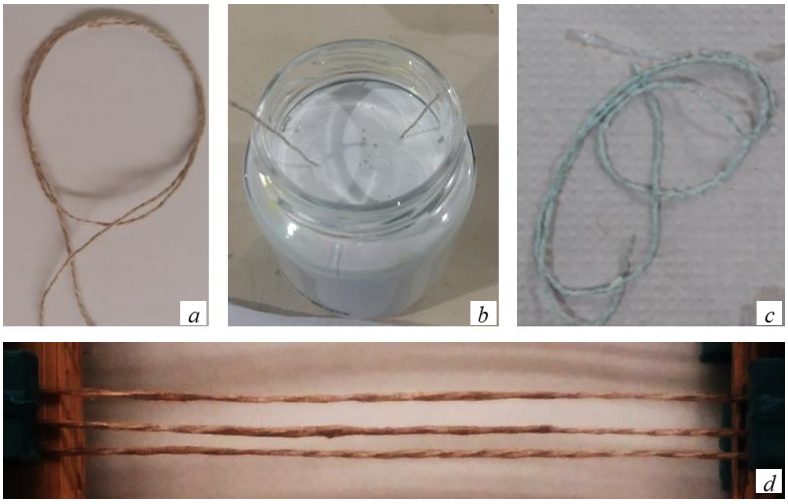

Figure 7.1: Fibres treatment procedure: a) Flax yarn; b) Yarn immersion; c) embedded yarn; d) Yarn drying.

Concerning the influence of the treatment on the morphology of the flax yarns, high resolution SEM images were detected to analyse the cross section of impregnated fibres and to compare it with that of dry fibres. The morphology of dry fibres and the procedure to assess cross section and perimeter are discussed in *Chapter 3*. The images were characterised by a magnification of 80X. A total of 30 coated fibres were compared with 30 dry ones. Figure 7.2 shows the analysed images of a representative sample of dry and coated flax yarn. The images were manipulated to get the geometric parameters, with the same procedure shown in *Chapter 3*. In order to quantify the irregular geometric shape of fibres, the relative Fibre Intrinsic Efficiency Ratio ($FIER_r$) was assessed for all the specimens. The latter is defined as the ratio between the actual yarn perimeter, P_f, and the equivalent perimeter, P_{eq}, defined as the circumference of a circle having the same area of the actual yarn section [76].

Tensile strength was assessed on both the impregnated and non-impregnated flax yarns. The following series of specimens were considered:

- non-impregnated-T-tensile: it consists of the yarn representing the main element of the fabric (labelled as Flax T in *Chapter 3*). The specimens, having a length of 70 mm were randomly extracted from the textile (Figure 7.3a);

- impregnated-T-tensile: it consists of specimens obtained by coating samples having the same characteristics of the non-impregnated-T-tensile threads (Figure 7.3b).

The series were characterised by 13 to 15 samples having a gauge length of 50 mm and clamped in each edge for a length of 10 mm. The tests were performed by a micro force machine Tytron 250 with 500 N load cell in displacement control by using a rate of 4 mm/min.

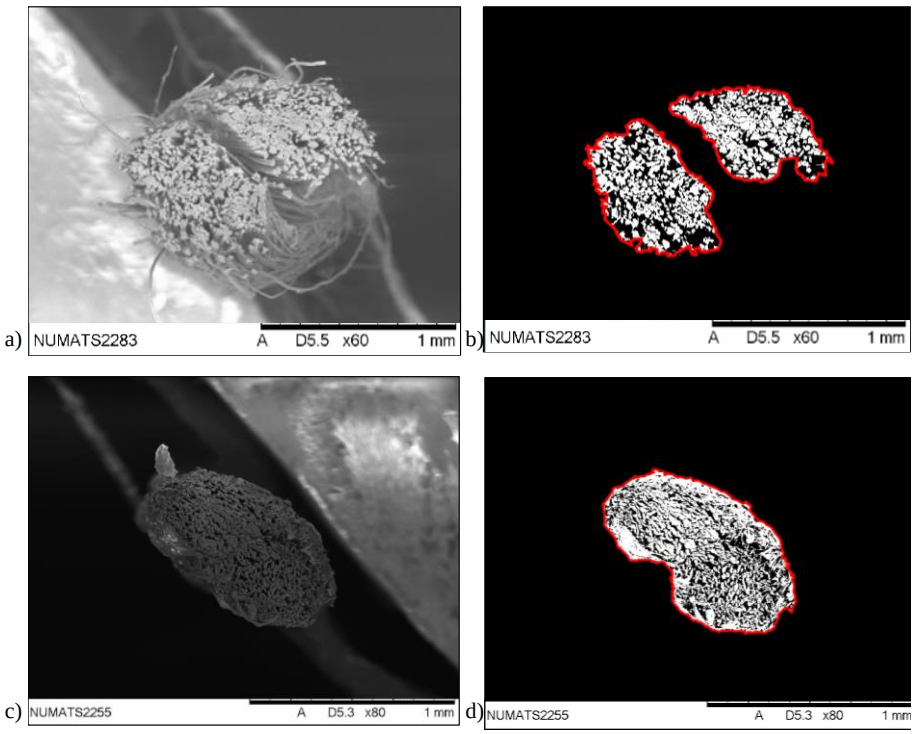

Figure 7.2: Flax yarn's morphology identification: a)Non-impregnated yarn SEM image; b) Non-impregnated yarn manipulated SEM image; c) Impregnated yarn SEM image; d) Impregnated yarn manipulated SEM image.

Pull-out tests were carried out to investigate the bond behaviour between flax fibres threads and the mortar. The specimens consist of a hydraulic lime cylinder with a diameter of 25 mm and a height of 25 mm, representing the embedded fibre length. The latter was chosen by ensuring the tensile failure of the thread was avoided and the debonding within matrix guaranteed.

The series of specimens tested in pull-out tests are as follows:

- non-impregnated-T-pullout: it consists of uncoated flax yarns embedded in the mortar cylinders;

- impregnated-T-pullout: it consists of impregnated flax threads embedded in the mortar cylinders.

Figure 7.3: Flax specimens tested in tension of the series: a) non-impregnated-T-tensile; b) impregnated-T-tensile.

Both series, characterised by the same geometry and test set-up, consist of 15 specimens. The threads, having a length of 35 mm, were immersed in the mortar element during their casting by ensuring it to be well placed in the middle, embedded for the entire cylinder length and in axis with it. The tests, conducted after 28 days of curing in environment conditions, were carried out by means of a micro force machine Tytron 250 with 500 N load in displacement control with a rate of 1 mm/min. On one side of the specimen the cylinder was clamped by means of a steel device specifically conceived for this purpose, on the other one the free edge of the thread was clamped for a length of 10 mm by ensuring the clampers to be at the cylinder edge not to record any fibre elastic elongation during the test (Figure 7.4).

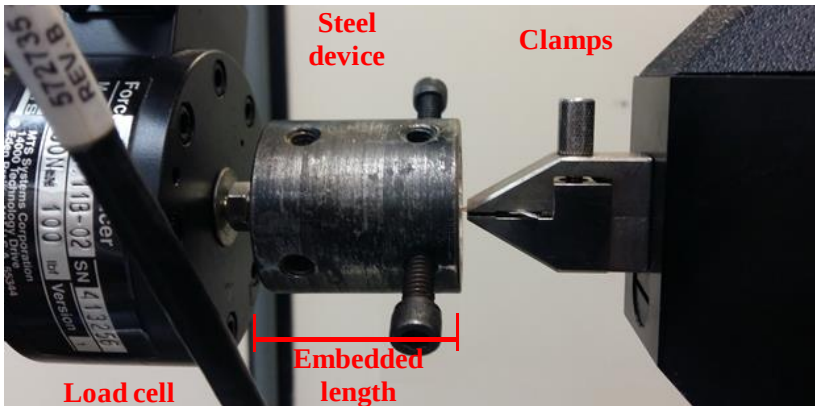

Figure 7.4: Pull-out test set-up.

7.2.2 Results and discussion

7.2.2.1 Morphological characterisation

The morphological characterisation was carried out by analysing 30 non-impregnated and 30 impregnated flax threads. Figure 7.5 shows SEM images of some representative non-impregnated and impregnated specimens.

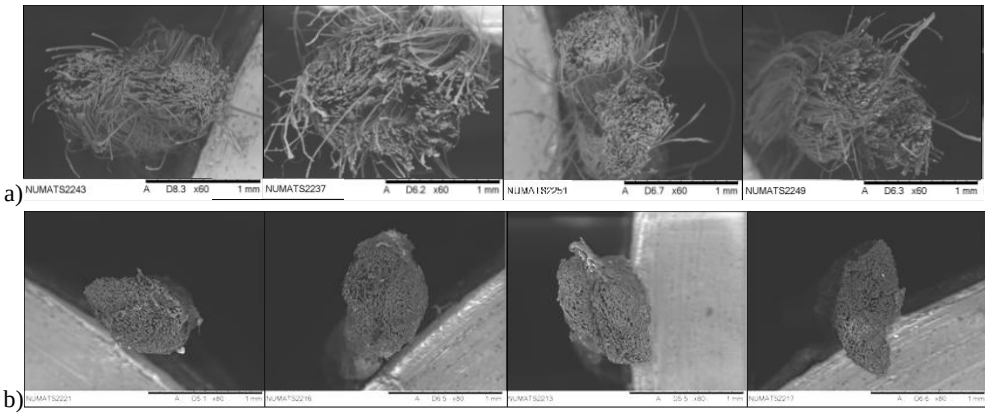

Figure 7.5: SEM images of representative specimens of the series: a) non-impregnated-T-pullout; b) impregnated-T-pullout.

Regarding the cross-section area, both groups of fibres showed the same average value equal to 0.28 mm^2. Being both groups of fibres derived from the same textile this aspect shows that the coating procedure does not affect this geometrical parameter. This is also confirmed by analysing the images proposed in Figure 7.6, where an impregnated yarn represented in different magnification scales shows that the coating polymer does not penetrate within the inner filaments of the yarn.

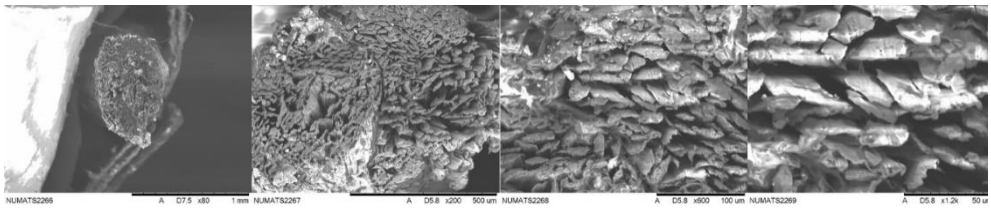

Figure 7.6: SEM images of an impregnated yarn in different magnification scales: 80X, 200X, 600X, 1200X.

As regards the perimeter of the flax bundles, the two groups of specimens show different average values equal to 4.89 mm for the non-impregnated specimens and 3.15 mm for the impregnated ones, respectively.

Focusing on the value's relative frequency distribution it can be observed that while in terms of cross-section area there is no discrepancy between non-impregnated and impregnated fibres (Figure 7.7), on the other hand, in terms of perimeter, there is a significant difference not only in terms of average values, but also in terms of probabilistic distribution (Figure 7.8).

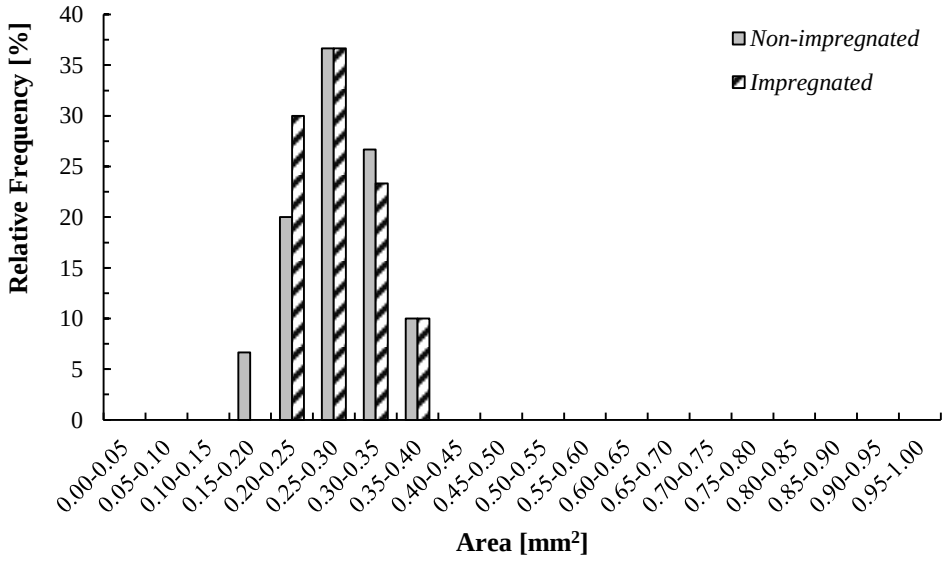

Figure 7.7: Frequency distribution of the cross-section area.

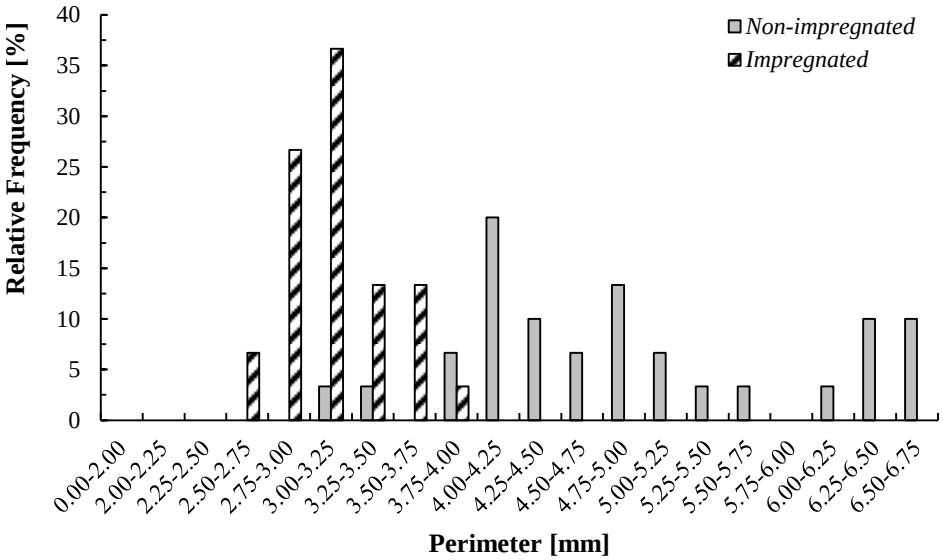

Figure 7.8: Frequency distribution of the perimeter.

In fact, when the impregnation is applied on the fibres, the distribution moves from a "multi-modal" to "quasi uni-modal" form: it means that the coating system tends to reduce the heterogeneity of the fibres' geometry. This evidence is also confirmed by analysing the results in terms of resulting relative FIER (Figure 7.9).

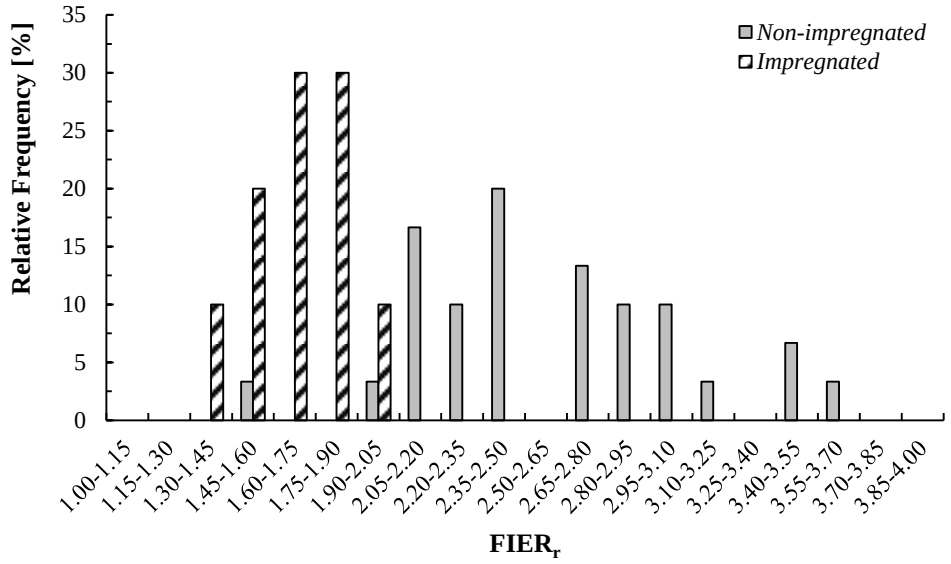

Figure 7.9: Frequency distribution of the $FIER_r$ parameter.

In fact, a significant reduction of around 35% is observed in terms of the $FIER_r$ the mean of which value moves from 2.61 (for non-impregnated threads) to 1.69 (for the impregnated specimens). Moreover, the $FIER_r$ value's relative frequency distributions in Figure 7.9 shows a difference also in terms of dispersion of the data, with a squeezed distribution for the coated threads and a more stretched one for the non-impregnated fibres. As a matter of fact, the impregnation process significantly affects the geometry of the yarns by making them more regular in shape with reduction in both lateral surface, due to a smaller space between the filaments, and variability of the properties.

7.2.2.2 Tensile behaviour

During tensile tests, both axial displacement and applied loads were recorded. The parameters considered for describing the tensile behaviour are: the maximum load, F_{max}, the displacement corresponding to the maximum load, $disp_{max}$, the tensile strength, f_t, the strain corresponding the maximum load, ε_{max}, the Young's modulus, E, calculated in the linear branch within the stress range from 50% to 90% of the maximum strength.

The main values of the parameters concerning the non-impregnated-T-tensile and impregnated-T-tensile series of specimens, together with the respective coefficient of variation are reported in Table 7.1.

Figure 7.10 shows the tensile responses, in terms of stress-strain, for both non-impregnated-T-tensile and impregnated-T-tensile series of specimen.

Table 7.1: Mean mechanical properties of specimens tested in tension.

Series	Number of specimens	F_{max} (N)	$disp_{max}$ (mm)	f_t (MPa)	ε_{max} (%)	E (GPa)
non-impregnated-T-tensile	15	100 (9)	3.0 (10)	341.2 (20)	6.1 (10)	9.06 (19)
impregnated-T-tensile	13	79 (15)	1.8 (18)	295.8 (18)	3.6 (18)	9.11 (18)

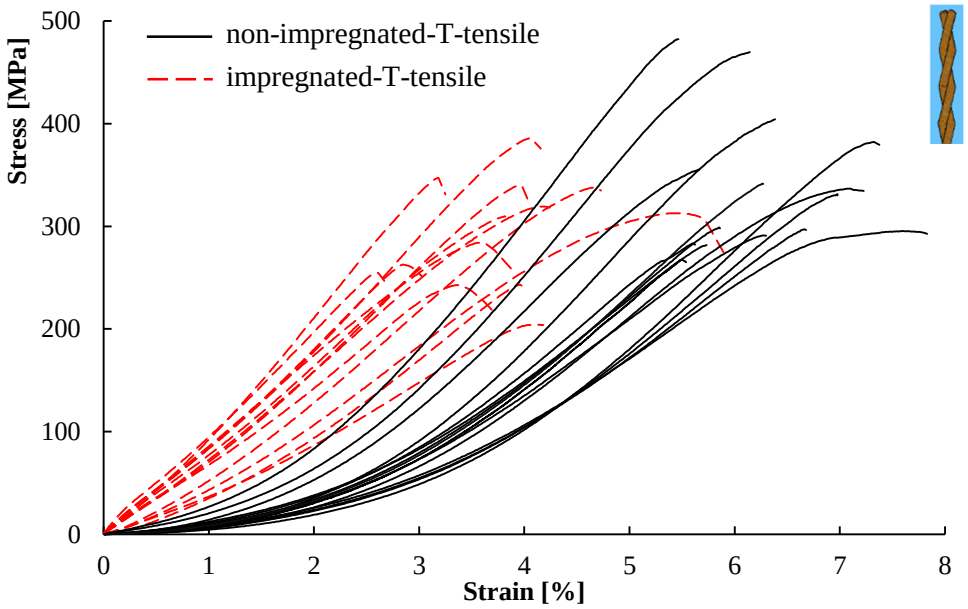

Figure 7.10: Tensile test results of non-impregnated-T-tensile and impregnated-T-tensile series of specimens.

Both series of specimens are characterised by a lower initial stiffness that increases up to a constant value before the failure. This result is in line with what observed in *Chapter 3*, and, as discussed in the state of the art review, it is due to the particular microstructure of plant fibres, and to the macrostructure of the yarn, hence the arrangement of the filaments creating the threads.

Although no significant differences in terms of Young's modulus (evaluated in the linear branch) were observed, the coated threads present a maximum strain smaller than the one exhibited by the non-impregnated ones and a lower strength. As a matter of fact, the impregnated yarns behaved as "polymeric composite" in which the amount of polymer strongly affects the failure mode. The lower initial stiffness observed in the non-impregnated specimens may be due to the fact that during the first phase of the tensile tests the yarns are stretched meanwhile the application of the coating system tends to reduce this effect resulting in a more "rigid" behaviour characterised by a quasi-constant value of the stiffness from the beginning of the test. Therefore, it can be assumed, that the coating treatment resulted in a macrostructure of the threads whose contribution to the lower initial stiffness is less significant. The resulting lower deformability of the impregnated fibres represents an important aspect in view of applications of the textile as reinforcement in mortar-based composites in which, as discussed in previous chapters and confirmed by the literature [82], one of the limitations is characterised by the significant difference in terms of deformability between mortar and plant fibres.

7.2.2.3 Bond behaviour

The pull-out behaviour of the non-impregnated-T-pullout and impregnated-T-pullout series is shown in terms of load-displacement curves in Figure 7.11.

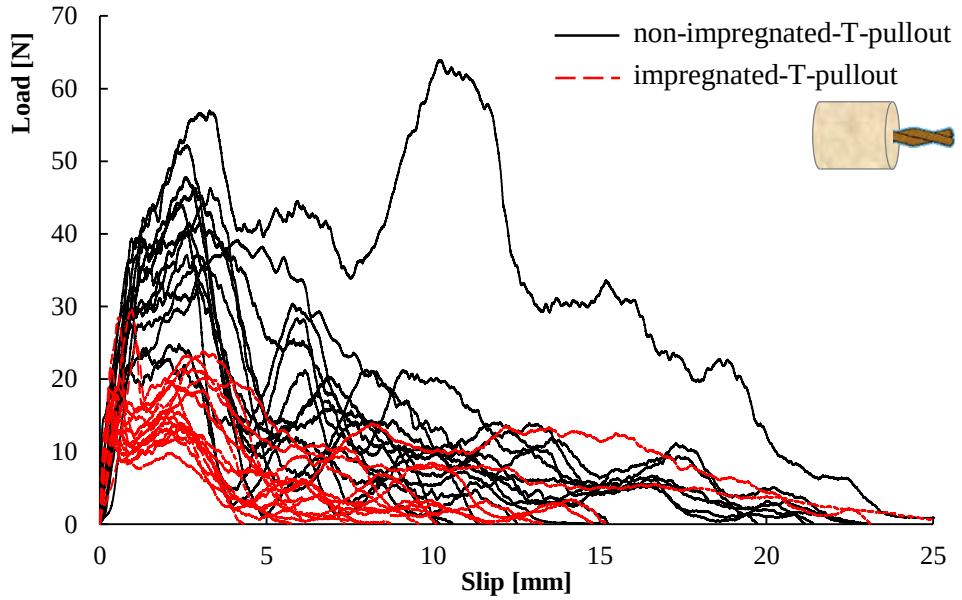

Figure 7.11: Pull-out test results of non-impregnated-T-pullout and impregnated-T-pullout series of specimens.

In all specimens the failure mode is characterised by the slipping of the bundle within the matrix up to the complete pull-out of the bundle from the mortar cylinder. Both groups of fibres exhibit a response typical of the cases in which debonding occurs [76]. This response is generally characterised by a first elastic branch, named as bond adhesive phase, and a frictional bond phase following a drop of the peak, characterised by a quasi-constant value due to the residual frictional force. In some cases, between the two phases another stage occurs in which the peak load is achieved after a non-elastic hardening branch, named as mechanical bond phase. In most of the non-impregnated samples, the peak load occurs after a non-elastic hardening phase, while the impregnated specimens mainly showed an elastic behaviour up to the achievement of the maximum load (Figure 7.11).

As regards the post peak phase, the non-impregnated samples are characterised by a softening behaviour in which a mechanical bond component, still present, makes the test last up to the complete pull-out of the yarn from the mortar. Conversely, the softening branch exhibited by the coated yarn specimens is mainly characterised by a residual frictional component that in most of the cases reaches zero load before the complete slipping of the yarns from the mortar. In terms of maximum load, the mean value achieved by the non-impregnated specimens, equal to 40.96 N, is two times higher than the one reached by the impregnated yarns, being the latter equal to 20.23 N. This experimental result highlights that the impregnation procedure employed in the study reduces the performance in terms of adherence between the fibres and the mortar. Although this aspect may be attributed to a loss of adherence due to the presence of the coating, it also depends, in part, on the different morphology of the impregnated fibres that are characterised, as shown above, by a smaller fibre-to-mortar interface surface.

To make the analysis independent from the geometry the results are also expressed in terms of adherence shear stress, τ_{max}, assessed for each sample by dividing the maximum load for its interface surface (the latter was assessed on the basis of the actual perimeter of the bundles). By looking at the interface shear stress relative frequency distribution (Figure 7.12), the two groups of data, having a similar dispersion, still show a difference in terms of average values.

By comparing the higher average maximum shear stress values, being 0.37 MPa and 0.25 MPa respectively for the non-impregnated and impregnated specimens, it is obvious that the discrepancy, although still significant and consisting in a reduction of the mean maximum stress of about the 30%, results to be lower with respect to the case in which the comparison is made in terms of load. This is due to the fact that the impregnation reduces the tortuousness of the threads. However, it is highlighted that the coated fibres are characterised by a local bond behaviour less performing than the one exhibited by putting the fibres directly in

contact with the mortar. It may be attributed to the specific polymer material or coating procedure used to impregnate the fibres. In fact, the impregnation creates a weak layer between the fibres and the mortar that reduces the adhesion of the reinforcement-to-mortar system.

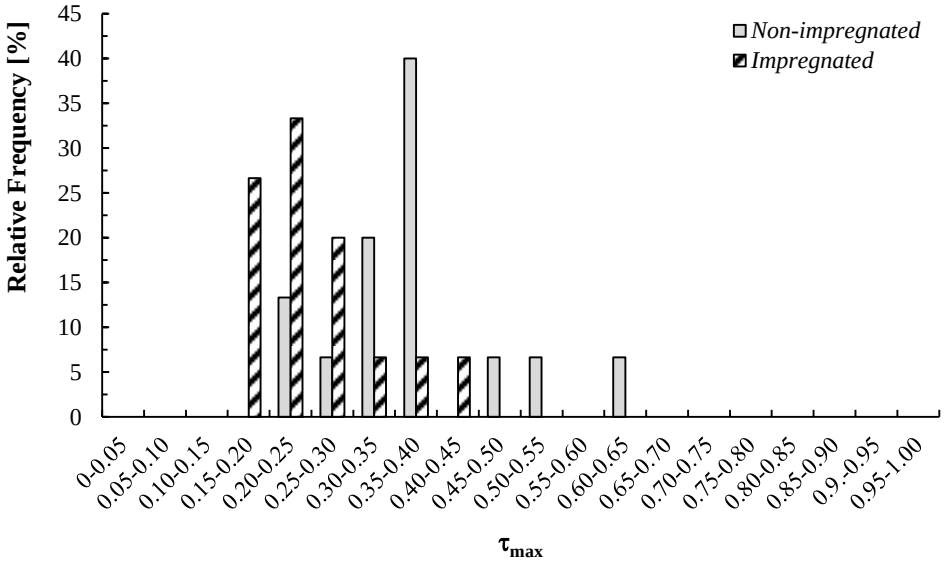

Figure 7.12: Frequency distribution of shear stress of non-impregnated-T-pullout and impregnated-T-pullout series of specimens.

The experimental evidences showed are the result of a preliminary study aimed at analysing the efficiency of the coating procedure adopted. Clearly, further investigations are needed, perhaps by adopting a different coating material and/or amount or impregnation treatment, in order to get an impregnation process that may confer mechanical benefits to the system also in terms of adherence response. Moreover, since one of the main issues related to the use of natural-based reinforcement in cement- and or lime-based matrix is the alkaline environment in which the fibres are embedded, it is worth mentioning that the application of impregnation processes could also mitigate these durability-related issues. Therefore, it would be useful a more comprehensive study for further analyse these fundamental aspects.

7.3 Influence of fibre treatment and matrix mix design modification on the tensile behaviour of Flax TRMs

As shown in the previous paragraph, the fibre treatment by means of a coating application affects the morphology and the tensile behaviour of flax threads, and also influences the bond between fibres and mortar.

With the aim of investigating the influence of such treatment on the mechanical behaviour of the composite, tensile tests are proposed on Flax TRMs performed by adopting textiles treated by means of the same coating treatment showed above. In addition, with the aim of achieving a more improved performance, the influence on the mechanical behaviour of matrix modifications, obtained by adding short fibres, was investigated as well.

7.3.1 Materials and methods

The textile adopted to perform the TRM coupons consisted of the flax fabric whose mechanical and physical properties were discussed in *Chapter 3*. The treatment applied on the textile consisted in the application of a Carboxylated Styrene Butadine Rubber (XSBR) latex on the surface of the fabric in order to reproduce the same treatment performed on the flax thread subjected to tensile and bond characterisation and whose behaviour is discussed in the previous paragraph.

The treatment was carried out on flax fabric portions 35 cm large and 60 cm long. The textile portions were arranged on a wood frame specifically conceived to keep them strained during the entire coating procedure. The coating substance was applied on the textile in environmental temperature conditions (Figure 7.13a), then the excess liquid was removed and the textile portions were dried at a controlled temperature of 38 ± 2 °C for 24h (Figure 7.13b). After the treatment flax strips, 60 mm large, were cut from the textile to be used as reinforcement in TRMs (Figure 7.13c). The mechanical characterisation of the strips was carried out by means of tensile tests, considering the follow series of specimens:

- Flax fabric 6cm, consisting in 5 specimens of flax textile with a width of 60 mm (containing 12 Flax-T threads) and a length of 500 mm;
- Flax fabric 6cm-imp, consisting in 5 specimens of impregnated flax textile with width of 60 mm (containing 12 Flax-T threads) and length of 500 mm.

Tensile tests were carried out by means of a Shimadzu (model AG-Xplus) universal testing machine with 10 kN load capacity, with a gauge length of 300 mm, in displacement control with a rate of 4mm/min. Each edge of the flax strips was glued by means of a resin within two aluminium plates for a length of 100 mm. The

elongation of the textile during the test was taken via extensometers placed at mid-length recording the relative displacements over a length of 200 mm (Figure 7.14).

Figure 7.13: Textile impregnation procedure: a) application of the coating substance; b) drying of the textile; c) coated flax strip.

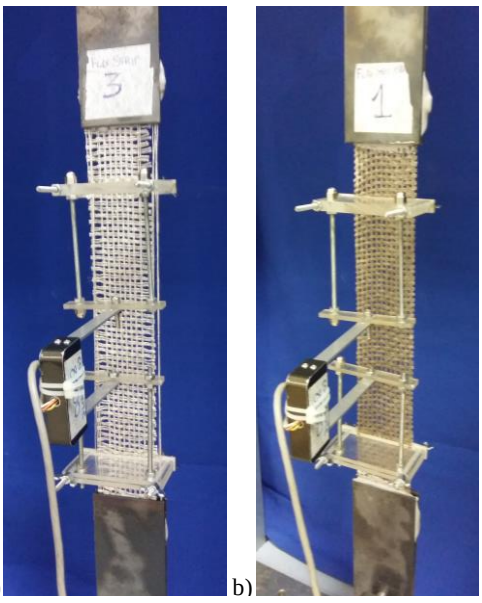

Figure 7.14: Tensile test set up of representative a) Flax fabric 6cm and b) Flax fabric 6cm-imp specimens.

Flax TRM specimens to be tested in tension were performed with the same manufacturing process already shown in *Chapter 4*, by alternating layers of mortar and textile (Figure 7.15a and b). Specifically, the specimens were characterised by the TRM-2L reinforcement configuration in which two layers of textile, alternated by a thin layer of mortar, were arranged within the sample. The series of specimens considered are shown as follows:

- Flax TRM-2L, consists of a series of specimens characterised by two layers of non-impregnated flax textile;
- Flax TRM-2L-imp, consist of a series of specimens characterised by two layers of impregnated flax textile (Figure 7.15c);
- Flax TRM-2L-imp-SF, consist of a series of specimens characterised by two layers of impregnated flax textile, and by a short-fibre reinforced mortar (Figure 7.15d).

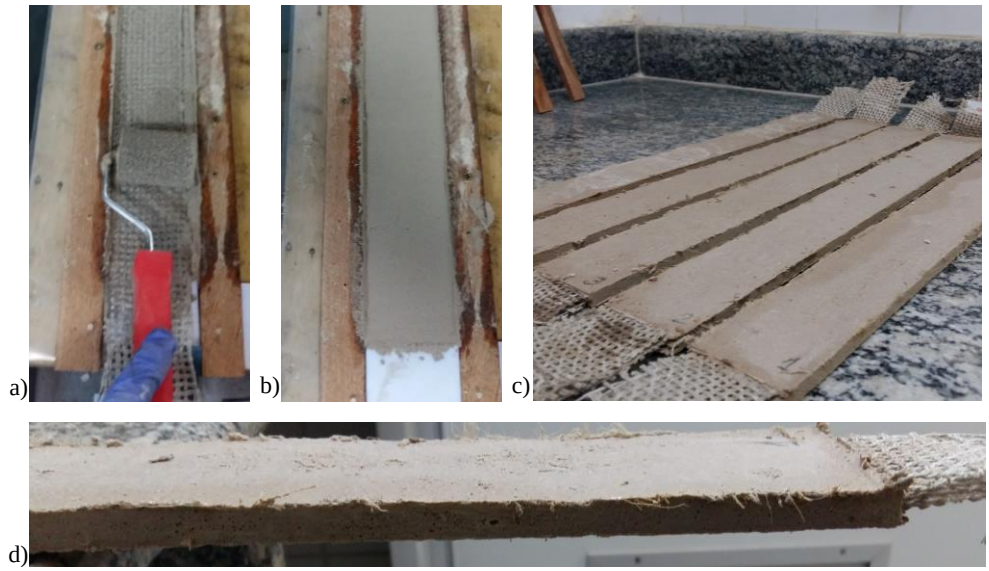

Figure 7.15: a) application of the impregnated textile within the mortar; b) smoothing of the outer layer of mortar; c) Flax TRM-2L-imp specimens; d) representative Flax TRM-2L-imp-SF specimen.

For each series of specimens the mechanical properties of the mortar were assessed by means of bending and compression tests carried out according to specific standards [111]. The consistence of the fresh mortar properties was assessed as well by means of flow table test, and was expressed in terms of mean diameter of the mortar after jolting the table for 15 times [110].

The mix design adopted for the mortar is the same shown in *Chapter 4*. With respect to the series Flax TRM-2L-imp-SF, short fibres were added to the mix

design. In accordance to the principles of sustainability on which the entire research study is based, plant fibres were chosen to strengthen the mortar. Specifically, 20 mm long curaua fibres were added to the mix design in a percentage of 1% in weight of the fresh mortar (Figure 7.16a). The fibres had a diameter of 77.7 μm [134]. Before their use the fibres were subjected to chemical and physical treatments to improve their strength and their durability once immersed in alkaline mortars [134]. As first they were submitted to three hornification cycles, each one consisting in 3 h of immersion in 80 °C and 24 h of drying at 40 °C in a ventilated chamber. Consequently, an alkaline treatment was adopted consisting in 50 min of immersion in an alkaline solution characterised by a concentration of 0.73% g/ml of $Ca(OH)_2$, followed by 24 h of drying at 40 °C in a ventilated chamber.

The addition of the short fibres within the mortar significantly increased the consistency of the fresh mortar (Figure 7.16 b and c). However, the short fibres conferred to the mortar a higher flexural strength and a post peak behaviour in flexion, thanks to their capacity to transfer the load between two edges of a crack within the mortar (Figure 7.16d).

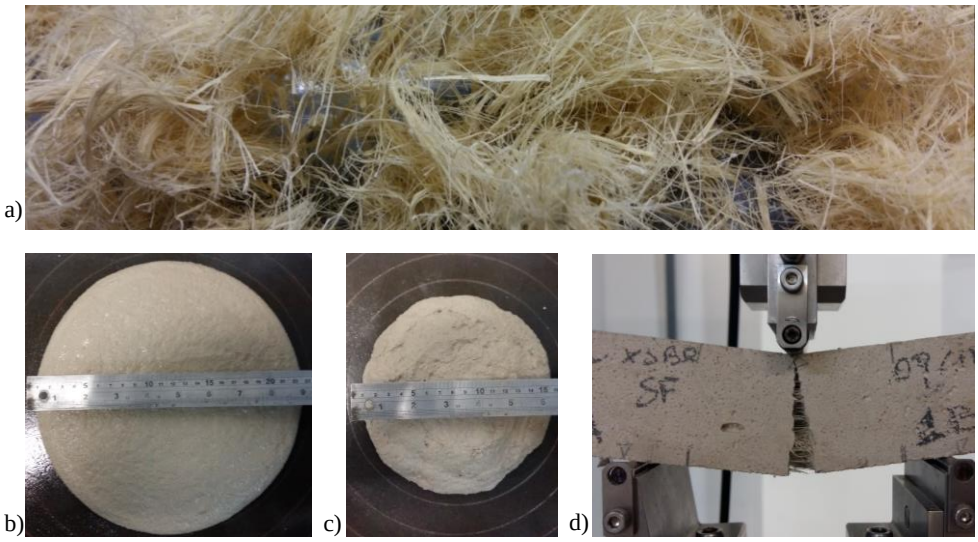

Figure 7.16: a) curaua short fibres; b) consistence of fresh mortar (Flax TRM-2L-imp series); c) consistence of fresh mortar (Flax TRM-2L-imp-SF); d) Bending test of curaua short fibre reinforced mortar (Flax TRM-2L-imp-SF series).

The main properties of the three series of specimens are listed in Table 7.2. All specimens were characterised by a length of 500 mm and a gauge length of 300 mm. Each edge was glued between two aluminium plates by means of a resin for a length of 100 mm. The gripping configuration was the clevis type. The test set up was arranged so that, by means of hinges, no bending and torsional moments were

applied to the specimen during the test. In order to be consistent with the experimental evidences showed in the previous chapters, the test set up was conceived to be as similar as possible to the one showed in *Chapter 4*. However, being the experimental analysis carried out at a different laboratory, the occurrence of differences in the specimens manufacturing process, and in the testing, was unavoidable. For this reason, the reference series, i.e. the Flax TRM-2L, although having the same characteristics of the series Flax TRM-2L-T showed in *Chapter 4*, was implemented again.

Table 7.2: Main properties of the tensile test series of specimens.

Series	Number of spec.	Section (mmxmm)	$A_{textile}$ (mm^2)	fibre vol. ratio	$f_{textile}$ (MPa)	$f_{c,mortar}$ (MPa)	$f_{t,mortar}$ (MPa)	$d_{flow\ table}$ (mm)
Flax TRM-2L	5	8 x 60	12.2	2.55%	331	10.4	4.4	238
Flax TRM-2L-imp	5	8 x 60	12.2	2.55%	266	8.4	3.9	223
Flax TRM-2L-imp-SF	5	8 x 60	12.2	2.55%	266	9.9	5.9	153

Tensile tests were carried out by means of a Shimadzu (model AG-Xplus) universal testing machine with 10 kN load capacity, in displacement control with a rate of 0.3 mm/min (Figure 7.17a).

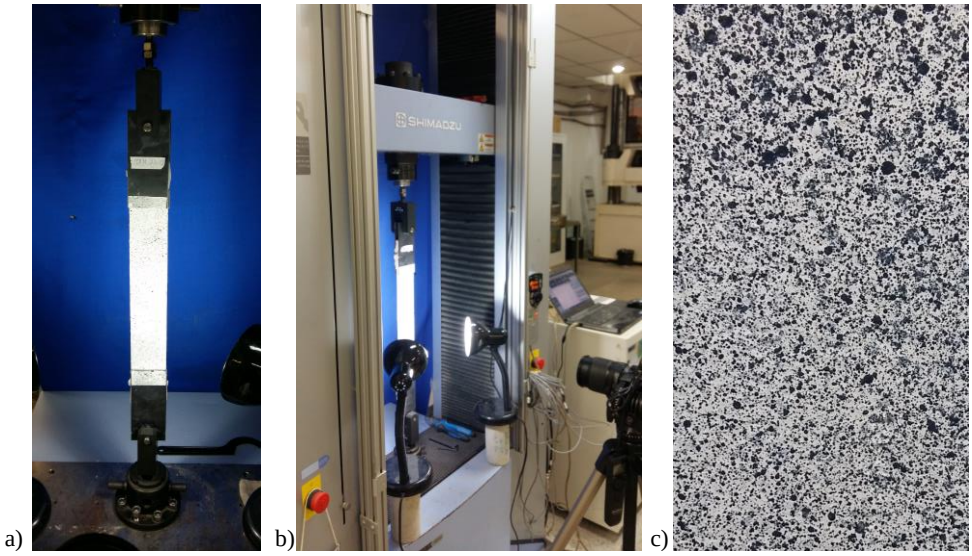

Figure 7.17: a) tensile test set up; b) light spots and camera and c) surface treatment for DIC analysis.

The external surface of the specimens was treated, by creating a white background on which black dots were stochastically sprinkled, in order to get images for Digital Image Correlation (DIC) analysis (Figure 7.17c). The acquisition of the

photos was carried out by means of a camera placed at a focal distance of 50 cm. The acquisition rate was of 3.75 ph/min and the resolution of the photos was of 4310 x 2868 pixels (0.08 mm/pix).

7.3.2 Results and discussion

The tensile response of the impregnated and non-impregnated flax textile is shown in terms of stress-strain in Figure 7.18.

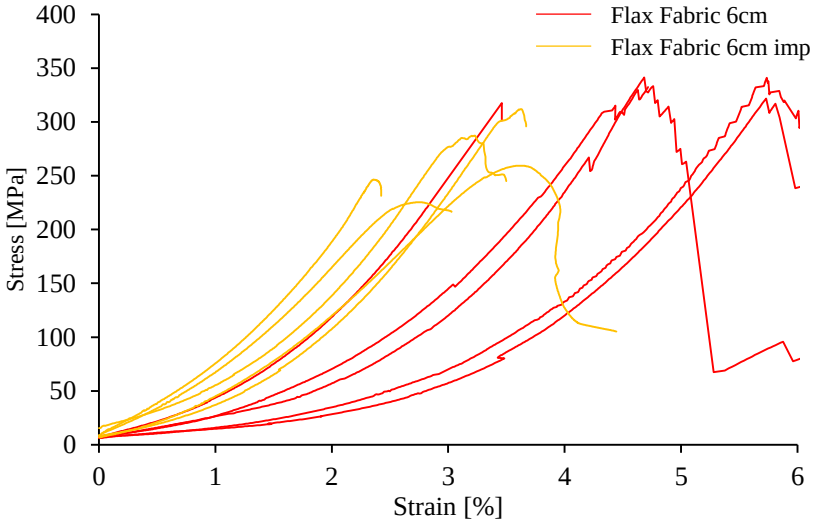

Figure 7.18: Stress-strain response of non-impregnated and impregnated flax strips.

The main parameters are listed in Table 7.3. As expected, in accordance with what was observed in previous chapters, the tensile response was characterised by a first step characterised by a lower stiffness that increases with the strain up to achieve a quasi-linear branch before the failure. The latter represents the stiffness E reported in the table.

Table 7.3: main parameters of flax strips tested in tension.

Series	Cross section (mm^2)	σ_{max} (MPa)	ε_{max} (%)	E (GPa)
Flax Fabric 6cm	6.12	331	4.9	12.50
Co.V. (%)	-	3	19	6
Flax Fabric 6cm imp	6.12	266	3.1	12.43
Co.V. (%)	-	13	18	14

The series Flax Fabric 6cm was characterised by a failure mode in which the progressive rupture of the fibres threads occurred. The Flax fabric 6cm-imp specimens failed at lower values of stress and with a mixed failure characterised by filament rupture and slipping of filaments within the coating polymer. Moreover, unlike non-impregnated fibres, the impregnated textile is also characterised by a transversal stiffness. By increasing the strain, due to the Poisson effect, the textile tends to get thinner in the middle contributing to a premature failure. Although being characterised by the same main value of stiffness in the linear branch, impregnated strips were characterised by lower values of the strain at failure. Such behaviour, in line with the evidences showed in previous paragraph where impregnated threads were tested in tension, confirmed that the coating reduces the deformability of the textile.

The tensile response of Flax TRMs in terms of load-displacement is shown in Figure 7.19, Figure 7.20 and Figure 7.21. The response is also shown in terms of stress-strain in Figure 7.22, Figure 7.23 and Figure 7.24. The stresses were assessed, and reported within the graphs, with respect to both the mortar and textile cross section in order to represent both configurations in which, in proximity of the cracks, the load is entirely borne by the textile, and, in proximity of the sections characterised by a full interaction between textile and mortar, the stress may be assumed uniformly distributed along the TRM cross section.

The main mechanical parameters deriving from the tests are reported, in terms of mean value, and for each series of specimen, in Table 7.4.

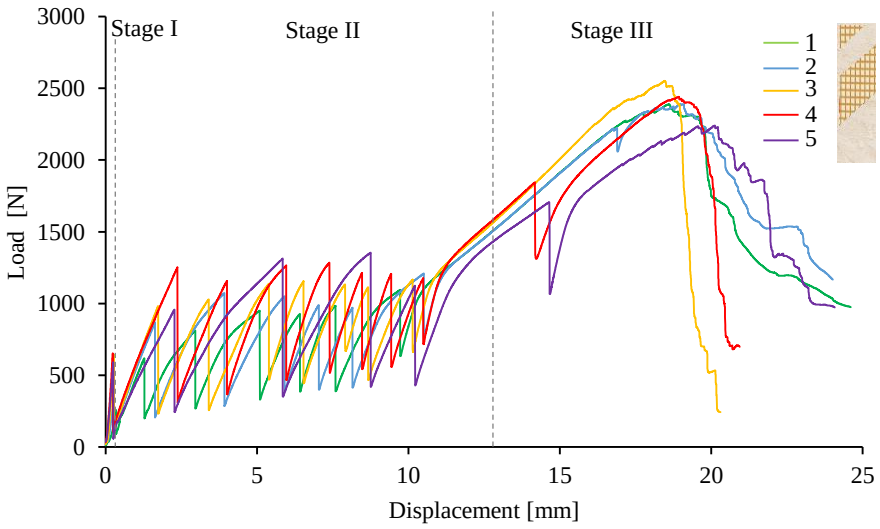

Figure 7.19: Load-displacement curves concerning Flax TRM-2L specimens.

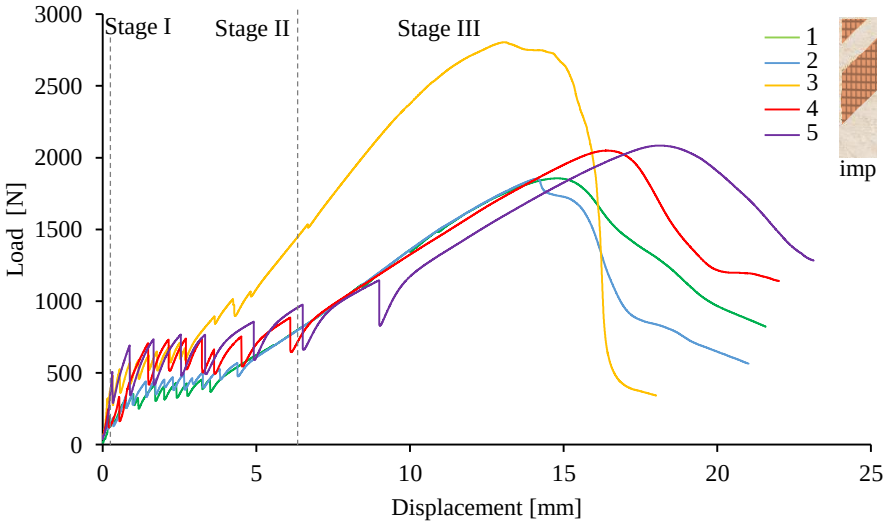

Figure 7.20: Load-displacement curves concerning Flax TRM-2L-imp specimens.

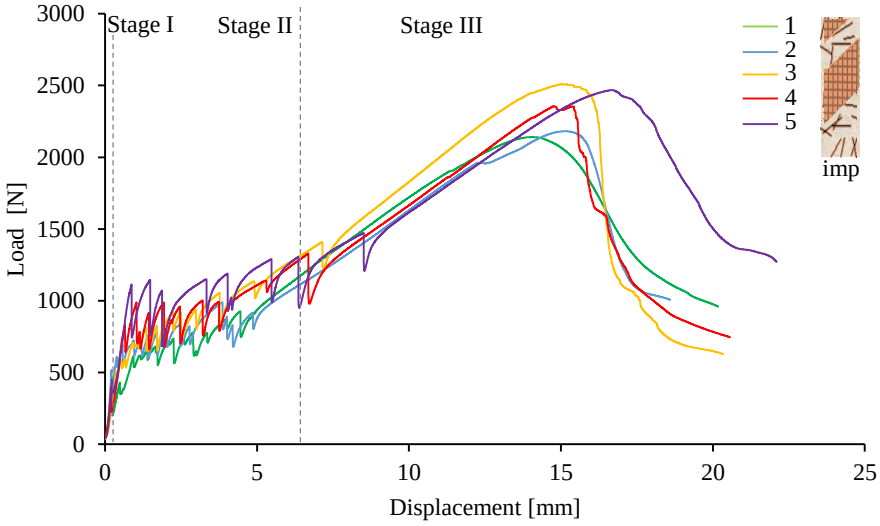

Figure 7.21: Load-displacement curves concerning Flax TRM-2L-imp-SF specimens.

It is worth highlighting that the tensile response of the reference Flax TRM-2L series resulted perfectly in line with the analogous series, Flax TRM-2L-T, whose behaviour is described in *Chapter 4*. Such experimental evidence confirms that the desired boundary conditions were properly reproduced.

As with as the reference series, also the others were characterised by the classical trilinear behaviour characterised by: the first elastic stage, the transition

behaviour characterised by the progressive development of several cracks, the third stage mainly governed by the textile mechanical contribution.

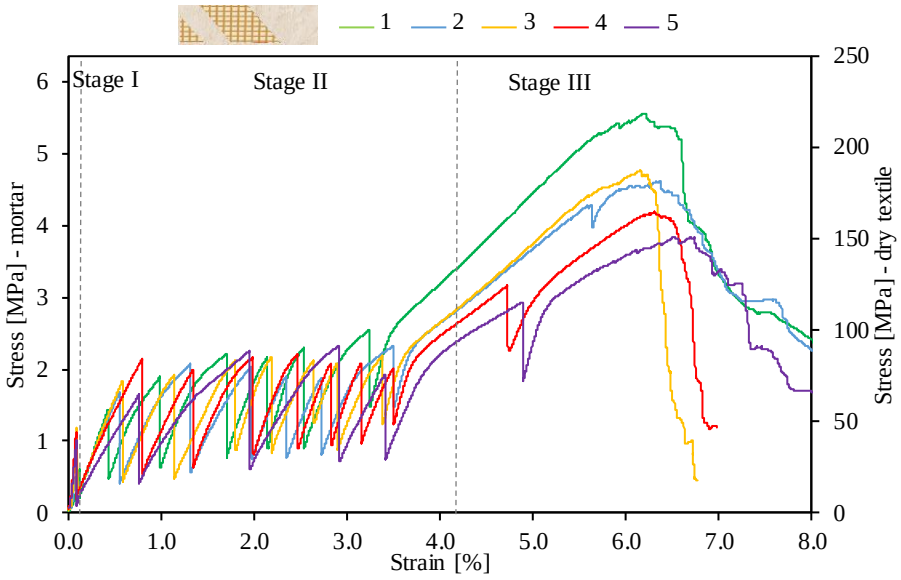

Figure 7.22: Stress-strain curves concerning Flax TRM-2L specimens.

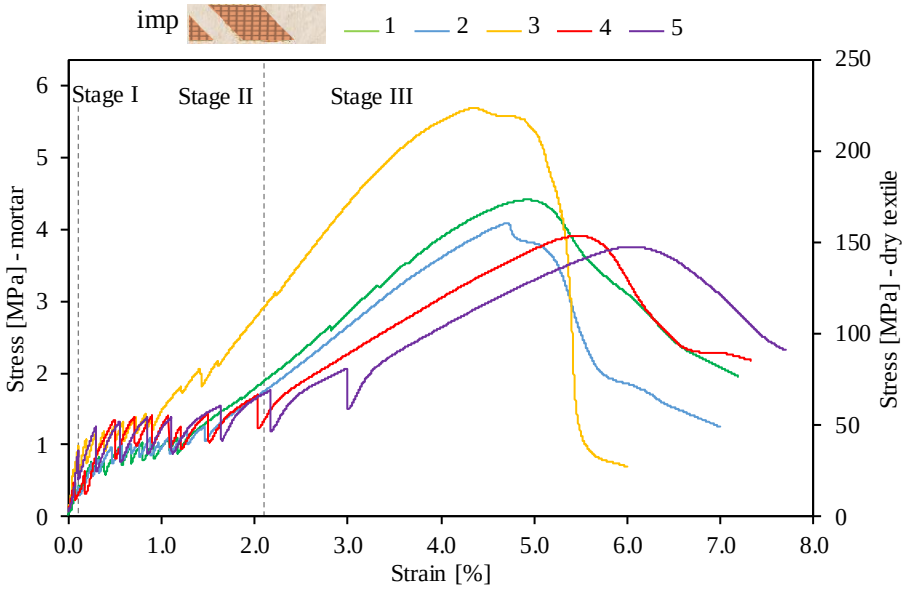

Figure 7.23: Stress-strain curves concerning Flax TRM-2L-imp specimens.

The main values of the stress and strain in correspondence to the transition points between the various stages were evaluated as well and reported in Table 7.5.

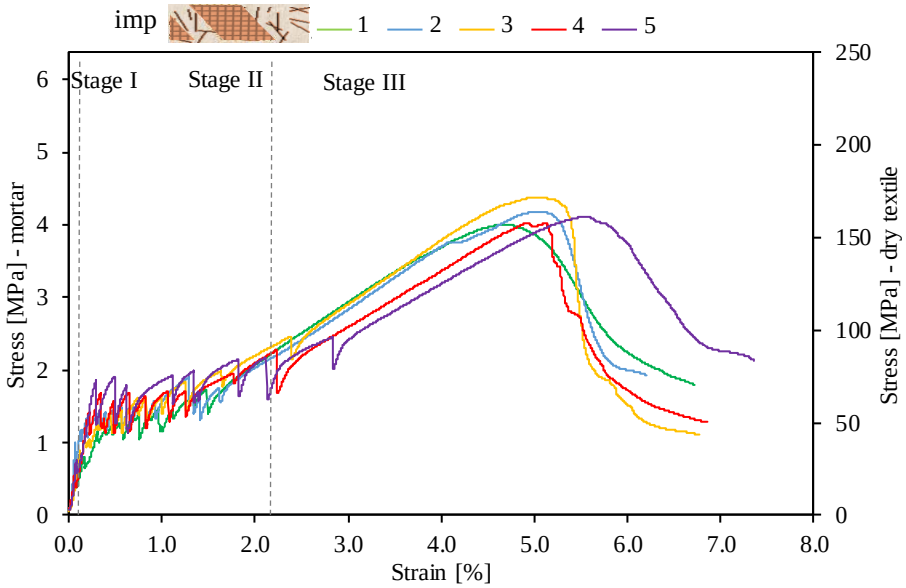

Figure 7.24: Stress-strain curves concerning Flax TRM-2L-imp-SF specimens.

Table 7.4: Main properties of Flax TRM specimens tested in tension.

Series	P_{max} (N)	$disp_{max}$ (mm)	σ_{max} (MPa)	ε_{max} (%)	$\sigma_{textile}$ (MPa)	$\sigma_{max}/f_{textile}$ (%)
Flax TRM-2L	2402	19.0	5.00	6.3	196	59
Co.V. (%)	5	3	5	3	5	5
Flax TRM-2L-imp	2129	15.3	4.44	5.1	174	65
Co.V. (%)	18	13	18	13	18	18
Flax TRM-2L-imp-SF	2331	15.1	4.86	5.0	191	72
Co.V. (%)	7	6	7	6	7	7

Table 7.5: Stress and strain corresponding to the different transition points.

Specimen	σ_1 (MPa)	ε_1 (%)	σ_2 (MPa)	ε_2 (%)
Flax TRM-2L	1.15	0.1	2.53	3.7
Co.V. (%)	24	7	6	5
Flax TRM-2L-imp	0.68	0.1	1.75	2.0
Co.V. (%)	48	25	37	40
Flax TRM-2L-imp-SF	0.96	0.1	2.34	2.1
Co.V. (%)	11	40	17	26

As expected, the series of specimen Flax TRM-2L, was characterised by a second stage in which, in correspondence of each crack, a significant drop of the load was observed. As widely discussed in previous chapters, such behaviour may be attributed to a matrix-to-textile bond problem, to the non-uniform stretching of the textile during the manufacturing process, and to the characteristic lower initial stiffness of plant fibre textiles.

As a matter of fact, both the improved Flax TRM configurations, i.e. Flax TRM-2L-imp and Flax TRM-2L-imp-SF series, showed a second stage in which the drops of load corresponding to the occurrence of cracks, were considerably lower with respect to what observed in the reference series. Moreover, it can be observed that the number of cracks exhibited in the two improved configurations, was higher with respect to the reference series. Such aspect, emphasized that the fibre treatment caused alterations in the fibre-to-mortar bond properties, and in the textile stiffness, that resulted in a higher capacity to transfer the stress from the textile to the matrix, with a consequent reduction of the distance between consecutive cracks.

With respect to the third stage, although dry and impregnated textile tested in tension exhibited the same stiffness, the average value of the slope of the curves concerning the improved Flax TRMs (series Flax TRM-2L-imp and Flax TRM-2L-imp-SF) was of about 10 % lower than what observed in the reference series. Such experimental evidence may be due to the higher number of cracks occurred in the improved Flax TRMs.

The specimen Flax TRM-2L-imp-3 was characterised by a much stiffer, and with a higher strength, response, with respect to the other specimens. Such behaviour can be attributed to the impregnation treatment adopted. Specifically, the impregnation treatment was manually performed, and applied on several textile portions. Such procedure, adopted without having at disposal standardized industrial techniques, unavoidably resulted in a heterogeneity among the textile strips. In order to reduce the influence of such variability in the composite behaviour, the TRM coupons were performed by uniformly distributing the flax strips deriving from the different portions, among the various specimens and series. The better performance exhibited by the specimen Flax TRM-2L-imp-3 may be attributed to the use of flax strips characterised by an impregnation treatment occurred in a proper manner. For the same reason the response of the series in which impregnated textiles were adopted, is characterised by a significant variability (see coefficient of variation of the mechanical parameters reported in Table 7.5).

By comparing the stress at the transition point between the Stages I and II, σ_1, it can be noticed that the average value of the reference series was higher with respect to the others. Such evidence may be attributed to the fact that the less significant contribution of the textile in the elastic phase let the specimen to be closer to the

mortar direct tensile conditions. However, by comparing the mean values of the stress σ_1 of the improved Flax TRMs, it is observed that the series Flax TRM-2L-imp-SF was characterised by a value of about the 30% higher than those of Flax TRM-2L-imp series. This aspect is clearly shown in Figure 7.25, where representative specimens of each series were compared.

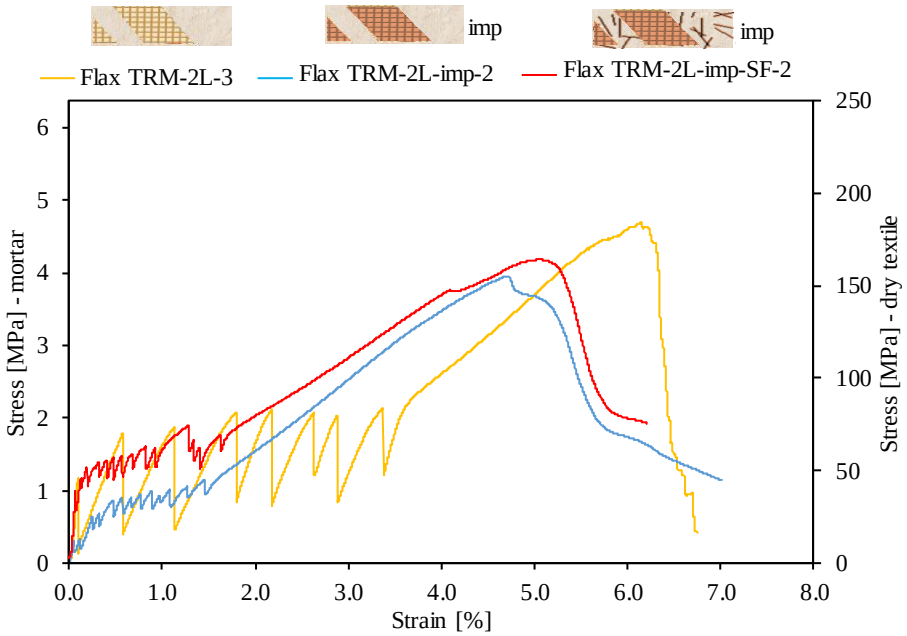

Figure 7.25: Comparison between representative specimens of the series tested in tension.

The comparison shows that the load values corresponding to each crack opening, is generally higher in improved Flax TRMs with respect to the reference series. Moreover, by comparing the Flax TRM-2L-imp and the Flax TRM-2L-imp-SF it is observed that the latter was characterised by an average value of the stress within the second stage, much higher than the one observed in the other series. This behaviour is due to the presence of the curaua short fibres that increased the tensile strength of the mortar. This aspect is of fundamental importance in view of applications of the TRM as reinforcement of structural elements. In fact, the higher stress values on the second stage, and the lower losses of strength corresponding to the crack openings, may lead toward a hardening post-elastic behaviour.

In terms of ε_2, the use of impregnated textiles led to an evident reduction of the deformability within the second stage, with a mean value of the strain that decreased of about the 50 % in the improved TRMs with respect to the reference series. The latter represents a fundamental aspect. In fact, as known, once applied on

a structural element, the TRM composite is considered to confer an actual contribution when behaving in the third stage. Therefore, the textile impregnation treatment leads to a TRM system capable to exhibit its contribution, once applied on structural element, at smaller values of deformation, with respect to the reference Flax TRM. The smaller deformability of the composite, may correspond, on the structural element scale, to a post elastic behaviour characterised by less significant abrupt losses of strength.

The failure mode was characterised, in all specimens, by a progressive development of cracking along the free length, up to the rupture of the textile in proximity of a crack (Figure 7.26d).

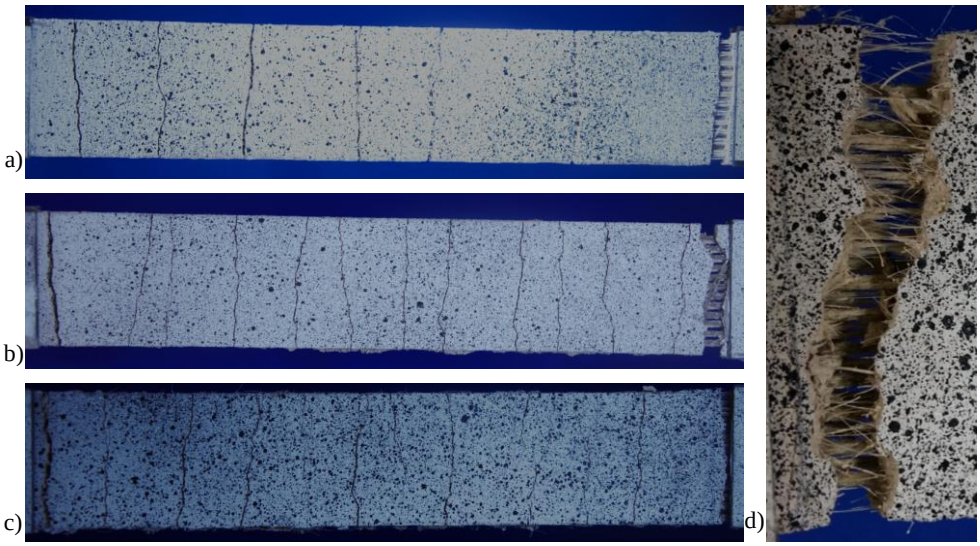

Figure 7.26: Failure mode of representative specimens: a) Flax TRM-2L-3; b) Flax TRM-2L-imp-2; c) Flax TRM-imp-SF-2; d) rupture of the textile.

The comparison between the cracked representative specimens of the three series, shows that Flax TRM-2L-imp and Flax TRM-2L-imp-SF specimens were characterised by a higher number of cracks, closely spaced with respect to the reference specimen (Figure 7.26a, b and c).

With respect to the maximum strength achieved, as expected considering the tensile strength exhibited by non-impregnated and impregnated textile strips, the reference series was characterised by higher values of the maximum stress. However, in terms of exploitation ratio, σ_{max}/f_{tex} (representing the ratio between the maximum stress achieved in the composite and the maximum strength achievable in the textile), a significant increase of 10 % and 20 % was observed with respect to Flax TRM-2L-imp and Flax TRM-2L-imp-SF series.

7.3.3 Analysis of the crack pattern

The analysis of the crack pattern was carried out on a representative specimen of each series tested in tension, i.e. Flax TRM-2L-3 (also referred to as reference Flax TRM), Flax TRM-2L-imp-2 and Flax TRM-2L-imp-SF-2 specimens (also referred to as improved Flax TRMs).

In line with what was proposed in paragraph 4.1.4, DIC images were treated in order to construct the displacement field of the external surface of the specimens, over a length of 200 mm in the middle of the free length of the specimens. For each specimen significant images were selected, corresponding to the occurrence of cracks, the transition points between different stages, and the cracked specimen at maximum. The displacement over a longitudinal section corresponding to the selected images, for each representative specimen, is shown in Figure 7.27, Figure 7.28 and Figure 7.29.

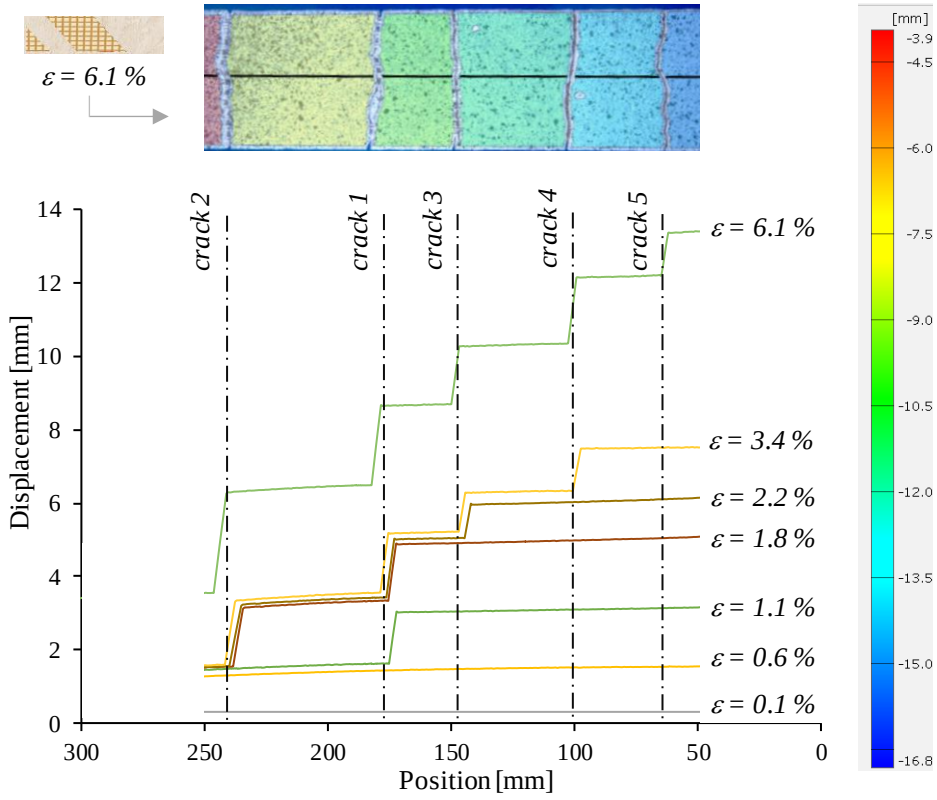

Figure 7.27: Displacement field of the middle longitudinal section (Flax TRM-2L-3).

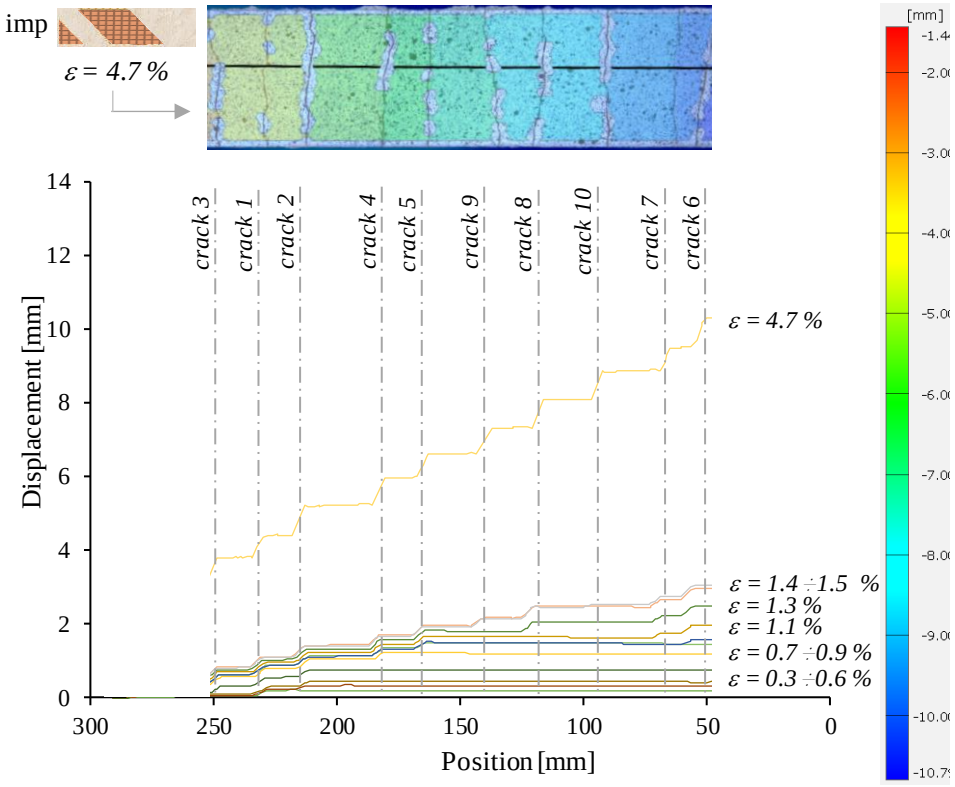

Figure 7.28: Displacement field of the middle longitudinal section (Flax TRM-2L-imp-2).

The image on the top of the figures represents the displacement field of the external surface of the TRMs, over a length of 200 mm, in correspondence to the achievement of the maximum strength.

By comparing the graphs, it is clear that the improved Flax TRMs were characterised by a much higher number of cracks developed during the test. Moreover, such cracks, developed at much lower values of the strain. Such behaviour confirms, from another perspective, the deformability of the improved Flax TRMs in the second stage, with respect to the reference TRM.

The capacity of developing cracks at lower values of strain, is clearly highlighted in Figure 7.30, where the evolution of the mean crack spacing as a function of the axial strain, is shown for the three representative specimens. The curves are a logarithmic approximation of discreet values. This representation clearly emphasises the best mechanical performance of the improved Flax TRMs with respect to the reference coupon.

By analysing the displacement fields it is also possible to see that the improved Flax TRMs were characterised by shorter distances between consecutive cracks, as well as smaller crack openings.

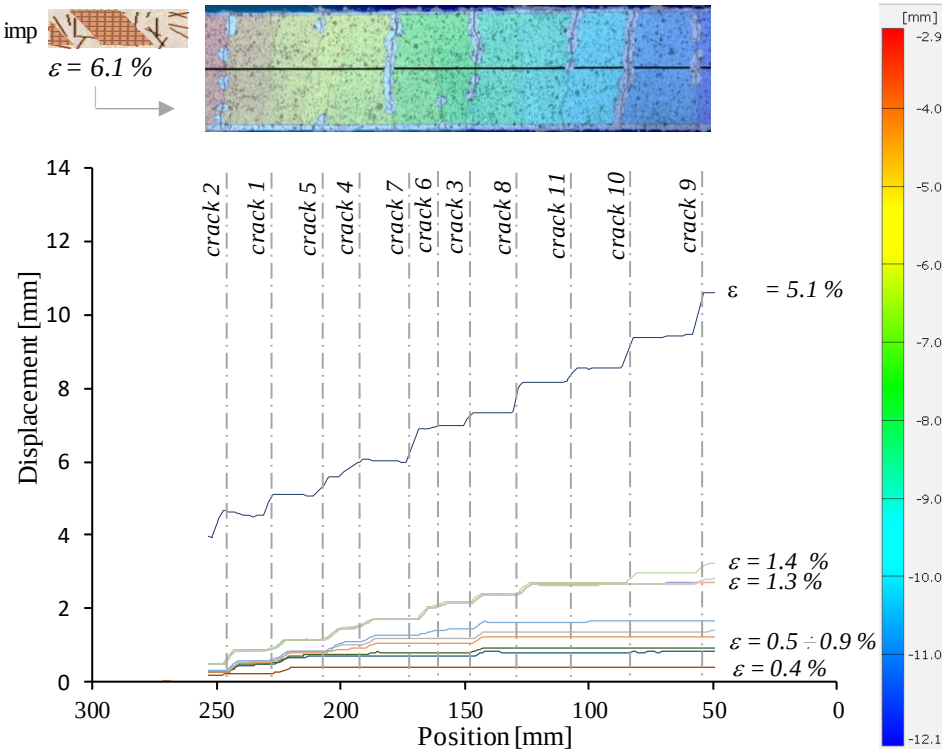

Figure 7.29: Displacement field of middle longitudinal section (Flax TRM-2L-imp-SF-2).

The mean values of the distance between consecutive cracks, $\delta_{0,mean}$, and the maximum crack opening, w_{max}, concerning the representative specimens are listed in Table 7.6. The maximum value of the crack opening resulted up to 3 times smaller in improved Flax TRMs with respect to the reference behaviour. Such aspect is fundamental in view of application of the composite as external reinforcement of structural elements. In fact, the closer space between cracks reduces the contact of the textile with the external environment, improving the capacity to resist to ageing processes.

With respect to the approximated analytical model proposed in paragraph 4.1.4, starting from the values of the mean spacing between consecutive cracks, the tensile strength of the mortar and the perimeter of non-impregnated and impregnated textile cross section, an approximated estimation of the maximum interfacial shear stress between the fabric and the mortar was carried out. The mean value for each

representative specimen is reported in Table 7.6. Although being an approximated estimation, this parameter provides interesting information.

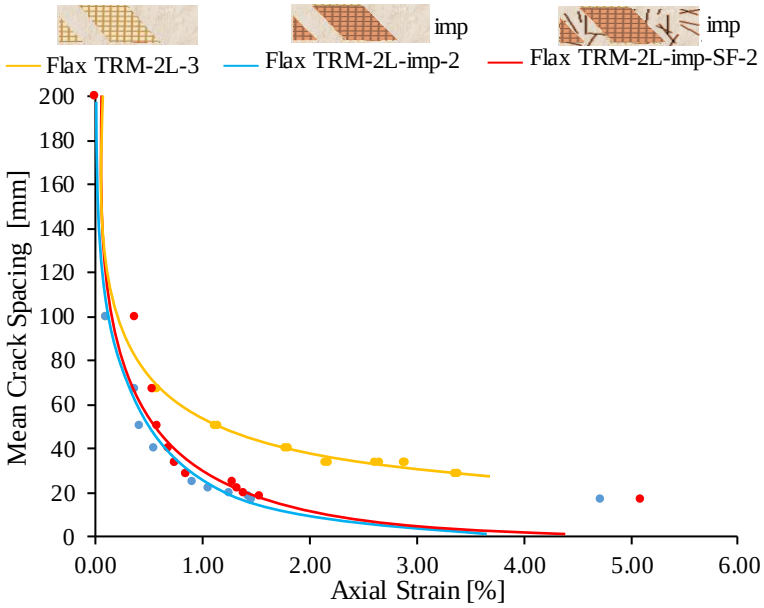

Figure 7.30: Mean crack spacing as a function of the strain for representative specimens.

Table 7.6: Main parameters of the analysis of cracks of representative specimens.

Series	Spec.	$\delta_{0,mean}$ (mm)	w_{max} (mm)	τ (MPa)
Flax TRM-2L	3	43	2.70	0.22
Co.V. (%)		29	-	25
Flax TRM-2L-imp	2	23	0.83	0.57
Co.V. (%)		31	-	28
Flax TRM-2L-imp-SF	2	27	1.12	0.74
Co.V. (%)		28	-	28

The mean shear stress value concerning the reference series is in line with what observed in *Chapter 4*, confirming once again the desired conditions were well reproduced. In both of the improved TRM configurations a significant increase of the mean shear stress was observed with respect to the reference series. This result is not in line with what observed in the previous paragraph where the bond between the mortar and non-impregnated and impregnated threads was analysed by means of

pull-out tests. Such experimental investigation showed that the impregnation caused a reduction in the matrix to fibre bond capacity.

This discrepancy may be due to two aspects. The approximated model, by considering constant the shear stress along the length, did not take into account the stiffness of the textile, that in fact plays an important role in the mechanical behaviour of the system. The other aspect is related to the fibre impregnation treatment. As a matter of fact, the impregnation of the single threads, did not reproduce the same conditions created by impregnating portions of textile. Specifically, the removal of the coating substance in excess from the flax thread was much easier than removing the polymer form the bidirectional fabric. As a result, the textile strips were characterised by a higher amount of coating substance with respect to the flax threads.

This aspect emphasizes that, although showing very satisfactory results in terms of mechanical behaviour of the composite, the impregnation procedure adopted still needs to be refined, perhaps by adopting industrial techniques, and further studies are needed to define the best coating substance. Moreover, for further investigation, it would be more reliable to extract flax threads to submit to pull-out tests, directly from the impregnated textile. By doing so it would be easier to reproduce, by means of pull-out tests, the bond conditions of composite tensile tests.

Although having a similar mean value of the distance between cracks, the Flax TRM-2L-imp-SF representative specimen showed a mean shear stress of about the 30 % higher than the one exhibited by the Flax TRM-2L-imp representative specimen. Such result is due to the higher tensile strength of the short-fibre reinforced mortar, that, according to the model, is directly proportional to the shear stress. However, although the approximated nature of the analytical model, it is reasonable to assert that the addition of short fibres within the mortar may result in an increased capacity of transferring the stress from the textile to the matrix, promoting an homogeneous distribution of the stress over the entire composite cross section.

7.4 Conclusions

The aim of the chapter is to show that by applying some of the techniques available in literature, it is possible to improve the mechanical performance of plant based TRM composite systems. At first, the influence of a fibre impregnation treatment on the morphology and tensile strength of flax threads, and on the bond behaviour with a hydraulic lime-based mortar, was investigated. Secondly, the tensile response of improved TRMs, obtained by means of the application of impregnated textiles, and

by means of the addition of curaua short fibres within the mortar, was investigated and compared with reference TRMs.

The main findings of the experimental investigation are listed as follows:

- the analysis of the SEM images showed that the impregnation treatment by means of XSBR latex significantly affected the flax thread shape, with a reduction of the $FIER_r$ of 35 %, and reduced the variability of the geometry of the threads characterised by a dispersion in the measurements much lower than the dispersion of the measurements carried out on non-impregnated fibres;
- a favourable effect of the impregnation on the mechanical response in tension was observed: despite a small reduction in tensile strength, the impregnated fibres exhibited an ultimate strain much smaller than the one observed by testing non-impregnated threads, due to a less significant initial less stiff branch;
- a decrease of the bond between fibres and mortar was observed with a reduction of the maximum shear stress of about 30 % because of a polymeric weak layer between the fibres and the mortar created by the impregnation;
- the impregnation of flax textile strips had a favourable effect on the tensile behaviour. In fact, although characterised by slightly lower strength values, impregnated textiles exhibited a lower deformability by achieving the linear stiffness at lower strains with respect to non-impregnated textiles;
- both the improved TRMs proposed in the study showed a second stage in which the typical drops of load corresponding to the occurrence of a crack in plant-based composites, were considerably lower with respect to what observed in the reference TRM;
- the use of impregnated flax textiles as reinforcement of TRMs significantly reduced the deformability of the system in the second stage, with a main value of the transition strain ε_2 reduced of about the 50 % with respect to the reference values;
- the addition of short fibres within the mortar resulted in a mean value of the stress within the second stage, significantly higher than the value observed in the improved TRMs conceived without improving the mortar;
- the improved TRMs failed assuming higher values of the exploitation ratio with respect to the reference series, behaving as a more efficient composite material;

- the analysis of the crack pattern showed that the improved TRMs were characterised by a much higher number of cracks developed at much lower values of strain with respect to the reference behaviour;
- the application of the improvement techniques resulted in lower cracks opening, reducing the contact with the external environment, hence letting hope to an improved durability performance.

It is worth emphasising that the showed results represent a preliminary study, and the impregnation procedure needs to be standardised in order to make the results more reliable (at present they are characterised by a considerable coefficient of variation). The experimental evidences showed within the chapter confirmed that the application of simple improving techniques can significantly improve the mechanical performance of plant based TRMs. Moreover, according to the critical observation reported in Chapter 6, these improvements may correspond to a much better performance of the composite system once applied to structural elements to enhance their strength. The lower deformability of the TRM in the cracked zone, the less significant loss of strength corresponding to the crack development, a more efficient behaviour as composite characterised by a wider development of cracks through the entire specimen, and the higher values of the stresses in the cracked zone, may possibly result in a more satisfying mechanical behaviour of externally strengthened masonry elements, perhaps by achieving higher elastic capacity, and an hardening post-elastic behaviour.

Finally, it is worth highlighting that the improvement solutions adopted, were not selected through sophisticated technical analysis, but were rather chosen with respect to the ease availability of the materials employed, and to few encouraging similar literature evidences. Nevertheless, the scientific outcomes resulted more than promising. Reasonably, further investigations aimed at optimizing improvement techniques, may only result in a mechanical behaviour even more satisfactory.

8. Conclusions

The Thesis was intended at assessing the potential of Flax TRM composite systems as external strengthening system of masonry structural elements. It order to meet the need of a deep understanding of the mechanical behaviour of plant fibre based TRMs, the study proposes a comprehensive characterisation that moves from the analysis of the microstructure of the flax threads constituting the textile, up to the investigation of the efficiency of the composite system as reinforcement of masonry walls. The main outcomes of the research study are discussed as follows.

As preliminary investigation, the physical and mechanical properties, as well as some durability aspects, of the flax textile adopted in the study were analysed. The results demonstrated that the flax fabric under investigation, with promising mechanical properties can be utilised as internal reinforcement for TRM systems. In terms of durability the fibres showed a good performance in the short term, and significant decreases of strength in accelerated ageing exposures, highlighting the need of specifically designed treatments to cope with this issue.

In light of the encouraging outcomes on the textile scale of analysis, the study moved to the investigation of Flax TRM composite systems. Tensile tests showed that the response in tension was characterised by a trilinear behaviour, differing from the typical behaviour exhibited by conventional high strength fibre based TRMs, in the exhibition of significant drops of the stress in correspondence to crack occurrence. Such experimental evidence may be due to the low initial stiffness of plant fibres when subjected to tensile loading conditions. However, the specimens exhibited a promising behaviour with a fibre exploitation ratio of about the 70 %. With respect to the Flax TRM-to-masonry substrate shear bond behaviour, the experimental evidences showed a rupture of the textile in the free length of the charging edge. This behaviour emphasised that the system is characterised by a good adhesion at the fibre-to-mortar interface with respect to the tensile strength of the flax textile itself. The experimental investigation carried out to analyse the durability of Flax TRM composites showed that the system, exposed to a conventional ageing protocol, complies with the acceptance criteria proposed by standards in the field.

Based on the satisfactory experimental evidences deriving from a characterisation at the composite scale of analysis, the reinforcement systems were

applied to masonry structural elements to assess their efficiency in enhancing the in-plane capacity of the walls. The application of the Flax TRM system significantly affected the mechanical response of the masonry elements tested in diagonal compression, by conferring them an increase in shear capacity, and a ductile behaviour completely absent in unreinforced elements. The experimental evidences also showed a significant loss of strength corresponding to the cracking of the wall in proximity of the maximum capacity, due to the significant deformability of the reinforcing flax textile at low values of strength. A comparative analysis with works available in the literature showed that the study is in line with similar investigations and is characterised by a low fibre reinforcement ratio. It was also showed that increasing the fibre amount by overlapping different textile layers not necessary ends up in a more performant behaviour.

A critical analysis of the strain fields of the TRM system, both in tensile and diagonal compression tests, showed that there is a relationship between the behaviour of the composite in the two different configurations. By analysing such correspondence, it was possible to define in which terms a more satisfactory tensile behaviour may lead to a better performance on the structural scale of analysis. Specifically, with respect to TRM tensile response, an increase of the mean stress in the second stage, a reduction of the loss of strength corresponding to the crack openings, an increase of the number of cracks developed at smaller strain levels, would probably results in a composite system that, once applied as reinforcement of structural elements, may confer them a behaviour tending toward a higher elastic capacity, and an hardening post-elastic behaviour.

Finally, with the aim of going further than merely confirm the promising potential of the proposed reinforcement system, the study proposed the application of technical solutions with the purpose of showing that there is still room for improvements in the mechanical behaviour of plant based TRM composites. Specifically, by means of Flax TRM tensile tests, the efficiency of a textile impregnation treatment, and of the addition of curaua short fibres within the mortar, was investigated. The use of impregnated flax textile resulted in a satisfactory improvement of the mechanical response of the system. In fact, although characterised by slightly lower strength, the improved TRMs exhibited a second stage with drops of the load corresponding to the occurrence of cracks, significantly lower with respect of the reference behaviour. Moreover, the application of the impregnated textiles considerably reduced the deformability of the system with a main value of the transition strain, ε_2, reduced of about the 50 % with respect to the reference behaviour. Furthermore, the addition of short fibres within the mortar resulted in a main value of the stress within the second stage, significantly higher than the value observed in the improved TRM conceived without improving the

mortar. As a matter of fact. the experimental evidences showed that the application of simple available techniques can significantly improve the mechanical performance of plant based TRMs.

The study, presenting a large amount of results, contributes to advancing knowledge about the use of plant textiles as reinforcement in mortar-based composites, and paves the way for further research activities aimed at optimising the sustainable strengthening system object of study. Many perspectives of the study may be defined:

- further mechanical investigations aimed at the definition of optimised improvement techniques, such as: performant textile treatments by means of chemical and/or physical procedures, the use of efficient coating substances improving the textile response and the fibre-to-mortar bond, the use of optimised fibre reinforcement amounts and textile arrangements, efficient matrix modifications improving the composite performance;
- comprehensive analysis on the durability of plant based TRMs, with respect to significant ageing environments, and by defining fibre treatments able to improve such aspect;
- multicriterial studies aimed at providing an exhaustive assessment of the sustainability of these types of reinforcement systems, and at comparing it with conventional composite systems nowadays largely adopted;
- the definition of actual possible applications of the studied composite system, according to its mechanical performance, as a reinforcement technique for structural elements and for elements of secondary importance.

Future research studies moving in the according to these directives, may end up in optimisation of the strengthening technique by means of plant based TRM composites, hence hopefully in a significant diffusion of these types of sustainable reinforcement systems in actual civil engineering applications.

References

1. N. Ambraseys, Earthquakes in the Mediterranean and Middle East: A Multidisciplinary Study of Seismicity up to 1900. *Cambridge University Press*, 2009.
2. H. Kaplan, H. Bilgin, S. Yilmaz, H. Binici, and A. Öztas, 'Structural damages of L'Aquila (Italy) earthquake', *Nat. Hazards Earth Syst. Sci.*, vol. 10, no. 3, pp. 499–507, Mar. 2010.
3. M. Indirli, L. A. S. Kouris, A. Formisano, R. P. Borg, and F. M. Mazzolani, 'Seismic Damage Assessment of Unreinforced Masonry Structures After The Abruzzo 2009 Earthquake: The Case Study of the Historical Centers of L'Aquila and Castelvecchio Subequo', *Int. J. Archit. Herit.*, vol. 7, no. 5, pp. 536–578, Jan. 2013.
4. Y. Zhuge and S. W. Chuang, 'Seismic retrofitting of unreinforced masonry buildings - a literature review', *Aust. J. Struct. Eng.*, vol. 6, pp. 25–36, 2005.
5. J. G. Tumialan, F. Micelli, and A. Nanni, 'Strengthening of Masonry Structures with FRP Composites', *Struct. 2001*, pp. 1–8.
6. L. Van Den Einde, L. Zhao, and F. Seible, 'Use of FRP composites in civil structural applications', *Constr. Build. Mater.*, vol. 17, no. 6, pp. 389–403, Sep. 2003.
7. T. Triantafillou, 'Innovative Textile-Based Composites for Strengthening and Seismic Retrofitting of Concrete and Masonry Structures', in *Advances in FRP Composites in Civil Engineering*, Berlin, Heidelberg, 2011, pp. 3–12.
8. M. Del Zoppo, M. Di Ludovico, and A. Prota, 'Analysis of FRCM and CRM parameters for the in-plane shear strengthening of different URM types', *Compos. Part B Eng.*, vol. 171, pp. 20–33, Aug. 2019.
9. C. Papanicolaou, T. Triantafillou, and M. Lekka, 'Externally bonded grids as strengthening and seismic retrofitting materials of masonry panels', *Constr. Build. Mater.*, vol. 2, no. 25, pp. 504–514, 2011.
10. G. Giacomin, 'Innovative strengthening materials for the post-earthquake reconstruction of L'Aquila masonries', *Proceedings of the 10th international conference on structural analysis of historical constructions, SAHC 2016, LEUVEN*, Belgium, 16-26 September 2016.
11. L. Ascione, G. de Felice, and S. De Santis, 'A qualification method for externally bonded Fibre Reinforced Cementitious Matrix (FRCM) strengthening systems', *Compos. Part B Eng.*, vol. 78, pp. 497–506, Sep. 2015.
12. RILEM Technical Committee 232-TDT (Wolfgang Brameshuber), 'Recommendation of RILEM TC 232-TDT: test methods and design of textile reinforced concrete', *Mater. Struct.*, vol. 49, no. 12, pp. 4923–4927, Dec. 2016.

13. L. A. S. Kouris and T. C. Triantafillou, 'State-of-the-art on strengthening of masonry structures with textile reinforced mortar (TRM)', *Constr. Build. Mater.*, vol. 188, pp. 1221–1233, Nov. 2018.
14. F. G. Carozzi and C. Poggi, 'Mechanical properties and debonding strength of Fabric Reinforced Cementitious Matrix (FRCM) systems for masonry strengthening', *Compos. Part B Eng.*, vol. 70, pp. 215–230, Mar. 2015.
15. A. Bilotta, F. Ceroni, G. P. Lignola, and A. Prota, 'Use of DIC technique for investigating the behaviour of FRCM materials for strengthening masonry elements', *Compos. Part B Eng.*, vol. 129, pp. 251–270, Nov. 2017.
16. S. De Santis, F. G. Carozzi, G. de Felice, and C. Poggi, 'Test methods for Textile Reinforced Mortar systems', *Compos. Part B Eng.*, vol. 127, pp. 121–132, Oct. 2017.
17. S. De Santis and G. de Felice, 'Tensile behaviour of mortar-based composites for externally bonded reinforcement systems', *Compos. Part B Eng.*, vol. 68, pp. 401–413, Jan. 2015.
18. Arboleda Diana, Carozzi Francesca Giulia, Nanni Antonio, and Poggi Carlo, 'Testing Procedures for the Uniaxial Tensile Characterization of Fabric-Reinforced Cementitious Matrix Composites', *J. Compos. Constr.*, vol. 20, no. 3, p. 04015063, Jun. 2016.
19. T. D'Antino and C. Papanicolaou, 'Mechanical characterization of textile reinforced inorganic-matrix composites', *Compos. Part B Eng.*, vol. 127, pp. 78–91, Oct. 2017.
20. F. G. Carozzi, A. Bellini, T. D'Antino, G. de Felice, F. Focacci, Ł. Hojdys, L. Laghi, E. Lanoye, F. Micelli, M. Panizza, and C. Poggi, 'Experimental investigation of tensile and bond properties of Carbon-FRCM composites for strengthening masonry elements', *Compos. Part B Eng.*, vol. 128, pp. 100–119, Nov. 2017.
21. S. De Santis, F. Ceroni, G. de Felice, M. Fagone, B. Ghiassi, A. Kwiecień, G. P. Lignola, M. Morganti, M. Santandrea, M. R. Valluzzi, and A. Viskovic, 'Round Robin Test on tensile and bond behaviour of Steel Reinforced Grout systems', *Compos. Part B Eng.*, vol. 127, pp. 100–120, Oct. 2017.
22. M. Leone, M. A. Aiello, A. Balsamo, F. G. Carozzi, F. Ceroni, M. Corradi, M. Gams, E. Garbin, N. Gattesco, P. Krajewski, C. Mazzotti, D. Oliveira, C. Papanicolaou, G. Ranocchiai, F. Roscini, and D. Saenger, 'Glass fabric reinforced cementitious matrix: Tensile properties and bond performance on masonry substrate', *Compos. Part B Eng.*, vol. 127, pp. 196–214, Oct. 2017.
23. G. P. Lignola, C. Caggegi, F. Ceroni, S. De Santis, P. Krajewski, P. B. Lourenço, M. Morganti, C. (Corina) Papanicolaou, C. Pellegrino, A. Prota, and L. Zuccarino, 'Performance assessment of basalt FRCM for retrofit applications on masonry', *Compos. Part B Eng.*, vol. 128, pp. 1–18, Nov. 2017.
24. C. Caggegi, F. G. Carozzi, S. De Santis, F. Fabbrocino, F. Focacci, Ł. Hojdys, E. Lanoye, and L. Zuccarino, 'Experimental analysis on tensile and bond properties of PBO and aramid fabric reinforced cementitious matrix for

strengthening masonry structures', *Compos. Part B Eng.*, vol. 127, pp. 175–195, Oct. 2017.
25. C. Caggegi, E. Lanoye, K. Djama, A. Bassil, and A. Gabor, 'Tensile behaviour of a basalt TRM strengthening system: Influence of mortar and reinforcing textile ratios', *Compos. Part B Eng.*, vol. 130, pp. 90–102, Dec. 2017.
26. J. Donnini and V. Corinaldesi, 'Mechanical characterization of different FRCM systems for structural reinforcement', *Constr. Build. Mater.*, vol. 145, pp. 565–575, Aug. 2017.
27. L. H. Sneed, T. D'Antino, C. Carloni, and C. Pellegrino, 'A comparison of the bond behavior of PBO-FRCM composites determined by double-lap and single-lap shear tests', *Cem. Concr. Compos.*, vol. 64, pp. 37–48, Nov. 2015.
28. T. D'Antino, C. Carloni, L. H. Sneed, and C. Pellegrino, 'Matrix–fiber bond behavior in PBO FRCM composites: A fracture mechanics approach', *Eng. Fract. Mech.*, vol. 117, pp. 94–111, Feb. 2014.
29. A. D'Ambrisi, L. Feo, and F. Focacci, 'Experimental and analytical investigation on bond between Carbon-FRCM materials and masonry', *Compos. Part B Eng.*, vol. 46, pp. 15–20, Mar. 2013.
30. F. G. Carozzi, P. Colombi, G. Fava, and C. Poggi, 'A cohesive interface crack model for the matrix–textile debonding in FRCM composites', *Compos. Struct.*, vol. 143, pp. 230–241, May 2016.
31. P. D. Askouni and C. (Corina) G. Papanicolaou, 'Comparison of Double-Lap/Double-Prism and Single-Lap/Single-Prism Shear Tests for the TRM-to-Masonry Bond Assessment', in *Strain-Hardening Cement-Based Composites*, Dordrecht, 2018, pp. 527–534, doi: 10.1007/978-94-024-1194-2_61.
32. G. de Felice, M. A. Aiello, C. Caggegi, F. Ceroni, S. De Santis, E. Garbin, N. Gattesco, Ł. Hojdys, P. Krajewski, A. Kwiecień, M. Leone, G. P. Lignola, C. Mazzotti, D. Oliveira, C. Papanicolaou, C. Poggi, T. Triantafillou, M. R. Valluzzi, and A. Viskovic, 'Recommendation of RILEM Technical Committee 250-CSM: Test method for Textile Reinforced Mortar to substrate bond characterization', *Mater. Struct.*, vol. 51, no. 4, p. 95, Jul. 2018.
33. C. Signorini, A. Nobili, E. I. Cedillo González, and C. Siligardi, 'Silica coating for interphase bond enhancement of carbon and AR-glass Textile Reinforced Mortar (TRM)', *Compos. Part B Eng.*, vol. 141, pp. 191–202, May 2018.
34. P. E. Mezrea, I.A. Yilmaz, M. Ispir, E. Binbir,E. Bal Ihsan, and A. Ilki, 'External Jacketing of Unreinforced Historical Masonry Piers with Open-Grid Basalt-Reinforced Mortar', *J. Compos. Constr.*, vol. 21, no. 3, p. 04016110, Jun. 2017.
35. C. G. Papanicolaou, T. C. Triantafillou, K. Karlos, and M. Papathanasiou, 'Textile-reinforced mortar (TRM) versus FRP as strengthening material of URM walls: in-plane cyclic loading', *Mater. Struct.*, vol. 40, no. 10, pp. 1081–1097, Dec. 2007.
36. C. G. Papanicolaou, T. C. Triantafillou, M. Papathanasiou, and K. Karlos, 'Textile reinforced mortar (TRM) versus FRP as strengthening material of

URM walls: out-of-plane cyclic loading', *Mater. Struct.*, vol. 41, no. 1, pp. 143–157, Jan. 2008.
37. M. Harajli, H. ElKhatib and J. T. San-Jose, 'Static and Cyclic Out-of-Plane Response of Masonry Walls Strengthened Using Textile-Mortar System', *J. Mater. Civ. Eng.*, vol. 22, no. 11, pp. 1171–1180, Nov. 2010.
38. ASTM E519-2: 2003. 'Standard test method for diagonal tension (shear) in masonry assemblages', *ASTM Committee C15 on Manufactured Masonry Units*, West Conshohocken, PA, United States, 2003.
39. N. Williams Portal, M. Flansbjer, P. Johannesson, K. Malaga, and K. Lundgren, 'Tensile behaviour of textile reinforcement under accelerated ageing conditions', *J. Build. Eng.*, vol. 5, pp. 57–66, Mar. 2016.
40. M. T. Tran, X. H. Vu, and E. Ferrier, 'Experimental and analytical analysis of the effect of fibre treatment on the thermomechanical behaviour of continuous carbon textile subjected to simultaneous elevated temperature and uniaxial tensile loadings', *Constr. Build. Mater.*, vol. 183, pp. 32–45, Sep. 2018.
41. F. Micelli and M. A. Aiello, 'Residual tensile strength of dry and impregnated reinforcement fibres after exposure to alkaline environments', *Compos. Part B Eng.*, vol. 159, pp. 490–501, Feb. 2019.
42. V. Rizzo, A. Bonati, F. Micelli, M. Leone, and M. A. Aiello, 'Influence of Alkaline Environments on the Mechanical Properties of FRCM/CRM and their Materials', *Key Eng. Mater.*, vol. 817, pp. 195-201, Aug. 2019.
43. S. De Santis and G. de Felice, 'Tensile behavior and durability of mortar-based strengthening systems with glass-aramid textiles, *Key Eng. Mater.*, vol. 624, pp. 346-353, Sep. 2014.
44. A. Nobili, 'Durability assessment of impregnated Glass Fabric Reinforced Cementitious Matrix (GFRCM) composites in the alkaline and saline environments', *Constr. Build. Mater.*, vol. 105, pp. 465–471, Feb. 2016.
45. A. Nobili and C. Signorini, 'On the effect of curing time and environmental exposure on impregnated Carbon Fabric Reinforced Cementitious Matrix (CFRCM) composite with design considerations', *Compos. Part B Eng.*, vol. 112, pp. 300–313, Mar. 2017.
46. T. Trapko, 'The effect of high temperature on the performance of CFRP and FRCM confined concrete elements', *Compos. Part B Eng.*, vol. 54, pp. 138–145, Nov. 2013, doi: 10.1016/j.compositesb.2013.05.
47. L. Bisby, T. Stratford, J. Smith, and S. Halpin, 'FRP versus Fiber Reinforced Cementitious Mortar Systems at Elevated Temperature', *Spec. Publ.*, vol. 275, pp. 1–20, Mar. 2011, doi: 10.14359/51682459.
48. J. Michels and M. Motavalli, 'Strength evolution after high temperature exposure of coated carbon fiber rovings used for a fiber-reinforced cementitious matrix (FRCM)', *Fourth Asia Pacific Conference on FRP in Structures (APFIS 2013)*, Melbourne, Australia, 2013 International Institute for FRP in Construction.

49. L. Bisby, T. Stratford, C. Hart, and S. Farren 'Fire performance of well-anchored TRM, FRCM and FRP flexural strengthening systems', *Adv Compos Constr 2013*, Network Group for Composites in Construction, Belfast, UK.
50. L. Bisby, 'Fire resistance of textile fiber composites used in civil engineering', in *Textile Fibre Composites in Civil Engineering*, T. Triantafillou, Ed. Woodhead Publishing, 2016, pp. 169–185.
51. Z. C. Tetta and D. A. Bournas, 'TRM vs FRP jacketing in shear strengthening of concrete members subjected to high temperatures', *Compos. Part B Eng.*, vol. 106, pp. 190–205, Dec. 2016, doi: 10.1016/j.compositesb.2016.09.026.
52. F. de A. Silva, M. Butler, S. Hempel, R. D. Toledo Filho, and V. Mechtcherine, 'Effects of elevated temperatures on the interface properties of carbon textile-reinforced concrete', *Cem. Concr. Compos.*, vol. 48, pp. 26–34, Apr. 2014.
53. J. Donnini, F. De Caso y Basalo, V. Corinaldesi, G. Lancioni, and A. Nanni, 'Fabric-reinforced cementitious matrix behavior at high-temperature: Experimental and numerical results', *Compos. Part B Eng.*, vol. 108, pp. 108–121, Jan. 2017.
54. E. Franzoni, C. Gentilini, M. Santandrea, S. Zanotto, and C. Carloni, 'Durability of steel FRCM-masonry joints: effect of water and salt crystallization', *Mater. Struct.*, vol. 50, no. 4, p. 201, Jul. 2017.
55. J. Donnini, 'Durability of glass FRCM systems: Effects of different environments on mechanical properties', *Compos. Part B Eng.*, vol. 174, p. 107047, Oct. 2019.
56. RILEM TC IMC: Durability of Inorganic Matrix Composites used for Strengthening of Masonry Constructions. Available online: https://www.rilem.net/groupe/imc-durability-of-inorganic-matrix-composites-used-for-strengthening-of-masonry-constructions-384 (accessed on December 2nd, 2019).
57. AC 434-1011-R1: Acceptance Criteria for Masonry and Concrete Strengthening using Fiber-Reinforced Cementitious Matrix (FRCM) Composite Systems, *ICC Evaluation Service*, LLC: Birmingham, AL, USA, 2018.
58. ACI 549.4R-13, Guide to Design and Construction of Externally Bonded Fabric-Reinforced Cementitious Matrix (FRCM) Systems for Repair and Strengthening Concrete and Masonry Structures; *ACI Committee 549*: Farmington Hills, MI, USA, 2013.
59. NTC 2018. 'Norme Tecniche per le Costruzioni', *Ministery of the Infrastractures and Transports of the Italian Republic*, decree 17 Jan. 2018.
60. Linea Guida per la identificazione, la qualificazione ed il controllo di accettazione di compositi fibrorinforzati a matrice inorganica (FRCM) da utilizzarsi per il consolidamento strutturale di costruzioni esistenti, *Consiglio Superiore Lavori Pubblici* (Italy), 2018.
61. CNR-DT 215/2018: Istruzioni per la Progettazione, l'Esecuzione ed il Controllo di Interventi di Consolidamento Statico mediante l'utilizzo di Compositi Fibrorinforzati a matrice inorganica, *Consiglio Nazionale delle*

Ricerche – Commissione per lo studio per la predisposizione e l'analisi di norme tecniche relative alle costruzioni (Italy), 2018.
62. UN. Report of the world commission on environment and development: our common future, UN documents, transmitted to the general assembly as an annex to document A/42/427 - development and international Co-operation: environment available online at: http://www.un-documents.net/wced-ocf.htm, Accessed date: 13 December 2019.
63. M. Geissdoerfer, P. Savaget, N. M. P. Bocken, and E. J. Hultink, 'The Circular Economy – A new sustainability paradigm?', *J. Clean. Prod.*, vol. 143, pp. 757–768, Feb. 2017.
64. C. Meyer, 'The greening of the concrete industry', *Cem. Concr. Compos.*, vol. 31, no. 8, pp. 601–605, Sep. 2009.
65. L. Coppola *et al.*, 'Binders alternative to Portland cement and waste management for sustainable construction – Part 2':, *J. Appl. Biomater. Funct. Mater.*, Jul. 2018.
66. Q. Liu, T. Stuart, M. Hughes, H. S. S. Sharma, and G. Lyons, 'Structural biocomposites from flax – Part II: The use of PEG and PVA as interfacial compatibilising agents', *Compos. Part Appl. Sci. Manuf.*, vol. 38, no. 5, pp. 1403–1413, May 2007.
67. M. Carus, L. Scholz, 'Targets for bio-based composites and natural fibres', *Biowerkstoff report*, ISSN 1867-1217, 8th ed.; March 2011. p. 24.
68. A.K. Mohanty, M. Misra, L.T. Drzal, S.E. Selke, B.R. Harte, G. Hinrichsen. In: Mohanty AK, Misra M, Drzal LT, editors. Natural fibres, biopolymers, and biocomposites: an introduction in natural fibres, natural fibres, biopolymers, and biocomposites. Boca Raton, FL: CRC Press, *Taylor & Francis Group;* 2005. p. 1–36.
69. L. Yan, B. Kasal, and L. Huang, 'A review of recent research on the use of cellulosic fibres, their fibre fabric reinforced cementitious, geo-polymer and polymer composites in civil engineering', *Compos. Part B Eng.*, vol. 92, pp. 94–132, May 2016.
70. L. Yan, N. Chouw, and K. Jayaraman, 'Flax fibre and its composites – A review', *Compos. Part B Eng.*, vol. 56, pp. 296–317, Jan. 2014.
71. A. Komuraiah, N. S. Kumar, and B. D. Prasad, 'Chemical Composition of Natural Fibers and its Influence on their Mechanical Properties', *Mech. Compos. Mater.*, vol. 50, no. 3, pp. 359–376, Jul. 2014.
72. K. Charlet, S. Eve, J. P. Jernot, M. Gomina, and J. Breard, 'Tensile deformation of a flax fiber', *Procedia Eng.*, vol. 1, no. 1, pp. 233–236, Jul. 2009.
73. M. P. M. Dicker, P. F. Duckworth, A. B. Baker, G. Francois, M. K. Hazzard, and P. M. Weaver, 'Green composites: A review of material attributes and complementary applications', *Compos. Part Appl. Sci. Manuf.*, vol. 56, pp. 280–289, Jan. 2014.
74. D. B. Dittenber and H. V. S. GangaRao, 'Critical review of recent publications on use of natural composites in infrastructure', *Compos. Part Appl. Sci. Manuf.*, vol. 43, no. 8, pp. 1419–1429, Aug. 2012.

75. D.S. Ramamurthi and M. Sophia, 'A review on modified lime based mortars – an alternative to cement mortar, *Int J Innov Res Sci Eng Technol*, vol. 2, no. 12, pp. 350-356, May 2016.
76. S. R. Ferreira, E. Martinelli, M. Pepe, F. de Andrade Silva, and R. D. Toledo Filho, 'Inverse identification of the bond behavior for jute fibers in cementitious matrix', *Compos. Part B Eng.*, vol. 95, pp. 440–452, Jun. 2016.
77. M. E. A. Fidelis, R. D. Toledo Filho, F. de Andrade Silva, B. Mobasher, S. Müller, and V. Mechtcherine, 'Interface characteristics of jute fiber systems in a cementitious matrix', *Cem. Concr. Res.*, vol. 116, pp. 252–265, Feb. 2019.
78. S. R. Ferreira, F. de A. Silva, P. R. L. Lima, and R. D. Toledo Filho, 'Effect of fiber treatments on the sisal fiber properties and fiber–matrix bond in cement based systems', *Constr. Build. Mater.*, vol. 101, pp. 730–740, Dec. 2015.
79. B. Ghiassi, A. Razavizadeh, D. V. Oliveira, V. Marques and P. B. Lourenço, 'Tensile and bond characterization of natural fibers embedded in inorganic matrices', *Proceed. of 2nd International Conference on natural fibers*, Azores/Portugal, 27-29 Apr. 2015.
80. R. Codispoti, D. V. Oliveira, R. S. Olivito, P. B. Lourenço, and R. Fangueiro, 'Mechanical performance of natural fiber-reinforced composites for the strengthening of masonry', *Compos. Part B Eng.*, vol. 77, pp. 74–83, Aug. 2015.
81. R. S. Olivito, O. A. Cevallos, and A. Carrozzini, 'Development of durable cementitious composites using sisal and flax fabrics for reinforcement of masonry structures', *Mater. Des.*, vol. 57, pp. 258–268, May 2014.
82. O. A. Cevallos and R. S. Olivito, 'Effects of fabric parameters on the tensile behaviour of sustainable cementitious composites', *Compos. Part B Eng.*, vol. 69, pp. 256–266, Feb. 2015.
83. C. B. de Carvalho Bello, I. Boem, A. Cecchi, N. Gattesco, and D. V. Oliveira, 'Experimental tests for the characterization of sisal fiber reinforced cementitious matrix for strengthening masonry structures', *Constr. Build. Mater.*, vol. 219, pp. 44–55, Sep. 2019.
84. L. Mercedes, L. Gil, and E. Bernat-Maso, 'Mechanical performance of vegetal fabric reinforced cementitious matrix (FRCM) composites', *Constr. Build. Mater.*, vol. 175, pp. 161–173, Jun. 2018.
85. R. S. Olivito, R. Codispoti, and O. A. Cevallos, 'Bond behavior of Flax-FRCM and PBO-FRCM composites applied on clay bricks: Experimental and theoretical study', *Compos. Struct.*, vol. 146, pp. 221–231, Jun. 2016.
86. O. A. Cevallos, R. S. Olivito, R. Codispoti, and L. Ombres, 'Flax and polyparaphenylene benzobisoxazole cementitious composites for the strengthening of masonry elements subjected to eccentric loading', *Compos. Part B Eng.*, vol. 71, pp. 82–95, Mar. 2015.
87. C. Menna, D. Asprone, M. Durante, A. Zinno, A. Balsamo, and A. Prota, 'Structural behaviour of masonry panels strengthened with an innovative hemp fibre composite grid', *Constr. Build. Mater.*, vol. 100, pp. 111–121, Dec. 2015.

88. R. S. Olivito, F. Dubois, A. Venneri and F. A. Zuccarello, 'Experimental and numerical analysis of masonry macroelements reinforced by natural-fibre-composite materials, *Proceed. of 4th International Conference on FRP Composites in Civil Engineering*, Rome/Italy, 13-15 Jun. 2012.
89. H. E. Gram, 'Durability of natural fibres in concrete, *Swedish Cement and Concrete Research Institute of Technology*, Stockholm, Sweden, 1983.
90. R. D. Toledo Filho, K. Scrivener, G. L. England and K. Ghavami, 'Durability of alkali-sensitive sisal and coconut fibres in cement mortar composites', *Cement Concrete Comp.*, vol. 22, pp. 127–143, Oct. 2000.
91. G. Ramakrishna and T. Sundararajan, 'Studies on the durability of natural fibres and the effect of corroded fibres on the strength of mortar', *Cem. Concr. Compos.*, vol. 27, no. 5, pp. 575–582, May 2005.
92. G. H. D. Tonoli, A. P. Joaquim, M.-A. Arsène, K. Bilba, and H. S. Jr, 'Performance and Durability of Cement Based Composites Reinforced with Refined Sisal Pulp', *Mater. Manuf. Process.*, vol. 22, no. 2, pp. 149–156, Feb. 2007.
93. F. Pacheco-Torgal and S. Jalali, 'Cementitious building materials reinforced with vegetable fibres: A review', *Constr. Build. Mater.*, vol. 25, no. 2, pp. 575–581, Feb. 2011.
94. R. M. de Gutiérrez, L. N. Díaz, and S. Delvasto, 'Effect of pozzolans on the performance of fiber-reinforced mortars', *Cem. Concr. Compos.*, vol. 5, no. 27, pp. 593–598, 2005.
95. A. D'Almeida, J. M. Filho, and R. T. Filho, 'Use of curaua fibers as reinforcement in cement composites', *Chem. Eng. Trans.*, vol. 17, pp. 1717–1722, May 2009.
96. R. D. Tolêdo Filho, K. Ghavami, G. L. England, and K. Scrivener, 'Development of vegetable fibre–mortar composites of improved durability', *Cem. Concr. Compos.*, vol. 25, no. 2, pp. 185–196, Feb. 2003.
97. L. A. Motta, V. M. John and V. Agopyan 'Thermo-mechanical treatment to improve properties of sisal fibres for composites', *Mater. Sci. Forum.*, vol. 636-637, pp. 253–259, Jan. 2010.
98. Technical Sheet, FIDFLAX GRID 300 HS20®, Tessuto a Rete Bilanciato in Fibra di Lino per il Rinforzo Strutturale. Available online: http://www.fidiaglobalservice.com (accessed on Decembre 29th, 2019).
99. A. Mustata and F. S. C. Mustata 'Moisture absorption and desorption in flax and hemo fibres and yarns', *FIBRES & TEXTILES in Eastern Europe*, vol. 31, 3(99), pp. 26–30, 2013.
100. ISO 13934-1. Textiles-Tensile properties of fabrics- Determination of maximum force and elongation at maximum force using the strip method, 2013.
101. J. Wei, S. Ma, and D. G. Thomas, 'Correlation between hydration of cement and durability of natural fiber-reinforced cement composites', *Corros. Sci.*, vol. 106, pp. 1–15, May 2016, doi: 10.1016/j.corsci.2016.01.020.

102. M. E. A. Fidelis, R. D. Toledo Filho, F. de A. Silva, V. Mechtcherine, M. Butler, and S. Hempel, 'The effect of accelerated aging on the interface of jute textile reinforced concrete', *Cem. Concr. Compos.*, vol. 74, pp. 7–15, Nov. 2016, doi: 10.1016/j.cemconcomp.2016.09.002.
103. M. Ardanuy, J. Claramunt, and R. D. Toledo Filho, 'Cellulosic fiber reinforced cement-based composites: A review of recent research', *Constr. Build. Mater.*, vol. 79, pp. 115–128, Mar. 2015, doi: 10.1016/j.conbuildmat.2015.01.035.
104. B. Coppola, L. Di Maio, P. Scarfato, and L. Incarnato, 'Use of polypropylene fibers coated with nano-silica particles into a cementitious mortar', *AIP Conf. Proc.*, vol. 1695, no. 1, p. 020056, Dec. 2015, doi: 10.1063/1.4937334.
105. M. Aly, M. S. J. Hashmi, A. G. Olabi, K. Y. Benyounis, M. Messeiry, A. I. Hussain and E. F. Abadir, 'Optimization of Alkaline Treatment Conditions of Flax Fiber Using Box–Behnken Method', *J. Nat. Fibers*, 9:4, 256-276, 2012, doi: 10.1080/15440478.2012.738036
106. T. P. Sathishkumar, P. Navaneethakrishnan, S. Shankar, R. Rajasekar, and N. Rajini, 'Characterization of natural fiber and composites – A review':, *J. Reinf. Plast. Compos.*, Jul. 2013, doi: 10.1177/0731684413495322.
107. Technical Sheet, FIDCALX NHL5®, Betoncino Strutturale di Calce Idraulica Naturale per L'impregnazione di Tessuti per il Rinforzo Strutturale. Available online: http://www.fidiaglobalservice.com (accessed on December 29th, 2019).
108. Innovations.srl Company Website. Available online: http://www.innovationssrl.it (accessed on December 29th, 2019).
109. ASTM C136 / C136M-14, Standard Test Method for Sieve Analysis of Fine and Coarse Aggregates; ASTM International: West Conshohocken, PA, USA, 2014.
110. EN 1015-3: 1999. Methods of Test Mortar for Masonry. Determination of Consistence of Fresh Mortar (by Flow Table); European Committee for Standardization: Brussels, Belgium, 1999.
111. EN 196-1:1994. Methods of Testing Cement—Part 1: Determination of Strength; European Committee for Standardization: Brussels, Belgium, 1994.
112. GOM Correlate 2017. Digital Image Correlation Software. https://www.gom.com/3d-software/gom-correlate.html (accessed on December 31th, 2019).
113. M. E. Alves Fidelis, F. de Andrade Silva, and R. D. Toledo Filho, 'The influence of fibre treatment on the mechanical behaviour of jute Textile Reinforced Concrete', *Key Eng. Mater.*, vol. 600, pp. 469-474, Mar. 2014.
114. San Marco Terreal Company Website. Available online: https://www.sanmarco.it/ (accessed on January 3rd, 2020).
115. RILEM TC-76-LUM. 'Diagonal tensile strength tests of small wall specimens, RILEM recommendations for the testing and use of constructions materials, pp. 488-9, 1994.
116. S. Babaeidarabad, F. De Caso, and A. Nanni, 'URM Walls Strengthened with Fabric-Reinforced Cementitious Matrix Composite Subjected to Diagonal

Compression', *J. Compos. Constr.*, vol. 18, no. 2, p. 04013045, Apr. 2014, doi: 10.1061/(ASCE)CC.1943-5614.0000441.
117. G. Marcari, M. Basili, and F. Vestroni, 'Experimental investigation of tuff masonry panels reinforced with surface bonded basalt textile-reinforced mortar', *Compos. Part B Eng.*, vol. 108, pp. 131–142, Jan. 2017, doi: 10.1016/j.compositesb.2016.09.094.
118. X. Wang, C. C. Lam, and V. P. Iu, 'Experimental investigation of in-plane shear behaviour of grey clay brick masonry panels strengthened with SRG', *Eng. Struct.*, vol. 162, pp. 84–96, May 2018, doi: 10.1016/j.engstruct.2018.02.027.
119. J. A. P. P. Almeida, E. B. Pereira, and J. A. O. Barros, 'Assessment of overlay masonry strengthening system under in-plane monotonic and cyclic loading using the diagonal tensile test', *Constr. Build. Mater.*, vol. 94, pp. 851–865, Sep. 2015, doi: 10.1016/j.conbuildmat.2015.07.040.
120. F. Parisi, I. Iovinella, A. Balsamo, N. Augenti, and A. Prota, 'In-plane behaviour of tuff masonry strengthened with inorganic matrix–grid composites', *Compos. Part B Eng.*, vol. 45, no. 1, pp. 1657–1666, Feb. 2013, doi: 10.1016/j.compositesb.2012.09.068.
121. N. Gattesco, I. Boem, and A. Dudine, 'Diagonal compression tests on masonry walls strengthened with a GFRP mesh reinforced mortar coating', *Bull. Earthq. Eng.*, vol. 13, no. 6, pp. 1703–1726, Jun. 2015, doi: 10.1007/s10518-014-9684-z.
122. F. Ferretti, A. Incerti, B. Ferracuti, and C. Mazzotti, 'FRCM Strengthened Masonry Panels: The Role of Mechanical Anchorages and Symmetric Layouts', *Key Engineering Materials*, vol. 747, pp. 334-341, 2017.
123. A. Incerti, A.R. Tilocca, F. Ferretti, and C. Mazzotti, 'Influence of masonry texture on the shear strength of FRCM reinforced panels', *Proc. of the 11th International Conference on Structural Analysis of Historical Constructions, SAHC2018*, Sep. 11 to 13, 2018, Cusco, Perù.
124. M. Del Zoppo, M. Di Ludovico, A. Balsamo, and A. Prota, 'Experimental In-Plane Shear Capacity of Clay Brick Masonry Panels Strengthened with FRCM and FRM Composites', *J. Compos. Constr.*, vol. 23, no. 5, p. 04019038, Oct. 2019, doi: 10.1061/(ASCE)CC.1943-5614.0000965.
125. L. De Lorenzis, N. Galati, and L. Ombres, 'In-plane shear strengthening of natural masonry walls with NSM CFRP strips and FRCM overlay' *Proceedings of the Fourth International Seminar on Structural Analysis of Historical Constructions*, pp. 847–856, Nov. 2004, Padova, Italy.
126. A. Prota, G. Marcari, G. Fabbrocino, G. Manfredi, and C. Aldea, 'Experimental In-Plane Behavior of Tuff Masonry Strengthened with Cementitious Matrix–Grid Composites', *J. Compos. Constr.*, vol. 10, no. 3, pp. 223–233, Jun. 2006, doi: 10.1061/(ASCE)1090-0268(2006)10:3(223).
127. C. Faella, E. Martinelli, E. Nigro, and S. Paciello, 'Shear capacity of masonry walls externally strengthened by a cement-based composite material: An experimental campaign', *Constr. Build. Mater.*, vol. 24, no. 1, pp. 84–93, Jan. 2010, doi: 10.1016/j.conbuildmat.2009.08.019.

128. A. Balsamo, M. Di Ludovico, A. Prota, and G. Manfredi, ‘Masonry walls strengthened with innovative composites, *American Concr. Inst.*, ACI spec publ., vol. 2, no. 275, pp. 769-786, 2012.
129. M. Del Zoppo, M. Di Ludovico, A. Balsamo, and A. Prota, ‘In-plane shear capacity of tuff masonry walls with traditional and innovative Composite Reinforced Mortars (CRM)’, *Constr. Build. Mater.*, vol. 210, pp. 289–300, Jun. 2019, doi: 10.1016/j.conbuildmat.2019.03.133.
130. S. Babaeidarabad, D. Arboleda, G. Loreto, and A. Nanni, ‘Shear strengthening of un-reinforced concrete masonry walls with fabric-reinforced-cementitious-matrix’, *Constr. Build. Mater.*, vol. 65, pp. 243–253, Aug. 2014, doi: 10.1016/j.conbuildmat.2014.04.116.
131. N. Ismail, T. El-Maaddawy, N. Khattak, and A. Najmal, ‘In-Plane Shear Strength Improvement of Hollow Concrete Masonry Panels Using a Fabric-Reinforced Cementitious Matrix’, *J. Compos. Constr.*, vol. 22, no. 2, p. 04018004, Apr. 2018.
132. B. Zukowski, E. R. F. dos Santos, Y. G. dos Santos Mendonça, F. de Andrade Silva, and R. D. Toledo Filho, ‘The durability of SHCC with alkali treated curaua fiber exposed to natural weathering’, *Cem. Concr. Compos.*, vol. 94, pp. 116–125, Nov. 2018, doi: 10.1016/j.cemconcomp.2018.09.002.
133. Y. Jia and B. Fiedler, ‘Influence of Furfuryl Alcohol Fiber Pre-Treatment on the Moisture Absorption and Mechanical Properties of Flax Fiber Composites’, *Fibers*, vol. 6, no. 3, p. 59, Sep. 2018, doi: 10.3390/fib6030059.
134. B. Zukowski, F. de Andrade Silva, and R. D. Toledo Filho, ‘Design of strain hardening cement-based composites with alkali treated natural curauá fiber’, *Cem. Concr. Compos.*, vol. 89, pp. 150–159, May 2018, doi: 10.1016/j.cemconcomp.2018.03.006.

Appendix A

Displacement field of the middle longitudinal section of specimens of the series Flax TRM-1L-T and Flax TRM-2L-T

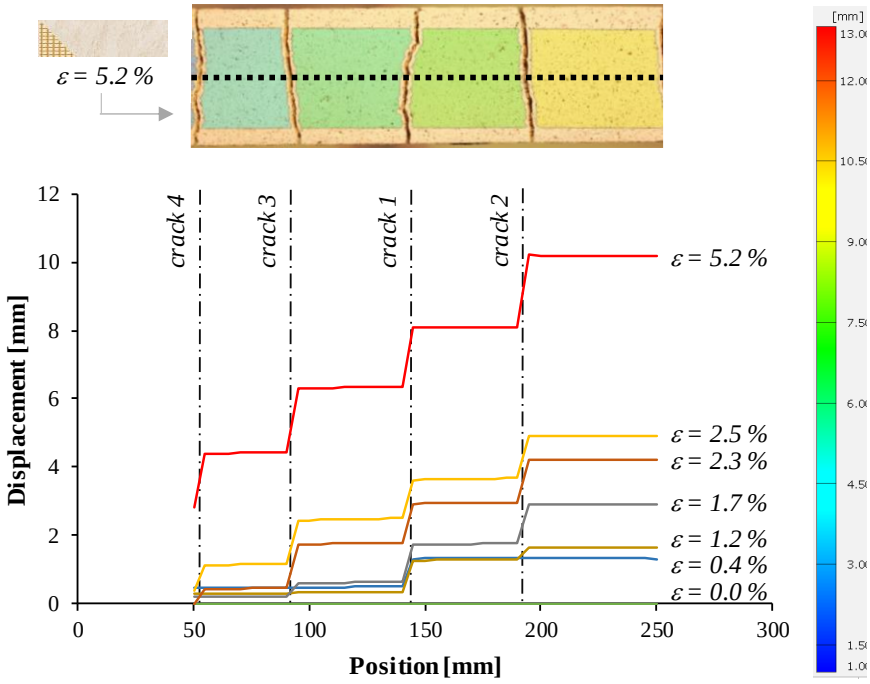

Figure A. 1: Displacement field of middle longitudinal section (specimen Flax TRM-1L-1).

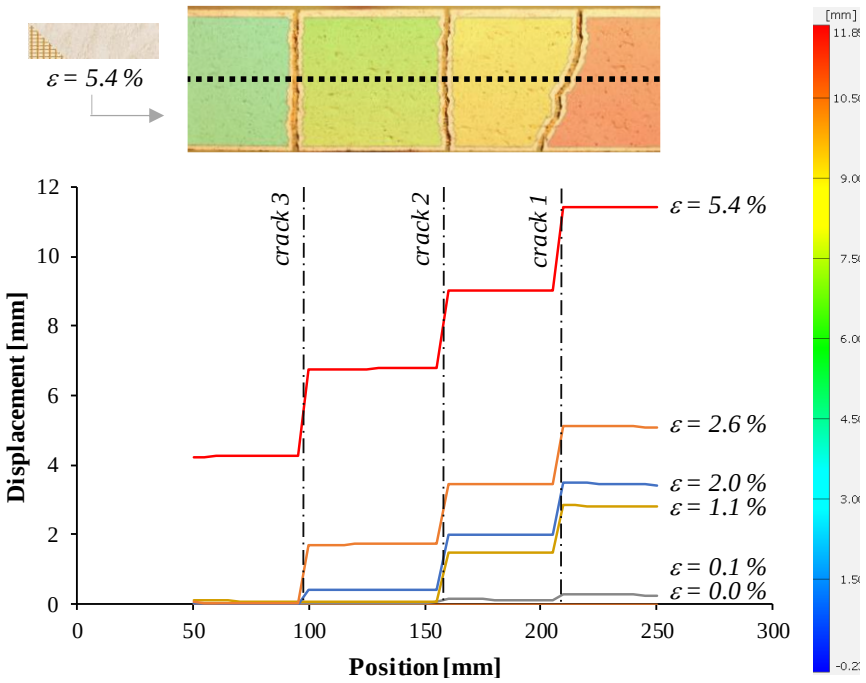

Figure A. 2: Displacement field of middle longitudinal section (specimen Flax TRM-1L-2).

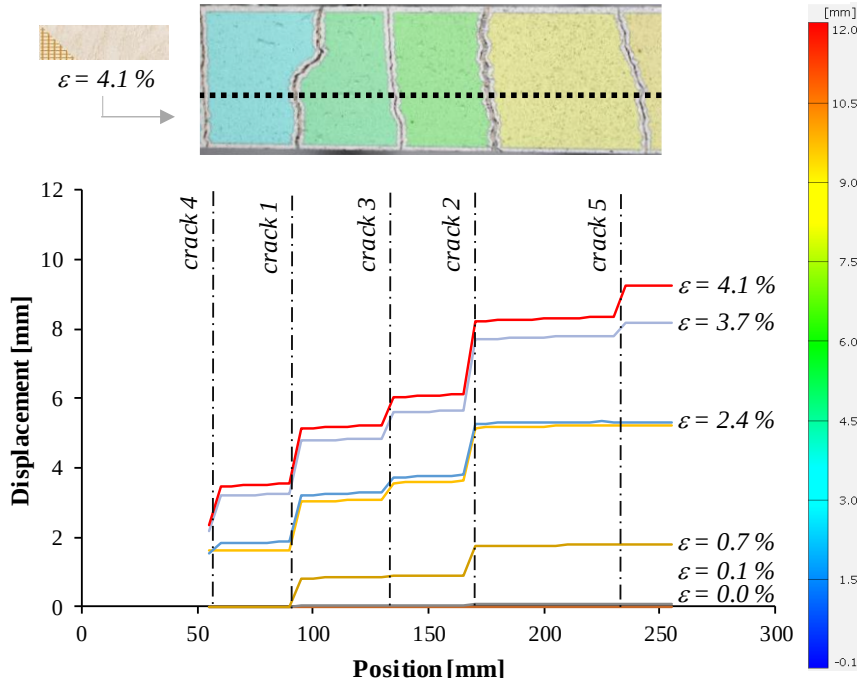

Figure A. 3: Displacement field of middle longitudinal section (specimen Flax TRM-1L-3).

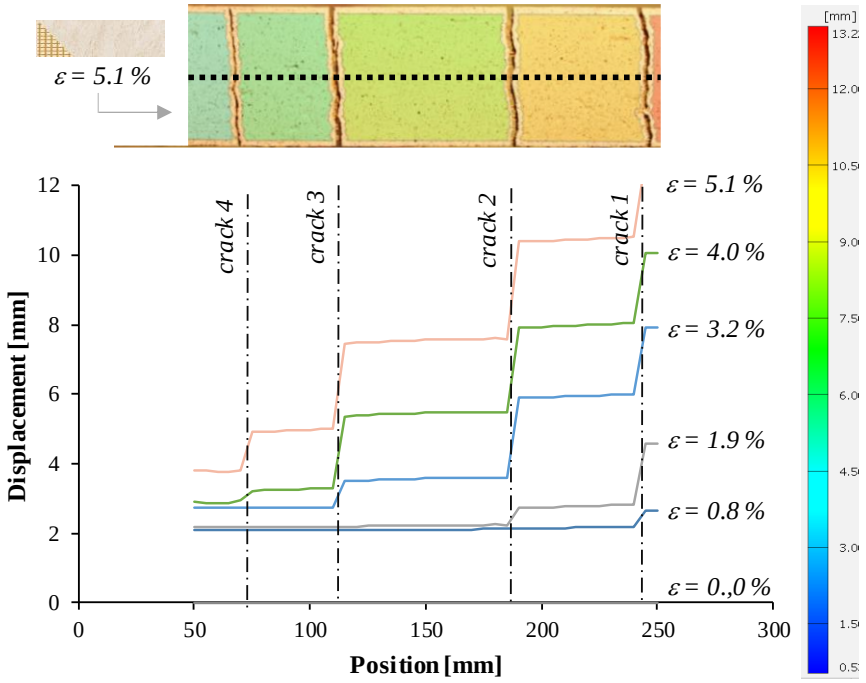

Figure A. 4: Displacement field of middle longitudinal section (specimen Flax TRM-1L-4).

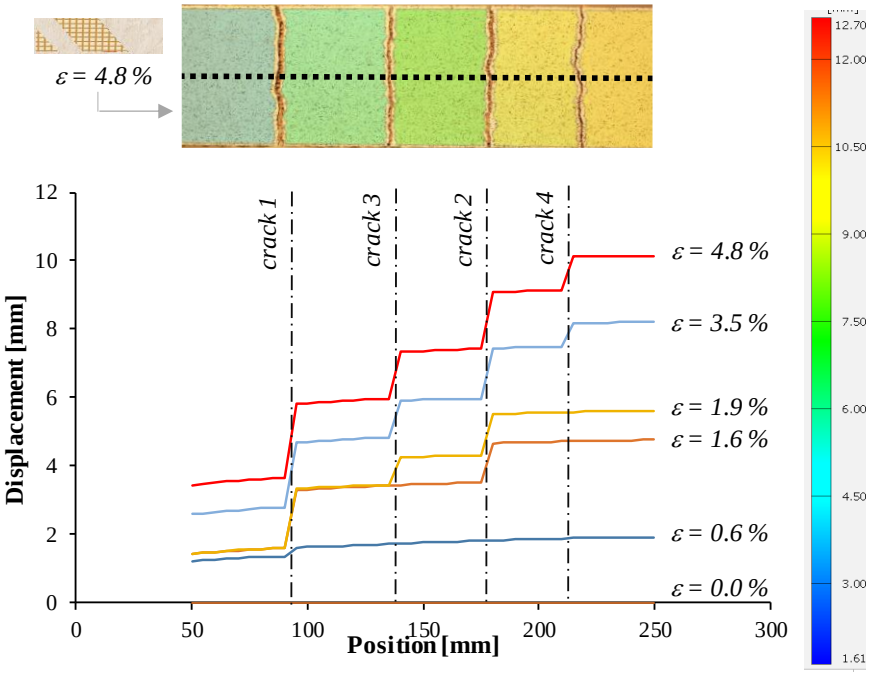

Figure A. 5: Displacement field of middle longitudinal section (specimen Flax TRM-2L-1).

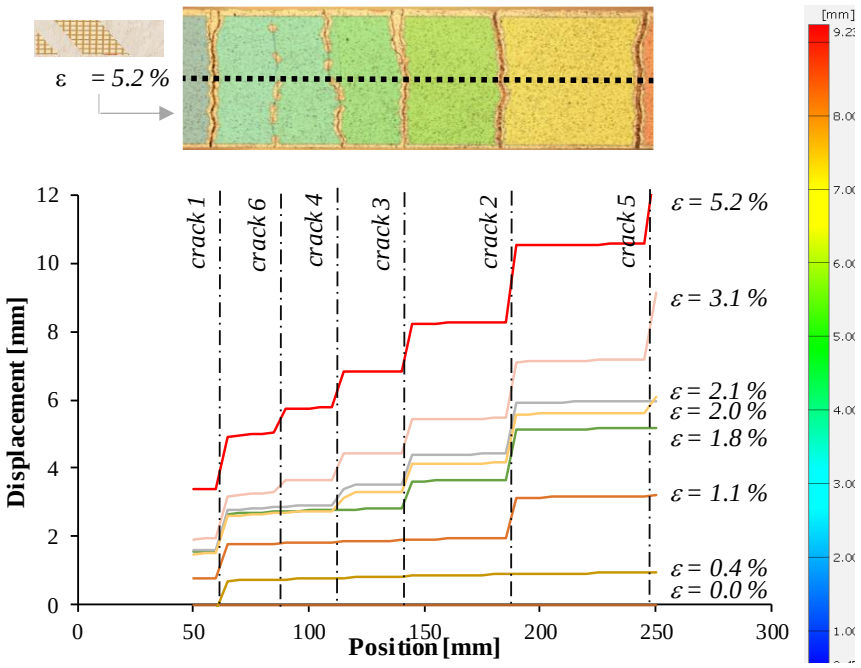

Figure A. 6: Displacement field of middle longitudinal section (specimen Flax TRM-2L-2).

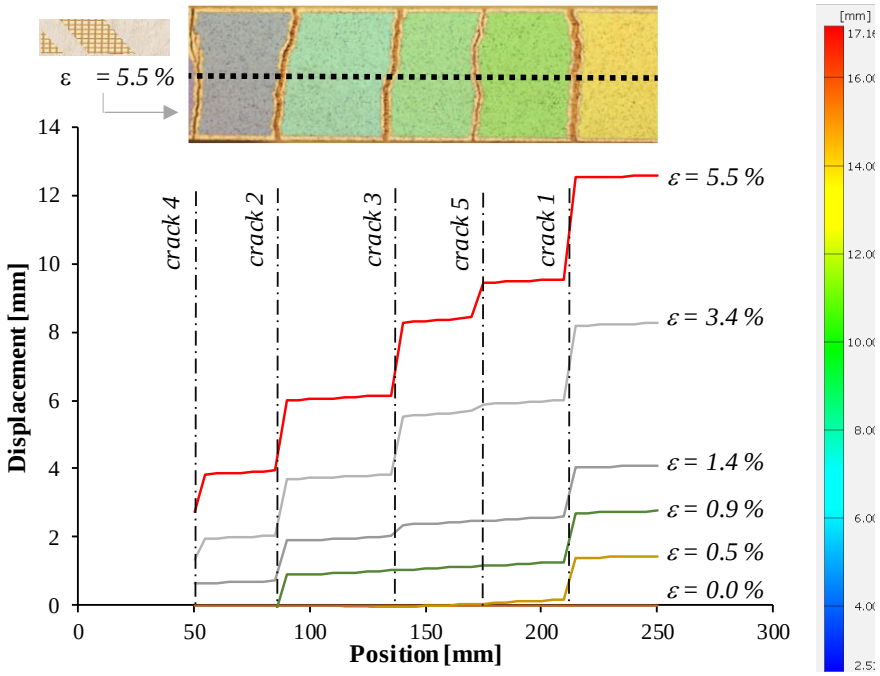

Figure A. 7: Displacement field of middle longitudinal section (specimen Flax TRM-2L-3).

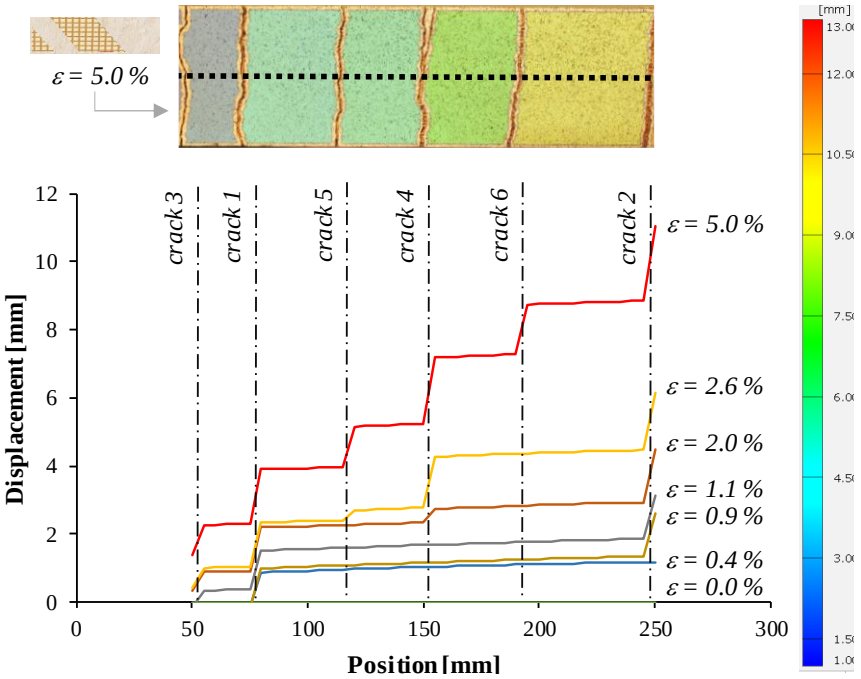

Figure A. 8: Displacement field of middle longitudinal section (specimen Flax TRM-2L-4).

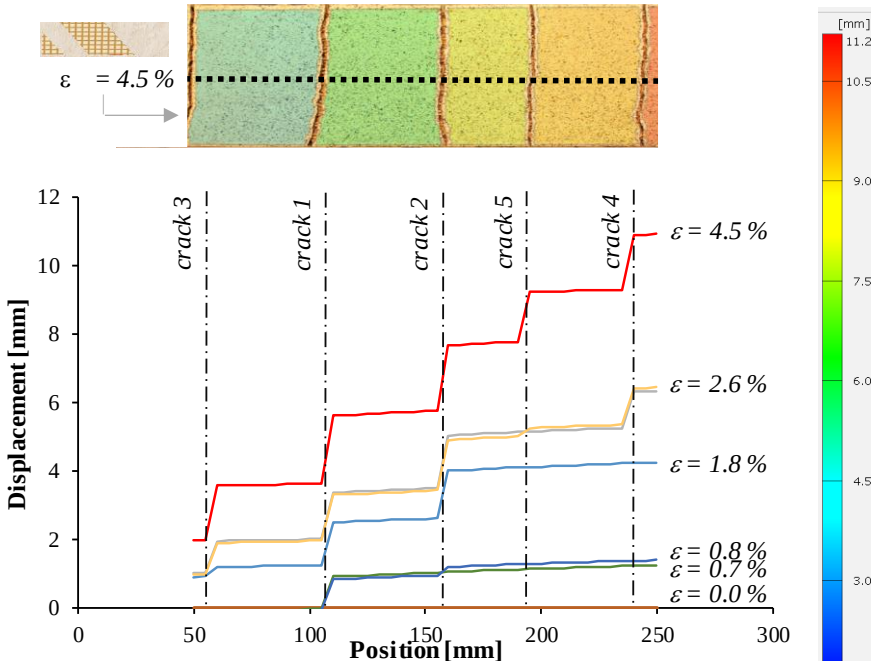

Figure A. 9: Displacement field of middle longitudinal section (specimen Flax TRM-2L-5).